
# The Controlled Synthesis of Interlocked Architectures

**Andrew John Wilson**

Submitted for the Degree of Doctor of Philosophy in Chemistry

University of Warwick

Department of Chemistry

October 2000

# Contents

## List of Figures

## List of Schemes

## List of Tables

# Acknowledgments

Of the many people I wish to thank for making my time as a postgraduate as enjoyable as it has been over the past three years I wish to first of all thank my supervisor Prof. David A. Leigh who has given me some fantastic projects to work on and also given me the freedom and enthusiastic support to explore many other avenues of research.

Dr. Guy. J. Clarkson has without doubt made this research successful as without his unbelievable knowledge of synthetic chemistry and his ideas I would have been unable to make many of the molecules that appear in this thesis. As if this were not already enough Guy deserves eternal thanks for reading and correcting this thesis!

Tim Kidd, Philip Nash and Richard Smith have all had to put up with me at home as well as in the lab at some time and all I can say is that at least they weren't Tony Wood who got lumbered with me for all three years! Thanks a lot Folks.

Thanks To everyone else past and present in the group: In particular Jenny Wong and Steven Lacy for crystallography and Francesco Gatti for NMR.

I must also thank Dr. Alex Slawin, Dr. Simon Teat and Dr. Nat Alcock whom have assisted with and run many of the crystal structure investigations.

I must also thank all the technical staff at both UMIST and the University of Warwick in particular Adam Clarke who has always helped with any NMR problems.

I would also like to thank my family, 'Moike' and Ian for their support and encouragement over the past three years and Claire for putting up with me this last year the most stressful for anyone who has had anything to do with me!

## Declaration

The work performed in this thesis was carried out in the Department of Chemistry, University of Manchester Institute of Science and Technology, between October 1997 and September 1998 and in the Chemistry Department, University of Warwick between September 1998 and September 2000. Unless otherwise stated, it is the work of the author and has not been submitted in whole or in support of an application for another degree or qualification of this or any other university or other institute of learning.

## Summary

An area of great current interest is the synthesis and characterisation of molecules possessing moving parts, with the goal that they can function as "nanoscopic machines" carrying out tasks that molecules with fixed conventional architectures cannot do. Rotaxanes and catenanes (mechanically interlocked architectures) represent one approach towards achieving these aims as their component *wheels* and /or *threads* are connected together but can still move in certain, controlled, directions. This thesis focuses on the problem that many of the reactions (*clipping* and *capping*) that lead to interlocked architectures are carried out under kinetic control and as a result if *clipping* or *capping* does not occur *via* an already *threaded precursor*, "mistakes"- non-interlocked molecules- are produced that cannot be "corrected" leading to lower yields.

**Chapter One** gives a brief outline of the common synthetic approaches to interlocked architectures and the thermodynamically controlled routes that are now being developed to address the problems outlined above.

**Chapters Two and Three** are concerned with probing the mechanism of hydrogen bond-assembled rotaxane formation and gaining insight into the requirements of a thermodynamically controlled synthesis of interlocked architectures.

**Chapter Four** outlines the remarkable binding properties of the component macrocycle of a hydrogen bond-assembled catenane.

**Chapter Five** uses the results of chapter four to synthesise a rotaxane under thermodynamic control using *slippage* illustrating exactly why this approach to synthesis is a poor one.

**Chapter Six** describes the true thermodynamically controlled synthesis of hydrogen bond-assembled rotaxanes employing the results of chapter four and olefin metathesis.

**Chapter Seven** describes an efficient synthesis of catenates using octahedral metal templates. These catenates complement structurally analogous hydrogen bond-assembled catenanes as they provide a way of fixing the conformational preference of the component rings. In addition there are elements of thermodynamic control built into the synthesis.

## Abbreviations Used in the Text

| | |
|---|---|
| $^{t}Boc_2O$ | *tertiary*-butoxycarbonyl anyhdride |
| *m*CPBA | *meta*-Chloroperbenzoic Acid |
| DNA | Deoxyribonucleic Acid |
| DEAD | Diethylazodicarboxylate |
| EDCI | 1-(3-Dimethylaminopropyl)-3-ethyl-carbodiimide hydrochloride |
| DMAP | Dimethylaminopyridine |
| DMF | Dimethylformamide |
| DMSO | Dimethylsulphoxide |
| EtOH | Ethanol |
| EtO | Ethoxide |
| EtOAc | Ethyl Acetate |
| en | Ethylenediamine |
| EDTA | Ethylenediaminetetra-acetic Acid |
| MeOH | Methanol |
| *m*NBA | *meta*-Nitrobenzyl Alcohol |
| RCM | Ring Closing Metathesis |
| THF | Tetrahydrofuran |
| TLC | Thin Layer Chromatography |
| TFA | Triflouroacetic Acid |

# Chapter One

# 1. From Statistical Beginnings to the Thermodynamically Controlled Synthesis of Interlocked Architectures

## 1.1. The Importance of Template-Directed Synthesis

*"Sun Paints Rainbows Over the Vast Waves" composed by David Bedford for Wind Ensemble and inspired by a jotting in Coleridges notebook during the time he was working on "The Rime of Ancient Mariner"... "The sea was then very much tossed and the Wind carrying of the Tops of the Waves made a kind of Rain, in which the Sun painted the colours of the Rainbow"*

Both in the literary inspiration and in the structure of the music (above), groups of components interacting in tandem with each other are used to construct a more complex entity. In much the same way, nature uses simple components in the controlled construction of more complex functional structures such as DNA[1,2] that carry out tasks within the human body that are essential for life. Over the past forty years, chemists have used nature as an example in a new area known as supramolecular chemistry[3]: - the designed chemistry of the intermolecular bond rather than molecular chemistry: - the chemistry of the covalent bond. Lehn defined the subject as "chemistry beyond the molecule, concerning the structure and functions of the entities formed by the association of two or more chemical species"[3c]. The goal has been to use well-defined arrays of molecules that function together to carry out tasks, which the individual components cannot do. Such a venture has only been possible with an increased understanding of self-assembly through non-covalent interactions in natural systems[4,5] and its application to unnatural systems.[5] More recently our understanding of non-covalent interactions

and template synthesis has allowed us to construct useful quantities of mechanically interlocked architectures: - catenanes, rotaxanes and knots[6] (not supramolecular species but discrete molecules)- that show the potential for the construction of nano-scale devices.[7] This short review which is by no means exhaustive discusses some of the principal synthetic routes to interlocked architectures and in particular the thermodynamically controlled syntheses that are now being developed in order to address the low yields that often arise even with the use of template directed synthesis.

## 1.2. Introducing the Interlocked Architectures: Catenanes, Rotaxanes and Knots

Since the first discussion of chemical topology with respect to interlocked architectures[6b] there has been a growing interest in the area. One of the major sources of interest derives from the fact that the individual components cannot be separated without cleavage of covalent bonds but can move independently of one another allowing for the development of molecular machinery.[7] There are three types of interlocked architecture:

A catenane from the Latin word " Catena" meaning chain can be thought of as two or more macrocycles that are mechanically interlocked together and cannot be separated without cleavage of a covalent bond (Figure 1.1).

**Figure 1.1.** A cartoon representation of a [2]catenane

A rotaxane, from the Latin "Rota" meaning wheel, and "Axis" meaning axle, is structurally one or more macrocycles mechanically locked around a "thread"

molecule that has two sterically bulky stoppers to constrain the macrocycle about its axis. In the absence of such stoppers the host-guest complex is named a *pseudo*-rotaxane (Figure 1.2).

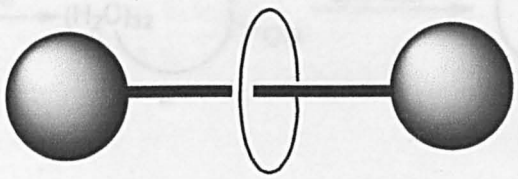

**Figure 1.2.** A cartoon representation of a [2]rotaxane

Molecular knots are arguably the most synthetically challenging, and hence most rare, of the interlocked topologically complex structures. The simplest of this type of structure is the trefoil knot (Figure 1.3).

**Figure 1.3.** A cartoon representation of a trefoil knot

As has already been stated it is possible to have more than two interlocked components. The number of components in an interlocked architecture is given a prefix e.g. a [3]rotaxane comprises a thread and two macrocycles.

## 1.3. Early Synthesis of Interlocked Architectures

The first synthesis of a catenane reported in 1960 by Wasserman[8] involved the synthesis of a hydrocarbon macrocycle **3** using acyloin ring closure of **1** to give macrocycle **2** followed by zinc reduction. Exploiting the statistical *"threading"* of **1** through **3** followed by a second acyloin ring closure resulted in small quantities of the catenane **4**. Oxidation of a mixture containing the acyloin fraction resulted in

addition to the acid **5**, the formation of small quantities of **3** proving the compound had been successfully synthesised (Scheme 1.1).

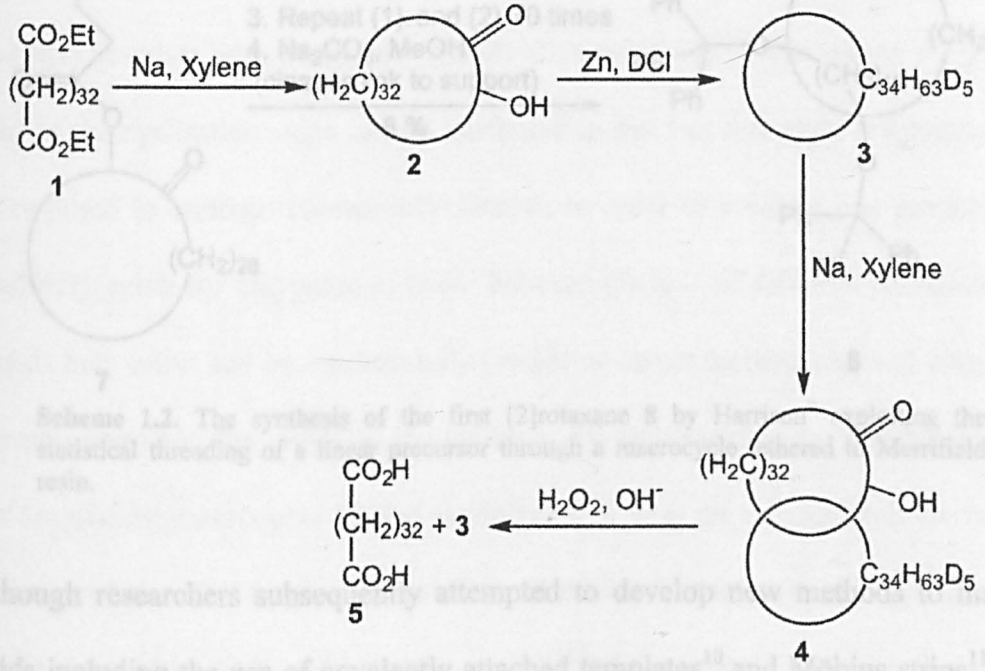


**Scheme 1.1.** The first synthesis of a [2]catenane **4** by Wasserman[8] exploiting the statistical *threading* of a linear chain through a macrocycle.

The first rotaxane synthesis reported seven years later by Harrison and Harrison[9] used similar methodology. The synthesis relied on the statistical *threading* of a reactive diol **6** through a pre-formed macrocycle tethered to a Merrifield resin **7**, followed by reaction of the diol **6** with bulky stopper groups (*via* $S_N1$ substitution). When the link to the support was cleaved a [2]rotaxane **7** was obtained because the macrocycle was prevented from falling off the linear component by the bulky stoppers (Scheme 1.2). The problem of low yield was highlighted by the fact that the threading and *"capping"* reaction was repeated 70 times to give only 6% of the rotaxane **8**.

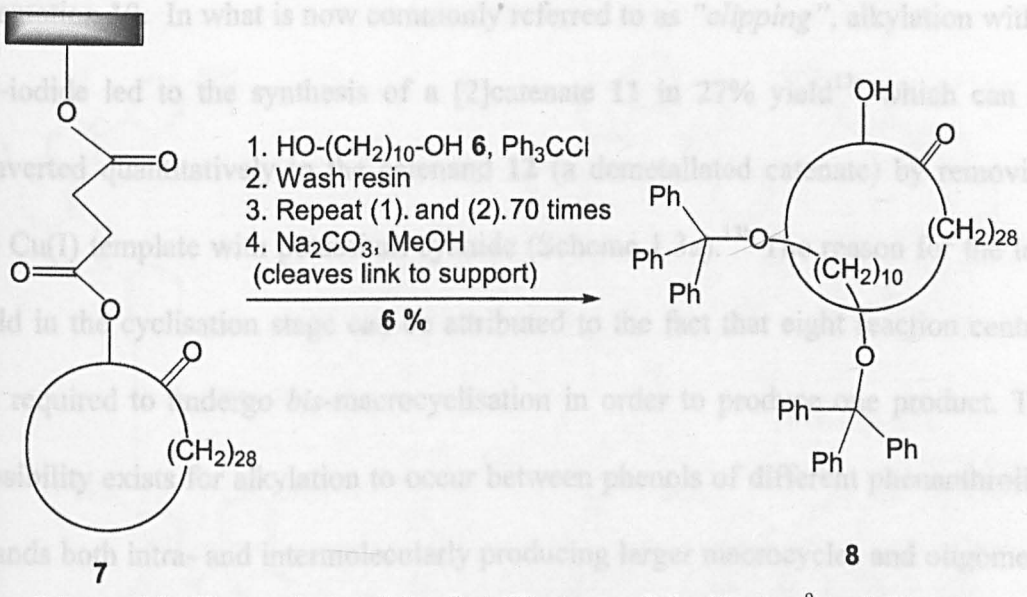


**Scheme 1.2.** The synthesis of the first [2]rotaxane **8** by Harrison[9] exploiting the statistical threading of a linear precursor through a macrocycle tethered to Merrifield resin.

Although researchers subsequently attempted to develop new methods to improve yields including the use of covalently attached templates[10] and Möbius strips[11] there was little improvement. Indeed, until the early 80's, the only noticeable improvement in yields was observed by Zilkha *et al.*[12] who returned to the formation of catenane synthesis *via* statistical methods. Realising that the conditions favouring *threading* through a macrocyclic ring (high concentration) were in opposition to the conditions favouring macrocyclisation (low concentration) they synthesised first a rotaxane *via* threading at high concentration and then converted it to a catenane *via* cyclisation at low concentration.

## 1.4. Template Directed Synthesis of Interlocked Architectures

### 1.4.1. The Synthesis of Interlocked Architectures Using a Metal Template

In 1984 Sauvage turned interlocked architectures from chemical curiosities into molecules of real scientific interest using template-directed synthesis.[13] He employed the preferred tetrahedral geometry of Cu(I) to quantitatively organise two appropriately derivatised phenanthroline ligands **9** in a fixed, mutually-orthogonal

orientation **10**. In what is now commonly referred to as *"clipping"*, alkylation with a *bis*-iodide led to the synthesis of a [2]catenate **11** in 27% yield[13c] which can be converted quantitatively to the catenand **12** (a demetallated catenate) by removing the Cu(I) template with potassium cyanide (Scheme 1.3a).[13b] The reason for the low yield in the cyclisation stage can be attributed to the fact that eight reaction centres are required to undergo *bis*-macrocyclisation in order to produce one product. The possibility exists for alkylation to occur between phenols of different phenanthroline ligands both intra- and intermolecularly producing larger macrocycles and oligomers. Sauvage improved the yields of the catenane forming reaction by first synthesising one component macrocycle **13** and complexing it with an appropriately derivatised phenanthroline unit **9** to give pre-catenate **14** which then underwent *clipping* to give the catenane **11** in 40 % yield (Scheme 1.3b).[13a] Unfortunately, the overall yield was poorer due to the difficulties encountered synthesising the macrocycle **13**.

The catenands themselves have been shown to stabilise the ordinarily disfavoured tetrahedral geometries of Ni(I) and Cu(0)[14] whilst the catenates derived from Cu(I) are believed to be amongst the most stable complexes that exist with neutral ligands.[15] In addition different ring closure techniques such as the use of acetylinic coupling extended the architectures available to [n]catenates (n = 2-8).[16]

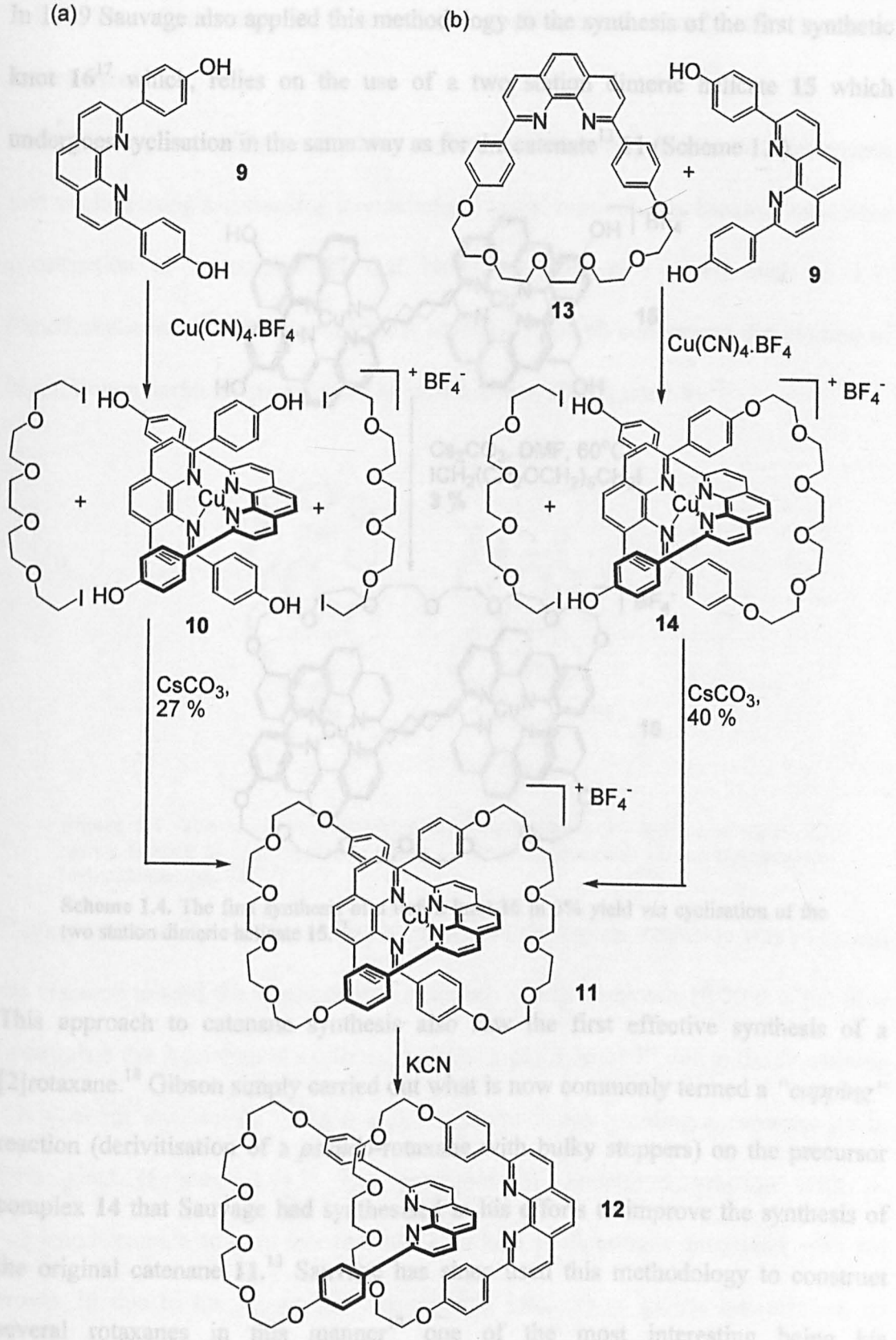


**Scheme 1.3.** The synthesis of a [2]catenante **11** and its corresponding [2]catenand **12** using a metal template (a) a double *clipping* strategy, (b) a single *clipping* strategy.[13]

In 1989 Sauvage also applied this methodology to the synthesis of the first synthetic knot **16**[17] which, relies on the use of a two station dimeric helicate **15** which undergoes cyclisation in the same way as for the catenate[13] **11** (Scheme 1.4).

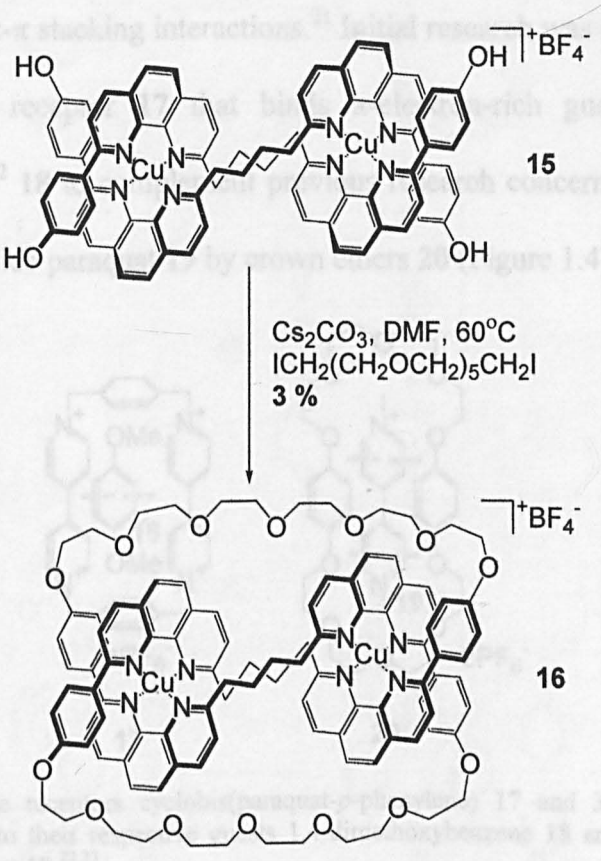


**Scheme 1.4.** The first synthesis of a trefoil knot **16** in 3% yield *via* cyclisation of the two station dimeric helicate **15**.[17]

This approach to catenane synthesis also saw the first effective synthesis of a [2]rotaxane.[18] Gibson simply carried out what is now commonly termed a *"capping"* reaction (derivitisation of a *pseudo*-rotaxane with bulky stoppers) on the precursor complex **14** that Sauvage had synthesised in his efforts to improve the synthesis of the original catenane **11**.[13] Sauvage has since used this methodology to construct several rotaxanes in this manner[19] one of the most interesting being his electrochemically controllable switch.[20]

### 1.4.2. The Synthesis of Interlocked Architectures Using π-π Stacking Interactions

In 1988, the group of Fraser Stoddart reported the discovery of a route to catenanes that worked using π-π stacking interactions.[21] Initial research was focused toward the construction of a receptor **17** that binds π-electron-rich guests such as 1,4-dimethoxybenzene[22] **18** to complement previous research concerning the binding of bipyridinium herbicide paraquat **19** by crown ethers **20** (Figure 1.4).[23]

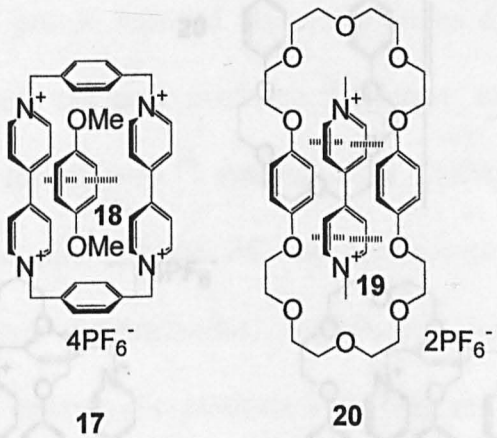


**Figure 1.4.** The receptors cyclobis(paraquat-*p*-phenylene) **17** and 34-crown-10 **20** shown binding to their respective guests 1,4-dimethoxybenzene **18** and bipyridinium herbicide paraquat **19**.[22,23]

Having successfully constructed such a receptor, the logical extension was to extend the research toward the synthesis of a catenane. Using 34-crown-10 **20** it is possible to template the formation of cyclobis(paraquat-*p*-phenylene) **17** due to the favourable π-π stacking interactions using a *clipping* methodology yielding a catenane **24** in 70% yield (Scheme 1.5).[21] The precursor **21** undergoes reaction with *p*-xylylenedibromide to give intermediate **22** which preferentially associates with the crown **20** due to the favourable π-π stacking interactions giving intermediate **23** which then rapidly undergoes cyclisation giving catenane **24**.

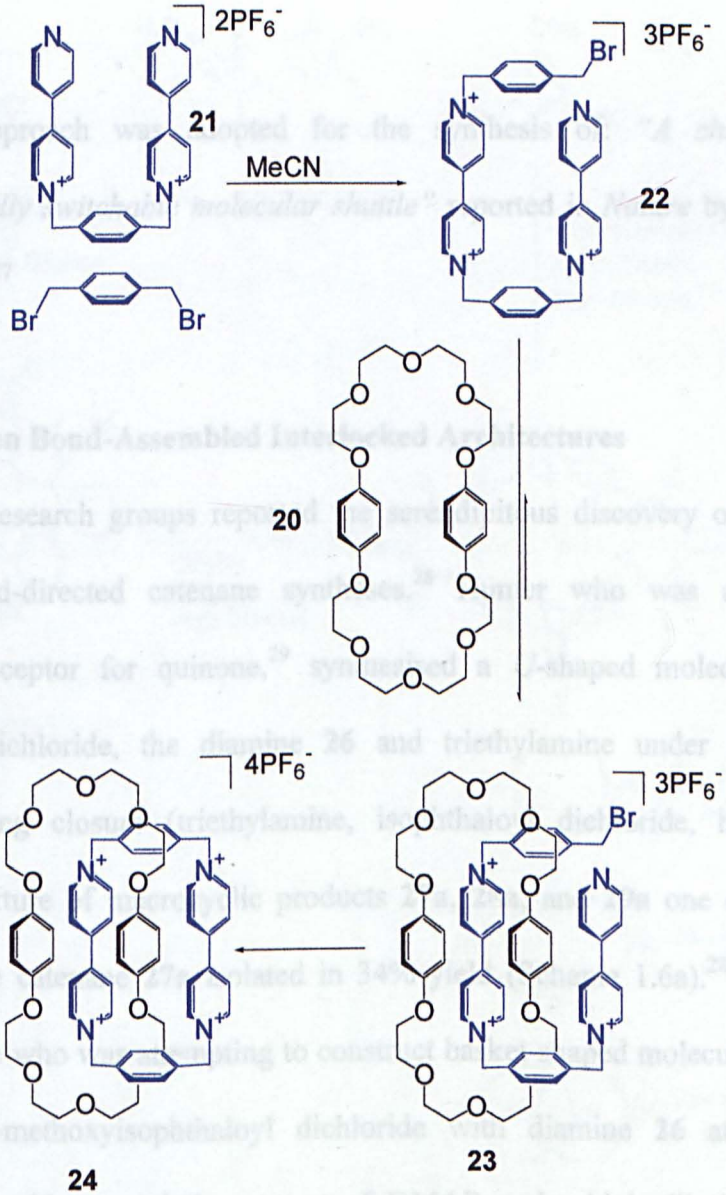


**Scheme 1.5.** The synthesis of a [2]catenane **24** using π-π stacking interactions to direct the formation of one macrocycle around another.[21]

This approach has since been adapted to allow the synthesis of rotaxanes by one of three general methods:

Threading of an appropriately functionalised bipyridinium residue through a crown ether followed by *capping*.[24]

Threading an appropriately derivatised electron rich aromatic through cyclobis(paraquat-*p*-phenylene) **17** followed by *capping*.[25]

Formation of cyclobis(paraquat-*p*-phenylene) around an electron rich thread *via clipping*.[26]

This latter approach was adopted for the synthesis of: *"A chemically and electrochemically switchable molecular shuttle"* reported in *Nature* by the Stoddart group in 1994.[27]

### 1.4.3. Hydrogen Bond-Assembled Interlocked Architectures

In 1992 two research groups reported the serendipitous discovery of two similar hydrogen bond-directed catenane syntheses.[28] Hunter who was attempting to construct a receptor for quinone,[29] synthesised a *U*-shaped molecule **25** from isophthaloyl dichloride, the diamine **26** and triethylamine under high dilution conditions. Ring closure (triethylamine, isophthaloyl dichloride, high dilution) afforded a mixture of macrocyclic products **27a**, **28a**, and **29a** one of which was reported as the catenane **27a** isolated in 34% yield (Scheme 1.6a).[28a] In a similar manner, Vögtle who was attempting to construct basket-shaped molecules found that reaction of 5-methoxyisophthaloyl dichloride with diamine **26** at 50-60°C in chlorobenzene with a catalytic amount of DMAP under high dilution conditions resulted in the formation of several macrocycles (Scheme 1.6b). These included the simple [2+2] tetralactam macrocycle **28b** (12.4 %), the [4+4] macrocyle **29b** (10 %) and an isomer identified as the catenane **27b** (8.4 %).[28b]

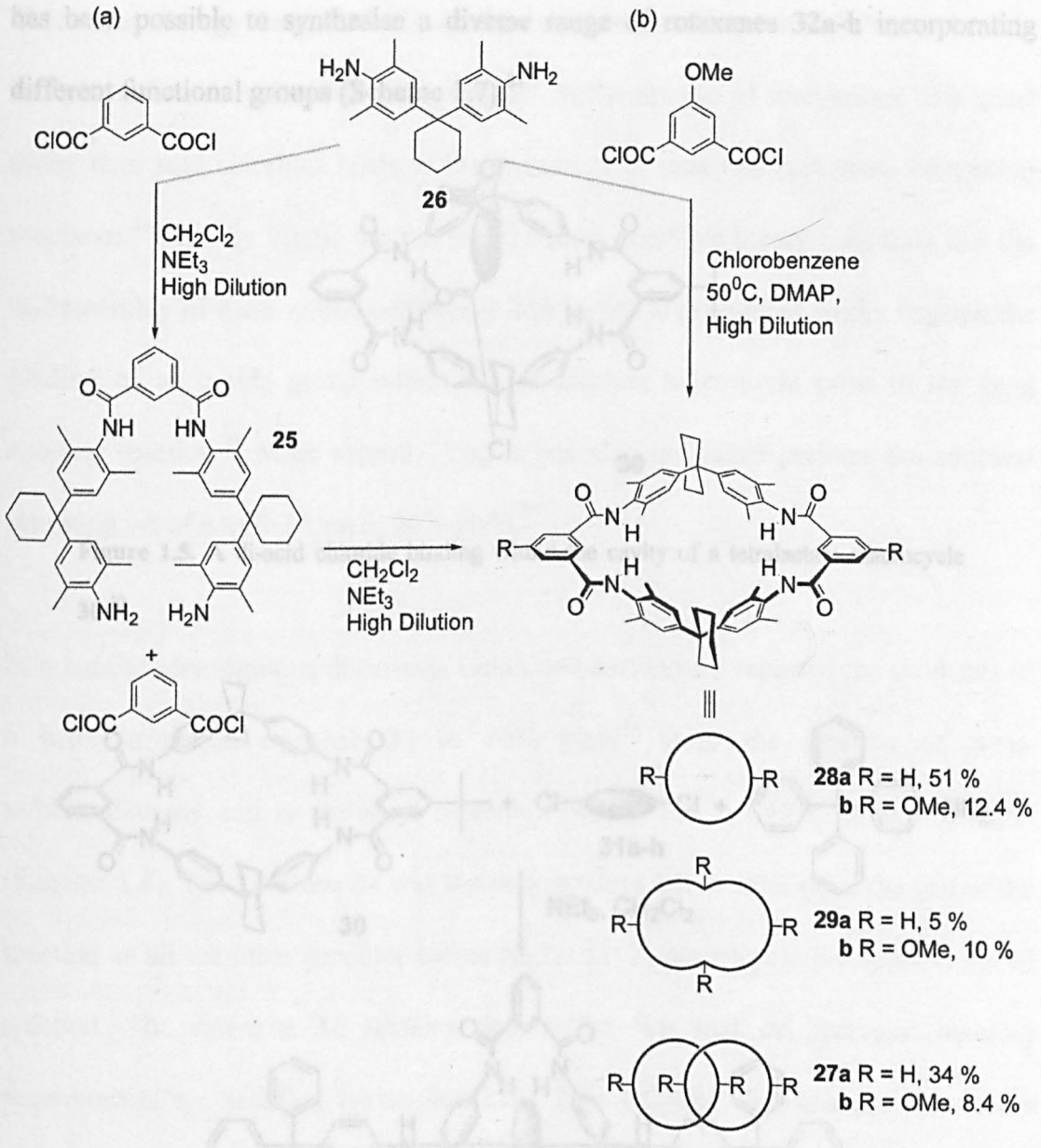


**Scheme 1.6.** The hydrogen bond-directed synthesis of catenane **27a,b** *via* (a) a two-step procedure (b) a one-pot procedure.[28]

Vögtle has since used a [2+2] macrocycle **30** similar to the component macrocycle **28b** of his catenane **27b** to construct hydrogen bond-assembled rotaxanes **32a-h** using a *threading* followed by *capping* methodology (Scheme 1.7). He initially proposed (incorrectly) that the catenane synthesis arose as a result of acid chlorides binding through hydrogen bonding within a tetralactam macrocycle (Figure 1.5).[30] Extending this by using different acid chlorides **31a-h** that undergo amide bond-forming *capping* reactions with the bulky tritylaniline group (acting as a stopper) it

has been possible to synthesise a diverse range of rotaxanes **32a-h** incorporating different functional groups (Scheme 1.7).[31]

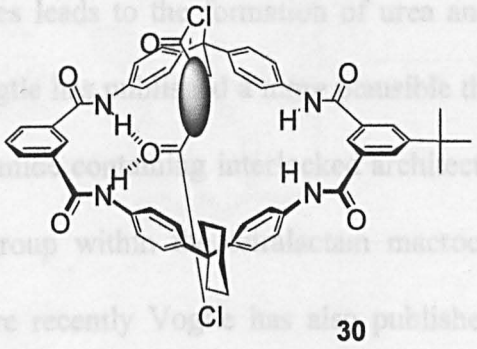

**30**

**Figure 1.5.** A di-acid chloride binding within the cavity of a tetralactam macrocycle **30**.[30]

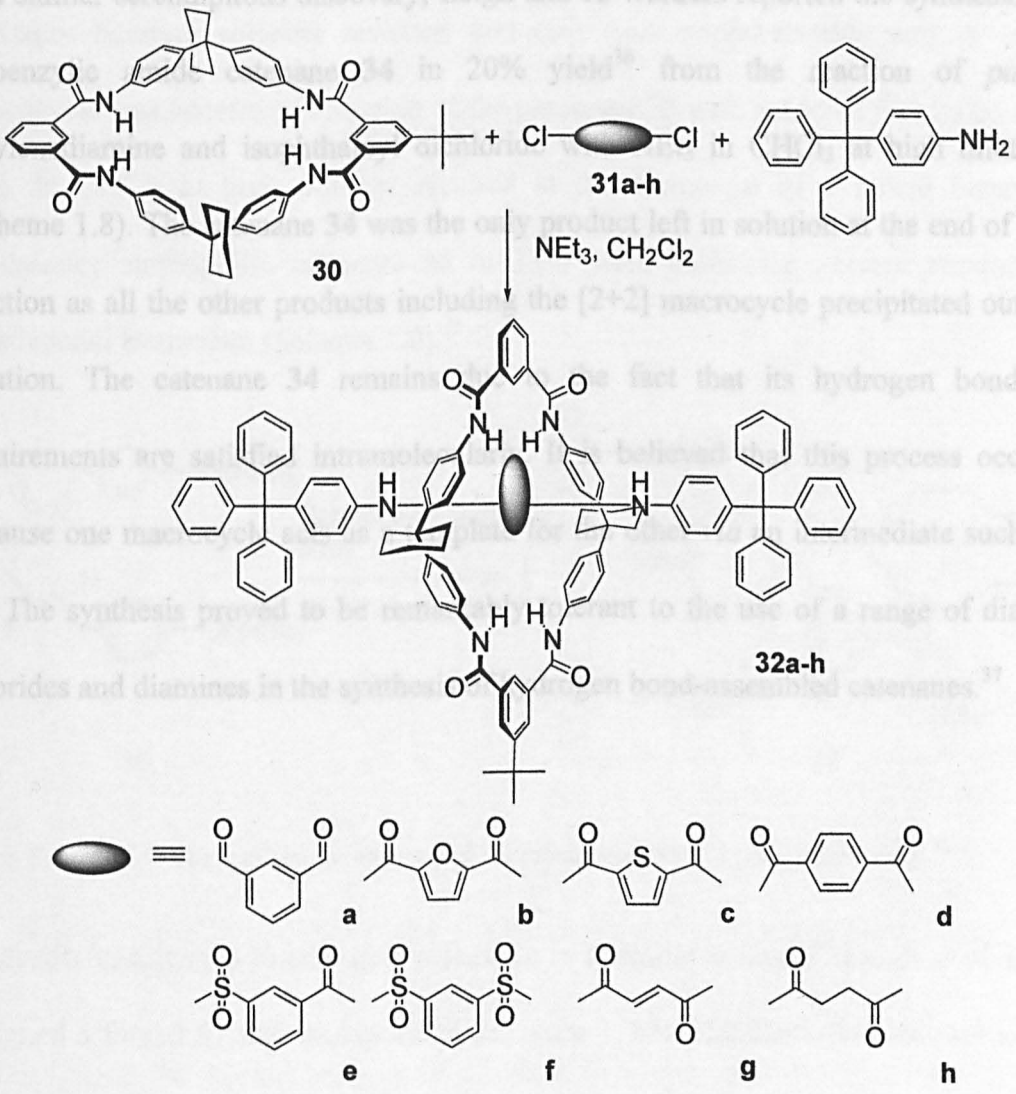


**Scheme 1.7.** The synthesis of hydrogen bond assembled rotaxanes **32a-h** using tetralactam macrocycle **30**.[31]

This same strategy has also been used to synthesise rotaxanes with benzophenone and cinnamic acid units within the thread[32] whilst the use of isocyanates as a guest rather than acid chlorides leads to the formation of urea and carbamate containing rotaxanes.[33] Latterly Vogtle has published a more plausible theory indicating that the self-assembly of these amide containing interlocked architectures works through the binding of an amide group within the tetralactam macrocycle prior to the final *capping* reaction.[34] More recently Vogtle has also published perhaps the simplest synthesis yet of a trefoil knot in 20% yield.[35]

In a similar serendipitous discovery, Leigh and co-workers reported the synthesis of a benzylic amide catenane **34** in 20% yield[36] from the reaction of *para*-xylylenediamine and isophthaloyl dichloride with $NEt_3$ in $CHCl_3$ at high dilution (Scheme 1.8). The catenane **34** was the only product left in solution at the end of the reaction as all the other products including the [2+2] macrocycle precipitated out of solution. The catenane **34** remains due to the fact that its hydrogen bonding requirements are satisfied intramolecularly. It is believed that this process occurs because one macrocycle acts as a template for the other *via* an intermediate such as **33**. The synthesis proved to be remarkably tolerant to the use of a range of diacid chlorides and diamines in the synthesis of hydrogen bond-assembled catenanes.[37]

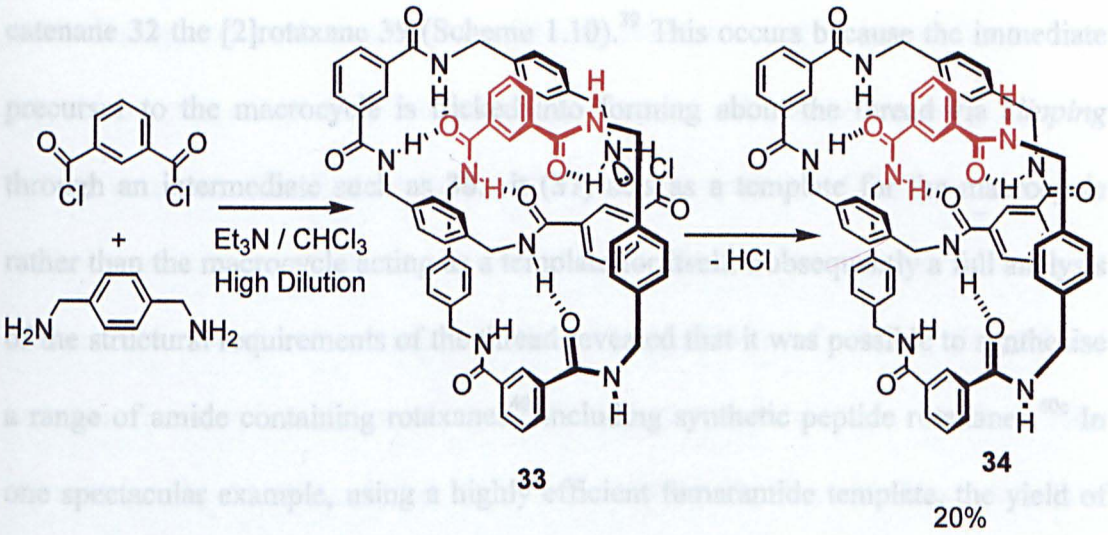


**Scheme 1.8.** The synthesis of [2]catenane **34** from *p*-xylylenediamine and isophthaloyl dichloride.[36]

Subsequently attempts to make the macrocyclic components more soluble in non-hydrogen bonding solvents revealed that only one isophthalamide unit in each macrocycle was necessary. Reaction of the precursor **35** with sebacoyl dichloride and $NEt_3$ in $CHCl_3$ at high dilution resulted in the formation of a mixed benzylic amide/ester amphiphilic catenane **36** in 18% yield exhibiting solvent dependent translational isomerism (Scheme 1.9).[38]

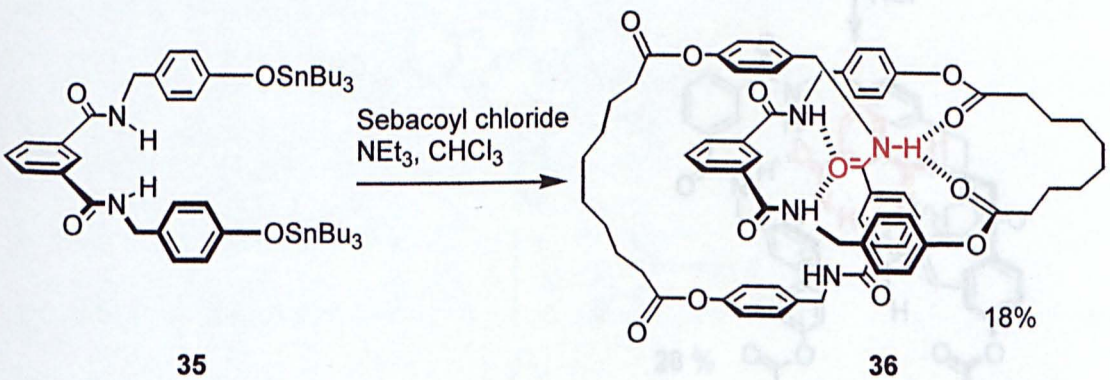


**Scheme 1.9.** The synthesis of an amphiphilic [2]catenane **36** from the precursor **35**.[38]

In successful attempts to assemble rotaxanes in a similar manner,[39] Leigh *et al.* later designed a thread **37** that incorporated the same 1,3-isophthaloyl diamide unit to be found in the component macrocycles of the original catenane **34**. In the presence of the thread **37** carrying out the original catenane synthesis[36] affords in addition to the

catenane **32** the [2]rotaxane **39** (Scheme 1.10).[39] This occurs because the immediate precursor to the macrocycle is tricked into forming about the thread via *clipping* through an intermediate such as **38**:- it (**37**) acts as a template for the macrocycle rather than the macrocycle acting as a template for itself. Subsequently a full analysis of the structural requirements of the thread revealed that it was possible to synthesise a range of amide containing rotaxanes[40] including synthetic peptide rotaxanes.[40c] In one spectacular example, using a highly efficient fumaramide template, the yield of rotaxane was almost quantitative.[40a]

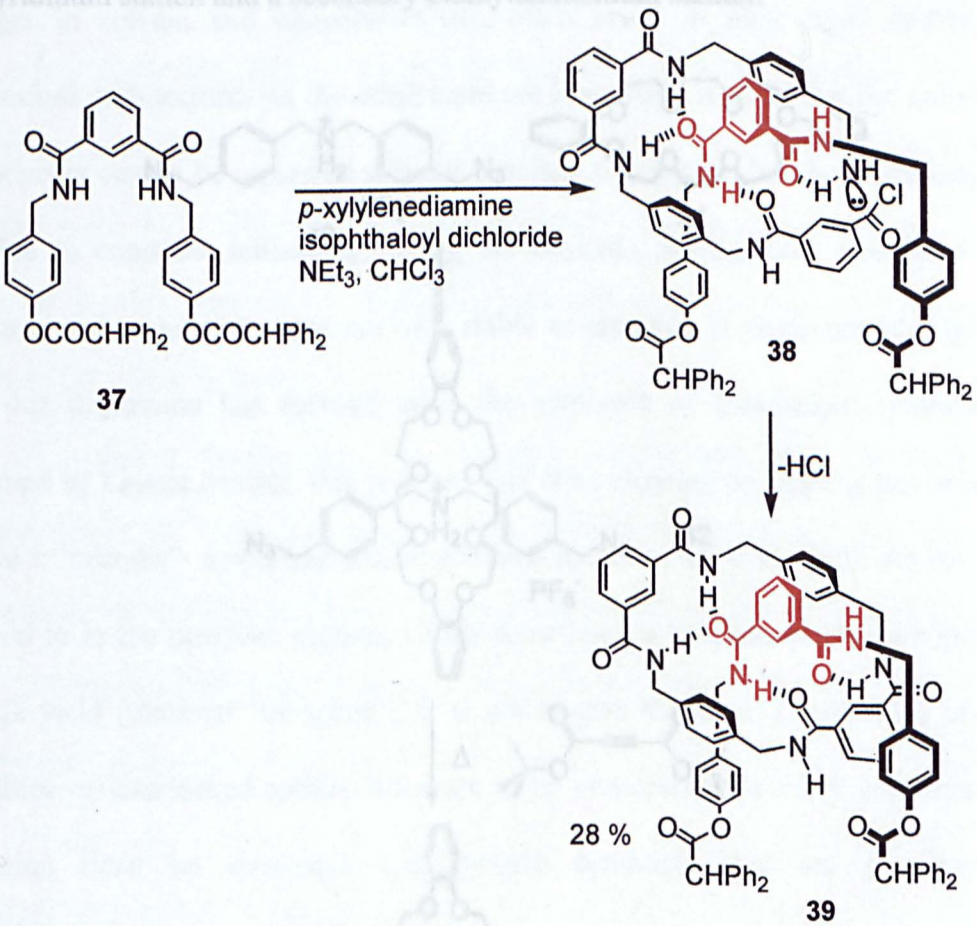


**Scheme 1.10.** The synthesis of the [2]rotaxane **39** in 28% from the thread **37**, *p*-xylylenediamine and isophthaloyl dichloride.[39]

Crown ethers have also been used to form rotaxanes by hydrogen bonding to secondary dialkylammonium salts.[41] Stoddart has adapted his use of bipyridinium binding by crown ethers[23] using instead secondary dialkylammonium salts as the

guest. Using crown ethers containing 24 ring atoms or more, it is possible to form *pseudo*-rotaxane complexes (Scheme 1.11),[42] that can subsequently undergo *capping* to form rotaxanes. The first rotaxane of this kind was synthesised thus: the secondary dialkyl ammonium salt **40** was dissolved in dichloromethane in the presence of dibenzo-24-crown-8 **41** giving complex **42**. Addition of excess di-tert-butyl acetylenedicarboxylate followed by refluxing for several days resulted after chromatography in the isolation of rotaxane **43** in 31 % yield. Since this time Stoddart has used this methodology to construct a pH driven switch comprising both a bipyridinium station and a secondary dialkylammonium station.[43]

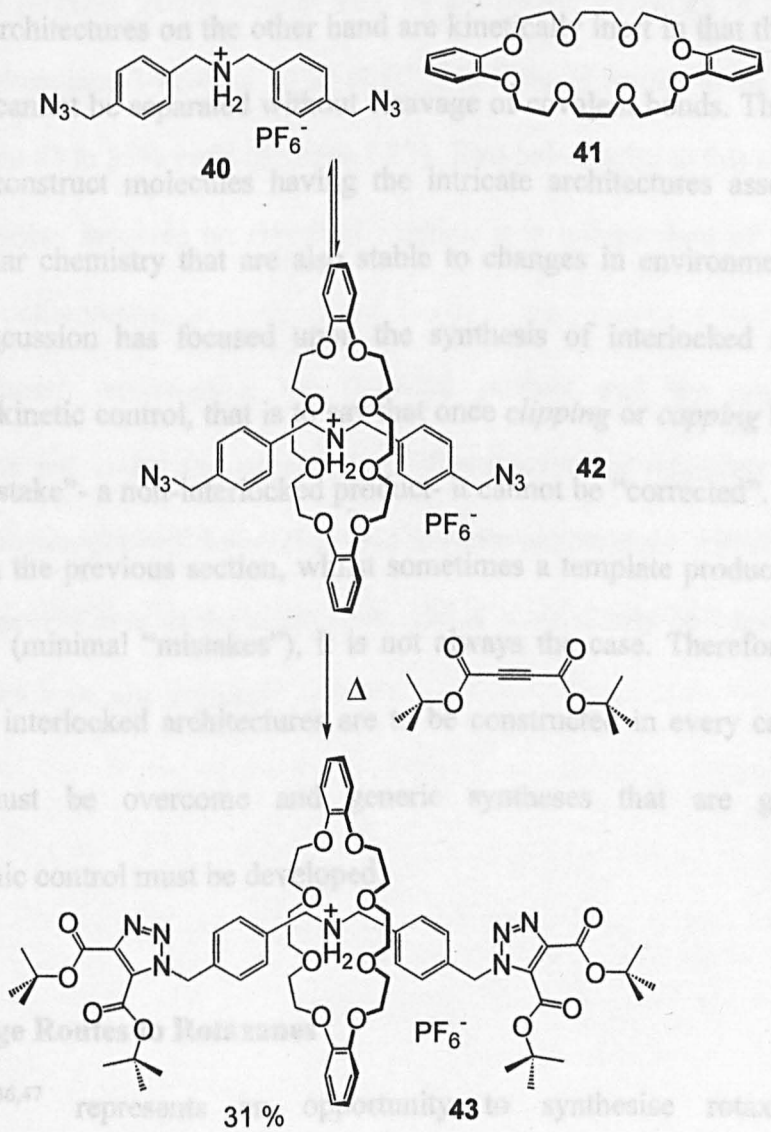


**Scheme 1.11.** The synthesis of the rotaxane **43** *via pseudo*-rotaxane **42** exploiting the binding of secondary dialkyl ammonium salts by crown ethers.[41]

## 1.5 Thermodynamically Controlled Synthesis of Interlocked Architectures

One of the features of self-assembled systems is that they are often constructed under thermodynamic control,[44] i.e. their syntheses are 'error-checking' and as a result well ordered arrays of molecules which function together for some overall purpose can be constructed. Unfortunately the use of weak reversible interactions that allow assembly with a high degree of structural integrity also make structures of this type fragile. Disruption of the equilibrium under which such structures are formed by changes in solvent and temperature etc. often result in their rapid destruction. Interlocked architectures on the other hand are kinetically inert in that the individual components cannot be separated without cleavage of covalent bonds. Therefore, it is possible to construct molecules having the intricate architectures associated with supramolecular chemistry that are also stable to changes in environment. Up until now this discussion has focused upon the synthesis of interlocked architectures governed by kinetic control, that is to say that once *clipping* or *capping* has occurred to give a "mistake"- a non-interlocked product- it cannot be "corrected". As has been referred to in the previous section, whilst sometimes a template produces rotaxanes in high yield (minimal "mistakes"), it is not always the case. Therefore if useable quantities of interlocked architectures are to be constructed in every case then this limitation must be overcome and generic syntheses that are governed by thermodynamic control must be developed.

### 1.5.1. Slippage Routes to Rotaxanes

"Slippage"[45,46,47] represents an opportunity to synthesise rotaxanes under thermodynamic control. This technique relies on the small increase in cavity size that occurs to a macrocycle when it is heated which allows it to slip onto a dumbbell

shaped thread whose stoppers have been judiciously chosen to allow such a process. The macrocycle then prefers to spend most of its time on the thread due to the thermodynamic stabilisation provided by the non-covalent interactions. Cooling results in the macrocycle becoming trapped upon the thread. Although several early papers have appeared utilising this approach,[45] only two groups have exploited it with any real success.[46,47]

Firstly the group of Fraser Stoddart have produced several papers[46] on the subject of slippage employing both aromatic π-π stacking interactions and the binding of secondary dialkylammonium salts by crown ethers. As an example, the first reported synthesis of a rotaxane in this manner shall be discussed.[46g] Heating of the thread **44** and *bis*-paraphenylene-34-crown-10 **20** at 60°C in $CH_3CN$ results in the synthesis of the [2]rotaxane **45** in 52% yield (Scheme 1.12). Two points arise at this stage:

As the process involves no chemical reaction it is independent of functionality within the components.

At the chosen temperature, the threaded product and the non-interlocked components are under the conditions of thermodynamic equilibrium; the non-covalent interactions will be weaker than at room temperature. Although the yield of 52% reported here seems reasonable, yields could surely be improved if high temperatures were not required.

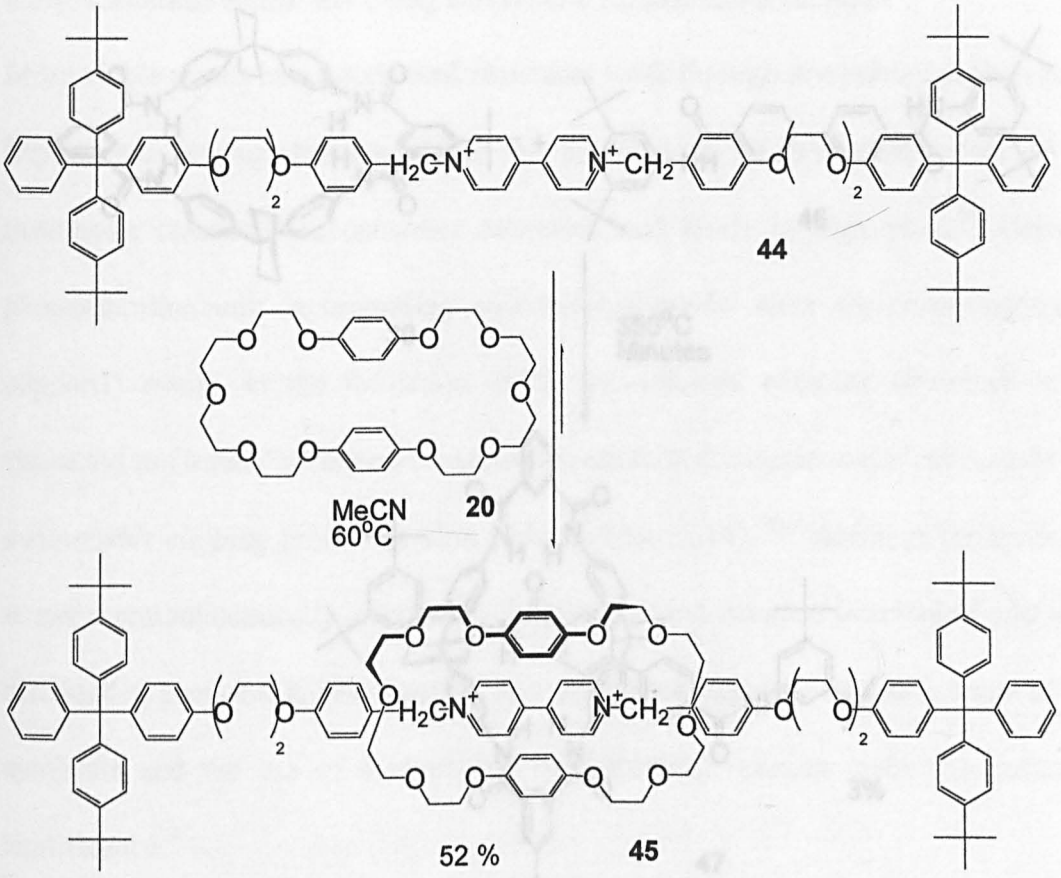


**Scheme 1.12.** The synthesis *via* slippage of rotaxane **45** from the component thread **44** and crown ether **20**.[46g]

The second group to make use of this methodology provide perhaps the best illustration of why slippage is a poor approach to the synthesis of interlocked architectures.[47] Fritz Vögtle *et al.* describe a slippage synthesis using the tetralactam macrocycle **30** (used to construct rotaxanes) which when heated to 350°C with various threads such as **46** in the melt can form small quantities of threaded species such as **47** in 3 % yield, (Scheme 1.13).[47b]

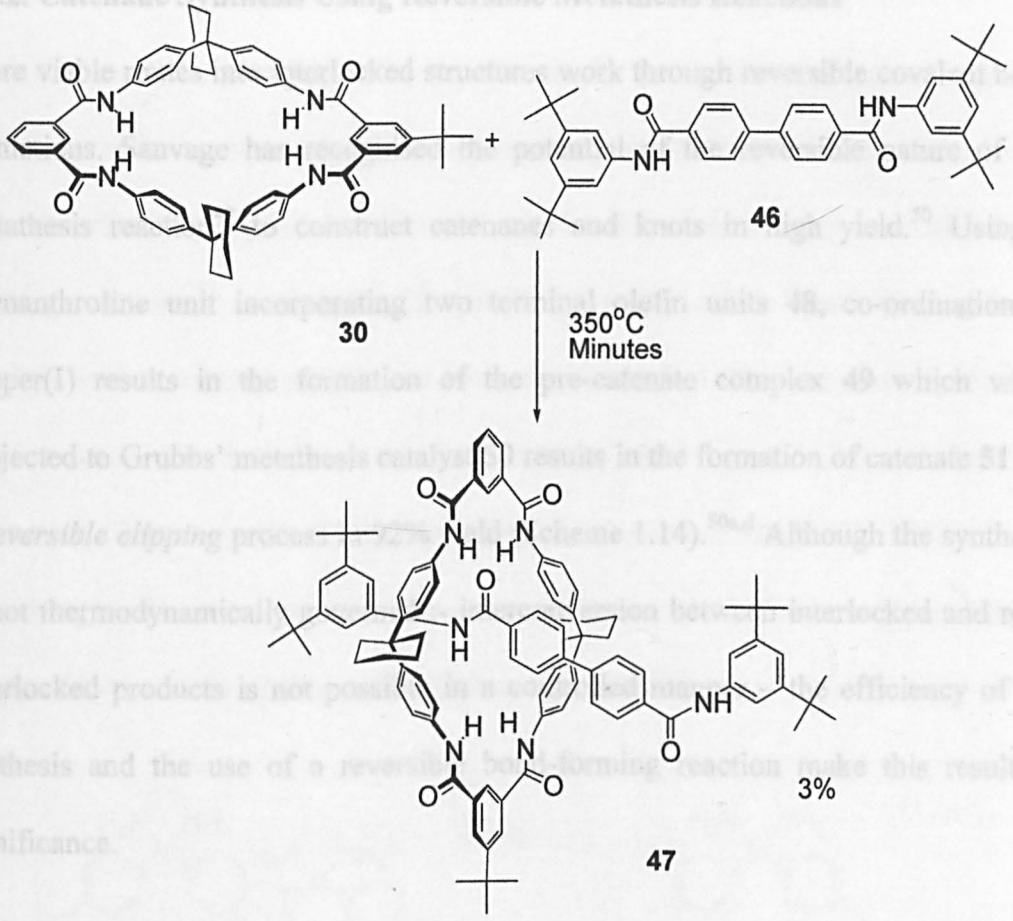


**Scheme 1.13.** The slippage synthesis of a hydrogen bond-assembled [2]rotaxane **47** by simple melting of the thread **46** and macrocycle **30** components.[47]

The problem of low yield highlights how high temperatures decrease the effects of non-covalent interactions, indeed, several of the threads described in the second paper[47a] contain no hydrogen bonding functionality suggesting the process may work under statistical conditions. Two other points arise form these results:

At these sorts of temperatures certain covalent bonds can break suggesting that the process may be working in a non-slippage manner: - possibly the anionic route which Vögtle has described.[48]

These rotaxanes undergo de-slippage indicating that rotaxanes synthesised in this way are not thermodynamically stable.

### 1.5.2. Catenane Synthesis Using Reversible Metathesis Reactions

More viable routes into interlocked structures work through reversible covalent bond formations. Sauvage has recognised the potential of the reversible nature of the metathesis reaction[49] to construct catenanes and knots in high yield.[50] Using a phenanthroline unit incorporating two terminal olefin units **48**, co-ordination to copper(I) results in the formation of the pre-catenate complex **49** which when subjected to Grubbs' metathesis catalyst **50** results in the formation of catenate **51** *via* a *reversible clipping* process in 92% yield (Scheme 1.14).[50a,d] Although the synthesis is not thermodynamically governed :- interconversion between interlocked and non-interlocked products is not possible in a controlled manner – the efficiency of the synthesis and the use of a reversible bond-forming reaction make this result of significance.

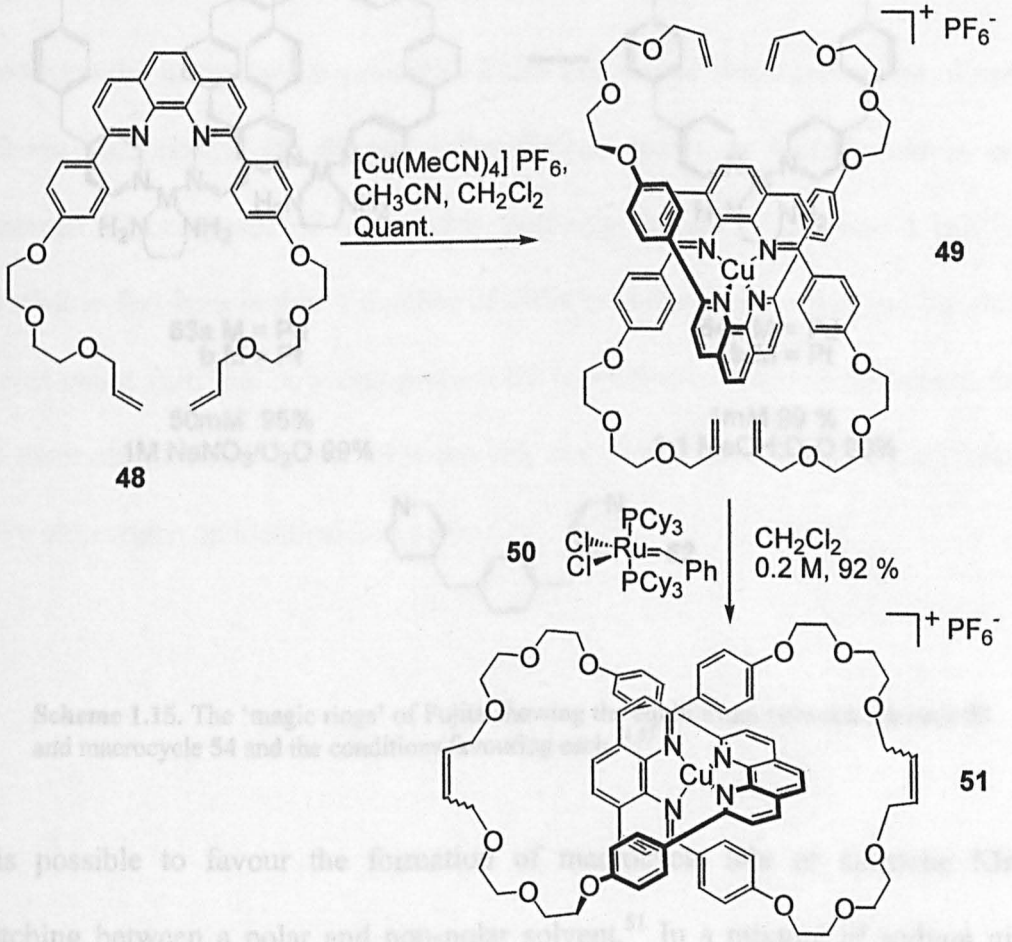


**Scheme 1.14.** Synthesis of a [2]catenante **51** in 92 % yield *via* the olefin metathesis of complex **49**.[50]

### 1.5.3. Catenane Synthesis Employing Kinetically Labile Co-ordinative Bonds

A more correct example of a thermodynamically controlled catenate synthesis has been described by Fujita who demonstrates the potential of using reversible bond forming reactions.[51] A mixture of $Pd(en)(NO_3)_2$ and pyridine ligand **52** in solution are involved in a rapid equilibrium between interlocked **53a** and macrocyclic **54a** species where the individual components are linked by palladium-pyridine co-ordination (Scheme 1.15). These co-ordinated species are kinetically labile and so interchanging between catenane **53a** and macrocycle **54a** is facile, a process Fujita proposes to occur *via* a Möbius strip type mechanism.[52]

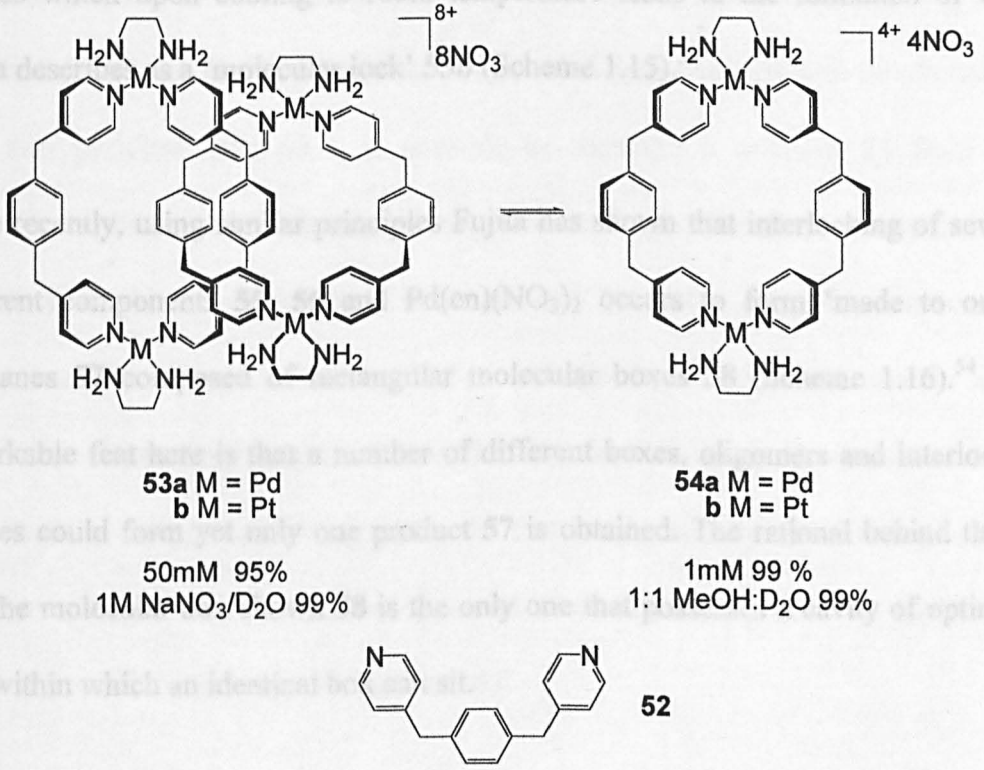


**Scheme 1.15.** The 'magic rings' of Fujita showing the equilibrium between catenane **53** and macrocycle **54** and the conditions favouring each.[51,53]

It is possible to favour the formation of macrocycle **54a** or catenane **53a** by switching between a polar and non-polar solvent,[51] In a mixture of sodium nitrate and water, the hydrophobic pyridine ligands want to shield themselves as much as

possible from the polar environment and so the two macrocycles reach a stage of equilibrium where this unwanted interaction is minimised by interlocking and shielding themselves as much as possible from the solvent to give 99% catenane **53a**. In methanol/water mixtures the hydrophobic pyridine ligands associate preferentially with the solvent to give macrocycles in 99 % yield **54a**. The same effect can also occur with changes in concentration. At 1mM, the species exist almost exclusively as the component macrocycles **54a** whereas at 50mM the equilibrium lies almost completely in favour of catenane **53a**. It is also possible to lock the equilibrium by using much less labile platinum complexes.[53] Heating the component macrocycle **54b** in highly polar media (sodium nitrate) leads to the formation of interlocked species which upon cooling to room temperature leads to the formation of what Fujita describes as a 'molecular lock' **53b** (Scheme 1.15).[53]

More recently, using similar principles Fujita has shown that interlocking of several different components **55**, **56** and $Pd(en)(NO_3)_2$ occurs to form 'made to order' catenanes **57** composed of rectangular molecular boxes **58** (Scheme 1.16).[54] The remarkable feat here is that a number of different boxes, oligomers and interlocked species could form yet only one product **57** is obtained. The rational behind this is that the molecular box shown **58** is the only one that possesses a cavity of optimum size within which an identical box can sit.

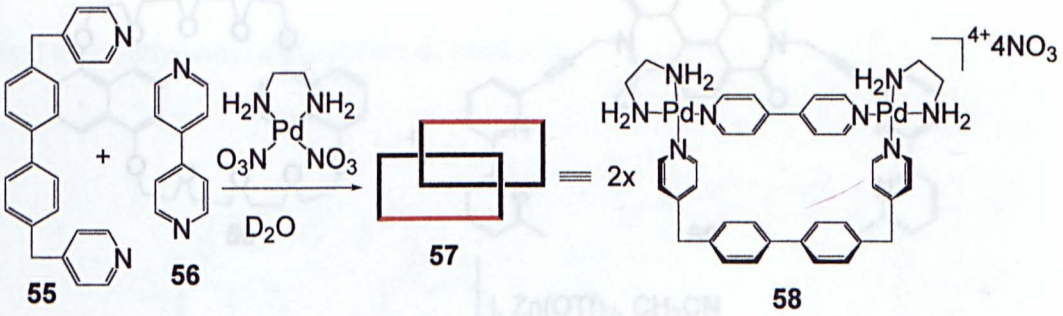


**Scheme 1.16.** The synthesis of 'made to order' catenanes **57** composed of molecular boxes **58**.[54]

In a similar manner to Fujita, Sanders *et al.* describe the synthesis of a catenane employing kinetically labile co-ordination to zinc[55], adapted from his previously reported synthesis of neutral catenanes using π-π stacking interactions.[56] Using a *bis*-naphthyl containing crown **59** and an electron deficient aromatic unit functionalised with two pyridine units **60** it is possible to construct a catenane **61** from five components under reversible conditions (Scheme 1.17). The linear component **60** threads through the crown and becomes stabilised due to π-donor/π-acceptor interactions. The linear component **60** then undergoes cyclisation with another linear component **60** *via* the formation of two zinc-bipyridyl moieties. As zinc forms labile co-ordination complexes the process is thermodynamically driven and so the metallomacrocycle component can open and close indefinitely until the most stable entity is formed: in this case the catenane **61**.

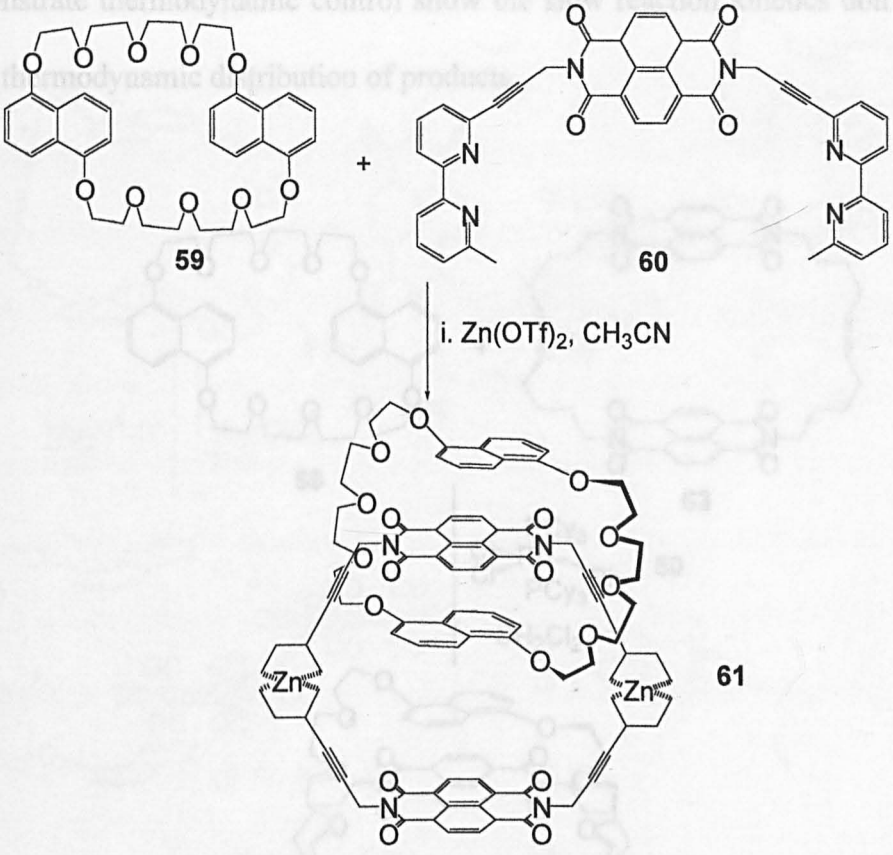


**Scheme 1.17.** The synthesis of a [2]catenane **61** under thermodynamic control comprising a crown **59** and a metallomacrocycle that can ring open/ring close easily because of kinetically labile co-ordinative zinc bonds.[56]

### 1.5.4. Synthesis of Wholly Organic Catenanes Under Thermodynamic Control

Sanders has subsequently recognised that such an approach whilst effective can suffer from the kinetic instability of the final product and that wholly organic systems represent a more attractive option. Whilst Fujita constructs a kinetically stable species under thermodynamic control employing his molecular lock,[53] Sanders has employed olefin metathesis[49] in a wholly organic system.[57] Exchanging the bipyridine ligands of **56** for olefins it is possible to synthesise catenanes **62** in up to 50% yield exposing the macrocycle **63** and crown **59** to Grubbs metathesis catalyst **50**[49d] in $CH_2Cl_2$ (Scheme 1.18). Unfortunately this yield doesn't really improve on current techniques and by Sanders' own admission control experiments to

demonstrate thermodynamic control show the slow reaction kinetics don't yield the ideal thermodynamic distribution of products.

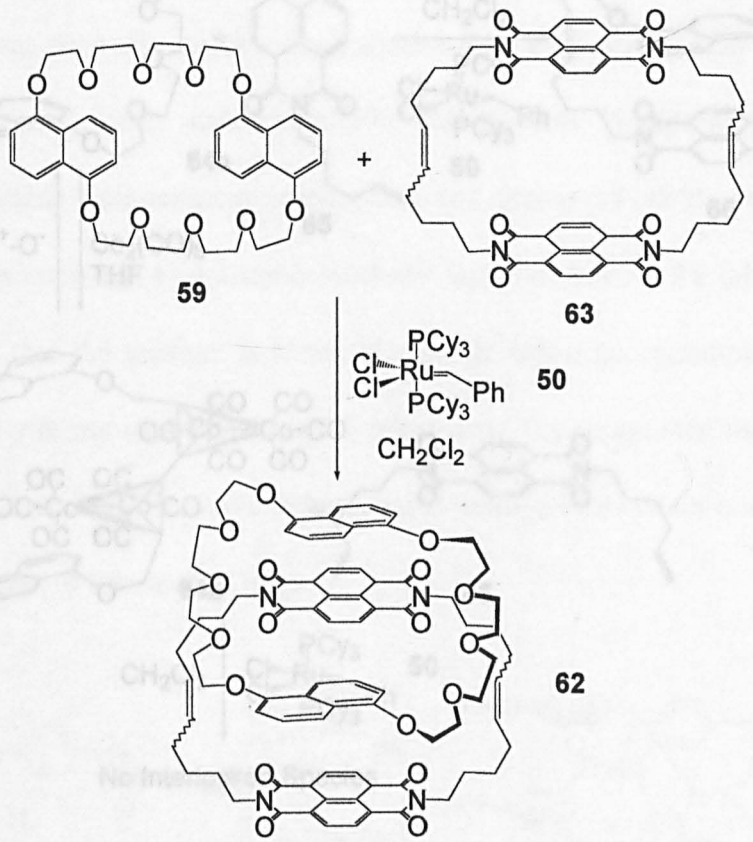


**Scheme 1.18.** The synthesis of a [2]catenane **62** under thermodynamic control from the macrocycles **59** and **63** using olefin metathesis.[57]

In a further paper by Sanders, he has shown it is possible to modulate reversibly, the binding properties of a macrocycle turning off intramolecular interactions *via* cobalt carbonyl complexation to the alkyne functionality.[58] In the presence of the macrocycle **64a**, metathesis of the dialkene **65** yields catenane **66** in 15% yield (Scheme 1.19). In the presence of macrocycle **64b** however metathesis yields no catenane even after three days, where-upon addition of macrocycle **64a** begins to allow the formation of interlocked species **66**. This paper represents an interesting development as it introduces a further control element to 'error checking' syntheses, showing that temporary modification of functionality can modulate the product distribution of a reaction.

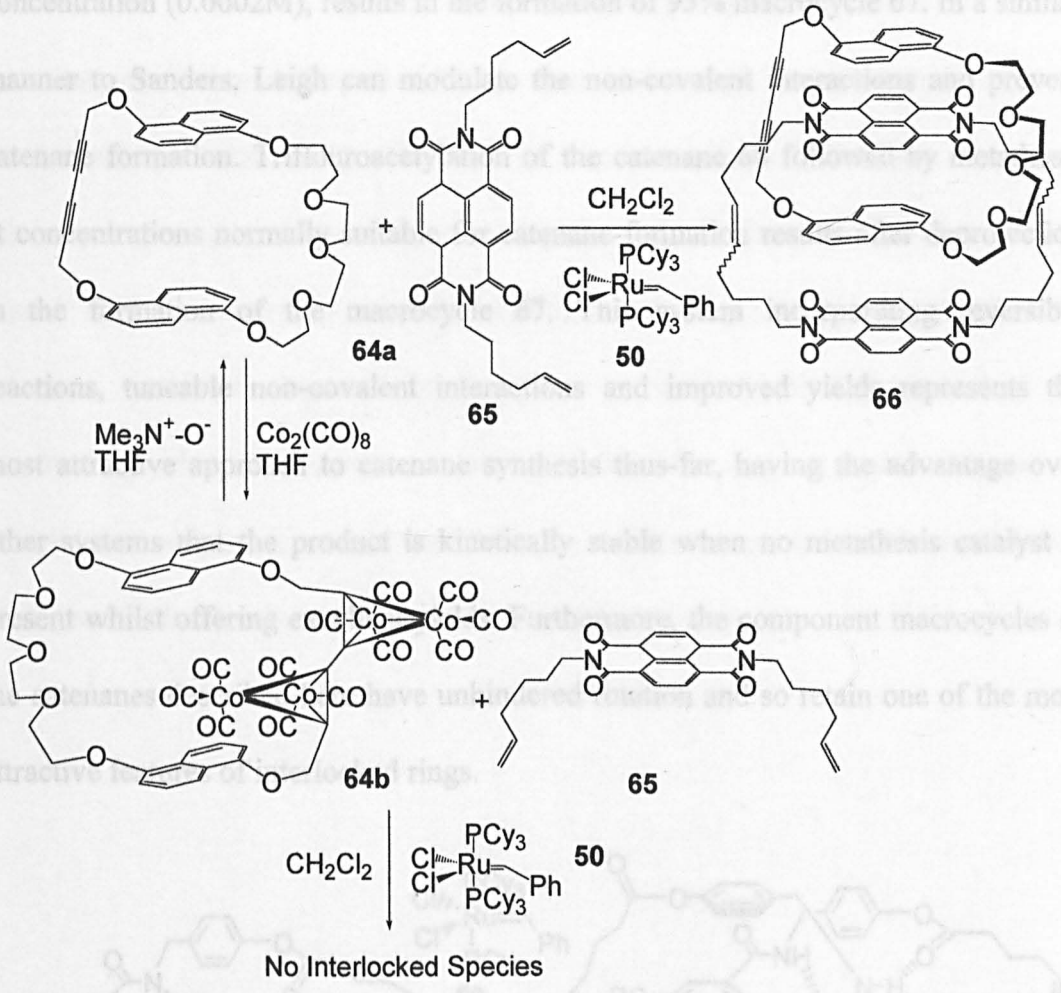


**Scheme 1.19.** The synthesis of a [2]catenane **66** modulated by structural modification of a macrocycle **64**.[58]

Most recently, Leigh has also achieved the goals of Sanders' work. Wholly organic ring systems using hydrogen bond-mediated assembly and the current generation of highly versatile olefin metathesis catalysts have been used to synthesise catenanes in greater than 95% yield.[59] The technique can be said to be similar to that of the conjurors' trick of interlocking seemingly 'magic rings'. When a macrocycle **67** containing an internal double bond is exposed to Grubbs' catalyst **50**,[49d] it can ring open and pass through the cavity of another macrocycle before closing again to form catenane **68** (Scheme 1.20). As the metathesis reaction is reversible this process can continue until the thermodynamic equilibrium is reached. At high concentration (0.2M) 95% catenane **68** is formed whereas metathesis of catenane **68** at low

concentration (0.0002M), results in the formation of 95% macrocycle **67**. In a similar manner to Sanders, Leigh can modulate the non-covalent interactions and prevent catenane formation. Triflouroacetylation of the catenane **68** followed by metathesis at concentrations normally suitable for catenane formation results after deprotection in the formation of the macrocycle **67**. This system incorporating reversible reactions, tuneable non-covalent interactions and improved yields represents the most attractive approach to catenane synthesis thus-far, having the advantage over other systems that the product is kinetically stable when no metathesis catalyst is present whilst offering excellent yields. Furthermore, the component macrocycles of the catenanes described here have unhindered rotation and so retain one of the most attractive features of interlocked rings.

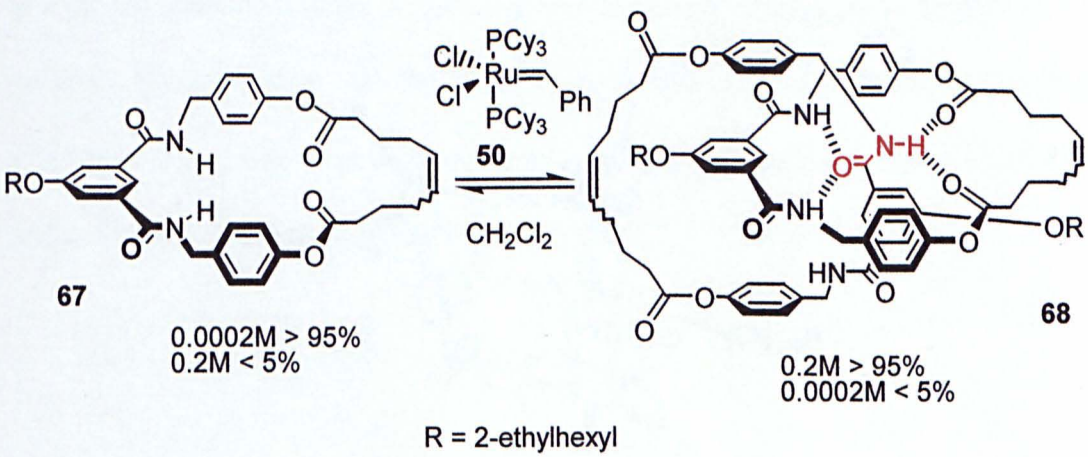


**Scheme 1.20.** The synthesis of a [2]catenane **68** from macrocycle **67** under thermodynamic control facilitated by olefin metathesis.[59]

### 1.5.5. Rotaxane Synthesis Employing Kinetically Labile Co-ordinative Bonds

Recently, like catenanes, rotaxanes have also been constructed using labile metal-ligand co-ordination.[60] Hydrogen bond-assembled rotaxanes similar to those described by Vögtle have recently been described. A tetralactam macrocycle **69** similar in structure to those described by Vögtle is assembled from osmium tetroxide, 2,3-dimethyl-2-butene and the precursor pyridine ligand **70**. In the

presence of a thread **71** with bulky stopper groups the macrocycle forms quantitatively a threaded species **72** by what is proposed as a *reversible clipping* mechanism (Scheme 1.21). The use of osmium allows the linear dipyridine macrocycle precursor **69** to ring-close/ring-open and in the presence of a suitable thread **71** form kinetically unstable rotaxanes in high yield. Once again, like the catenane syntheses discussed in the previous section, this approach has the disadvantage that if reversible metal-ligand bond-forming reactions are used to achieve thermodynamic control then there are very few ways to lock the equilibrium giving a kinetically robust product.

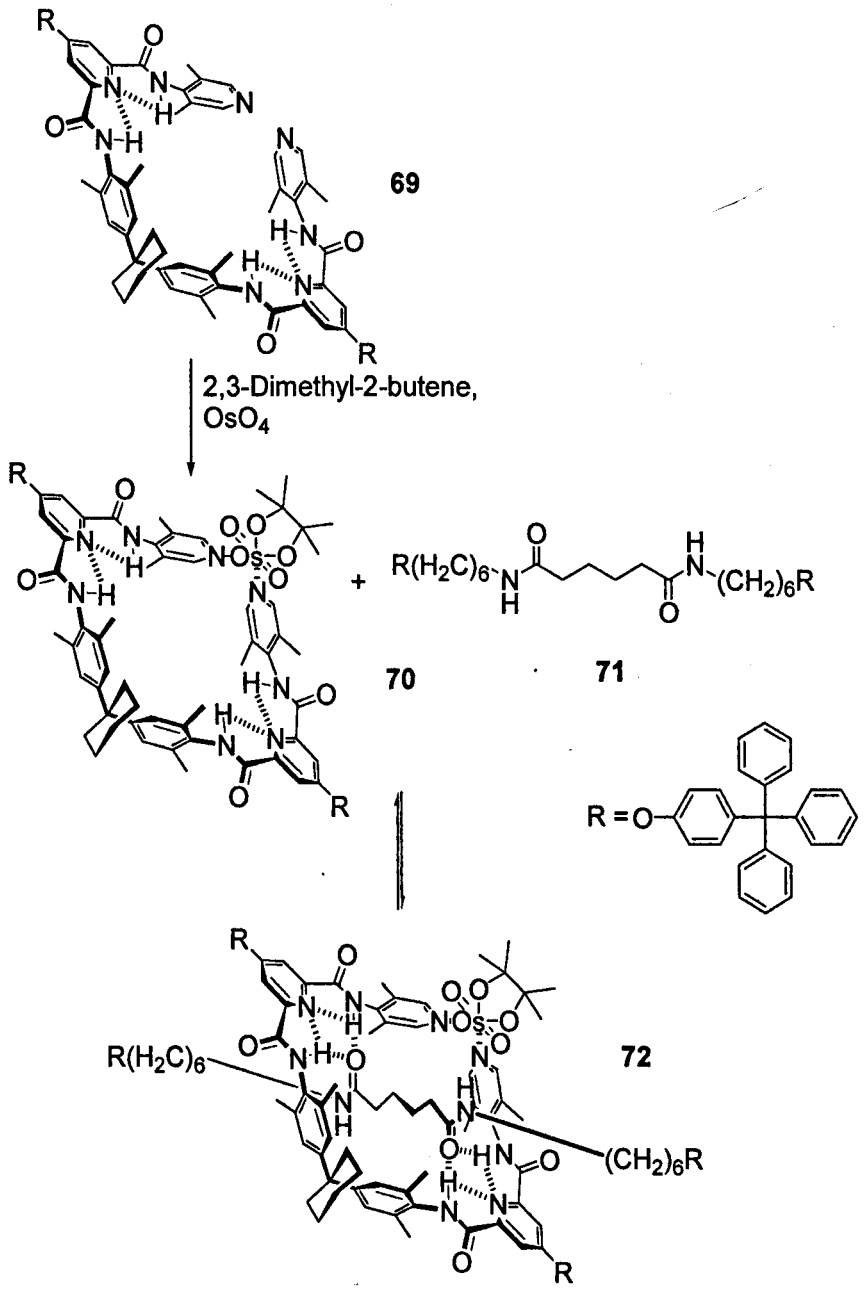


**Scheme 1.21.** The quantitative formation of a threaded species **72** facilitated by the reversible clipping of macrocycle **70**.[60]

### 1.5.6. Synthesis of Wholly Organic Rotaxanes Under Thermodynamic Control

For the first time Stoddart has made use of chemical reactions to achieve rotaxane synthesis under thermodynamic control.[61] Using well known reversible imine bond formations[62] and exploiting the interactions that promote mechanical interlocking it is possible to construct rotaxanes in high yield. This new approach to synthesis is an adaptation of the methodology already developed using cyclobis(paraquat-*p*-

phenylene) **17** which, forms favourable π-π aromatic interactions with diphenoxy residues. When a solution of diphenoxy thread **73** and cyclobis(paraquat-*p*-phenylene) **17** are mixed together over a period of time, almost quantitative formation of interlocked species **74** is observed (Scheme 1.22). As hydrolysis of the imine bond is facile the process probably works *via* hydrolysis of the imine to give the aldehyde then threading of the diphenoxy residue through cyclobis(paraquat-*p*-phenylene) **17** followed by regeneration of the imine. The rotaxane **74** is then trapped giving rotaxane **75** *via* reduction of the imine bonds using sodium borohydride. This last step of the synthesis brings up an interesting point: the imine containing rotaxane **75** itself is not isolated. Although the rotaxane formation is under thermodynamic control it is impossible to isolate any product and so the rotaxane itself behaves as any supramolecular host-guest complex would until it is trapped by reduction. The synthesis therefore falls into the category of syntheses Stoddart describes as 'self-assembly followed by covalent modification processes' and not in the strictest sense rotaxane formation under thermodynamic control.[63]

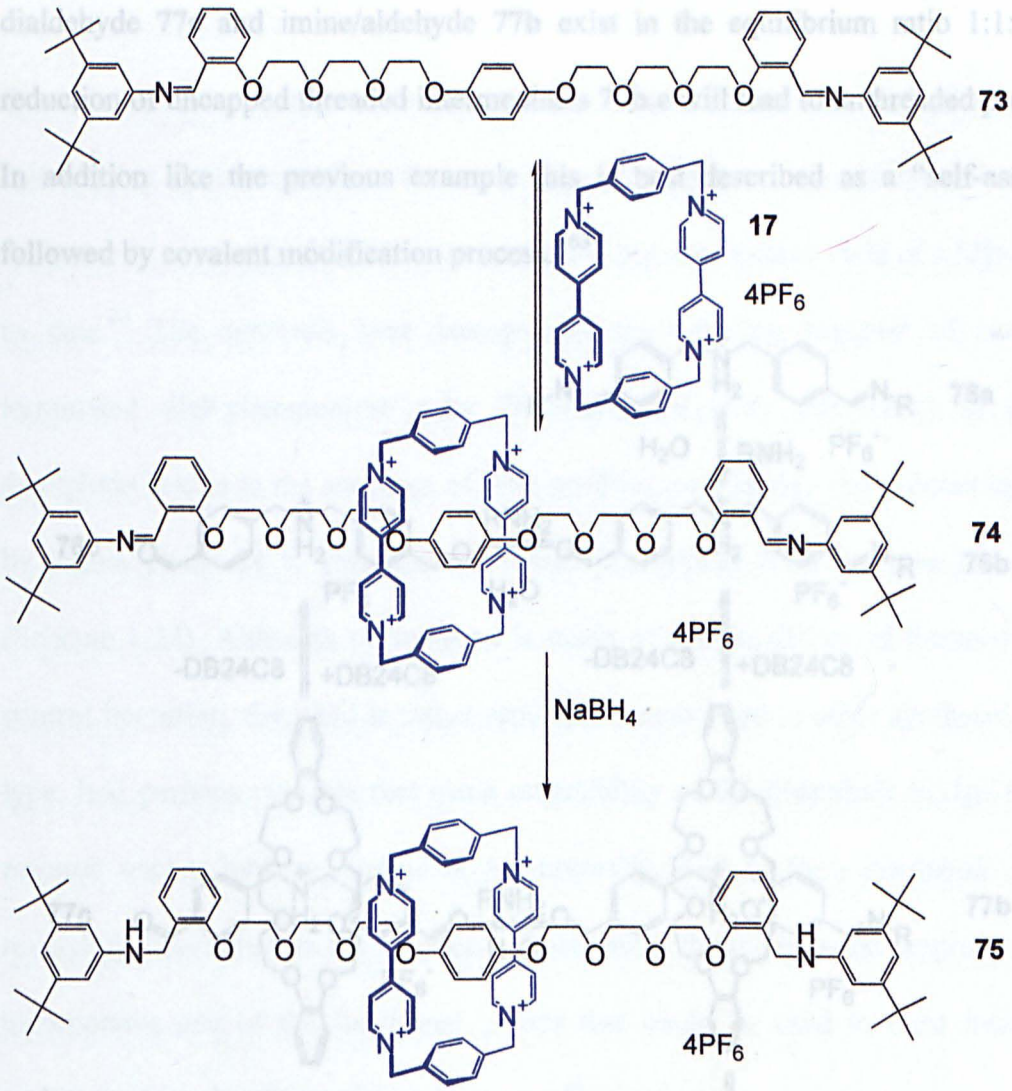


**Scheme 1.22.** The synthesis under thermodynamic control of rotaxane **74** and its subsequent trapping to give rotaxane **75**.[61]

Stoddart has also used hydrogen-bonding together with imine bond formations to achieve a similar result.[64] Using the dibenzo crown **41** and an ammonium thread functionalised with imine stoppers **76a** that exists in an equilibrium mixture with dialdehyde **76c**, monoaldehyde/monoimine **76b** it has been possible to synthesise rotaxane **77a**. Mixing of the crown **41** and thread components **76** leads to the formation of rotaxanes driven by ammonium binding of the crown. The process proceeds *via* slow complexation of the uncapped ammonium threads **76b,c** by the crown ether. Reduction of rotaxane **77a** with PhSeH traps the rotaxane **78** in 17% yield (Scheme 1.23). One reason for the low yield may be that diimine **77a**,

dialdehyde **77c** and imine/aldehyde **77b** exist in the equilibrium ratio 1:1:2, and reduction of uncapped threaded intermediates **77b,c** will lead to unthreaded products. In addition like the previous example this is best described as a "self-assembly followed by covalent modification process."[63]

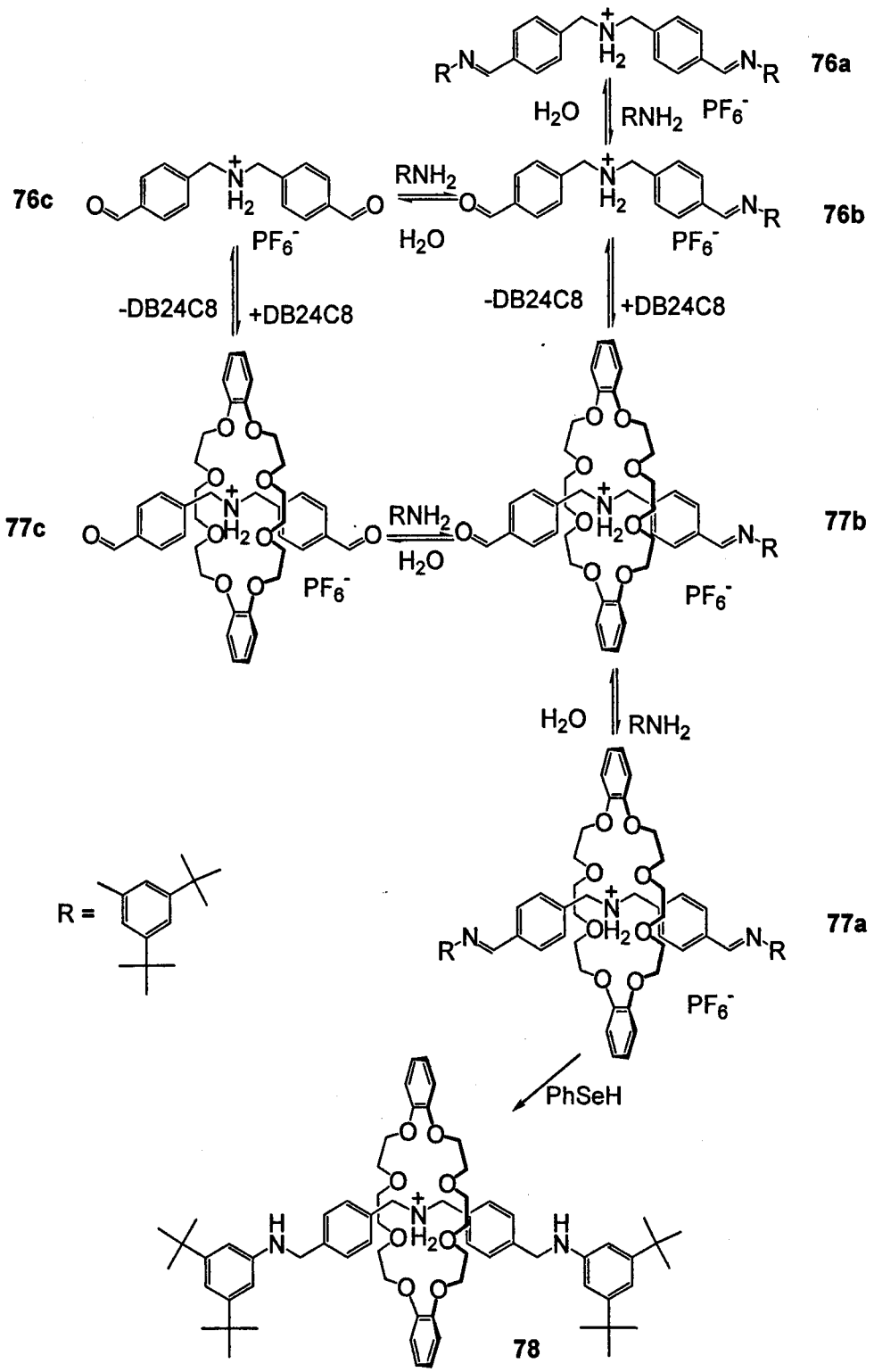


**Scheme 1.23.** The synthesis of hydrogen bond assembled rotaxane **77a** under thermodynamic control using reversible imine bond formations.[64]

There is another example of rotaxane formation using secondary dialkylammonium salt binding by crown ethers that may have an element of thermodynamic control built into its synthesis. Daryl Busch reports the highest isolated yield of a [3]rotaxane to date.[65] The synthesis here incorporates the coupling together of two thiol terminated dialkylammonium salts **79** (*stoppered* with anthracene) to form a disulphide bridge in the presence of dibenzo-24-crown-10 **41**. The process mediated by iodine yields 84 % rotaxane **80**, which precipitates from the reaction mixture (Scheme 1.24). Although no mention is made of the possibility of thermodynamic control operating, the yield is rather remarkable compared to other syntheses of this type. It is perhaps possible that some reversibility of the disulphide bridge forming reaction occurs however iodine is not normally used to form disulphide bridges reversibly. Nevertheless the synthesis if not under thermodynamic control certainly incorporates one of the functional groups that could be used to form interlocked architectures under thermodynamic control.[66]

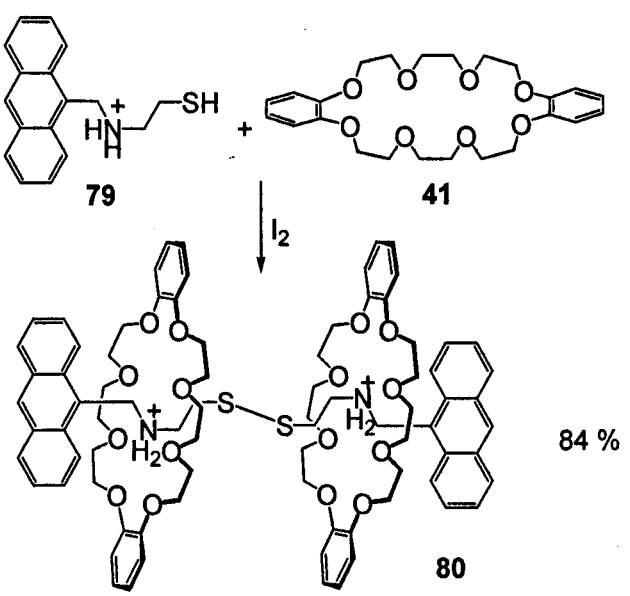


**Scheme 1.24.** The synthesis of [2]rotaxane **80** *via* the coupling of two thiols **79** in the presence of crown **41**.[66]

## 1.6. Conclusions and Outlook

From the general routes to interlocked architectures described here[67] it is clear that our greater understanding of self-assembly and template directed synthesis using non-covalent interactions has allowed us to construct interlocked architectures with relative ease. If useful quantities of interlocked architectures are to be constructed however, it will be necessary to develop thermodynamically controlled syntheses of interlocked architectures marrying the best attributes of traditional supramolecular species with the kinetically robust structures of interlocked compounds. From the examples detailed in this short review it seems clear that reversible covalent bond-forming reactions represent perhaps the best approach to this goal. Such reactions incorporate functional groups discussed here such as alkenes, imines or disulphide bridges, or those not discussed such as esters[68] and acetals.[69] A detailed study of hydrogen bond-directed routes to interlocked architectures will therefore allow us to study and develop two things:

Our understanding of template processes in particular those that occur in the *clipping* route to hydrogen bond assembled rotaxanes.

Develop thermodynamically controlled syntheses of interlocked architectures as a direct result of understanding the features of amide containing interlocked architecture assembly.

## 1.7. The objectives of this thesis

In this chapter the basic approaches to interlocked architecture assembly have been outlined and thus a deficiency in their syntheses was highlighted. Such processes are often governed by kinetic control, which limits their potential usefulness if low yields are obtained. The latter part of chapter one was concerned with the development of thermodynamically controlled routes to interlocked architectures that have recently come to the fore. In particular it was suggested that no true thermodynamically controlled synthesis of a rotaxane giving a kinetically robust product exists. In light of the results laid out in Appendix I (p. 179) (and also described in chapter one as the most ideal synthetic route to catenanes p. 29) where the synthesis of wholly organic interlocking rings is achieved in high yield under thermodynamic control, it was decided that the ultimate goal of this thesis would be to seek out a similar route allowing the synthesis of rotaxanes. The successful development of such a route (chapter six pg. 126) means that as a result of the results described in this thesis the controlled assembly of catenanes and rotaxanes is now possible and hence the title of the thesis: *"The controlled assembly of interlocked architectures"*. It was believed at the start of this project that a thorough understanding of the structural requirements for rotaxane assembly would be necessary for such an undertaking.

## 1.8. Understanding the role of the template

A clearer understanding of the rotaxane assembly first described in chapter one (pg. 16) was expected to aid the research directed toward a thermodynamically controlled synthesis. In Chapter two, the discussion regarding the basic rotaxane assembly process is elaborated upon from the previous chapter introducing a possible mechanistic intermediate. From this it was suggested that perhaps the traditional

synthesis of rotaxanes around a diamide from *p*-xylyenediamine and isophthaloyl dichloride could be simplified allowing the formation of rotaxanes around a single amide functional group. This concept forms the basis of Chapter two wherein a thorough study for the requirements of the template involved in the hydrogen bond-directed assembly of interlocked architectures is undertaken. These results expand upon the basic assembly process described in chapter one giving a greater choice of templates with which rotaxane assembly can be carried out. The results also provide a fuller understanding of the mechanism of the process first described in this chapter (p. 16), thus laying some elementary foundations for the results to be described in subsequent chapters.

## 1.9. References


1. (a) A. D. Bates, A. Maxwell. *DNA topology*, Oxford University Press, New York, **1993**. (b) W. Saenger, *Principles of Nucleic acid structure*; Springer-Verlag: New York, **1984**.
2. (a) H. E. Moser, P. B. Dervan, *Science* **1987**, *238*, 645-650. (b) J. D. Watson, F. H. C. Crick, *Nature* **1953**, *171*, 737-738.
3. For reviews of supramolecular chemistry see: (a) S. Mann, *Nature* **1993**, *365*, 499-505, (b) G. M. Whitesides, J. P. Mathias, C. T. Seto, *Science* **1991**, *254*, 1312-1319, (c) J-M. Lehn, *Angew. Chem. Int. Ed. Engl.* **1988**, *27*, 89. (d) D. J. Cram, *Angew. Chem. Int. Ed. Engl.* **1988**, *27*, 1009-1020, (e) C. J. Pedersen, *Angew. Chem. Int. Ed. Engl.* **1988**, *27*, 1021-1027.
4. For self-assembly in natural systems see: A. Klug, *Angew. Chem. Int. Ed. Engl.* **1983**, *22*, 565-582.
5. For reviews describing self-assembly in natural and unnatural systems see: (a) D. Philp, J. F. Stoddart, *Angew. Chem. Int. Ed. Engl.* **1996**, *35*, 1154-1196. (b) D. S. Lawrence, T. Jing, M. Levett, *Chem. Rev.* **1995**, *95*, 2229-2260.
6. (a) G. Schill, *Catenanes, Rotaxanes and Knots*, Academic Press, New York, **1971**. (b) H. L. Frisch, E. Wasserman, *J. Am. Chem. Soc.* **1961**, *83*, 3789-3795.
7. (a) D. Amabilino, J. F. Stoddart, *New Scientist* **19th February 1994**, 25-29. (b) J-P. Sauvage, *Acc. Chem. Res.* **1998**, *31*, 611-619.
8. E. Wasserman, *J. Am. Chem. Soc.* **1960**, *82*, 4433-4434.
9. I. T. Harrison, S. Harrison, *J. Am. Chem. Soc.* **1967**, *89*, 5723-5724.
10. (a) E. Logeman, K. Rissler, G. Schill, H. Fritz, *Ber. Dtsch. Chem. Ges.* **1981**, *114*, 2245-2260. (b) E. Logeman, G. Schill, W. Vetter, *Ber. Dtsch. Chem. Ges.* **1978**, *111*, 2615-2629. (c) G. Schill, A. Luttringhaus, *Angew. Chem., Int. Ed. Engl.* **1964**, *3*, 546.

11. (a) D. M. Walba, *Tetrahedron* **1985**, *41*, 3161. (b) D. M. Walba, R. M. Richards, P. C. Haltwanger, *J. Am. Chem. Soc.* **1982**, *104*, 3219-3221. (c) R. Wolovsky, *J. Am. Chem. Soc.* **1970**, *92*, 2132-2133. (d) D. A. Ben-Afraim, C. Batich, E. Wasserman, *J. Am. Chem. Soc.* **1970**, *92*, 2133-2135.

12. (a) G. Agam, A. Zilkha, *J. Am. Chem. Soc.* **1976**, *98*, 5214-5216. (b) G. Agam, D. Gravier, A. Zilkha, *J. Am. Chem. Soc.* **1976**, *98*, 5206-5214.

13. (a) C. O. Dietrich-Buchecker, J-P. Sauvage, J-M. Kern, *J. Am. Chem. Soc.* **1984**, *106*, 3043-3045. (b) C. O. Dietrich-Buchecker, J-P. Sauvage, J-P. Kintzinger, *Tetrahedron Lett.* **1983**, *24*, 5095-5098. (c) C. O. Dietrich-Buchecker, J-P. Sauvage, *Tetrahedron* **1990**, *36*, 503-512.

14. C. O. Dietrich-Buchecker, J-P. Sauvage, J-M. Kern, *J. Am. Chem. Soc.* **1989**, *111*, 7791-7800.

15. N. Armaroli, L. De Cola, V. Balzani, J-P. Sauvage, C. O. Dietrich-Buchecker, J-M. Kern, A. Bailal, *J. Chem. Soc., Dalton Trans.* **1993**, 3241-3247.

16. F. Bitsch, C. O. Dietrich-Buchecker, A-K. Khémiss, J-P. Sauvage, A. V. Dosselaer, *J. Am. Chem. Soc.* **1991**, *113*, 4023-4025.

17. C. O. Dietrich-Buchecker, J-P. Sauvage, *Angew. Chem. Int. Ed. Engl.* **1989**, *28*, 189-192.

18. C. Wu, P. R. Lecavalier, Y. X. Shen, H. W. Gibson, *Chem. Mater.* **1991**, *3*, 569-572.

19. (a) N. Armaroli, F. Diederich, C. O. Dietrich-Buchecker, L. Flamigni, G. Marconi, J-F. Nierengarten, J-P. Sauvage, *Chem. Eur. J.* **1998**, *4*, 406-416. (b) D. J. Cárdenas, P. Gaviña, J-P. Sauvage, *J. Chem. Soc., Chem. Commun.* **1996**, 1915-1916. (c) N. Solladié, J-C. Chambron, C. O. Dietrich-Buchecker, J-P. Sauvage, *Angew. Chem. Int. Ed. Engl.* **1996**, *35*, 906-909. (d) J-C. Chambron, V. Heitz, J-P. Sauvage, *J. Chem. Soc., Chem. Commun.* **1992**, 1131-1133.

20. N. Armaroli, V. Balzani, J-P. Collin, P. Gavina, J-P. Sauvage, B. Ventura, *J. Am. Chem. Soc.* **1999**, *121*, 4397-4408.

21. P. Ashton, T. T. Goodnow, A. E. Kaifer, M. V. Reddington, A. M. Z. Slawin, N. Spencer, J. F. Stoddart, C. Vicent, D. J. Williams, *Angew. Chem. Int. Ed. Engl.* **1989**, *28*, 1396-1399.

22. (a) B. Odell, M. V. Reddington, A. M. Z. Slawin, N. Spencer, J. F. Stoddart, D. J. Williams, *Angew. Chem. Int. Ed. Engl.* **1988**, *27*, 1547-1550. (b) P. R. Ashton, B. Odell, M. V. Reddington, A. M. Z. Slawin, J. F. Stoddart, D. J. Williams, *Angew. Chem. Int. Ed. Engl.* **1988**, *27*, 1550-1553.

23. (a) J-Y Ortholand, A. M. Z. Slawin, N. Spencer, J. F. Stoddart, D. J. Williams, *Angew. Chem. Int. Ed. Engl.* **1988**, *28*, 1394-1395. (a) P. R. Ashton, A. M. Z. Slawin, N. Spencer, J. F. Stoddart, D. J. Williams, *J. Chem. Soc., Chem. Commun.* **1987**, 1066-1069. (b) B. L. Allwood, H. Shahriari-Zavareh, J. F. Stoddart, D. J. Williams, *J. Chem. Soc., Chem. Commun.* **1987**, 1064-1066 (c) B. L. Allwood, H. Shahriari-Zavareh, J. F. Stoddart, D. J. Williams, *J. Chem. Soc., Chem. Commun.* **1987**, 1058-1061.

24. For an example of threading a bispyridimium residue through a crown ether followed by *capping* see: P. R. Ashton, D. Philp, N. Spencer, J. F. Stoddart, *J. Chem. Soc., Chem. Commun.* **1992**, 1124-1128.

25. For an example of threading an electron rich aromatic through cyclobisparaquat followed by *capping* see: P. L. Anelli, P. R. Ashton, R. Ballardini, V. Balzani, M. Delgado, M. T. Gandolfi, T. T. Goodnow, A. E. Kaifer, D. Philp, M. Pietraszkiewicz, L. Prodi, M. V. Reddington, A. M. Z. Slawin, N. Spencer, J. F. Stoddart, C. Vicent, D. J. Williams, *J. Am. Chem. Soc.* **1992**, *114*, 193-218.

26. For an example of clipping of cylcobisparaquat around an electron rich aromatic containing thread see: P. R. Ashton, M. Grognuz, A. M. Z. Slawin, J. F. Stoddart, D. J. Williams, *Tetrahedron Lett.* **1991**, *32*, 6235-6238.

27. R. A. Bissel, E. Cordova, A. E. Kaifer, J. F. Stoddart, *Nature* **1994**, *369*, 133-137.

28. (a) C. A. Hunter, *J. Am. Chem. Soc.* **1992**, *114*, 5303-5311. (b) F. Vögtle, S. Meier, R. Hoss, *Angew. Chem. Int. Ed. Engl.* **1992**, *31*, 1619-1622.

29. (a) H. Adams, F. J. Carver, C. A. Hunter, N. J. Osborne. *J. Chem. Soc. Chem. Commun.* **1996**, 2529-2530. (b) P. A. Brooksby, C. A. Hunter, A. J. McQuillan, D. H. Purvis, A. E. Rowan, R. J. Shannon, R. Walsh, *Angew. Chem. Int. Ed. Engl.* **1994**, *33*, 2489-2491. (c) F. J. Carver, C. A. Hunter, R. J. Shannon, *J. Chem. Soc. Chem. Commun.* **1994**, 1277-1280. (c) C. A. Hunter, D. H. Purvis, *Angew. Chem. Int. Ed. Engl.* **1992**, *31*, 792-795. (d) C. A. Hunter, *J. Chem. Soc., Chem. Commun.* **1991**, 749-751.

30. For a review of the early studies on the hydrogen bond-assembled catenane formation and its mechanism see: F. Vögtle, T. Dünnwald, T. Schmidt, *Acc. Chem. Res.* **1996**, *29*, 451-460.

31. (a) R. Jäger, S. Baumann, M. Fischer, O. Safarowsky, M. Nieger, F. Vögtle, *Liebigs Ann./Recueil* **1997**, 2269-2273. (b) F. Vögtle, M. Händel, S. Ottens-Hildebrandt, W. Schmidt, *Synthesis* **1996**, 353-356. (c) F. Vögtle, M. Händel, S. Meier, S. Ottens-Hildebrandt, F. Ott, T. Schmidt, *Liebigs Ann./Recuiel* **1995**, 739-743.

32. T. Dünnwald, A. H. Parham, F. Vögtle, *Synthesis*, **1998**, 339-347.

33. O. Braun, F. Vögtle, *Synlett*, **1997**, 1184-1186.

34. C. Seel, O. Safarowsky, G. M. Hübner, F. Vögtle, *J. Org. Chem.* **1999**, *64*, 7236-7242.

35. O. Safarowsky, M. Nieger, R. Frohlich, F. Vögtle, *Angew. Chem. Int. Ed. Engl.* **2000**, *39*, 1616-1618.

36. A. G. Johnston, D. A. Leigh, R. J. Pritchard, M. D. Deegan, *Angew. Chem. Int. Ed. Engl.* **1995**, *34*, 1209-1212.

37. A. G. Johnston, D. A. Leigh, L. Nezhat, J. P. Smart, M. D. Deegan, *Angew. Chem. Int. Ed. Engl.* **1995**, *34*, 1212-1216.

38. D. A. Leigh, K. Moody, J. P. Smart, K. J. Watson, A. M. Z. Slawin, *Angew. Chem., Int. Ed. Engl.* **1996**, *35*, 306-310.

39. A. G. Johnston, D. A. Leigh, A. Murphy, J. P. Smart, M. D. Deegan, *J. Am. Chem. Soc.* **1996**, *118*, 10662-10663.

40. (a) F. Gatti, D. A. Leigh, S. Nepogdiev, S. J. Teat, A. M. Z. Slawin, J. K. Y. Wong, *J. Am. Chem. Soc.* In Press. (b) W. Clegg, C. Gimenez-Saiz, D. A. Leigh, A. Murphy, A. M. Z. Slawin. S. J. Teat, *J. Am. Chem. Soc.* **1999**, *121* 4124-4129. (c) A. S. Lane, D. A. Leigh, A. Murphy, *J. Am. Chem. Soc.* **1997**, *119*, 11092-11093. (d) D. A. Leigh, A. Murphy, J. P. Smart, A. M. Z. Slawin, *Angew. Chem. Int. Ed. Engl.* **1997**, *36*, 728-732.

41. P. R. Ashton, P. T. Glink, J. F. Stoddart, P. A. Tasker, A. J. P. White, D. J. Williams, *Chem. Eur. J.* **1996**, *2*, 729-736.

42. P. R. Ashton, E. J. T. Crystal, P. T. Glink, S. Menzer, C. Schiavo, N. Spencer, J. F. Stoddart, P. A. Tasker, A. J. P. White, D. J. Williams, *Chem. Eur. J.* **1996**, *2*, 709-728.

43. M-V. Martinez-Diaz, N. Spencer, J. F. Stoddart, *Angew. Chem. Int. Ed. Engl.* **1997**, *36*, 1904-1907.

44. (a) J. P. Mathias, E. E. Simanek, J. A. Zerkowski, C. T. Seto, G. M. Whitesides, *J. Am. Chem. Soc.*, **1994**, *116*, 4316-4325. (b) F. H. Beijer, H. Kooijman, A. L. Spek, R. P. Sijbesma, E. W. Meijer, *Angew. Chem. Int. Ed. Engl.* **1998**, *37*, 75-

78. (c) R. P. Sijbesma, F. H. Beijer, L. Brunsveld, B. J. B. Folmer, J. H. K. Ky Hirschberg, R. F. M. Lange, J. K. L. Lowe, E. W. Meijer, *Science* **1997**, *278*, 1601-1605.

45. For early attempts to synthesise rotaxanes *via* slippage see: (a) G. Schill, W. Beckmann, N. Schweikert, H. Fritz, *Chem. Ber.* **1986**, *119*, 2647. (b) I. T. Harrison, *J. Chem. Soc., Perkin. Trans. 1* **1974**, 301. (c) I. T. Harrison, *J. Chem. Soc., Chem. Commun.* **1972**, 231.

46. (a) F. M. Raymo, K. N. Houk, J. F. Stoddart, *J. Am. Chem. Soc.* **1998**, *120*, 9318-9322. (b) M. Asakawa, P. R. Asthton, R. Ballardini, V. Balzani, M. Bělohradský, M. T. Gandolfi, O. Kocian, L. Prodi, F. M. Raymo, J. F. Stoddart, M. Venturi, *J. Am. Chem. Soc.* **1997**, *119*, 302-310. (c) P. R. Ashton, R. Ballardini, V. Balzani, M. Bělohradský, M. T. Gandolfi, D. Philp, L. Prodi, F. M. Raymo, M. V. Reddington, N. Spencer, J. F. Stoddart, M. Venturi, D. J. Williams, *J. Am. Chem. Soc.* **1996**, *118*, 4931-4951. (d) D. B. Amabilino, P. R. Ashton, M. Bělohradský, F. M. Raymo, J. F. Stoddart, *J. Chem. Soc., Chem. Comm.*, **1995**, 747-750. (e) D. B. Amabilino, P. R. Ashton, M. Bělohradský, F. M. Raymo, J. F. Stoddart, *J. Chem. Soc., Chem. Comm.* **1995**, 751-753. (f) P. R. Ashton, M. Bělohradský, D. Philp, J. F. Stoddart, *J. Chem. Soc., Chem. Comm.* **1993**, 1274-1277. (g) P. R. Ashton, M. Bělohradský, D. Philp, J.F. Stoddart, *J. Chem. Soc., Chem. Comm.* **1993**, 1269-1274.

47. (a) C. Heim, A. Affeld, F. Vögtle. *Helv. Chim. Acta* **1999**, *82*, 746-759. (b) M. Händel, M. Pleovets, S. Gestermann, *Angew. Chem. Int. Ed. Engl.* **1997**, *36*, 1199-1201.

48. (a) G. M. Hübner, G. Nachtsheim, Q. Yi Li, C. Seel, F. Vögtle, *Angew. Chem. Int. Ed. Engl.* **2000**, *39*, 1269-1272; (b) C. Seel, F. Vögtle, *Chem. Eur. J.* **2000**, *6*, 21-24; (c) C. Reuter, W. Wienand, G. M. Hübner, C. Seel, F. Vögtle, *Chem. Eur.*

*J.* **1999**, *5*, 2692-2697; (d) G. M. Hübner, J. Gläser, C. Seel, F. Vögtle, *Angew. Chem. Int. Ed. Engl.* **1999**, *38*, 383-386.

49. P. Schwab, M. B. France, J. W. Ziller, R. H. Grubbs, *Angew. Chem. Int. Ed. Engl.* **1995**, *34*, 2039-2041; M. Schuster, S. Blechert, *Angew. Chem. Int. Ed. Engl.* **1997**, *36*, 2036-2056; S. K. Armstrong, *J. Chem. Soc., Perkin Trans. 1*, **1998**, 371-338; R. H. Grubbs, S. Chang, *Tetrahedron*, **1998**, *54*, 4413-4450.
50. (a) M. Weck, B. Mohr, J-P. Sauvage, R. H. Grubbs, *J. Org. Chem.* **1999**, *64*, 5463-5471. (b) G. Rapenne, C. O. Dietrich-Buchecker, J-P. Sauvage *J. Am. Chem. Soc.* **1999**, *121*, 994-1001. (c) C. O. Dietrich-Buchecker, J-P. Sauvage, *Chem. Commun.* **1999**, 615-616. (d) B. Mohr, M. Weck, J-P. Sauvage, R. H.Grubbs, *Angew. Chem. Int. Ed. Engl.* **1997**, *36*, 1308-1310.
51. M. Fujita, F. Ibukuro, H. Hagihara, K. Ogura, *Nature*, **1994**, *367*, 720-723
52. M. Fujita, F. Ibukuro, H. Seki, O. Kamo, M. Imanari, K. Ogura, *J. Am. Chem. Soc*, **1996**, *118*, 899-900.
53. M. Fujita, F. Ibukuro, K. Yamaguchi, K. Ogura, *J. Am. Chem. Soc*, **1995**, *117*, 4175-4176.
54. M. Fujita, M. Aoyagi, F. Ibukuro, K. Ogura, K. Yamaguchi, *J. Am. Chem. Soc.* **1998**, *120*, 611-612.
55. A. C. Try, M. M. Harding, D. G. Hamilton, J. K. M. Sanders, *Chem. Commun.* **1998**, 723-724.
56. (a) D. G. Hamilton, N. Feeder, L. Prodi, S. J. Teat, W. Clegg, J. K. M. Sanders, *J. Am. Chem. Soc.* **1998**, *120*, 1096-1097. (b) D. G. Hamilton, J. E. Davis, L. Prodi, J. K. M. Sanders, *Chem. Eur. J.* **1998**, *4*, 608-620.
57. D. G. Hamilton, N. Feeder, S. J. Teat, J. K. M. Sanders, *New J. Chem.* **1998**, 1019-1021.
58. D. G. Hamilton, J. K. M. Sanders, *Chem. Commun.* **1998**, 1749-1750.

59. T. J. Kidd, D. A. Leigh, A. J. Wilson, *J. Am. Chem. Soc.* **1999**, *121*, 1599-1600.

60. K-Y. Jeong, J. S. Choi, S-Y. Chang, H-Y. Chang, *Angew. Chem. Int. Ed. Engl.* **2000**, *39*, 1692-1695.

61. S. J. Rowan, J. F. Stoddart, *Org. Lett.* **1999**, *1*, 1913-1916.

62. S. Dayagi, Y. Degani, In *The chemistry of the Carbon-Nitrogen Double Bond*, Ed. S. Pati, Interscience, New York, **1970**, 64-83.

63. Processes that utilise noncovalent forces to assemble an interlocked complex that is subsequently "captured" by irreversible bond formation ("self assembly with covalent modification") only operate under thermodynamic control before the final bond-forming reaction [D. B. Amabilino, P. R. Ashton, L. Perez-Garcia, J. F. Stoddart, *Angew. Chem. Int. Ed. Engl.* **1995**, *34*, 2378-2380]. "Strict self assembly" pathways spontaneously convert components into products at thermodynamic equilibrium [D. Philp, J. F. Stoddart, *Angew. Chem. Int. Ed. Engl.* **1996**, *35*, 1154-1196].

64. S. J. Cantrill, S. J. Rowan, J. F. Stoddart, *Org. Lett.* **1999**, *1*, 1363-1366.

65. A. G. Kolchinski, N. W. Alcock, R. A. Roesner, D. H. Busch, *Chem. Commun.* **1998**, 1437-1438.

66. For examples of reversible disulphide bridge forming reactions see: (a) S-W. Tam-Chang, J. S. Stehouwer, J. Hao, *J. Org. Chem.* **1999**, *64*, 334-335. (b) H. Hioki, W. C. Still, *J. Org. Chem.* **1998**, *63*, 904-905

67. There are many other examples of synthetic routes to molecules incorporating mechanical links: for examples of interlocked architectures incorporating co-ordinative bonds see: (a) C. P. McArdle, M. J. Irwin, M.C. Jennings, R. J. Puddephatt, *Angew. Chem. Int. Ed. Engl.* **1999**, *38*, 3376-3378; (b) D. Whang, K-M. Park, J. Heo, P. Ashton, K. Kim, *J. Am. Chem. Soc.* **1998**, *120*, 4899-4900; (c) R. B. Hannak, G. Farber, R. Konrat, B. Krautler, *J. Am. Chem. Soc.* **1997**, *119*,

2313-2314; (d) D. M. P. Mingos, J. Yau, S. Menzer, D. J. Williams, *Angew. Chem. Int. Ed. Engl.* **1995**, *34*, 1894-1895; (e) C. Piguet, G. Bernardinelli, A. F. Williams, B. Bocquet, *Angew. Chem. Int. Ed. Engl.* **1995**, *34*, 582-584; (f) G-J. M. Gruter, F. J. J. de Kanter, P. R. Markies, T. Nomoto, O. S. Akkerman, F. Bicklehaupt, *J. Am. Chem. Soc.* **1993**, *115*, 12179-12180; (g) H. Ogino, *J. Am. Chem. Soc.* **1981**, *103*, 1303-1304; For wholly organic interlocked architectures see: (h) S. Anderson, W. Clegg, H. L. Anderson, *J. Chem. Soc., Chem. Commun.* **1998**, 2379-2380; (i) H. Murakami, A. Kawabuchi, K. Kotoo, M. Kunitake, N. Nakashima, *J. Am. Chem. Soc.* **1997**, *119*, 7605-7606; (j) S. Anderson, T. D. W. Claridge, *Angew. Chem. Int. Ed. Engl.* **1997**, *36*, 1310-1313; (k) S. Anderson, H. L. Anderson, *Angew. Chem. Int. Ed. Engl.* **1996**, *35*, 1956-1959; For catenane-like coordination interpenetrating networks see: (l) A. J. Blake, N. R. Champness, H. Hubberstey, W-S. Li, M. A. Withersby, M. Schröder, *Coord. Chem. Rev.* **1999**, *183*, 117-138; (m) S. R. Batten, R. Robson *Angew. Chem. Int. Ed. Engl.* **1998**, *37*, 1460-1494; for polymeric rotaxanes see: (n) H. W. Gibson, S. Liu, P. Lecavalier, C. Wu, Y. X. Shen, *J. Am. Chem. Soc.* **1995**, *117*, 852-874; (o) A. Harada, J. Li, M. Kamachi, *Nature*, **1992**, *356*, 325-327;

68. For an example see S. J. Rowan, J. K. M. Sanders, *J. Org. Chem.* **1998**, *63*, 1536-1546.

69. For an example used in the synthesis of natural products see: A. Nadin, K. C. Nicolaou, *Angew. Chem. Int. Ed. Engl.* **1996**, *35*, 1622-1656.

# Chapter Two

## 2. Probing the Mechanism of Hydrogen-Bond Assembled Rotaxane Formation

Mechanically interlocked molecules[1] such as knots, catenanes and rotaxanes, of both natural[2] and synthetic origin[3] continue to attract widespread interest, in part because of the properties and functions that can be conferred by their unusual molecular architectures. Previous examples of synthetic *biomolecular* interlocked structures: - artificial DNA knots and catenanes,[4] are seen as forerunners to novel drug delivery systems, nanoscale mechanical devices and even 'biochips'.[5] Here the synthesis of hydrogen bond-assembled rotaxanes containing simple amide, urea and carbamate functionality within the thread is reported: - results which allow for greater understanding of the mechanism of hydrogen-bond-assembled rotaxane formation and shown why other two site systems[6] are more suitable for the construction of useful quantities of interlocked molecules. Understanding the mechanism of template processes is considered an important aspect of the development of efficient routes into functional architectures.

Leigh *et al.* recently described rotaxane formation from *para*-xylylene diamine, isophthaloyl dichloride and the simplest dipeptide (glycylglycine), incorporating a tetrabenzylic amide macrocycle using a five-molecule, hydrogen bond-directed 'clipping' strategy in yields of up to 62%.[6b] More recently the methodology has been extended to the use of a fumaramide template which, because of the additional rigidity and decreased inter-carbonyl distance results in higher yields of up to 95%.[6a] The first rotaxane synthesised using the tetra-amide macrocycle was with the 1,3-

benzylic diamide **37** which yielded [2]rotaxane **39** in 28% yield (Scheme 2.1).[6c] This thread **37** was simply half of one of the constituent macrocyclic components of the original benzylic amide catenane **34**, the interlocked molecule that inspired these investigations.[7] Changing the substitution pattern of the aromatic ring (using a 1,4-diamide thread rather than 1,3) resulted in lower yields of [2]rotaxane (15%),[6d] These results and the solid-state structure of the catenane led us to postulate that rotaxane formation required a multi-point interaction with the thread and emphasised the key importance of the distance between two amide carbonyls within the thread and the rigidity with which they were held in a transoid arrangement suitable for rotaxane formation.

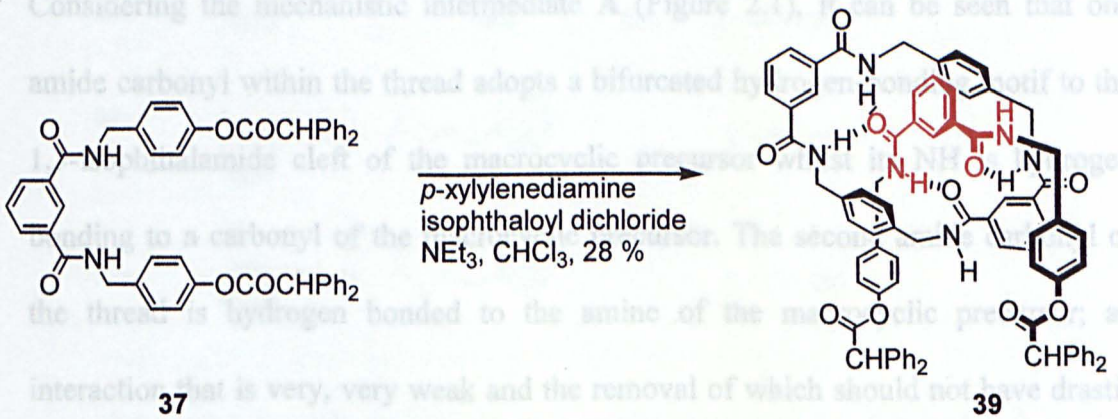


**37** **39**

**Scheme 2.1.** The first synthesis of a hydrogen bond-assembled rotaxane **39** incorporating a tetrabenzylic amide macrocycle.[6c]

Initially in light of these results, it was assumed that for rotaxane formation to occur it must be necessary for two amides to be present in the thread. Closer inspection of one of the possible mechanistic intermediates revealed however, that this might not be so.

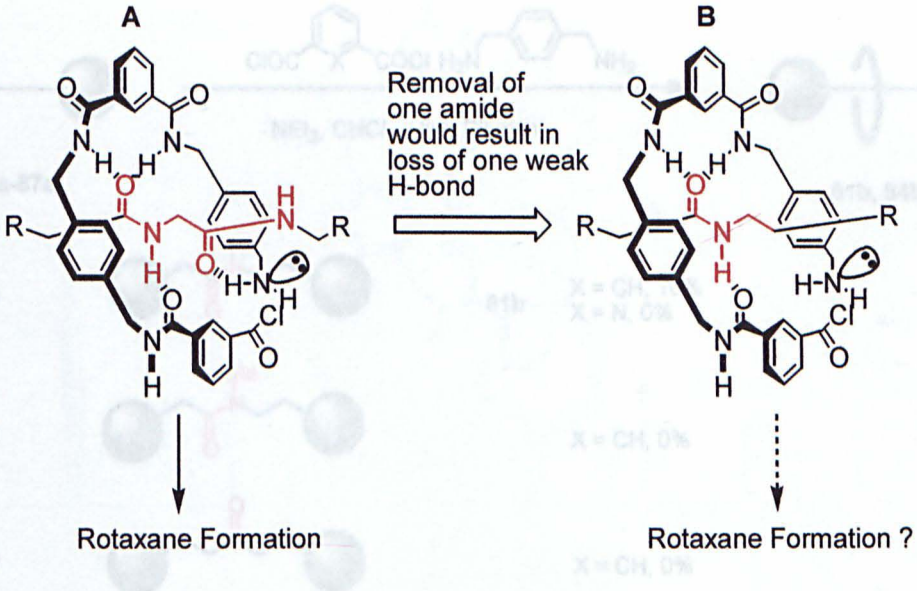


**Figure 2.1.** A possible mechanistic intermediate in the hydrogen bond-directed synthesis of a rotaxane around a two-site template **A** that may also be viable for a one-site template **B**.

Considering the mechanistic intermediate **A** (Figure 2.1), it can be seen that one amide carbonyl within the thread adopts a bifurcated hydrogen-bonding motif to the 1,3-isophthalamide cleft of the macrocyclic precursor whilst its NH is hydrogen bonding to a carbonyl of the macrocyclic precursor. The second amide carbonyl of the thread is hydrogen bonded to the amine of the macrocyclic precursor; an interaction that is very, very weak and the removal of which should not have drastic consequences (mechanistic intermediate **B**). Indeed the simple mono-amide thread **81a** undergoes rotaxane formation in 10% yield (Scheme 2.2).

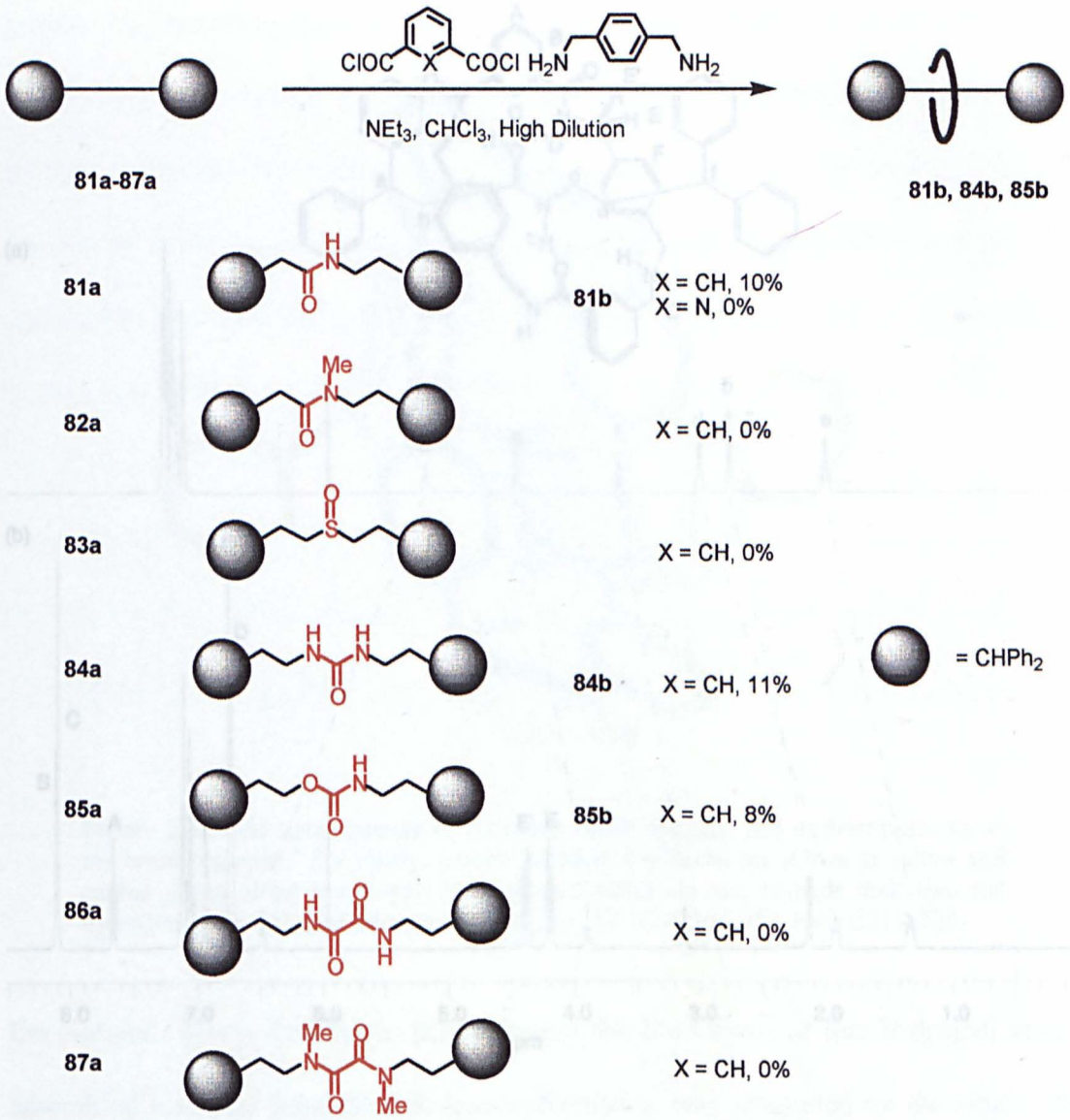


**Scheme 2.2.** The hydrogen bond-directed assembly of rotaxanes **81b**, **84b** and **85b** from threads **81a-87a**.

$^1$H NMR spectra in $C_2D_2Cl_4$ of rotaxane **81b** display some of the typical features of hydrogen bond-assembled rotaxanes (Figure 2.2). The ABX system for the benzylic protons $H_{E,E'}$ results from the unsymmetrical nature of the thread, as the two faces of the macrocycle are enantiotopic. The thread protons $H_{a\text{-}f}$ are all shielded by the macrocyclic sheath and thus move upfield relative to the component thread, except the amide $NH_c$ which moves downfield indicating that the shielding effect is offset by hydrogen-bonding to the macrocycle.

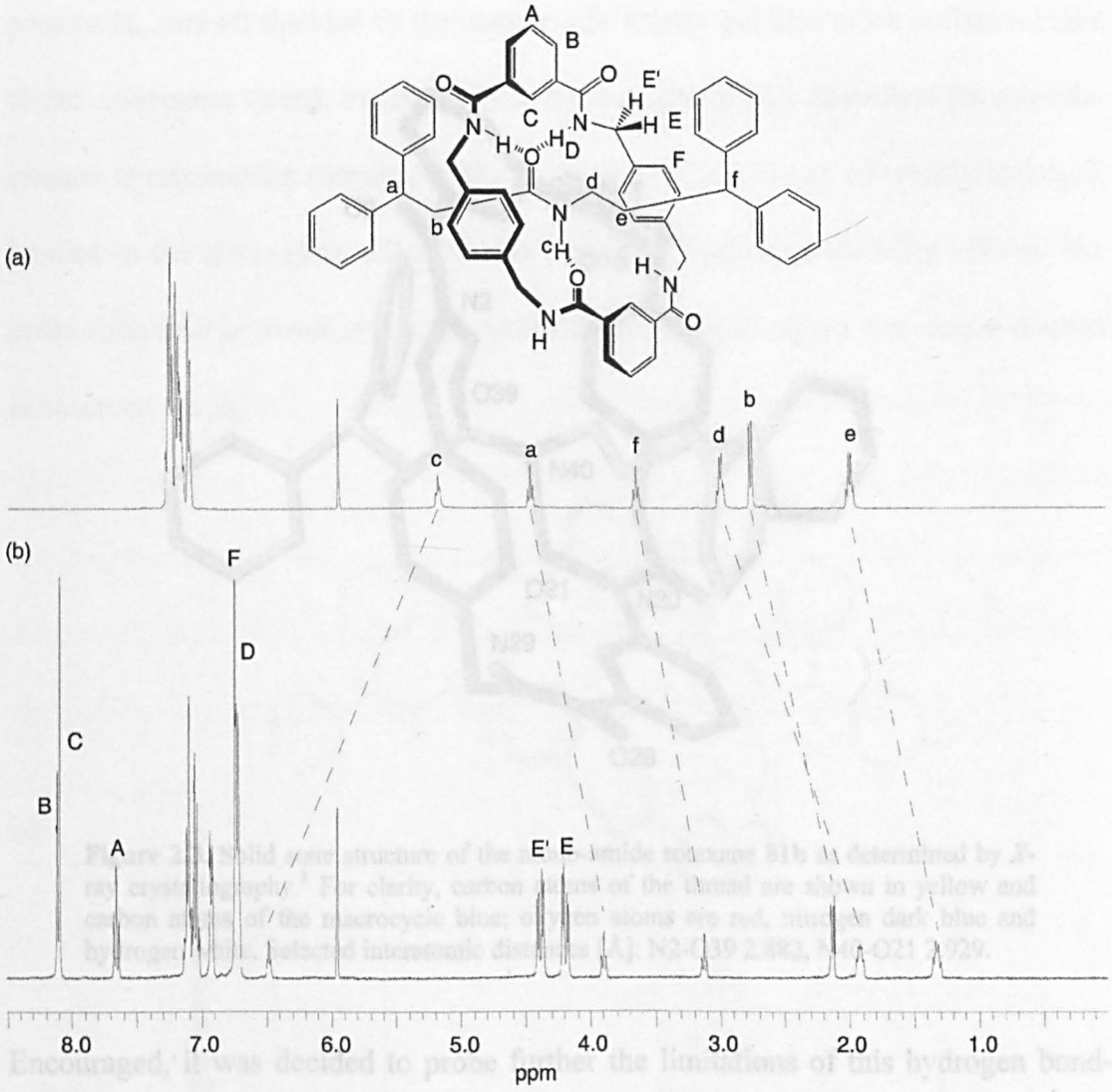


**Figure 2.2.** 1H NMR spectra (400 MHz, $C_2D_2Cl_4$) of (a) one amide thread **81a** and (b) one amide rotaxane **81b**.

Single crystals suitable for investigation by crystallography were obtained from the slow evaporation of water into a solution of the rotaxane **81b** in dimethylsulphoxide.[8] The results confirm the interlocked architecture and support the possibility of an even simpler mechanistic intermediate than **B** involving only one H-bond from the amide carbonyl of the thread to one 1,3 isophthalamide cleft and another H-bond from the amide NH to the other (Figure 2.3).

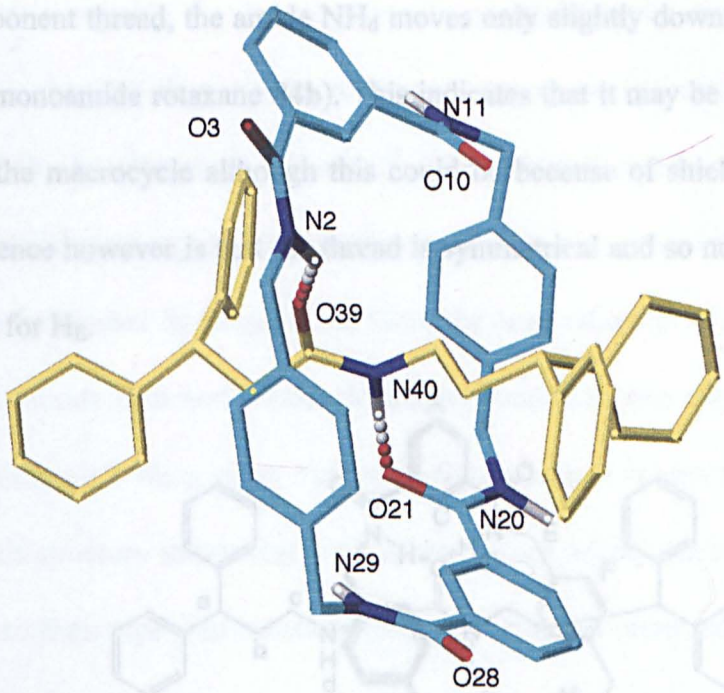


**Figure 2.3.** Solid state structure of the mono-amide rotaxane **81b** as determined by *X*-ray crystallography.[8] For clarity, carbon atoms of the thread are shown in yellow and carbon atoms of the macrocycle blue; oxygen atoms are red, nitrogen dark blue and hydrogen white. Selected interatomic distances [Å]: N2-O39 2.882, N40-O21 2.929.

Encouraged, it was decided to probe further the limitations of this hydrogen bond-assembled rotaxane formation. Rotaxane formation was attempted on the single site template mono-amide **81a**, methylated mono-amide **82a**, sulphoxide **83a**, urea **84a** and carbamate **85a** threads (Scheme 2.2). In addition rotaxane formation was also attempted around the simplest two-site oxalamide thread **86a** and its methylated derivative **87a** (Scheme 2.2). The urea thread yielded 11% rotaxane **84b** whilst the carbamate thread yielded rotaxane **85b** in 8%:[9,10] both comparable yields to the 10% obtained for mono-amide **81b** and indicating that hydrogen bonding strength does not necessarily play a significant role.[11]

$^1$H NMR spectra in $C_2D_2Cl_4$ of the urea rotaxane **84b** and its component thread exhibit similar behaviour to that of the mono-amide system (Figure 2.4). The thread

protons $H_{a-c}$ are all shielded by the macrocyclic sheath and thus move upfield relative to the component thread, the amide $NH_d$ moves only slightly downfield (in a similar manner to monoamide rotaxane **84b**). This indicates that it may be weakly hydrogen bonded to the macrocycle although this could be because of shielding effects. The main difference however is that the thread is symmetrical and so now only a doublet is observed for $H_E$.

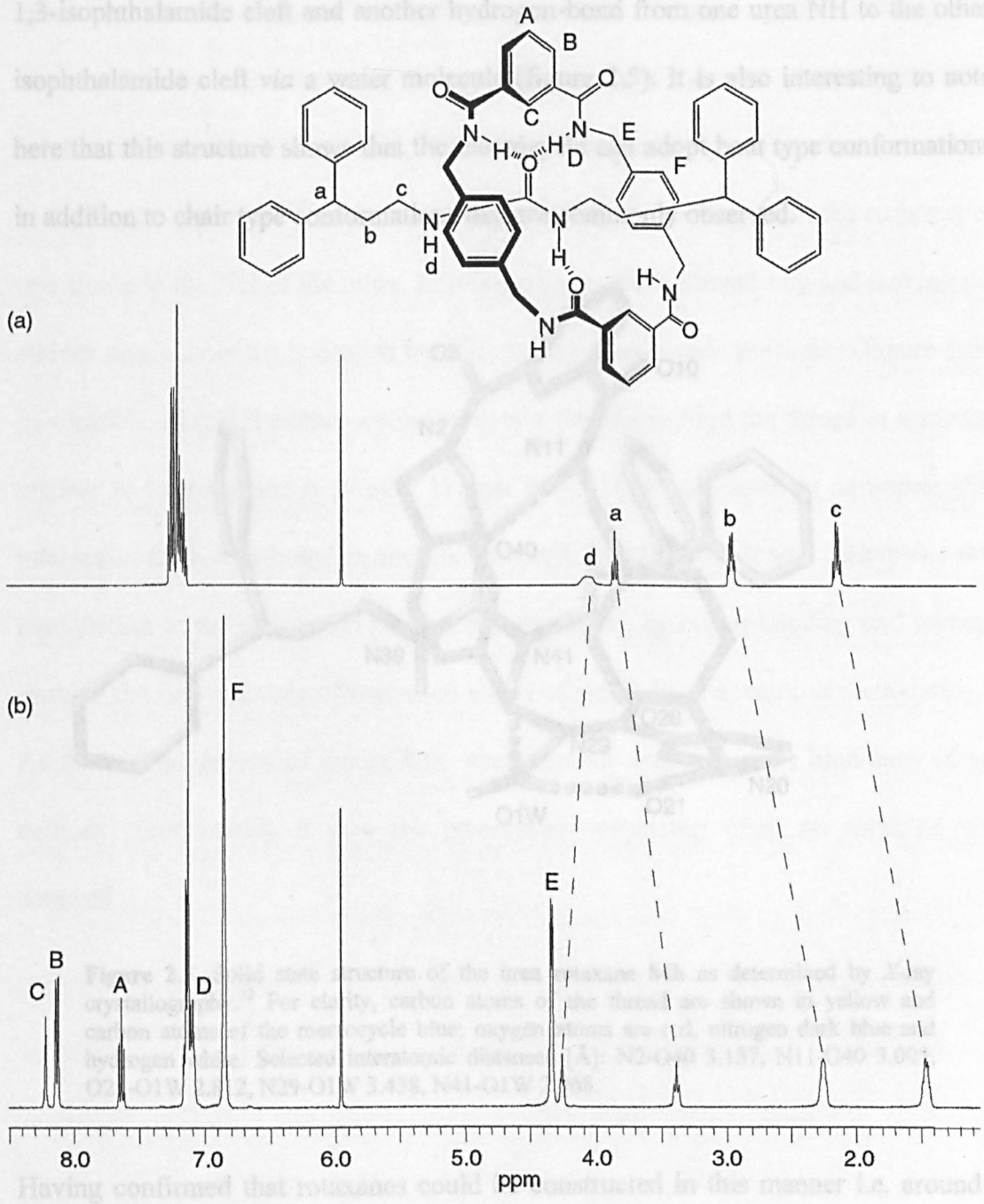


**Figure 2.4.** 1H NMR spectra (400 MHz, $C_2D_2Cl_4$) of (a) urea thread **84a** and (b) one urea rotaxane **84b**.

Single crystals suitable for investigation by crystallography using a synchotron source were obtained from the slow evaporation of water into a solution of the rotaxane **84b** in dimethylsulphoxide.[12] The results confirm the interlocked architecture and once again support the possibility of mechanistic intermediate **B** involving a bifurcated hydrogen-bond from the urea carbonyl of the thread to one 1,3-isophthalamide cleft and another hydrogen-bond from one urea NH to the other isophthalamide cleft *via* a water molecule (figure 2.5). It is also interesting to note here that this structure shows that the macrocycle can adopt boat type conformations in addition to chair type conformations that are commonly observed.

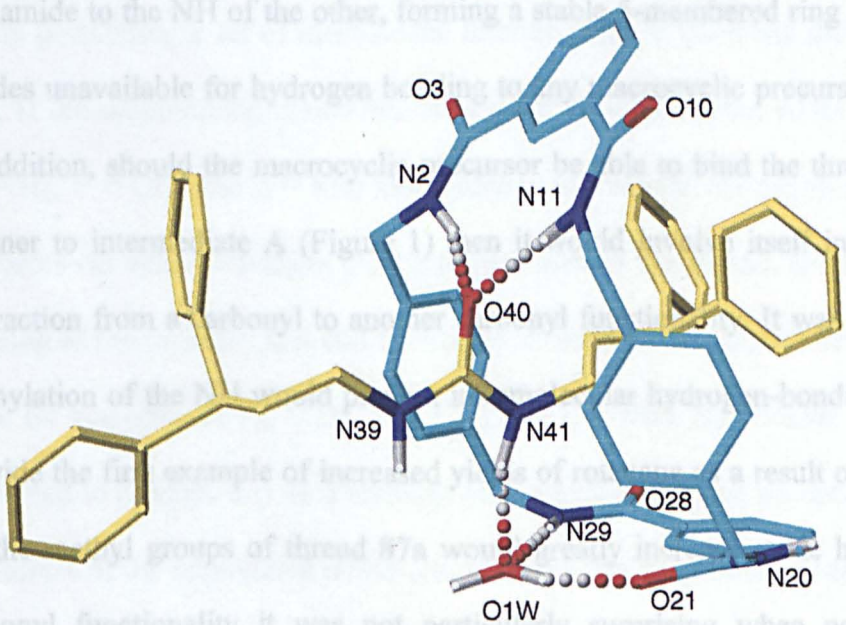


**Figure 2.5.** Solid state structure of the urea rotaxane **84b** as determined by *X*-ray crystallography.[12] For clarity, carbon atoms of the thread are shown in yellow and carbon atoms of the macrocycle blue; oxygen atoms are red, nitrogen dark blue and hydrogen white. Selected interatomic distances [Å]: N2-O40 3.137, N11-O40 3.005, O21-O1W 2.812, N29-O1W 3.438, N41-O1W 2.968.

Having confirmed that rotaxanes could be constructed in this manner i.e. around a single-site template, an attempt was made to explain the failure of the other threads to yield rotaxanes and thus, build up an extended theory of the mechanism of this

process. The simplest to explain was the oxalamide thread **86a**, which was synthesised to assess the boundaries at which two-site mechanisms become possible. Malonamide thread had previously been shown to form rotaxane in 8% yield, presumably through a one-site mechanism even though it possesses two amide groups.[13] The amide NH in the $^1$H NMR spectrum of the oxalamide thread **86a** didn't move from its chemical shift of around 8 ppm when the sample was diluted indicating its involvement in hydrogen-bonding. Single crystals suitable for investigation by crystallography were obtained from the slow evaporation of a solution of acetonitrile containing thread **86a**.[14] The results confirm that the amides in the thread are involved in intra-molecular hydrogen-bonding from the carbonyl of one amide to the NH of the other, forming a stable 5-membered ring and making the amides unavailable for hydrogen bonding to any macrocyclic precursor (Figure 2.6). In addition, should the macrocyclic precursor be able to bind the thread in a similar manner to intermediate **A** (Figure 1) then it would involve itself in an undesirable interaction from a carbonyl to another carbonyl functionality. It was anticipated that methylation of the NH would prevent intramolecular hydrogen-bonding and perhaps provide the first example of increased yields of rotaxane as a result of methylation.[15] As the methyl groups of thread **87a** would greatly increase steric hindrance of the carbonyl functionality it was not particularly surprising when no rotaxane was detected.

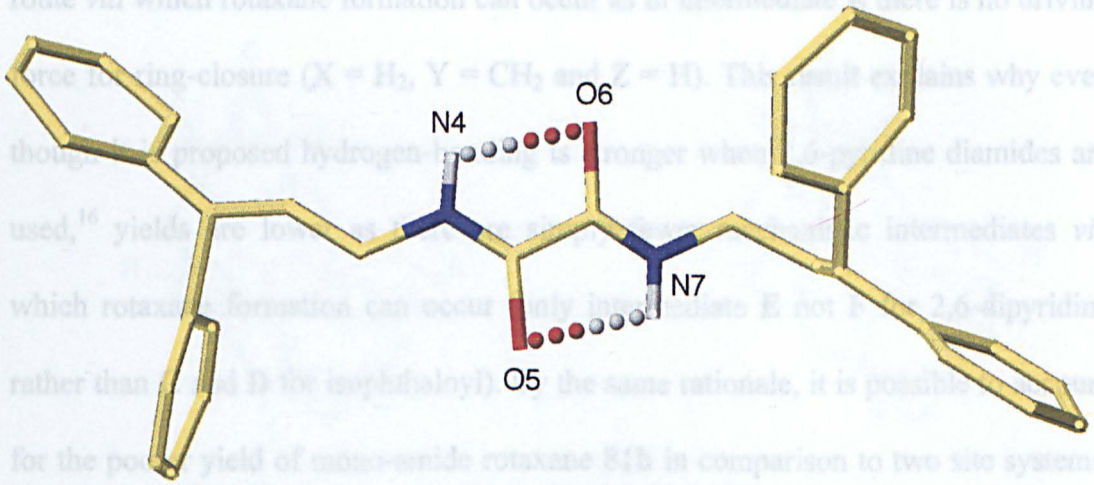


**Figure 2.6.** Solid state structure of the oxalamide thread **86a** as determined by X-ray crystallography.[14] For clarity, carbon atoms of the thread are shown in yellow and carbon atoms of the macrocycle blue; oxygen atoms are red, nitrogen dark blue and hydrogen white. Selected interatomic distances [Å]: N4-O6/O5-N7 2.342.

Finally methylated mono-amide and sulphoxide threads **82a** and **83a** were accounted for by postulating a set of mechanistic intermediates to complete the picture (Figure 2.7). If the mono-amide thread becomes methylated, it cannot adopt intermediate **C** (X = $H_2$, Y = $CH_2$ and Z = Me) as a pathway to rotaxane formation and so there are no routes *via* which rotaxanes can be formed around this thread. Bifurcated hydrogen bonding to the carbonyl can still take place in intermediate **D**, but there is no driving force for ring-closure (X = $H_2$, Y = $CH_2$ and Z = Me). Sulphoxide thread **83a** was attempted to confirm this as it contains only a hydrogen-bond accepting group whilst the failure of the methylated mono-amide thread **82a** may be attributable to the steric hindrance of the methyl group pointing in the direction were a macrocyclic precursor may attempt to ring close. As the sulphoxide thread also failed to yield rotaxane, the theory seems plausible although as sulphur is tetrahedral here steric hindrance cannot be discounted. In a similar manner, mono-amide thread **81a** failed to yield rotaxane when 2,6-pyridine dicarbonyl chloride was used rather than the traditional isophthaloyl dichloride. 2,6-Pyridine diamides are held in a rigid cisoid conformation, as the NH's are hydrogen-bonded to the pyridine. This means that mechanistic intermediate **F** (Figure 2.7) cannot be adopted and so there is no-valid

route *via* which rotaxane formation can occur as in intermediate **E** there is no driving force for ring-closure (X = $H_2$, Y = $CH_2$ and Z = H). This result explains why even though it is proposed hydrogen-bonding is stronger when 2,6-pyridine diamides are used,[16] yields are lower as there are simply fewer mechanistic intermediates *via* which rotaxane formation can occur (only intermediate **E** not **F** for 2,6-dipyridine rather than **C** and **D** for isophthaloyl). By the same rationale, it is possible to account for the poorer yield of mono-amide rotaxane **81b** in comparison to two site systems. Even though the mechanistic intermediate *via* which mono-amide rotaxane **81b** forms differs from its two-site counterpart by only one weak hydrogen bond from a carbonyl to an amine (intermediate **C**) there are several other pathways to rotaxane formation for two-site systems which are simply not valid for one site-systems (intermediate **D**). These results in combination seem to suggest that a major consideration when undertaking hydrogen bond-directed rotaxane formations should be the number of 'handles' and hence mechanistic intermediates which can be accessed by the precursors. In short, templates with two-sites are better than those with one-site and indeed necessary in addition to intercarbonyl distance, sterics, rigidty and hydrogen-bond strength.

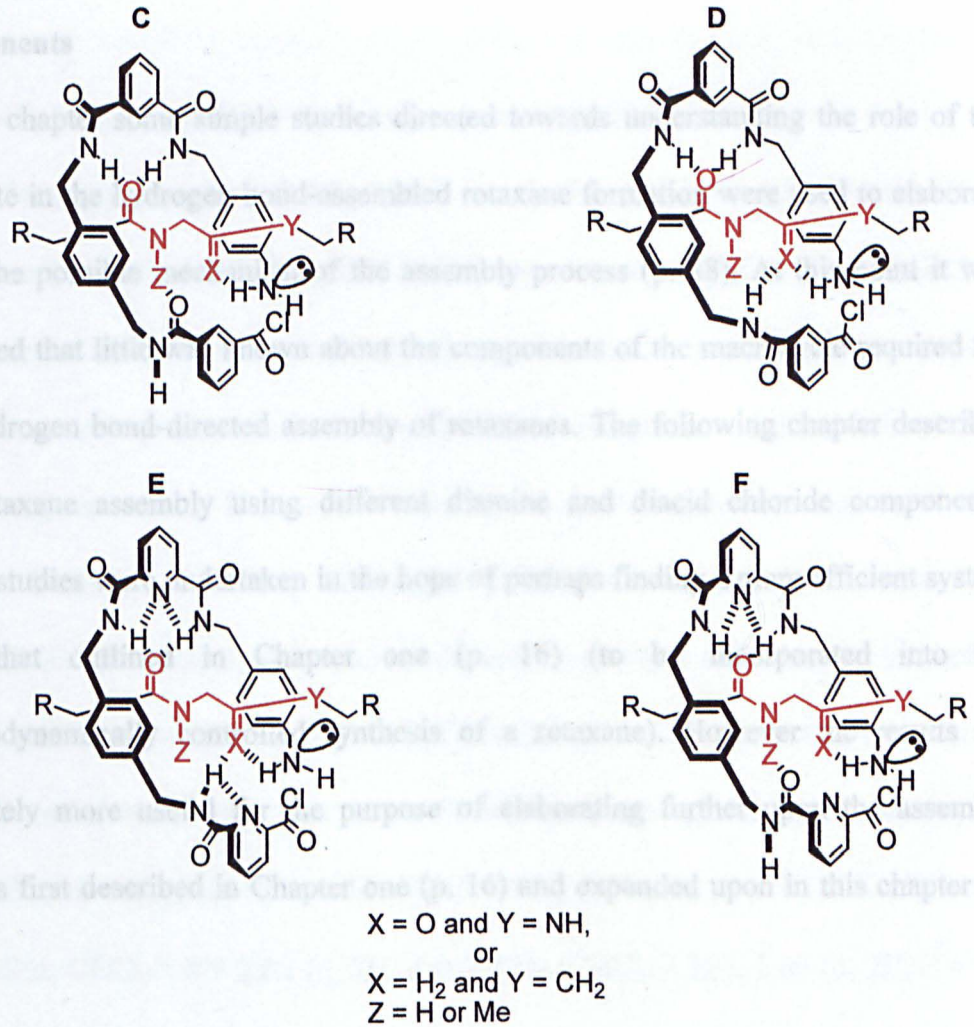


**Figure 2.7.** Possible mechanistic intermediates **C-F** that may be adopted as pathways *via* which hydrogen bond-assembled rotaxanes containing one and two-site templates may form.

In conclusion a new family of rotaxanes based around single-site templates has been synthesised providing a greater understanding of the mechanisms involved in the template-directed synthesis of amide containing rotaxanes. In addition there now exists, an expanded toolbox of amide, carbamate and in particular urea components that may in the future be incorporated into interlocked architectures. For example urea is involved in biological processes and is present in many commercial dyes and it may be possible to exploit the attributes of the mechanical bond to change some of the properties of these systems.

## 2.1. Understanding the assembly process in terms of the macrocyclic components

In this chapter some simple studies directed towards understanding the role of the template in the hydrogen bond-assembled rotaxane formation were used to elaborate upon the possible mechanism of the assembly process (p. 48). At this point it was observed that little was known about the components of the macrocycle required for the hydrogen bond-directed assembly of rotaxanes. The following chapter describes the rotaxane assembly using different diamine and diacid chloride components. These studies were undertaken in the hope of perhaps finding a more efficient system than that outlined in Chapter one (p. 16) (to be incorporated into the thermodynamically controlled synthesis of a rotaxane). However the results are ultimately more useful for the purpose of elaborating further upon the assembly process first described in Chapter one (p. 16) and expanded upon in this chapter (p. 48).

## 2.2. Experimental

### *N*-(3,3-diphenylpropyl)-3,3-diphenylpropanamide 81a

3,3-Diphenylpropylamine (5.14 g, 24.3 mmol), 3,3-diphenylpropionic acid (5 g, 22.1 mmol) and DMAP (2.97 g, 24.3 mmol) were stirred in DMF (100 ml) at 0°C for ten minutes. EDCI (4.66 g, 24.3 mmol) was then added to the reaction mixture, which was subsequently allowed to warm to room temperature and then stirred for a further eighteen hours. The reaction mixture was then extracted between water (100 ml) and EtOAc (5 x 100 ml). The organic layer was then washed with water (100 ml), HCl (0.2 M, 100 ml) and saturated sodium bicarbonate solution (100 ml) before being dried over $MgSO_4$ and filtered. The solvent was then removed in *vacuo* to leave a brown solid, which was recrystallised, from isopropyl alcohol/water to yield the product as creamy fluffy needles. Yield: 3.06 g (33%); m.p. 117-118°C; $^1$H NMR (400 MHz, $CDCl_3$): $\delta$ = 2.02 (q, 2H, $J$ = 7.0 Hz, $CHC\underline{H}_2CH_2$), 2.80 (d, 2H, $J$ = 7.5 Hz, $COC\underline{H}_2CH$), 3.07 (dt, 2H, $J$ = 5.5, 7.0, Hz, $CH_2C\underline{H}_2NH$), 3.68 (t, 1H, $J$ = 7.0 Hz, $C\underline{H}CH_2CH_2$), 4.53 (t, 1H, $J$ = 7.5 Hz, $COCH_2C\underline{H}$), 5.13 (bt, 1H, $J$ = 5.5 Hz, $N\underline{H}$), 7.11-7.30 (m, 20H, ArCH); $^{13}$C NMR (100 MHz, $CDCl_3$): $\delta$ = 35.28 ($CH_2$), 38.60 ($CH_2$), 43.89 ($CH_2$), 47.91 (CH), 49.04 (CH), 126.76 (ArCH), 127.03 (ArCH), 128.13 (ArCH), 128.16 (ArCH), 128.94 (ArCH), 129.04 (ArCH), 144.07 (q, ArC), 144.54 (q, ArC) and 171.30 (CO); FAB-MS (*m*BNA matrix): *m/z* = 420 [M+H$^+$]; anal. calcd for $C_{30}H_{29}NO$ (419.56): C, 85.9; H, 6.9; N, 3.3. found: C, 85.7; H, 7.1; N, 3.5.

### *N*-(3,3-diphenylpropyl)-*N*-methyl-3,3-diphenylpropanamide 82a

To a stirred solution of **81a** (0.2 g, 0.48 mmol) in tetrahydrofuran (20 ml) under an atmosphere of argon was added NaH (60% dispersion in oil 0.83 g, 20.8 mmol)

portion wise followed by methyl iodide (1.30 ml, 20.8 mmol). The solution was heated at 40°C until the reaction was complete and then ammonia solution (1M, 20 ml) added and the reaction stirred until effervescence ceased. The reaction mixture was diluted with EtOAc (50 ml) and then separated. The organic layer was then washed with dilute HCl (0.1M, 2 x 75 ml), saturated sodium bicarbonate solution (2 x 75 ml) and dried over $MgSO_4$ and filtered. Finally the solvent was removed by rotary evaporation and the product purified by column chromatography (30% EtOAc in hexane) to give a yellow oil. Yield: 0.20 g (95%); $^1$H NMR (400 MHz, $C_2D_2Cl_4$): ration E:Z = 1:1, δ = 2.15 (m, 4H, *J* = 7.0 Hz, $Ph_2CHC\underline{H}_2CH_2$ {E+Z}), 2.66 (d, 2H, *J* = 7.0 Hz, $Ph_2CHC\underline{H}_2CONCH_3$ {E}), 2.78 (s, 3H, $CH_3$ {E}), 2.80 (s, 3H, $CH_3$ {Z}), 2.94 (d, 2H, *J* = 7.0 Hz, $Ph_2CHC\underline{H}_2CONCH_3$ {Z}), 3.04 (t, 2H, *J* = 7.0 Hz, $PhCHCH_2C\underline{H}_2$ {E}), 3.19 (t, 2H, *J* = 7.0 Hz, $PhCHCH_2C\underline{H}_2$ {Z}), 3.77 (d, 2H, *J* = 7.0 Hz $Ph_2C\underline{H}CH_2CONH$ {E}), 3.79 (d, 2H, *J* = 7.0 Hz $Ph_2C\underline{H}CH_2CONH$ {Z}), 4.53 (t, 1H, *J* = 7.0 Hz, $PhC\underline{H}CH_2CH_2$ {E}), 4.623 (t, 1H, *J* = 7.0 Hz, $PhC\underline{H}CH_2CH_2$ {Z}), 7.04-7.33 (m, 40H, ArCH {E+Z}); $^{13}$C NMR (100 MHz, $C_2D_2Cl_4$): δ = 33.87 ($CH_2$ {E}), 34.57 ($CH_3$ {E}), 35.18 ($CH_2$ {Z}), 36.82 ($CH_3$ {Z}), 39.60 ($CH_2$ {E}), 40.42 ($\underline{C}H_2$ {Z}), 48.04 ($Ph_2\underline{C}HCH_2$ {E}), 48.08 ($Ph_2\underline{C}HCH_2$ {Z}), 48.29 ($CH_2$ {Z}), 49.32 ($CH_2$ {Z}), 49.57 ($Ph_2\underline{C}HCH_2$ {E}), 50.29 ($Ph_2\underline{C}HCH_2$ {Z}), 127.45 (ArCH), 127.50 (ArCH), 127.52 (ArCH), 127.87 (ArCH), 128.72 (ArCH), 128.82 (ArCH), 128.93 (ArCH), 129.02 (ArCH), 129.61 (ArCH), 129.69 (ArCH), 129.74 (ArCH), 130.01 (ArCH), 144.91 (q, ArC), 145.45 (q, ArC). 171.75 (CO), 171.83 (CO); FAB-MS (*m*BNA matrix): *m/z* = 434 [$M+H^+$].

**3,3-Diphenyl-1-bromopropane**

The procedure described in reference 17 was modified as follows: 3,3-Diphenylpropan-1-ol (5.0g, 23.55 mmol), and tetrabromomethane (10.2 g, 30.68

mmol) were stirred in tetrahydrofuran (50 mL) at 0°C. To the stirred solution was added portion wise; triphenylphosphine (8.0 g, 30.68 mmol) and then the mixture allowed to rise to room temperature and stirred for sixteen hours. The solution was then poured into water and the product extracted with dichloromethane (4 x 50 mL). The organic layer was then dried over magnesium sulphate and concentrated *in vacuo* to give a brown oil that was purified *via* passage through a short pad of silica (hexane) to give a clear oil. Yield: 6.2 g, 95 %; $^{1}$H NMR (400 MHz, $CDCl_3$) $\delta$ = 3.06 (dt, 2H, $J$ = 8.0 Hz, 6.5 Hz, $CHC\underline{H}_2CH_2$), 3.79 (t, 2H, $J$ = 6.5 Hz, $CH_2C\underline{H}_2Br$), 4.68 (t, 1H, J = 8.0 Hz, $C\underline{H}CH_2CH_2$), 7.74 (m, 10H, ArCH); $^{13}$C NMR (100 MHz, $CDCl_3$) $\delta$ = 31.42 ($CH_2$), 38.79 ($CH_2$), 49.61 (CH), 127.04 (ArCH), 128.36 (ArCH), 129.14 (ArCH), 143.90 (q, ArC); FAB-MS (mBNA matrix) m/z 276 $[M+H]^+$ ($^{79}$Br).

***Bis*-(3,3-diphenylpropyl)thioether**

To a stirred solution of 3,3-diphenyl-1-bromopropane (2.00 g, 7.26 mmol) in ethanol (25 mL) was added sodium sulphide hydrate (0.35 g, 3.63 mmol) and the mixture allowed to stir for 16 hours. The reaction mixture was then concentrated, re-dissolved in dichloromethane (50 mL) and washed with saturated sodium bicarbonate solution (25 mL). The organic layer was then dried over magnesium sulphate filtered and concentrated then purified by column chromatography (20% toluene in hexane) to give the product as a clear oil. Yield: 0.40 g, 23.5 %; $^{1}$H NMR (400 MHz, $CDCl_3$) $\delta$ = 2.26 (q, 4H, $J$ = 7.6 Hz, $CHC\underline{H}_2CH_2$), 2.41 (t, 4H, $J$ = 7.6 Hz, $CH_2C\underline{H}_2S$), 4.07 (t, 2H, $J$ = 7.6 Hz, $C\underline{H}CH_2CH_2$), 7.22 (m, 20H, ArCH); $^{13}$C NMR (100MHz, $CDCl_3$) $\delta$ = 30.50 ($CH_2$), 35.69 ($CH_2$), 50.30 (CH), 126.69 (ArCH), 128.26 (ArCH), 128.91 (ArCH), 144.62 (q, ArC); FAB-MS (mBNA matrix) m/z = 423 $[M+H]^+$

***Bis*-(3,3-diphenylpropyl)sulphoxide 83a**

To a stirred solution of *bis*-(3,3-diphenylpropyl)thioether (0.142 g, 0.337 mmol) in dichloromethane (20 mL) was added 50-55% *m*CPBA (0.116 g, 0.675 mmol). When the reaction was complete (around 25 minutes) the solution was washed with sodium metabisulphate (20 mL) and saturated sodium bicarbonate solution (20 mL). The organic layer was then dried over magnesium sulphate, filtered, concentrated and then purified via passage through a short pad of silica (dichloromethane) to give the product as a clear oil. Yield: 0.098 g, 66 %; $^{1}$H NMR (400 MHz, $CDCl_3$) $\delta$ = 2.47 (m, 8H, $CHC\underline{H_2}C\underline{H_2}SO$), 3.97 (t, 2H, J = 7.0 Hz, $C\underline{H}CH_2CH_2SO$), 7.20 (m, 20H, ArCH); $^{13}$C NMR (100 MHz, $CDCl_3$) $\delta$ = 28.79 ($CH_2$), 50.66 (CH), 51.12 ($CH_2$), 127.06 (ArCH), 128.16 (ArCH), 129.14 (ArCH), 143.64 (ArC); FAB-MS (*m*BNA matrix) m/z 439 $[M+H]^+$.

***N,N'-bis*(3,3-diphenylpropyl)urea 84a**

3,3-Diphenylpropylamine (13.0 g, 61.7 mmol) and carbonyldiimidazole (5.5 g, 33.9 mmol) were allowed to stir in THF (50 ml) for a period of two days. The solvent was removed in *vacuo* and the resulting white solid dissolved in DCM and washed with a solution of HCl (0.1N, 10 ml) followed by saturated sodium bicarbonate solution (2 x 30 ml). Finally the organic layer was dried over $MgSO_4$ and the solvent removed in *vacuo* to give a white solid identified as the product. Yield: 14.4 g (95%); m.p. 128-131°C; $^{1}$H NMR (400 MHz, $CDCl_3$): $\delta$ = 2.13 (q, 4H, *J* = 7.0 Hz, $CHC\underline{H_2}CH_2$), 2.88 (dt, 4H, *J* = 5.5, 7.0, Hz, $CHCH_2C\underline{H_2}$), 3.97 (t, 2H, *J* = 7.0 Hz, $Ph_2C\underline{H}CH_2$), 5.91 (bt, 2H, *J* = 5.5 Hz, NH), 7.14-7.34 (m, 20H, ArCH); $^{13}$C NMR (100 MHz, $CDCl_3$): $\delta$ = 35.86 ($CH_2$), 38.42 ($CH_2$), 48.32 (CH), 126.39 (ArCH), 127.83 (ArCH), 128.76 (ArCH), 145.21 (q, ArC), 158.44 (CO); FAB-MS (*m*BNA matrix): *m/z* = 449

[M+H$^+$]; anal. calcd for $C_{31}H_{32}N_2O$ (448.60): C, 83.0; H, 7.1; N, 6.25. found: C, 83.23; H, 7.09; N, 6.48.

***N-N'-Bis*-(3,3-diphenylpropyl)oxalamide 86a**

3,3-Diphenylpropylamine (7.33 g, 34.76 mmol) and triethylamine (5.48 ml, 39.4 mmol) were stirred in anhydrous THF (150 ml) and cooled to 0°C. Oxaloyl dichloride (1.37 ml, 15.76 mmol) was then added dropwise and the solution left to stir for 12 hours. The reaction mixture was filtered and the solvent removed in *vacuo*. The resulting white solid was dissolved in DCM and washed with dilute HCl (50 mL) followed by saturated sodium bicarbonate solution (50 mL). Finally the organic layer was dried over $MgSO_4$, the solvent removed in *vacuo* and the white solid recrystallised from EtOAc. The product was collected as a white crystalline solid. Yield: 3.70 g (50%); m.p. 175-177°C; $^1$H NMR (400 MHz, $CDCl_3$): $\delta$ = 2.36 (q, 4H, $J$ = 6.5 Hz, C$\underline{H_2}$NH), 3.32 (q, 4H, $J$ = 7.5 Hz, CHC$\underline{H_2}$), 3.93 (t, 2H, $J$ = 7.5 Hz, CH), 7.22-7.35 (m, 20H, ArCH) and 7.44 (bt, 2H, $J$=5.5 Hz, N$\underline{H}$); $^{13}$C NMR (100 MHz, $CDCl_3$): $\delta$ = 35.10 (CH$\underline{C}H_2$), 38.82 ($\underline{C}H_2$NH), 49.21 (CH), 126.95 (ArCH), 128.11 (ArCH), 129.10 (ArCH), 144.25 (q, ArC), 160.26 (CO); FAB-MS (*m*BNA matrix): *m/z* = 477 [M+H$^+$]; anal. calcd for $C_{32}H_{32}N_2O_2$ (476.61): C, 80.67; H, 6.54; N, 6.06. found: C, 81.15; H, 6.85; N, 5.95.

***N-N'-Bis*-(3,3-diphenylpropyl)-*N,N'*-dimethyloxalamide 87a**

To a stirring solution of *bis*-(3,3-diphenylpropyl)oxalamide **86a** (0.23 g, 0.48 mmol) in tetrahydrofuran (20 ml) under an atmosphere of argon was added NaH (60% dispersion in oil 0.83 g, 20.80 mmol) portion wise followed by methyl iodide (1.30 ml, 20.80 mmol). The solution was heated at 40°C until the reaction was complete and then ammonia solution (1M, 20 ml) added and the reaction stirred until

effervescence ceased. The reaction mixture was diluted with dichloromethane (50 ml) and then separated. The organic layer was then washed with dilute HCl (0.1M, 2 x 75 ml), saturated sodium bicarbonate solution (2 x 75 ml) and dried over $MgSO_4$. Finally the organic layer was filtered, the solvent was removed by rotary evaporation and the product purified by column chromatography (dichloromethane) to give pale yellow crystals. Yield 0.23 g, 95 %; $^1$H NMR (100 MHz, $CDCl_3$) ratio EE:EZ:ZZ = 1:2:1, $\delta$ = 2.38 (m, 4H, $CH_2$), {6H: 2.86 (s, $CH_3$), 2.88 (s, $CH_3$), 2.97 (s, $CH_3$), 3.03 (s, $CH_3$)}, {4H: 3.05 (t, $J$ = 8.0 Hz, $CH_2$), 3.22 (t, $J$ = 8.0 Hz, $CH_2$), 3.26 (t, $J$ = 8.0 Hz, $CH_2$), 3.42 (t, $J$ = 8.0 Hz, $CH_2$)}, {2H: 3.84 (t, $J$ = 8.0 Hz, CH), 3.89 (t, $J$ = 8.0 Hz, CH), 4.03 (q 4H, $J$ = 8.0 Hz, 2 x CH)}, 7.31 (m, ArCH); $^{13}$C NMR (100 MHz, $CDCl_3$) $\delta$ = 30.75 ($CH_3$ {EE}), 31.88 ($CH_3$ {EZ}), 32.07 ($CH_3$ {EZ}), 32.61 ($CH_2$ {EE}), 32.84 ($CH_2$ {EZ}), 33.83 ($CH_2$ {EZ}), 34.05 ($CH_2$ {EE}), 35.64 ($CH_3$ {ZZ}), 35.67 (CH {EZ}), 46.02 ($CH_2$ {EZ}), 46.05 ($CH_2$ {EE}), 49.17 (CH {EE}), 49.33 (CH {EZ}), 49.45 (CH {EZ}), 49.54 ($CH_2$ {EZ}), 49.60 ($CH_2$ {EZ}), 126.61 (ArCH {EE}), 127.95 (ArCH {EZ}), 128.07 (ArCH {EZ}), 129.14 (ArCH {EE}), 143.97 (q, ArC), 144.03 (q, ArC), 144.34 (q, ArC), 165.08 (CO), 165.29 (CO), 165.37 (CO), 165.47 (CO); FAB-MS (*m*BNA matrix) m/z = 505 $[M+H]^+$; anal. calcd for $C_{34}H_{36}N_2O_2$ (504): C, 80.92; H, 7.19; N, 5.55. found: C, 80.65; H, 7.21; N, 5.34.

**General method for the preparation of benzylic amide macrocycle [2]rotaxanes.** The thread (1.00 mmol) and triethylamine (3.9 ml, 27.5 mmol) were dissolved in anhydrous chloroform (100 ml), and stirred vigorously whilst solutions of the diamine (1.45 g, 14 mmol) in anhydrous chloroform (45 ml) and the acid chloride (2.85 g, 14 mmol) in anhydrous chloroform (45 ml) were simultaneously added over a period of 4 hours using motor-driven syringe pumps. The resulting suspension was filtered and concentrated under reduced pressure to afford the crude product. This

mixture was then re-dissolved in chloroform (100 mL); washed with dilute HCl acid (0.1M, 50 mL), saturated sodium bicarbonate solution (50 mL), then dried over magnesium sulphate and filtered. The solvent was then removed in *vacuo* and the resulting cream solid subjected to column chromatography to yield, in order of elution, the unconsumed thread and the [2]rotaxane.

**Mono-amide rotaxane 81b**

The rotaxane was isolated using column chromatography (silica gel, 1% MeOH/$CHCl_3$). Yield: 0.086 g (9%); m.p. 299-300°C; $^1$H NMR (400 MHz, DMSO-$d_6$): δ = 0.96 (bm, 2H, CHC$\underline{H}_2$CH$_2$), 1.46 (m, 2H, CH$_2$C$\underline{H}_2$NH), 2.17 (d, 2H, $J$ = 7.5 Hz, CHC$\underline{H}_2$CO), 2.27 (t, 1H, $J$ = 7.5, C$\underline{H}$CH$_2$CH$_2$), 4.08 (dd, 4H, $J$ = 5.0 and 13.9 Hz, $H_E$ or $H_{E'}$), 4.11 (t, 1H, $J$ = 7.5 Hz, COCH$_2$C$\underline{H}$), 4.37 (dd, 4H, $J$ = 6.0 Hz and 13.9 Hz, $H_E$ or $H_{E'}$), 6.51 (m, 5H, ArCH + N$\underline{H}$CH$_2$CH$_2$), 6.61 (s, 8H, Ar$CH_F$), 7.02 (m, 10H, ArCH), 7.13 (t, 2H, $J$ = 8.0 Hz, ArCH), 7.23 (m, 4H, ArCH), 7.71 (t, 2H, $J$ = 8.0 Hz, Ar$CH_C$), 8.15 (d, 4H, $J$ = 7.5 Hz, Ar$CH_B$), 8.36 (s, 2H, Ar$CH_A$), 8.66 (t, 4H, $J$ = 5.5 Hz, $NH_D$); $^{13}$C NMR (100 MHz, DMSO-$d_6$): δ = 33.83 ($\underline{C}$H$_2$), 37.69 ($\underline{C}$H$_2$), 39.43 (from HMQC underneath DMSO-$d_6$, CH$_2$) 43.14 (CH), 46.05 (CH), 48.85 (CH), 126.06 (ArCH), 126.29 (ArCH), 127.25 (ArCH), 127.79 (ArCH), 128.40 (ArCH), 128.49 (ArCH), 128.56 (ArCH), 128.64 (ArCH), 129.24 (ArCH), 130.62 (ArCH), 134.73 (q, ArC), 137.57 (q, ArC) 144.37 (q, ArC), 145.21 (q, ArC), 165.61 (CO) 170.82 (CO); FAB-MS (*m*BNA matrix): *m/z* = 952 [M+H$^+$], 974 [M+Na$^+$]; anal. calcd for $C_{62}H_{57}N_5O_5$ (952.15): C, 78.2; H, 6.0; N, 7.4; found: C, 78.0; H, 6.0; N, 7.4.

**Urea rotaxane 84b**

The rotaxane was isolated using column chromatography (silica gel, 1% MeOH/$CHCl_3$). Yield: 0.120 g (12%); m.p. 137-139°C; $^1$H NMR (400 MHz, $CDCl_3$): $\delta$ = 1.55 (q, 4H, $J$ = 7.5 Hz, CHC$\underline{H}_2$), 2.35 (dt, 4H, $J$ = 7.5 Hz, $J$ = 5.0 Hz, C$\underline{H}_2$NH), 3.48 (t, 2H, $J$ = 7.5 Hz, $Ph_2C\underline{H}$), 4.31 (t, 2H, $J$ = 5.0 Hz, N$\underline{H}$CON$\underline{H}$), 4.43 (d, 8H, $J$ = 5.5 Hz, $H_E$), 6.89-6.93 (m, 14H, 12ArCH+ $2NH_D$), 7.23-7.14 (m, 16H, ArCH), 7.69 (t, 2H, $J$ = 7.5 Hz, ArCH), 8.23 (dd, 4H, $J$ = 7.5 Hz, $J$ = 1.51 Hz, $ArCH_B$), 8.31 (t, 2H, $J$ = 1.5 Hz, $ArCH_C$); $^{13}$C NMR (100 MHz, $CDCl_3$): $\delta$ = 36.19 ($CH_2$), 39.44 ($CH_2$), 44.60 ($CH_2$), 49.14 ($Ph_2\underline{C}HCH_2$), 125.34 (ArCH), 126.85 (ArCH), 127.12 (ArCH), 128.84 (ArCH), 128.92 (ArCH), 129.81 (ArCH), 131.41 (ArCH), 134.31 (q, ArC), 137.60 (q, ArC) 144.26 (q, ArC), 159.54 (CO) 166.51 (CO); FAB-MS (*m*BNA matrix): *m/z* = 981 [M+H$^+$], 1003 [M+Na$^+$]; anal. calcd for $C_{63}H_{60}N_6O_5$ (981.19): C, 77.14; H, 6.12; N, 8.57; found: C, 77.39; H, 5.98; N, 8.42.

## 2.3. References


1. (a) D. B. Amabilino, J. F. Stoddart, *Chem. Rev.* **1995**, 2725-2828. (b) G. Schill, *Catenanes, Rotaxanes and Knots*, Academic Press, New York, **1971**.
2. C. Liang, K. Mislow, *J. Am. Chem. Soc.* **1995**, *117*, 4201-4213. (b) C. Liang, K. Mislow, *J. Am. Chem. Soc.* **1994**, *116*, 11189-11190. (c) A. J. Lapthorne, D. C. Harris, A. Littlejohn, J. W. Lustbader, R. E. Cranfield, K. J. Machin, F. J. Morgan, N. W. Issacs, *Nature* **1994**, *369*, 455-461. (d) A. D. Bates, A. Maxwell. *DNA topology*, Oxford University Press, New York, **1993**. (e) F. B. Dean, A. Stasiak, T. Koller, N. R. Corazelli, *J. Biol. Chem.* **1985**, *260*, 4975.
3. (a) D. B. Amabilino, P. R. Ashton, C. L. Brown, E. Córdova, L. A. Godinez, T. T. Goodnow, A. E. Kaifer, S. P. Newton, M. Pietraszkiewicz, D. Philp, F. M. Raymo, A. S. Reder, M. T. Rutland, A. M. Z. Slawin, N. Spencer, J. F. Stoddart, D. J. Williams, *J. Am. Chem. Soc.* **1995**, *117*, 1271-1293. (b) M. Momenteau, F. Le Bras, B. Loock, *Tetrahedron Lett.* **1994**, *35*, 3289-3292 (c) M. Fujita, F. Ibukuro, H. Hagihara, K. Ogura, *Nature* **1994**, *367*, 720-723. (d) J-F. Nierengarten, C. O. Dietrich-Buchecker, J-P Sauvage, *J. Am. Chem. Soc.* **1994**, *116*, 375-376. (e) C. A. Hunter, *J. Am. Chem. Soc.* **1992**, *114*, 5303-5311. (f) F. Vögtle, S. Meier, R. Hoss, *Angew. Chem. Int. Ed. Engl.* **1992**, *31*, 1619-1622. (g) M. J. Gunter, M. R. Johnston, *J. Chem. Soc., Chem. Commun.* **1992**, 1163-1165.
4. N. C. Seeman, *Angew. Chem. Int. Ed. Engl.* **1997**, *36*, 3220-3238 and references therein.
5. D. H. Freedman, *Science* **1991**, *254*, 1308-1310
6. (a) F. G. Gatti, D. A. Leigh, S. Nepogdiev, S. J. Teat, A. M. Z. Slawin, J. K. Y. Wong, *J. Am. Chem. Soc.* In Press. (b) D. A. Leigh, A. Murphy, J. P. Smart, A. M. Z. Slawin, *Angew. Chem. Int. Ed. Engl.* **1997**, *36*, 728-732. (c) A. G.

Johnston, D. A. Leigh, A. Murphy, J. P. Smart, M. D. Deegan, *J. Am. Chem. Soc.* **1996**, *118*, 10662-10663. (d) A. Murphy, D. A. Leigh, *unpublished results*.

7. A. G. Johnston, D. A. Leigh, R. J. Pritchard, M. D. Deegan, *Angew. Chem. Int. Ed. Engl.* **1995**, *34*, 1209-1212.

8. $C_{64.75}H_{66}N_5O_{6.75}S$, $M$ = 1054.29, crystal size 0.25 × 0.18 × 0.10 mm, monoclinic $P2_1/n$, $a$ = 14.0609(9), $b$ = 20.0392(13), $c$ = 21.6344(14) Å, $\beta$ = 96.8120(10)°, $V$ = 6052.9(7)Å$^3$, $Z$ = 4, $\rho_{calcd}$ = 1.157 Mg m$^{-3}$; MoK/α radiation (graphite monochromator, $\lambda$ = 0.71073 Å), $\mu$ = 0.108 mm$^{-1}$, $T$ = 293(2)K. 28938 data (8630 unique, $R_{int}$ = 0.3315, $1.39<\theta<23.29°$), were collected on a Siemens SMART CCD diffractometer using narrow frames (0.3 in ω), and were corrected semi-empirically for absorption and incident beam decay. The structure was solved by direct methods and refined by full-matrix least-squares on $F^2$ values of all data (G.M.Sheldrick, SHELXTL manual, Siemens Analytical *X*-ray Instruments, Madison WI, USA, 1993, version 5.0) to give $wR = \{\Sigma[w(F_o^2-F_c^2)^2]/\Sigma[w(F_o^2)^2]\}^{1/2}$ = 0.5656, conventional $R$ = 0.1821 for $F$ values of 8580 reflections with $F_o^2>2\sigma(F_o^2)$, $S$ = 1.408 for 391 parameters. Residual electron density extremes were 0.280 and 0.037 Å$^{-3}$. Hydrogens were added in calculated positions and constrained to a Riding model.

9. The carbamate rotaxane was synthesised by A. M. Wood of the Leigh group. Although no data is presented here, the result is considered of significant importance and relevance for it to be included in this discussion.

10. For a hydrogen bond-assembled synthesis of urea and carbamate containing rotaxanes see: O. Braun, F. Vögtle, *Synlett* **1997**, 1184-1186.

11. E. M. Arnett, E. J. Mitchell, T. S. S. R. Murty, *J. Am. Chem. Soc.* **1974**, *96*, 3875-3891.

12. $C_{66}H_{70}N_6O_8S$, $M$ = 1095.33, crystal size 0.10 × 0.06 × 0.02 mm, monoclinic P2(1)/c, $a$ = 25.979(2), $b$ = 11.7341(10), $c$ = 19.473(2) Å, β = 106.529(2)°, $V$ = 5690.9(9)Å$^3$, $Z$ = 4, $\rho_{calcd}$ = 1.278 Mg m$^{-3}$; MoK/α synchotron radiation (graphite monochromator, λ = 0.68840 Å), μ = 0.120 mm$^{-1}$, $T$ = 150(2)K. 39607 data (15730 unique, $R_{int}$ = 0.0877, 1.86<θ<29.44°), were collected on a Siemens SMART CCD diffractometer using narrow frames (0.3° in ω), and were corrected semi-empirically for absorption and incident beam decay. The structure was solved by direct methods and refined by full-matrix least-squares on $F^2$ values of all data (G.M.Sheldrick, SHELXTL manual, Siemens Analytical *X*-ray Instruments, Madison WI, USA, 1993, version 5.0) to give $wR$ = $\{\Sigma[w(F_o^2-F_c^2)^2]/\Sigma[w(F_o^2)^2]\}^{1/2}$ = 0.2364, conventional $R$ = 0.0941 for $F$ values of 15680 reflections with $F_o^2>2\sigma(F_o^2)$, $S$ = 1.013 for 735 parameters. Residual electron density extremes were 0.658 and -0.432 Å$^{-3}$. Hydrogens were added in calculated positions and constrained to a Riding model.

13. The malonamide rotaxane was synthesised by G. J. Clarkson of the Leigh group. Although no data is presented here, the result is considered of significant importance and relevance for it to be included in this discussion. The author points out however that there is no evidence to support the assumption that the reaction proceeds *via* a one-site mechanism other than its comparable yield to the mono-amide rotaxane and that there may be other factors that affect this reaction.

14. $C_{32}H_{32}N_2O_2$, $M$ = 476.60, crystal size 0.22 × 0.16 × 0.12 mm, triclinic P1, $a$ = 9.2452(2), $b$ = 15.2765(2), $c$ = 19.7857(10) Å, α = 110.5160(10), β = 98.6820(10), γ = 91.2660(10)° $V$ = 2578.69(7)Å$^3$, $Z$ = 4, $\rho_{calcd}$ = 1.228 Mg m$^{-3}$; MoK/α radiation (graphite monochromator, λ = 0.71073 Å), μ = 0.076 mm$^{-1}$, $T$ = 180(2)K. 17380 data (11998 unique, $R_{int}$ = 0.1633, 1.43<θ<29.08°), were

collected on a Siemens SMART CCD diffractometer using narrow frames (0.3° in ω), and were corrected semi-empirically for absorption and incident beam decay. The structure was solved by direct methods and refined by full-matrix least-squares on $F^2$ values of all data (G.M.Sheldrick, SHELXTL manual, Siemens Analytical *X*-ray Instruments, Madison WI, USA, 1993, version 5.0) to give $wR = \{\Sigma[w(F_o^2-F_c^2)^2]/\Sigma[w(Fo^2)^2]\}^{1/2} = 0.3332$, conventional $R = 0.1192$ for $F$ values of 11998 reflections with $F_o^2 > 2\sigma(F_o^2)$, $S = 1.083$ for 665 parameters. Residual electron density extremes were 2.234 and –0.755 $Å^{-3}$. Hydrogens were added in calculated positions and constrained to a Riding model.

15. W. Clegg, C. Gimenez-Saiz, D. A. Leigh, A. Murphy, A. M. Z. Slawin. S. J. Teat, *J. Am. Chem. Soc.* **1999**, *121* 4124-4129.

16. (a) H. Adams, F. J. Carver, C. A. Hunter, N. J. Osborne. *J. Chem. Soc. Chem. Commun.* **1996**, 2529-2530. (b) P. A. Brooksby, C. A. Hunter, A. J. McQuillan, D. H. Purvis, A. E. Rowan, R. J. Shannon, R. Walsh, *Angew. Chem. Int. Ed. Engl.* **1994**, *33*, 2489-2491. (c) F. J. Carver, C. A. Hunter, R. J. Shannon, *J. Chem. Soc. Chem. Commun.* **1994**, 1277-1280. (c) C. A. Hunter, D. H. Purvis, *Angew. Chem. Int. Ed. Engl.* **1992**, *31*, 792-795. (d) C. A. Hunter, *J. Chem. Soc., Chem. Commun.* **1991**, 749-751.

17. G. Leclerc, N. Decker, J. Schwartz, *J. Med. Chem.* **1982**, *25*, 709-714.

# Chapter Three

## 3. Regioisomeric hydrogen bond-assembled [2]rotaxanes

Rotaxanes[1] currently enjoy a great deal of interest due to their unique topological and dynamic properties.[2] Further to our initial studies on the hydrogen bond-directed synthesis of peptide rotaxanes[3] we report here the synthesis of regioisomeric rotaxanes based on the original peptide template and the more efficient fumaramide template.[4] The incorporation of different macrocyclic components into the interlocked framework has the potential of increasing yields, inducing thus-far unobserved properties and increasing our understanding of template processes.[5]

Leigh *et al.* recently reported the 5-component assembly of rotaxanes from *para*-xylylene diamine, isophthaloyl dichloride and isophthalamide or peptide-based threads in good yields (typically 28-62%).[3,6] The five component clipping reactions (Figure 3.1) produce rotaxanes because of a change in the preferred conformation of the immediate precursor to macrocycle formation **G** in the presence of a suitable template **88**. In the absence of such a template, 1,3-diamide units like **G** preferentially adopt *syn-anti* conformations.[7] In the presence of template **88** however, co-operative multi-point hydrogen-bonding interactions between thread and macrocyclic precursor shift the conformational preference of the 1,3-diamide unit to *syn-syn* as a direct result of bifurcated hydrogen-bonding to a carbonyl of the thread **G.88**. Additional 'handles' on the template **88** hold the reactive end groups in mutual proximity such that cyclisation of **G** occurs rapidly around the template **88** to give the mechanically interlocked product. Such a pathway is also proposed for the synthesis of the benzylic amide catenane **34**: - the molecule that inspired these

investigations.[8] The use of *meta*-xylylene diamine and terephthaloyl dichloride components together or in tandem with the appropriate traditional component to synthesise regioisomeric rotaxanes: - rotaxanes incorporating macrocycles whose substitution patterns differ - was anticipated to change the effectiveness of these precursor hydrogen-bonding interactions.

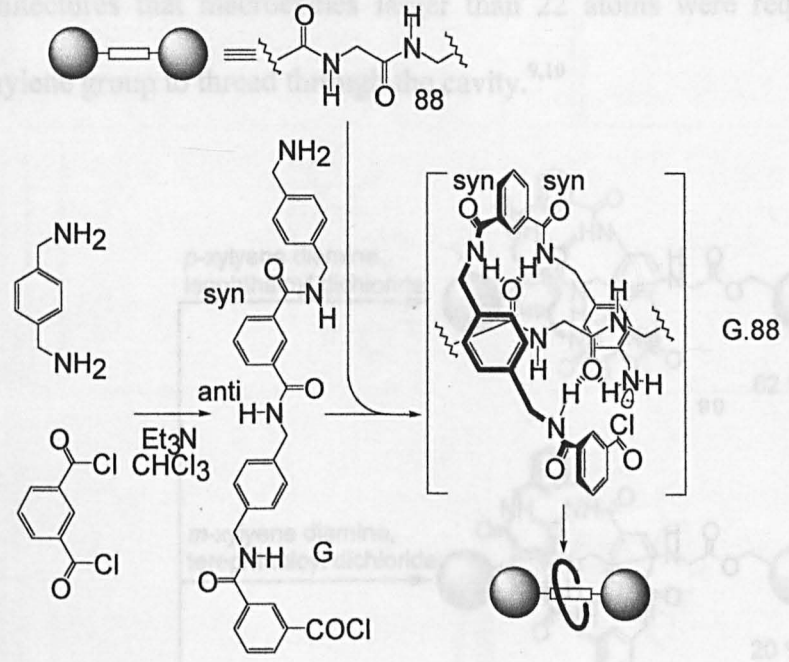


**Figure 3.1.** A possible mechanistic pathway to hydrogen bond-assembled rotaxane formation illustrating how the template **88** induces a conformational change in the immediate precursor to ring closure **G**.

Initially, rotaxane formation using peptide thread **89** was attempted with all four combinations of amine and acid chlorides (Scheme 3.1). The results indicate that the must suitable macrocyclic component for the interlocked architecture was in fact the original benzylic amide macrocycle (rotaxane **90** in 62%, isophthaloyl dichloride/ *para*-xylylene diamine).[3] Two new rotaxanes were obtained: rotaxane **91** in 20% and rotaxane **92** in 2%, however, no rotaxane was detected using terephthaloyl dichloride/ *para*-xylylene diamine. Interestingly, the macrocycle does not self-template to yield catenane for any of the new acid chloride/ diamine combinations indicating that the macrocycles don't have the right dimensions or cannot adopt the

appropriate conformations to act as templates and so only the thread acts as a template. It is also interesting to note here that the yield of 2% [2]rotaxane **92** obtained for the *meta-meta* substituted benzylic amide macrocycle represents the tightest ring (24 atoms) through which penetration of a thread has been shown to occur thus far. Indeed, Wasserman indicated in his early studies concerning interlocked architectures that macrocycles larger than 22 atoms were required in order for a methylene group to thread through the cavity.[9,10]

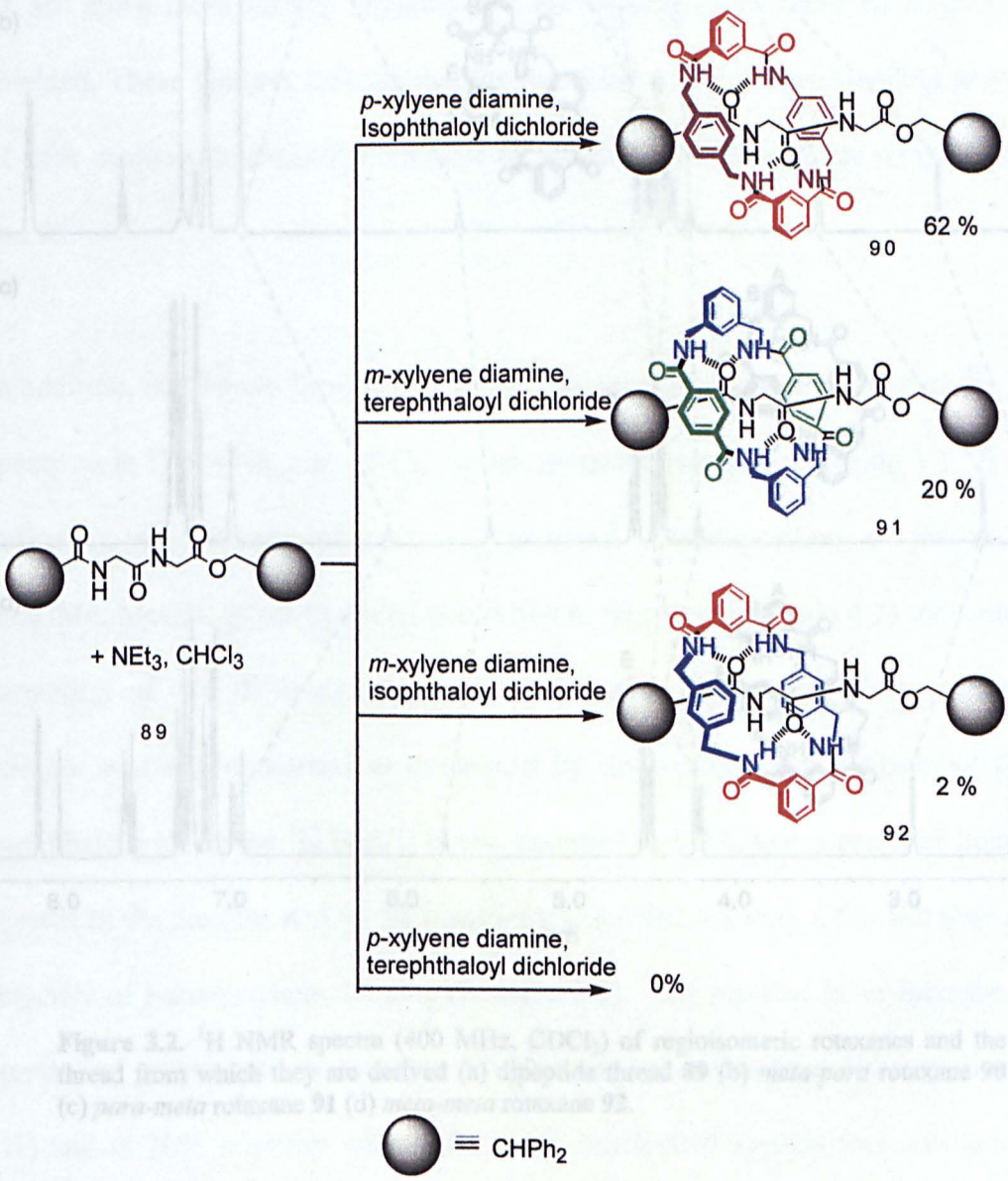


**Scheme 3.1.** The hydrogen bond-directed synthesis of regioisomeric [2] rotaxanes **90,91** and **92** from the dipeptide template **89**.

The solution behaviour of the rotaxanes was assessed from the $^1$H NMR spectra in $CDCl_3$ (Figure 3.2). All three rotaxanes **90-92** exhibit several of the typical features that interlocked architectures of this kind possess.

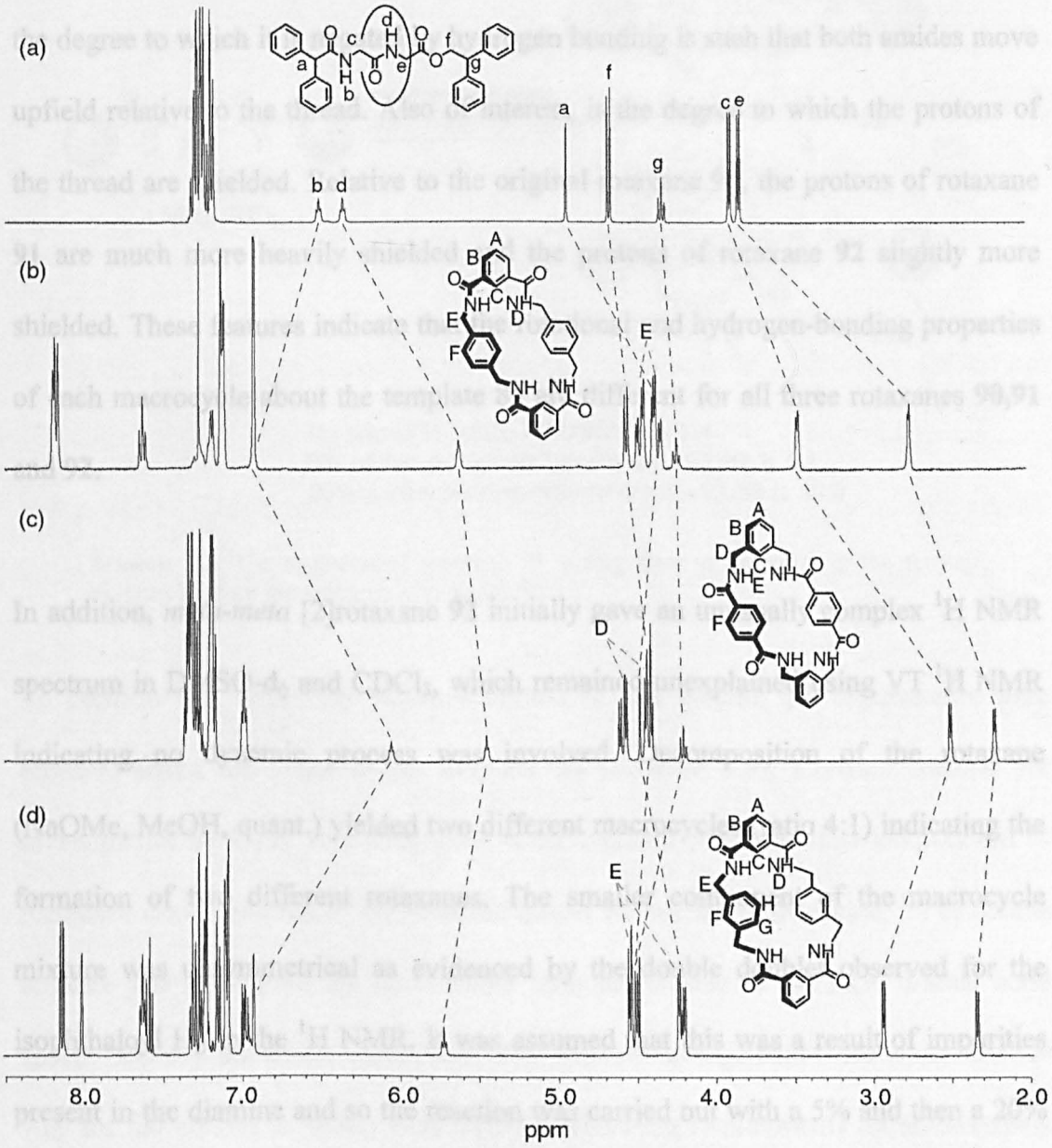


**Figure 3.2.** $^1$H NMR spectra (400 MHz, $CDCl_3$) of regioisomeric rotaxanes and the thread from which they are derived (a) dipeptide thread **89** (b) *meta-para* rotaxane **90** (c) *para-meta* rotaxane **91** (d) *meta-meta* rotaxane **92**.

In all three cases, an ABX system is observed for the benzylic protons, which expresses the enantiotopicity of the two benzylic protons due to the asymmetry of the thread. Also common to each of the three spectra, all the protons of the thread $H_{a-g}$

are shifted downfield as a result of shielding by the macrocycle except the amide NH protons $H_{b,d}$. In rotaxanes **90** and **92**, $H_b$ shifts downfield relative to the thread as the effect of shielding is offset by hydrogen bonding to the macrocycle whilst $H_d$ becomes shielded and moves upfield. In rotaxane **91** however, the shielding effect or the degree to which it is negated by hydrogen bonding is such that both amides move upfield relative to the thread. Also of interest, is the degree to which the protons of the thread are shielded. Relative to the original rotaxane **90**, the protons of rotaxane **91** are much more heavily shielded and the protons of rotaxane **92** slightly more shielded. These features indicate that the rotational and hydrogen-bonding properties of each macrocycle about the template **89** are different for all three rotaxanes **90,91** and **92**.

In addition, *meta-meta* [2]rotaxane **92** initially gave an unusually complex $^1$H NMR spectrum in DMSO-$d_6$ and $CDCl_3$, which remained unexplained using VT $^1$H NMR indicating no dynamic process was involved. Decomposition of the rotaxane (NaOMe, MeOH, quant.) yielded two different macrocycles (ratio 4:1) indicating the formation of two different rotaxanes. The smaller component of the macrocycle mixture was unsymmetrical as evidenced by the double doublet observed for the isophthaloyl $H_B$ in the $^1$H NMR. It was assumed that this was a result of impurities present in the diamine and so the reaction was carried out with a 5% and then a 20% impurity of *para*-xylylene diamine (Scheme 3.2). This resulted in an increase in the amount of unsymmetrical rotaxane **93** (thus far not isolated) at 5% impurity (ratio 1:1) and at 20% impurity where almost all interlocked species was unsymmetrical rotaxane **93**. Further studies are now underway directed towards the isolation of the unsymmetrical rotaxane **93** and the understanding of the processes that occur to yield

a significant amount of rotaxane **93** where the impure amine component from which it is derived is not even observed in the $^1$H NMR spectrum of the starting material!

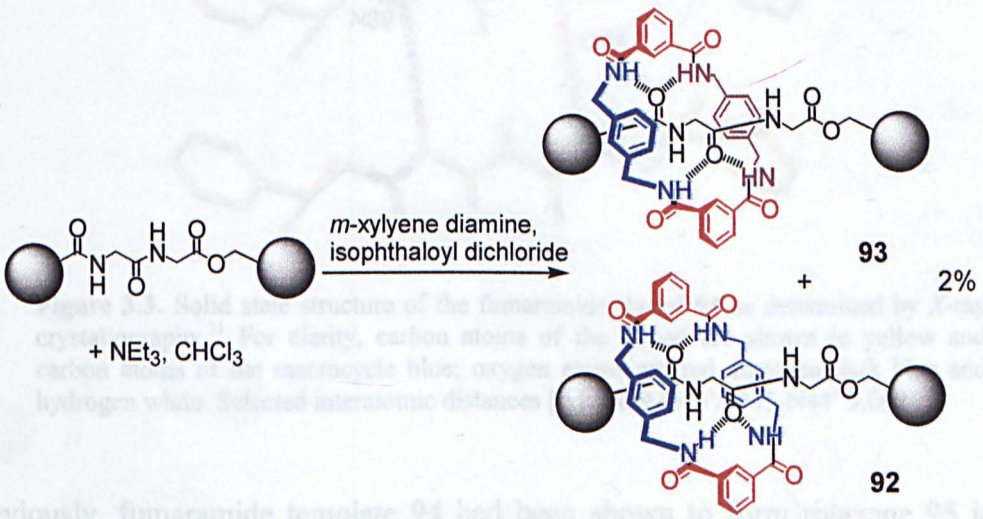


No added impurity, ratio **93:92** is 1:4
5% added *p*-xylyenediamine ratio **93:92** is 1:1
20% added *p*-xylyenediamine ratio **93:92** is 95:5

**Scheme 3.2.** The synthesis of rotaxane **93** arising from an impurity in the starting diamine used for the synthesis of rotaxane **92**

To confirm this behaviour was not limited to one system, the experiments were repeated using the fumaramide template **94** (Scheme 3.3). Crystals suitable for investigation by *X*-ray crystallography were obtained from the slow evaporation of methanol into a solution of fumaramide thread **94** in tetrachloroethane.[11] The results indicate just how good the fumaramide template is; due to the rigid double bond spacer between the amide bonds, and their transoid arrangement there is no efficient way for the amides to satisfy their hydrogen-bonding requirements intramolecularly and so in this case self-association occurs (Figure 3.3). This feature probably accounts for the poor solubility of the thread **94** in non-hydrogen-bonding solvents.

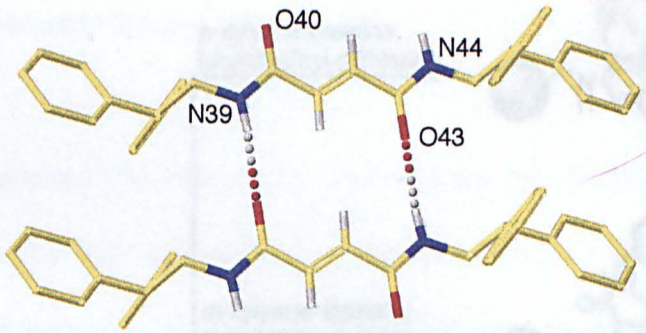


**Figure 3.3.** Solid state structure of the fumaramide thread **94** as determined by *X*-ray crystallography.[11] For clarity, carbon atoms of the thread are shown in yellow and carbon atoms of the macrocycle blue; oxygen atoms are red, nitrogen dark blue and hydrogen white. Selected interatomic distances [Å]: N39-O40'/ O43-N44' 3.069

Previously, fumaramide template **94** had been shown to form rotaxane **95** in near quantitative yield using the original isophthaloyl dichloride/ *para*-xylylene diamine components.[4] Repeating the experiments carried out on the glycylglycyl template **89**, similar behaviour was observed with the fumaramide template **94** (Scheme 3.3). The new rotaxanes **96** and **97** derived from terephthaloyl dichloride/*meta*-xylylene diamine and isophthaloyl dichloride/*meta*-xylylene diamine were obtained in 30% and 3% yields respectively. Once again, no new catenanes were observed and neither was any rotaxane for the *para*-xylylene/ terephthaloyl dichloride combination.

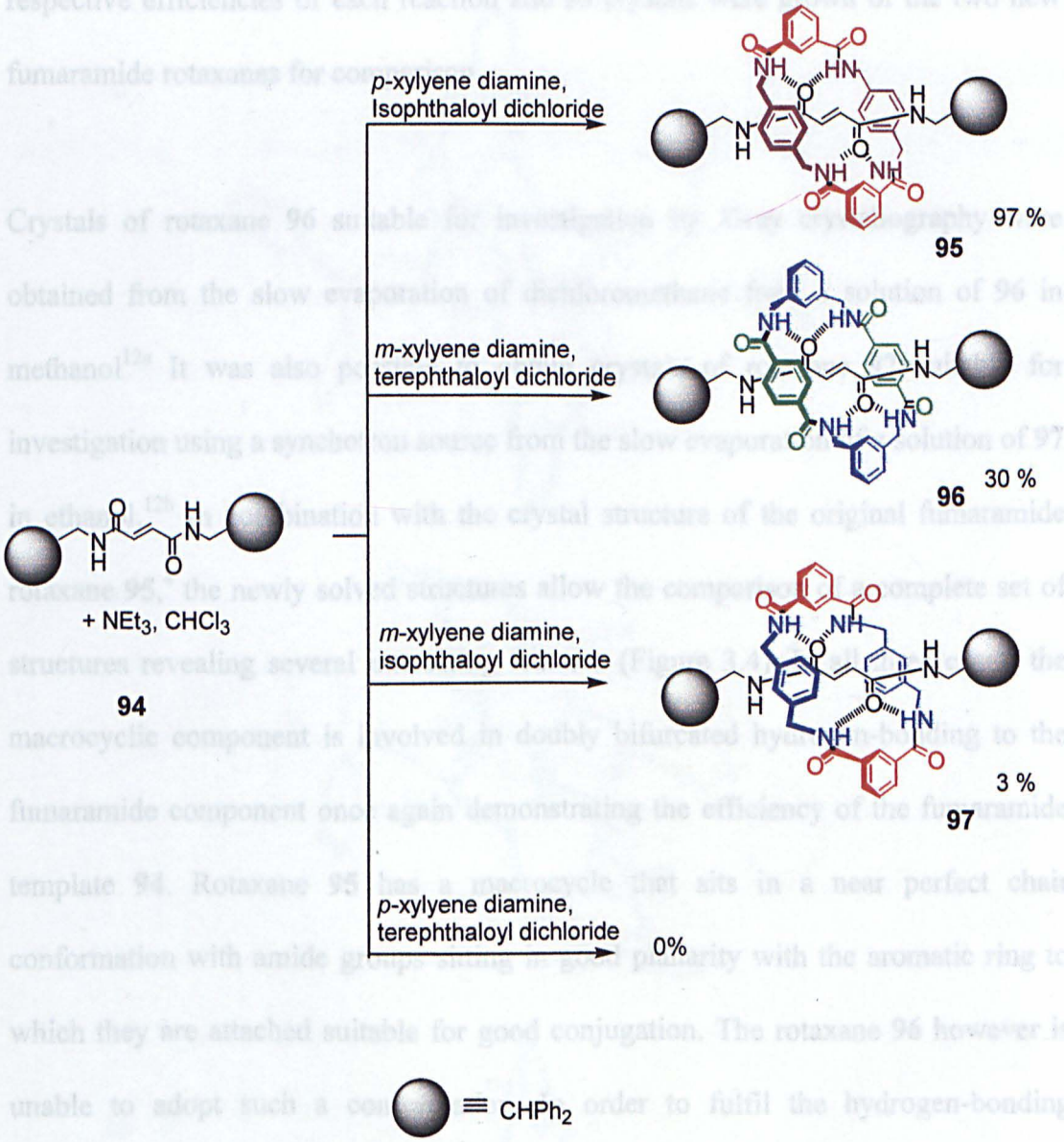


**Scheme 3.3.** The hydrogen bond-directed synthesis of regioisomeric [2] rotaxanes **95,96** and **97** from the fumaramide template **94**.

Having shown the methodology to be transferable it was necessary to explain the efficiency of each combination of components. CPK modelling indicated that *para*-xylylenediamine/ terephthaloyl dichloride combinations might not be able to form immediate precursors to rotaxane formation having well defined binding sites that the template could employ to promote ring closure. Similarly, the *para-para* substituted macrocycle may have a cavity large enough to allow unthreading of any rotaxane formed. It was not possible however to postulate any further theories for the

respective efficiencies of each reaction and so crystals were grown of the two new fumaramide rotaxanes for comparison.

Crystals of rotaxane **96** suitable for investigation by *X*-ray crystallography were obtained from the slow evaporation of dichloromethane from a solution of **96** in methanol[12a] It was also possible to obtain crystals of rotaxane **97** suitable for investigation using a synchotron source from the slow evaporation of a solution of **97** in ethanol.[12b] In combination with the crystal structure of the original fumaramide rotaxane **95**,[4] the newly solved structures allow the comparison of a complete set of structures revealing several interesting features (Figure 3.4). In all three cases, the macrocyclic component is involved in doubly bifurcated hydrogen-bonding to the fumaramide component once again demonstrating the efficiency of the fumaramide template **94**. Rotaxane **95** has a macrocycle that sits in a near perfect chair conformation with amide groups sitting in good planarity with the aromatic ring to which they are attached suitable for good conjugation. The rotaxane **96** however is unable to adopt such a conformation. In order to fulfil the hydrogen-bonding requirements of the fumaramide template the chair confirmation becomes slightly distorted as a result of the elongated cavity and more importantly the amide groups distort out of the ideal planarity with the aromatic unit to which they are attached making conjugation less effective. In the case of the *meta*-xylylene diamine/ isophthaloyl dichloride rotaxane **97**, the macrocycle becomes extremely distorted (now bearing little resemblance to a chair conformation) such that the xylylene units orientate themselves in opposing directions.

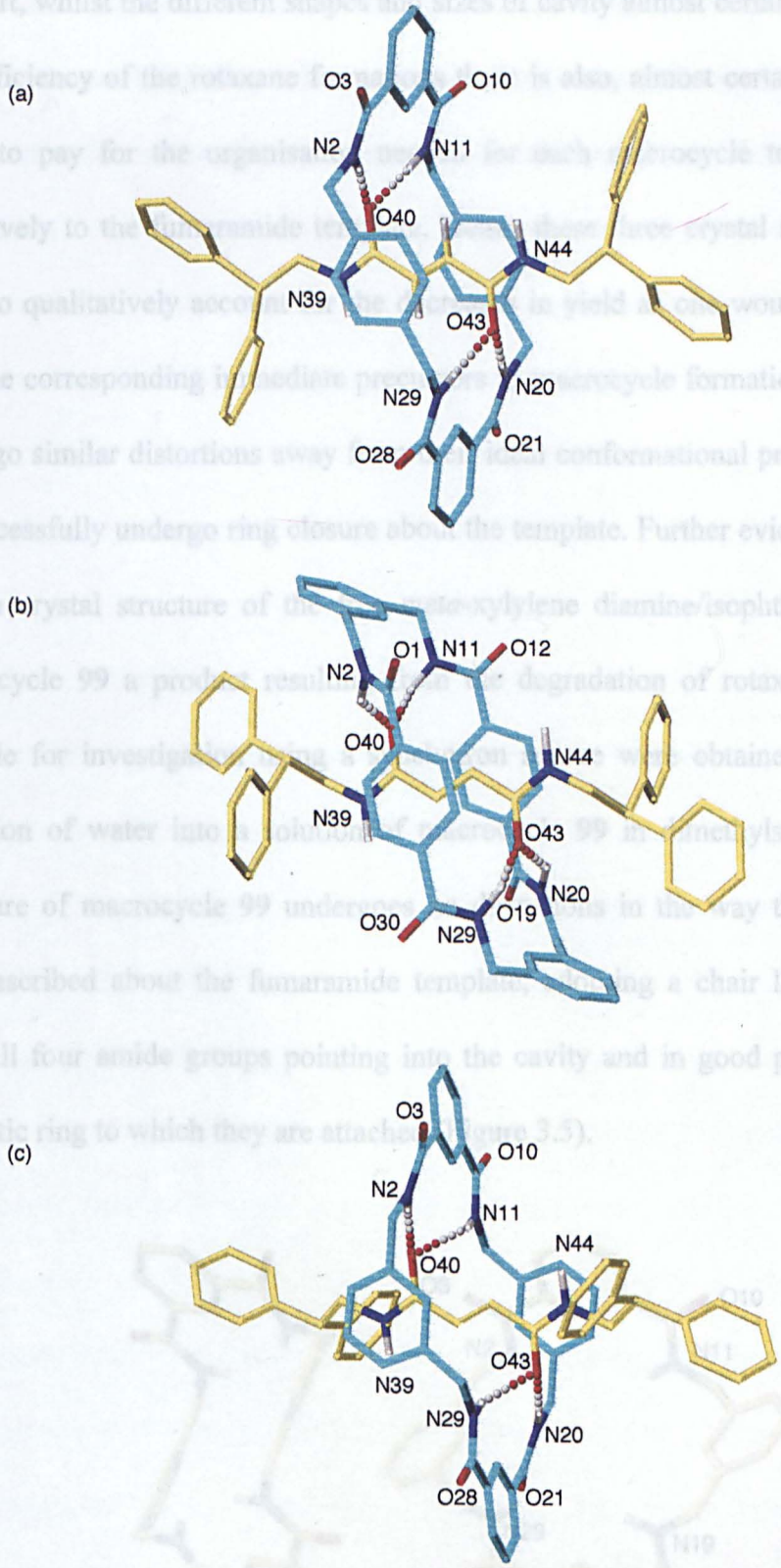


**Figure 3.4.** Solid state structure of the regioisomeric rotaxanes as determined by *X*-ray crystallography. For clarity, carbon atoms of the thread are shown in yellow and carbon atoms of the macrocycle blue; oxygen atoms are red, nitrogen dark blue and hydrogen white. (a) rotaxane **95**[4] selected interatomic distances [Å]: N2-O40/ N29-O43 2.06, N11-O4O/ N20-O43 1.98; dihedral angles [°]: O3-C3-C4-C9 –16.983, C7-C6-C10-O10 16.301, O21-C21-C22-C27 16.983, O28-C28-C24-C25 –16.301, (b) rotaxane **96**[12a] selected interatomic distances [Å]: N2-O40/ N29-O43 3.107, N11-O4O/ N20-O43 2.975; dihedral angles [°]: O1-C1-C34-C33 45.989, C14-C13-C12-O12 –42.243, O19-C19-C15-C16 –45.989, O30-C30-C31-C36 –45.989, (c) rotaxane **97**[12b] selected interatomic distances [Å]: N2-O40/N20-O43 3.007, N11-O40/ N29-O43 3.096 dihedral angles [°]:O3-C3-C4-C9 –28.855, C7-C6-C10-O10 6.329, O21-C21-C22-C27 –28.855, O28-C28-C24-C25 –6.329

In short, whilst the different shapes and sizes of cavity almost certainly play a role in the efficiency of the rotaxane formations there is also, almost certainly an energetic price to pay for the organisation needed for each macrocycle to hydrogen-bond effectively to the fumaramide template. Hence these three crystal structures can be used to qualitatively account for the decreases in yield as one would expect to find that the corresponding immediate precursors to macrocycle formation would have to undergo similar distortions away from their ideal conformational preference in order to successfully undergo ring closure about the template. Further evidence is provided by the crystal structure of the free *meta*-xylylene diamine/isophthaloyl dichloride macrocycle **99** a product resulting from the degradation of rotaxane **92**. Crystals suitable for investigation using a synchotron source were obtained from the slow diffusion of water into a solution of macrocycle **99** in dimethylsulphoxide.[12] The structure of macrocycle **99** undergoes no distortions in the way that it does when circumscribed about the fumaramide template, adopting a chair like conformation with all four amide groups pointing into the cavity and in good planarity with the aromatic ring to which they are attached (Figure 3.5).

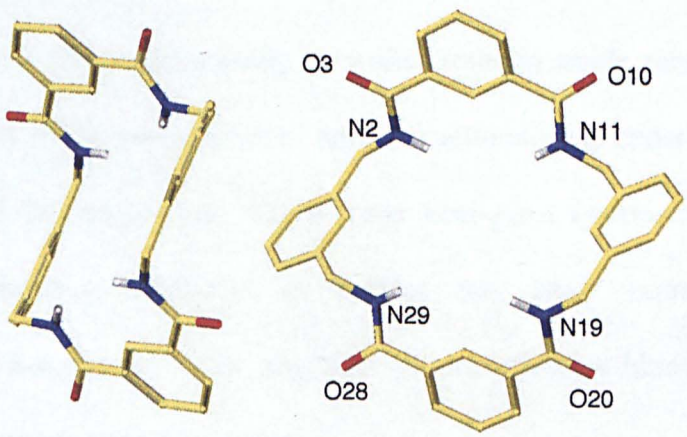


**Figure 3.5.** Solid state structure of the 1,3-1,3 macrocycle **99** as determined by *X*-ray crystallography.[13] For clarity, carbon atoms of the thread are shown in yellow and carbon atoms of the macrocycle blue; oxygen atoms are red, nitrogen dark blue and hydrogen white. Selected dihedral angles [°]:O3-C3-C4-C9 2.020, C7-C6-C10-O10 –4.047, O21-C21-C22-C27 –2.020, O28-C28-C24-C25 4.047

In conclusion, it has been shown that different macrocyclic components can be used in the hydrogen bond-directed construction of rotaxanes. The results may now allow the construction of threaded species with new and interesting rotational and shuttling properties.

## 3.1. A soluble macrocycle whose properties may be useful for the thermodynamically controlled assembly of rotaxanes

In Chapters two (p. 48) and this chapter (p.72) the hydrogen bond-assembled rotaxane formation described in Chapter one (p. 16) was studied to acquire more information about the assembly process. These systems were however also identified as being unsuitable for thermodynamically controlled rotaxane assembly as it would be difficult to incorporate functionality suitable for carrying out reversible bond forming reactions. In the following chapter the direction of the research is changed somewhat to find some property, which can be used in the thermodynamically controlled synthesis of rotaxanes. In light of the catenane synthesis described in Chapter one (p. 15) (incorporating chloroform soluble macrocycles) and its subsequent modification resulting in the results outlined in appendix I (p. 179), it was thought that the binding of an amide within the cavity of the component macrocycle may contribute to the assembly process of this structural class of catenane. In the following chapter, binding studies on the component mixed benzylic amide-ester macrocycles show the selective binding to single amide functionality over a wide variety of functional groups and some simple anions. Moving momentarily away from the goal of a thermodynamically controlled route to amide containing rotaxanes a thorough study of the recognition of amide functionality is undertaken by varying the structure of the macrocycle. Whilst many host-guest systems currently employ the hydrogen-bonding attributes of amides this study represents the first comprehensive assessment of the requirements for effective binding of the amide functionality over other functionalities.

## 3.2. Experimental

### Diphenylacetylglycylglycine, 2,2-diphenylester 89

The synthesis was carried out as is outlined in reference 3

### Glycylcglycine rotaxane 91

To a stirred solution of thread **89** (0.50 g, 0.99 mmol) and triethylamine (2.2 mL, 15.80 mmol) in anhydrous chloroform (150 mL) was added simultaneously over a period of four hours, solutions of *meta*-xylylene diamine (1.08 g, 7.91 mmol) in anhydrous chloroform (50 mL) and terephthaloyl dichloride (1.61 g, 7.91 mmol) in anhydrous chloroform (50 mL) using motor driven syringe pumps. When addition had been completed the reaction mixture was allowed to stir for a further eighteen hours after which time the reaction mixture was filtered. The filtrate was then washed with hydrochloric acid (0.2M, 100 mL) and saturated sodium bicarbonate solution (100 mL). The organic layer was then dried over magnesium sulphate, filtered and the solvent removed in *vacuo* to leave a cream solid. The rotaxane **91** was isolated using column chromatography (silica gel, 10% EtOAc/$CH_2Cl_2$). Yield: 0.28 g (20%); mp 154.5-156.3°C; $^1$H NMR (400 MHz, $CDCl_3$): $\delta$ = 2.04 (d, 2H, $J$ = 4.5 Hz, NHC$\underline{H}_2$CO), 2.49 (d, 2H, $J$ = 5.0 Hz, NHC$\underline{H}_2$CO), 3.19 (t, 1H, $J$ = 8.0 Hz, C$\underline{H}$CH$_2$), 4.41 (dd, 6H, $J$ = 14.0, 5.0 Hz, C$\underline{H}_2$NHCO$_{macrocylic}$ and CHC$\underline{H}_2$ from COSY), 4.47 (s, 1H, CHCO), 4.58 (dd, 4H, $J$ = 14.0, 5.5 Hz, C$\underline{H}_2$NHCO$_{macrocylic}$), 5.44 (t, 1H, J = 4.5 Hz, NH), 6.04 (t, 1H, $J$ = 5.0 Hz, NH), 6.98 (t, 4H, $J$ = 5.0 Hz, NH), 7.15-7.22 (m, 16H, ArCH), 7.23-7.37 (m, 20H, ArCH) $^{13}$C NMR (100 MHz, DMSO-$d_6$): $\delta$ = 40.52 ($CH_2$), 41.69 ($CH_2$), 43. 77 ($CH_2$), 49.29 (CH), 56.31 (CH), 67.13 ($CH_2$), 127.07 (ArCH), 127.26 (ArCH), 128.04 (ArCH), 128.13 (ArCH),

128.27 (ArCH), 128.53 (ArCH), 128.74 (ArCH), 128.81 (ArCH), 128.92 (ArCH), 128.94 (ArCH), 137.49 (q, ArC), 139.07 (q, ArC), 140.28 (q, ArC) 141.64 (q, ArC), 166.22 (CO) 167.00 (CO), 168.15 (CO) 173.03 (CO); FAB-MS (*m*BNA matrix): *m/z* = 1039 $[M+H]^+$ anal. calcd. for $C_{64}H_{58}N_6O_8$ (1038): C, 73.97; H, 5.63; N, 8.09; found: C, 73.78; H, 5.83; N, 7.99.

**Glycylglycine rotaxane 92**

To a stirring solution of thread **89** (0.50 g, 0.988 mmol) and triethylamine (2.2 mL, 15.8 mmol) in anhydrous chloroform (150 mL) was added simultaneously over a period of four hours, solutions of *meta*-xylylene diamine (1.08 g, 7.91 mmol) in anhydrous chloroform (50 mL) and isophthaloyl dichloride (1.61 g, 7.91 mmol) in anhydrous chloroform (50 mL) using motor driven syringe pumps. When addition had been completed the reaction mixture was allowed to stir for a further eighteen hours after which time the reaction mixture was filtered. The filtrate was then washed with hydrochloric acid (0.2M, 100 mL) and saturated sodium bicarbonate solution (100 mL). The organic layer was then dried over magnesium sulphate and the solvent removed in *vacuo* to leave a cream solid. The rotaxane was isolated using column chromatography (silica gel, 10% EtOAc/$CH_2Cl_2$). Yield: 0.02 g (2%); mp 125°C (decomp); $^1$H NMR (400 MHz, $CDCl_3$): δ = 2.27 (d, 2H, *J* = 5.5 Hz, NHC$\underline{H_2}$CO), 2.89 (d, 2H, *J* = 5.5 Hz, NHC$\underline{H_2}$CO), 4.20 (m, 5H, $H_E$ and CH from COSY) (m, 7H, $H_E$ and CH and $CH_2$ from COSY), 5.68 (t, 1H, *J* = 5.5 Hz, NH), 6.91 (s, 2H, ArCH), 6.96 (m, 4H, ArCH), 7.08 (m, 8H, ArCH), 7.14 (d, 4H, *J* = 7.5 Hz ArCH), 7.22 (m, 7H, ArCH + NH) 7.30 (m, 4H, ArCH), 7.58 (t, 2H, *J* = 7.5 Hz, $H_A$), 7.64 (t, 4H, *J* = 6.0 Hz, $H_D$), 7.99 (s, 2H, $H_C$), 8.13 (dd, 4H, *J* = 7.5, 1.5 Hz, $H_B$); $^{13}$C NMR (100 MHz, DMSO-$d_6$): δ = 40.92 ($CH_2$), 41.57 ($CH_2$), 44.65 ($CH_2$), 50.22 (CH), 58.78 (CH), 68.19 ($CH_2$), 121.66 (ArCH), 124.74 (ArCH), 128.04 (ArCH),

128.13 (ArCH), 128.27 (ArCH), 124.74 (ArCH), 127.55 (ArCH), 128.06 (ArCH), 128.44 (ArCH), 129.16 (ArCH), 130.89 (ArCH) 131.60 (ArCH), 132.05 (q, ArC), 138.85 (q, ArC), 139.21 (q, ArC) 140.76 (q, ArC), 167.31 (CO) 169.59 (CO), 170.52 (CO) 173.42 (CO); FAB-MS (*m*BNA matrix): *m/z* = 1039 $[M+H]^+$; anal. calcd. for $C_{64}H_{58}N_6O_8$ (1038): C, 73.97; H, 5.63; N, 8.09; found: C, 73.90; H, 5.81; N, 8.12.

**(*E*)-*N,N'-bis* (2,2-diphenylethyl)-2-butendiamide 94**

To a stirred solution of 2,2-diphenylethylamine (3.80 g, 19.40 mmol) in $CHCl_3$ (50 mL) and triethylamine (3.7 mL, 27.75 mmol) at 0 °C was added dropwise a solution of fumaryl acid chloride (1.0 mL, 9.25 mmol) in $CHCl_3$ (20 mL) over a period of 30 minutes. The solution was then allowed to warm to room temperature and stirred for twelve hours under an $N_2$ atmosphere after which time a white precipitate had formed. The reaction mixture was then filtered and the white solid was washed with ether (3 x 10 mL) to afford the product as a flocculent white solid. Yield 2.70 g, 62%; mp 280°C; $^1$H NMR (400 MHz, $CDCl_3$): δ = 3.90 (dd, 4H, *J* = 7.9, 5.9 Hz, $CH_2$), 4.11 (t, 2H, *J* = 7.9 Hz, C<u>H</u>), 5.59 (t, 2H, *J* = 5.9 Hz, N<u>H</u>), 6.58 (s, 2H, COC<u>H</u>C<u>H</u>CO) and 7.17-7.34 (m, 20 H, ArCH); $^{13}$C NMR (100 MHz, DMSO-$d_6$): δ = 43.69 ($CH_2$), 50.30 (CH), 126.73 (ArCH), 128.20 (ArCH), 128.79 (ArCH), 132.89 (CO<u>C</u>H<u>C</u>HCO), 143.10 (q, ArC), 164.10 (CO); MS (FAB, *m*BNA): *m/z* = 475 $[M+H^+]$; anal. calcd. for $C_{32}H_{30}N_2O_2$ (474.59): C, 80.98; H, 6.37; N, 5.90; found: C, 80.63; H, 6.50; N, 5.69.

**Fumaramide rotaxane 96**

To a stirred solution of thread **94** (0.50 g, 0.99 mmol) and triethylamine (1.60 g, 2.20 mL, 15.80 mmol) in anhydrous chloroform (150 mL) was added simultaneously over a period of four hours, solutions of *meta*-xylylene diamine (1.08 g, 7.91 mmol) in

anhydrous chloroform (50 mL) and terephthaloyl dichloride (2.61 g, 7.91 mmol) in anhydrous chloroform (50 mL) using syringe pumps. When addition had been completed the reaction mixture was allowed to stir for a further eighteen hours after which time the reaction mixture was filtered. The filtrate was then washed with hydrochloric acid (0.2M, 100 mL) and saturated sodium bicarbonate solution (100 mL). The organic layer was then dried over magnesium sulphate and the solvent removed in *vacuo* to leave a cream solid. The rotaxane was isolated using column chromatography (silica gel, 2% methanol/$CH_2Cl_2$); Yield: 0.32 g, 30 %; mp 329.9-331.9°C; $^1$H NMR (400 MHz, DMSO-$d_6$): δ = 3.77 (4H, t, *J* = 6.5 Hz, CHC$\underline{H}_2$) 4.21 (2H, t, *J* = 6.5 Hz, C$\underline{H}$C$H_2$), 4.58 (d, 8H, *J* = 5.5 Hz, C$\underline{H}_2$NHCO), 4.85 (2H, s, COC$\underline{H}$C$\underline{H}$CO), 6.80 (8H, s, ArC$H_F$), 7.19 (4H, t, *J* = 7.5 Hz, ArCH), 7.31 (22H, m, ArCH), 7.74 (2H, s, ArC$H_C$), 8.00 (4H, t, *J* = 5.5 Hz, $CH_2N\underline{H}CO_{macrocycle}$), 8.35 (2H, t, *J* = 6.5 Hz, N$\underline{H}$COCH); $^{13}$C NMR (100 MHz, DMSO-$d_6$): δ = 43.37 ($CH_2$), 43.97 ($CH_2$), 50.76 (CH), 125.40 (ArCH), 126.54 (ArCH), 126.66, (ArCH), 126.93 (ArCH), 128.80 (ArCH), 128.91 (ArCH), 131.96 (ArCH), 132.08 (COC$\underline{H}$C$\underline{H}$CO), 138.15 (q, ArC), 139.54 (q, ArC), 143.21 (q, ArC), 165.30 (CO), 167.60 (CO); FAB-MS (*m*BNA matrix): *m/z* 1007 $[M+H]^+$; anal. calcd. for $C_{64}H_{58}O_6N_6$ (1006): C, 76.32; H, 5.80; N, 8.34; found C, 75.96; H, 5.83; N, 8.19.

**Fumaramide rotaxane 97**

To a stirred solution of thread **94** (0.50 g, 0.99 mmol) and triethylamine (1.60 g, 2.20 mL, 15.80 mmol) in anhydrous chloroform (150 mL) was added simultaneously over a period of four hours, solutions of *meta*-xylylene diamine (1.08 g, 7.91 mmol) in anhydrous chloroform (50 mL) and isophthaloyl dichloride (2.61 g, 7.91 mmol) in anhydrous chloroform (50 mL) using syringe pumps. When addition had been completed the reaction mixture was allowed to stir for a further eighteen hours after

which time the reaction mixture was filtered. The filtrate was then washed with hydrochloric acid (0.2M, 100 mL) and saturated sodium bicarbonate solution (100 mL). The organic layer was then dried over magnesium sulphate and the solvent removed in *vacuo* to leave a cream solid. The rotaxane was isolated using column chromatography (silica gel, 2% methanol/$CH_2Cl_2$); Yield: 0.03, 3%; mp: 332.2-334.2°C; $^1$H NMR (400 MHz, DMSO-$d_6$): δ = 3.67 (2H, t, *J* = 7.0 Hz, C<u>H</u>$CH_2$), 3.75 (4H, t, J = 7.0 Hz, CHC<u>H</u>$_2$), 4.06 (8H, d, *J* = 5.5 Hz, CONHC<u>H</u>$_{2macrocycle}$), 6.08 (2H, s, COC<u>H</u>C<u>H</u>CO), 6.68 (m, 4H, $ArCH_{macrocycle}$), 6.79 (m, 4H, $ArCH_{macrocycle}$), 7.19 (m, 8H, ArCH), 7.28 (m, 14H, ArCH + $CHCH_2N$<u>H</u>), 7.69 (2H, t, *J* = 8.0 Hz, $ArCH_A$), 8.03 (4H, d, *J* = 8.0 Hz, $ArCH_B$), 8.292 (4H, t, *J* = 5.0 Hz, NH), 8.52 (2H, brs, $ArCH_C$). $^{13}$C NMR (100 MHz, DMSO-$d_6$): δ = 42.51 ($CH_2$), 43.50 ($CH_2$), 50.07 (CH), 126.59 (ArCH), 126.91 (ArCH), 127.71, (ArCH), 127.80 (ArCH), 128.20 (ArCH), 128.51 (ArCH), 128.58 (ArCH), 128.64 (ArCH), 130.48 (ArCH), 131.59 (COC<u>H</u>C<u>H</u>CO), 134.77 (q, ArC), 137.94 (q, ArC), 142.72 (q, ArC), 166.04 (CO), 166.12 (CO); FAB-MS (*m*BNA matrix): *m/z* 1007 $[M+H]^+$; anal. calcd. for $C_{64}H_{58}O_6N_6$ (1006): C, 76.32; H, 5.80; N, 8.34; found C, 76.51; H, 5.64; N, 8.16.

**Macrocycle 98**

To a stirred solution containing rotaxane **91** (0.10 g, 0.096 mmol) in methanol (20 mL) was added sodium methoxide (0.05 g, 0.926 mmol) in methanol (5 mL), which resulted in the reaction mixture turning a cloudy white almost immediately. After stirring for a further hour a precipitate had formed which was filtered, washed with methanol (10 mL), dichloromethane (10 mL) and then dried *in vacuo* to leave the product as a white solid. Yield: 0.05 g, 95 %; mp: decomp 295°C; $^1$H NMR (400 MHz, DMSO-$d_6$): δ = 4.51 (d, 8H, *J* = 5.5 Hz, C<u>H</u>$_2$NHCO), 7.18 (d, 4H, *J* = 7.0 Hz,

$ArCH_B$), 7.29 (m, 4H, $ArCH_{A,C}$), 7.76 (s, 8H, $ArCH_F$), 9.15 (t, 4H, $J$ = 5.5 Hz, NH) $^{13}C$ NMR (100 MHz, DMSO-$d_6$): $\delta$ = 42.29 ($CH_2$), 122.83 (ArCH), 125.61 (ArCH), 127.31 (ArCH)), 128.16 (ArCH), 137.12 (q, ArC), 140.26 (q, ArC), 166.24 (CO); FAB-MS (*m*BNA matrix): *m/z* = 532 $[M+H]^+$; anal. calcd for $C_{32}H_{28}N_4O_4$ (532): C, 72.16; H, 5.30; N, 10.52; found: C, 71.90; H, 5.42; N, 10.54.

**Macrocycle 99**

To a stirred solution containing rotaxane **92** (0.10 g, 0.0963 mmol) in methanol (20 mL) was added sodium methoxide (0.05 g, 0.9259 mmol) in methanol (5 mL), which resulted in the reaction mixture turning a cloudy white almost immediately. After stirring for a further hour a precipitate had formed which was filtered, washed with methanol (10 mL), dichloromethane (10 mL) and then dried *in vacuo* to leave the product as a white solid. Yield: 0.05 g, 97 %; mp 300°C (decomp); $^1H$ NMR (400 MHz, DMSO-$d_6$) $\delta$ = 4.44 (d, 8H, $J$ = 6.0 Hz, $CH_2$), 7.20 (m, 8H, ArCH), 7.48 (t, 2H, $J$ = 7.5 Hz, ArCH), 7.97 (dd, 4H, $J$ = 7.5 Hz, 1.5 Hz, ArCH), 8.29 (s, 2H, ArCH) 9.06 (t, 4H, $J$ = 6.0 Hz, NH); $^{13}C$ NMR (100 MHz, DMSO-$d_6$) $\delta$ = 43.06 ($CH_2$), 126.23 (ArCH), 126.40 (ArCH), 126.96 (ArCH), 128.34 (ArCH), 128.44 (ArCH), 128.57 (ArCH), 134.50 (q, ArC), 140.16 (q, ArC), 165.21 (CO); FAB-MS (*m*BNA matrix): *m/z* = 532 $[M+H]^+$.

### 3.3. References


1. (a) D. B. Amabilino, J. F. Stoddart, *Chem. Rev.* **1995**, 2725-2828. (b) G. Schill, *Catenanes, Rotaxanes and Knots*, Academic Press, New York, **1971**.
2. (a) V. Bermudez, N. Capron, T. Gase, F. G. Gatti, F. Kajzar, D. A. Leigh, F. Zerbetto, S. Zhang, *Nature* **2000**, *406*, 608-611. (b) N. Amaroli, V. Balzani, J-P. Collin, P. Gavina, J-P. Sauvage, B. Ventura, *J. Am. Chem. Soc.* **1999**, *121*, 4397-4408. (c) R. A. Bissel, E. Córdova, A. E. Kaiefer, J. F. Stoddart, *Nature* **1994**, *369*, 133-137. (d) M. Fujita, F. Ibukuro, H. Hagihara, K. Ogura, *Nature* **1994**, *367*, 720-723.
3. D. A. Leigh, A. Murphy, J. P. Smart, A. M. Z. Slawin, *Angew. Chem. Int. Ed. Engl.* **1997**, *36*, 728-732.
4. F. G. Gatti, D. A. Leigh, S. Nepogdiev, S. J. Teat, A. M. Z. Slawin, J. K. Y. Wong, *J. Am. Chem. Soc.* In Press.
5. For accounts referring to self-assembly and template directed synthesis see: (a) D. Philp, J. F. Stoddart, *Angew. Chem. Int. Ed. Engl.* **1996**, *35*, 1154-1196. (b) D. S. Lawrence T. Jing, M. Levett, *Chem. Rev.* **1995**, 2229-2260. (c) J-M. Lehn, *Angew. Chem. Int. Ed. Engl.* **1990**, *29*, 1304-1319.
6. A. G. Johnston, D. A. Leigh, A. Murphy, J. P. Smart, M. D. Deegan, *J. Am. Chem. Soc.* **1996**, *118*, 10662-10663.
7. (a) A. G. Johnston, D. A. Leigh, L. Nezhat, J. P. Smart, M. D. Deegan, *Angew. Chem. Int. Ed. Engl.* **1995**, *34*, 1212-1216. (b) F. J. Carver, C. A. Hunter, R. J. Shannon, *J. Chem. Soc., Chem. Commun.* **1994**, 4124-4129. (c) S. G. Geib, C. Vincent, E. Fan, A. D. Hamilton. *Angew. Chem. Int. Engl.* **1993**, *32*, 119-121. (d) C. A. Hunter, D. H. Purvis, *Angew. Chem. Int. Ed. Engl.* **1992**, *31*, 792-795.

8. A. G. Johnston, D. A. Leigh, R. J. Pritchard, M. D. Deegan, *Angew. Chem. Int. Ed. Engl.* **1995**, *34*, 1209-1212.

9. H. L. Frisch, E. Wasserman, *J. Am. Chem. Soc.* **1961**, *83*, 3789-3795.

10. It has been shown that it is possible to synthesise rotaxanes incorporating 24-crown-10 as the macrocycle for examples see: (a) S. J. Cantrill, S. J. Rowan, J. F. Stoddart, *Org. Lett.* **1999**, *1*, 1363-1366. (b) A. G. Kolchinski, N. W. Alcock, R. A. Roesner, D. H. Busch, *Chem. Commun.* **1998**, 1437-1438. (c) P. R. Ashton, P. T. Glink, J. F. Stoddart, P. A. Tasker, A. J. P. White, D. J. Williams, *Chem. Eur. J.* **1996**, *2*, 729-736; It has also been shown that it is possible to synthesise rotaxanes incorporating cucurbituril; (d) D. Whang, K-M. Park, J. Heo, P. Ashton, K. Kim, *J. Am. Chem. Soc.* **1998**, *120*, 4899-4900.

11. $C_{34}H_{32}Cl_4N_2O_2$, $M$ = 642.42, crystal size 0.4 × 0.2 × 0.04 mm, triclinic P1, $a$ = 5.161(6), $b$ = 8.8928(10), $c$ = 17.013(2) Å, $\alpha$ = 101.723(3), $\beta$ = 95.524(3), $\gamma$ = 95.947(3)°, $V$ = 754.9(9)Å$^3$, $Z$ = 4, $\rho_{calcd}$ = 1.413 Mg m$^{-3}$; MoK/$\alpha$ radiation (graphite monochromator, $\lambda$ = 0.71073 Å), $\mu$ = 0.427 mm$^{-1}$, $T$ = 180(2)K. 3926 data (2629 unique, $R_{int}$ = 0.0406, $2.36<\theta<25.00°$), were collected on a Siemens SMART CCD diffractometer using narrow frames (0.3° in $\omega$), and were corrected semi-empirically for absorption and incident beam decay. The structure was solved by direct methods and refined by full-matrix least-squares on $F^2$ values of all data (G.M.Sheldrick, SHELXTL manual, Siemens Analytical *X*-ray Instruments, Madison WI, USA, 1993, version 5.0) to give $wR = \{\Sigma[w(F_o^2-F_c^2)^2]/\Sigma[w(F_o^2)^2]\}^{1/2}$ = 0.1404, conventional $R$ = 0.0552 for $F$ values of 2629 reflections with $F_o^2>2\sigma(F_o^2)$, $S$ = 0.909 for 190 parameters. Residual electron density extremes were 0.537 and –0.432 Å$^{-3}$. Hydrogens were added in calculated positions and constrained to a Riding model.

12. (a) $C_{66}H_{66}N_6O_8$, $M$ = 1071.25, crystal size 0.5 × 0.4 × 0.4 mm, monoclinic P2(1)/n, $a$ = 9.9757(2), $b$ = 18.3235(2), $c$ = 16.7744(3) Å, β = 106.04(6), $V$ = 2946.86(9)Å$^3$, $Z$ = 2, $\rho_{calcd}$ = 1.207 Mg m$^{-3}$; MoK/α radiation (graphite monochromator, λ = 0.71073 Å), μ = 0.080 mm$^{-1}$, $T$ = 180(2)K. 18241 data (7113 unique, $R_{int}$ = 0.0313, 2.22<θ<29.01°), were collected on a Siemens SMART CCD diffractometer using narrow frames (0.3° in ω), and were corrected semi-empirically for absorption and incident beam decay. The structure was solved by direct methods and refined by full-matrix least-squares on $F^2$ values of all data (G.M.Sheldrick, SHELXTL manual, Siemens Analytical *X*-ray Instruments, Madison WI, USA, 1997 version 5.0) to give $wR = \{\Sigma[w(F_o^2-F_c^2)^2]/\Sigma[w(F_o^2)^2]\}^{1/2}$ = 0.1089, conventional $R$ = 0.0428 for $F$ values of 7113 reflections with $F_o^2>2\sigma(F_o^2)$, $S$ = 0.942 for 366 parameters. Residual electron density extremes were 0.198 and –0.211 Å$^{-3}$. Hydrogens were added in calculated positions and constrained to a Riding model. (b) $C_{62}H_{58}N_6O_6$, $M$ = 983.14, crystal size 0.6 × 0.4 × 0.3 mm, monoclinic P2(1)/n, $a$ = 15.8946(5), $b$ = 21.4713(6), $c$ = 17.3090(4) Å, β = 109.692(2), $V$ = 5561.7(3)Å$^3$, $Z$ = 4, $\rho_{calcd}$ = 1.174 Mg m$^{-3}$; MoK/α radiation (graphite monochromator, λ = 0.71073 Å), μ = 0.076 mm$^{-1}$, $T$ = 180(2)K. 20463 data (6371 unique, $R_{int}$ = 0.1231, 1.36<θ<21.49°), were collected on a Siemens SMART CCD diffractometer using narrow frames (0.3° in ω), and were corrected semi-empirically for absorption and incident beam decay. The structure was solved by direct methods and refined by full-matrix least-squares on $F^2$ values of all data (G.M.Sheldrick, SHELXTL manual, Siemens Analytical *X*-ray Instruments, Madison WI, USA, 1997 version 5.0) to give $wR = \{\Sigma[w(F_o^2-F_c^2)^2]/\Sigma[w(F_o^2)^2]\}^{1/2}$ = 0.2839, conventional $R$ = 0.0899 for $F$ values of 6371 reflections with $F_o^2>2\sigma(F_o^2)$, $S$ = 1.009 for 709

parameters. Residual electron density extremes were 0.388 and –0.420 $Å^{-3}$. Hydrogens were added in calculated positions and constrained to a Riding model.

13. $C_{35}H_{40}N_4O_6S_2$, $M$ = 568.68, crystal size 0.3 × 0.2 × 0.14 mm, clinic, $a$ =8.9383(6), $b$ =9.5214(6), $c$ = 19.8899(13) Å, α = 86.169(2) β = 87.615(2) γ = 88.170(2)°, $V$ = $Å^3$, $Z$ = 2, $\rho_{calcd}$ 1.120 = Mg $m^{-3}$; MoK/α radiation (graphite monochromator, λ = 0.69290 Å), μ = 0.192 = $mm^{-1}$, $T$ = 293(2)K. 8840 data (7091 unique, $R_{int}$ = 0.0212, 2.00<θ<29.37°), were collected on a Siemens SMART CCD diffractometer using narrow frames (0.3° in ω), and were corrected semi-empirically for absorption and incident beam decay. The structure was solved by direct methods and refined by full-matrix least-squares on $F^2$ values of all data (G.M.Sheldrick, SHELXTL manual, Siemens Analytical *X*-ray Instruments, Madison WI, USA, 1997 version 5.0) to give $wR$ = $\{\Sigma[w(F_o^2-F_c^2)^2]/\Sigma[w(F_o^2)^2]\}^{1/2}$ = 0.1973, conventional $R$ = 0.0660 for $F$ values of reflections with $F_o^2>2\sigma(F_o^2)$, $S$ = 1.090 for 471 parameters. Residual electron density extremes were –0.696 and 0.090 $Å^{-3}$. Hydrogens were added in calculated positions and constrained to a Riding model.

# Chapter Four

## 4. The Selective Non-Covalent Recognition of a Functional Group Type

Selective biological recognition through the non-covalent interactions of neutral and anionic substrates is of relevance in many cases such as orthophosphate and sulphate binding in proteins,[1] and the self assembly of DNA.[2] As a result, the last decade has seen the development of synthetic receptors for neutral[3] and anionic guests[4] with a view to the development of receptor-based sensoric devices,[5] synthetic reagents and catalysts[6] (synthetic enzymes) facilitated by non-covalent interactions. Currently, the development of host-guest systems tends to focus on networks of complementary hydrogen bonding interactions between host and guest.[3] There has however been little attention paid to the construction of receptors capable of binding selectively to specific functional group types. Such an approach would be desirable in extrapolating from simple 'host-guest' chemistry to reagents and catalysts that recognise and orientate their substrates through non-covalent interactions. However, multi-point binding is normally required to generate strong and selective binding and few functional groups possess a sufficient number of 'handles' for this approach to be viable. Amides represent a class of functional group which posses a sufficient number of 'handles' suitable for the selective binding of neutral and anionic substrates. Here this concept is exemplified using amphiphilic benzylic amide macrocycles, the unlocked components of hydrogen bond-assembled catenanes.[7] These macrocycles are shown to form host-guest complexes selectively with secondary amides over a wide range of other carbonyl-containing functional group

types and also exhibit superior binding affinities for amides over simple anionic guests.

The synthesis and unusual solution properties of amphiphilic hydrogen bond assembled catenanes such as **36** (Figure 4.1) was recently reported.[7] These catenanes contain 1,3 isophthalamide clefts first introduced by Hamilton[3d,6] and so it was desirable to exploit this feature of the unlocked component macrocycles. The *X*-ray crystal structure of **36** shows that one macrocycle acts as a 'host' for a secondary amide group of the other macrocycle through four-point double bifurcated hydrogen bonding (Figure 4.1). $^1$H NMR spectra in $CDCl_3$ also indicate that both types of amide proton are involved in hydrogen bonding.

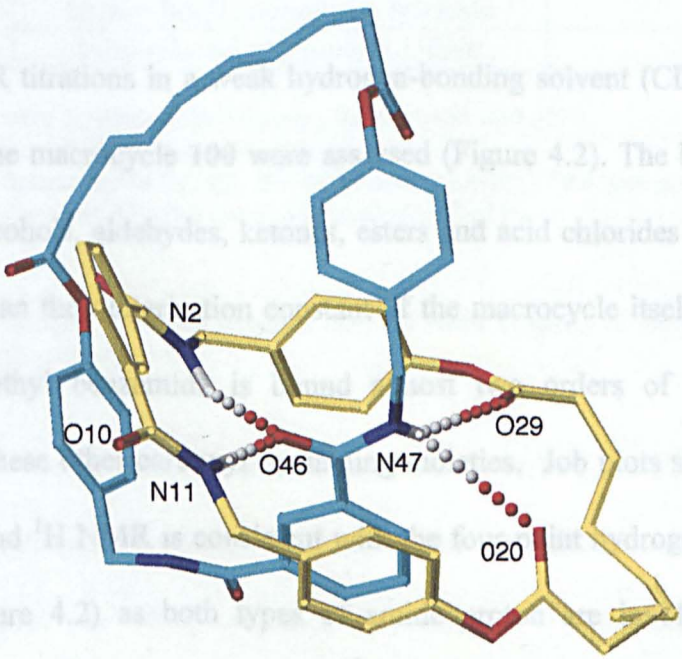


**Figure 4.1.** Solid state structure of the [2]catenane **36** as determined by *X*-ray crystallography.[7] For clarity, carbon atoms of one macrocycle are shown in yellow and carbon atoms of the other macrocycle blue; oxygen atoms are red, nitrogen dark blue and hydrogen white. Selected interatomic distances [Å]: N2-O46 3.232, N11 O46 2.989, 029-N47 3.365, O20-N47 3.483.

Encouraged, it was decided to assess the binding properties of the individual macrocyclic component **100** of the catenane **36** (Figure 4.2).

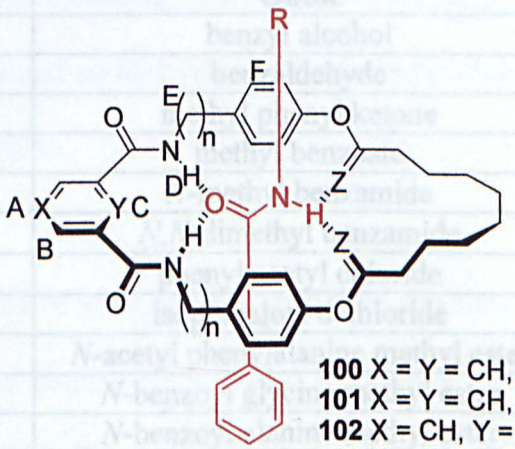


**100** X = Y = CH, Z = O, n = 1
**101** X = Y = CH, Z = $H_2$, n = 1
**102** X = CH, Y = N, Z = O, n = 1
**103** X = N, Y = CH, Z = O, n = 1
**104** X = $N^+MeI^-$, Y = CH, Z = O, n =1
**105** X = Y = CH, Z = O, n = 2

**Figure 4.2.** Proposed binding motif for recognition of secondary amides by benzylic amide macrocycles **100-105**.

Using $^1$H NMR titrations in a weak hydrogen-bonding solvent ($CDCl_3$) the binding properties of the macrocycle **100** were assessed (Figure 4.2). The binding constants of **100** with alcohols, aldehydes, ketones, esters and acid chlorides are all small and actually less than the dimerisation constant of the macrocycle itself (Table 4.1). In contrast, *N*-methyl benzamide is bound almost two orders of magnitude more strongly than these other carbonyl containing moieties. Job plots show that this is a 1:1 complex and $^1$H NMR is consistent with the four-point hydrogen bond structure indicated (Figure 4.2) as both types of amide proton are involved in hydrogen bonding. As the results also show, binding of simple amino-acid derivatives to **100** is one order of magnitude higher than that found for *N*-methylbenzamide. Bulkier amino-acid derivatives such as phenylalanine however, cannot be accommodated in the cavity of **100** because the bulky side-chain inhibits binding within the macrocycle. This feature is of particular interest because of its potential use in the recognition of peptide fragments. Tertiary amides, such as *N*,*N*-dimethylbenzamide

are not bound strongly because the second alkyl group prevents the bifurcated hydrogen-bonding motif adopted by secondary amides.

| Macrocycle | Guest | Binding Constant $M^{-1}$ |
|---|---|---|
| **100** | benzyl alcohol | ~0.1 |
| **100** | benzaldehyde | 5.2 |
| **100** | methyl phenyl ketone | 7.78 |
| **100** | methyl benzoate | 3.45 |
| **100** | *N*-methyl benzamide | 588 |
| **100** | *N*,*N*-dimethyl benzamide | 9.5 |
| **100** | phenyl acetyl chloride | 10.2 |
| **100** | isophthaloyl dichloride | 9.2 |
| **100** | *N*-acetyl phenylalanine methyl ester | ~4 |
| **100** | *N*-benzoyl glycine methyl ester | 1300 |
| **100** | *N*-benzoyl alanine methyl ester | 2370 |
| **101** | *N*-methyl benzamide | 11.1[a] |
| **102** | *N*-methyl benzamide | 380[b] |
| **103** | *N*-methyl benzamide | 825 |
| **104** | *N*-methyl benzamide | 99 |
| **105** | *N*-methyl benzamide | ~1.0[a] |
| **100** | tetra-*n*-butyl ammonium chloride | 304 |
| **100** | tetra-*n*-butyl ammonium bromide | 251 |
| **100** | tetra-*n*-butyl ammonium iodide | 146 |

Binding constants were determined by following the chemical shift of $H_c$
Self-association constant of the macrocycle 8.4 $M^{-1}$
[a] binding constant determined in $C_2D_2Cl_4$ due to the poor solubility of the host in $CDCl_3$
[b] binding constant determined by following the chemical shift of $H_E$

**Table 4.1.** Binding constants obtained from $^1H$ NMR titrations of macrocyclic hosts **100-105** with various guests.

The selectivity for secondary amides over other carbonyl containing functional groups can be rationalised on two accounts. In the first instance, amide carbonyls as H-bond acceptors are vastly superior to other C=O functional group types.[8] Secondly, the co-operative binding of the proton of the guest amide group[9] (i) increases the number of host-guest hydrogen-bonding interactions from two to four and (ii) increases the basicity of the amide oxygen atom making it an even stronger hydrogen bond acceptor. Put simply, both 'handles' within the amide functionality are made use of in the recognition process. The advantages of having such an arrangement of atoms to construct one binding site that can subsequently bind all the

functionality within an amide group are clear; selective binding of a functional group type is made possible. In contrast, the tetra-amide macrocycles of Hunter and Vogtle[10] have two binding sites and as a result bind to dicarbonyl compounds, esters, acid chlorides and amides with little selectivity other than that defined by hydrogen bonding basicities.

The importance of secondary (co-operative) binding interactions is clearly shown by comparing the binding of *N*-methyl benzamide by **100** with a range of analogous macrocycles **101-105** which were synthesised in order to asses the structural tolerance of this system (Figure 4.2). In the case where the ester linkages are replaced with ether linkages to give macrocycle **101**, primary amide selectivity is 'switched off' and the binding is very low. Considering that ester carbonyls are poor hydrogen-bond acceptors this result shows the real power and importance of co-operative binding interactions. Similarly, the use of a 2,6-pyridine unit (macrocycle **102**) decreases binding (a result conflicting with Hunter's proposals),[10b] as the lone-pair of the pyridine would point directly in the direction of the lone-pair of any carbonyl atom bound within the cavity: a highly disfavoured interaction. In contrast, there is a slight increase when a 3,5-pyridine unit is used (macrocycle **103**): the *exo*-nitrogen can pull electron density in its direction and away from the nitrogen atoms of the amides making them more acidic. Surprisingly the methylated counterpart of the *exo*-pyridyl macrocycle (macrocycle **104**) shows much weaker binding. This decrease in binding suggests that the iodide counterion is associated closely with the macrocycle sitting in or near the cavity preventing the guest from entering and binding. Crystals suitable for investigation using a synchotron radiation source were grown from the slow evaporation of **104** in a solution of ethanol.[11] The results of the

investigation confirm this theory showing that each macrocycle shares the iodine counterion through hydrogen-bonding to alternating amide groups (Figure 4.3).

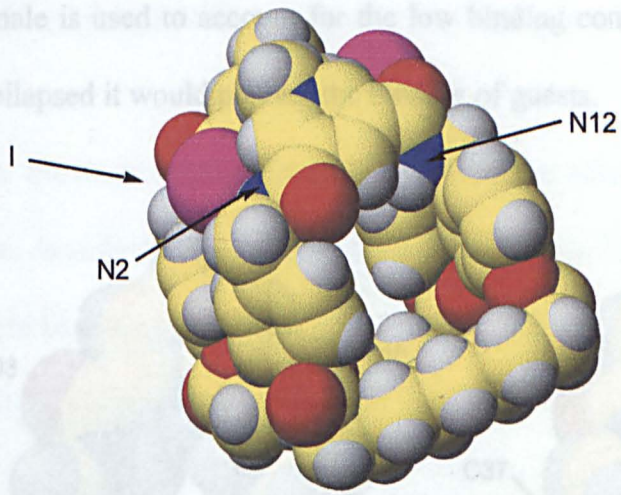


**Figure 4.3.** Solid state structure of the macrocycle **104** as determined by *X*-ray crystallography.[11] Carbon atoms are shown in yellow; oxygen atoms are red, nitrogen dark blue, iodide purple and hydrogen white. Selected interatomic distances [Å]: N2-I 3.636, N12-I 4.172.

Other subtle structural changes within the macrocycle also have remarkable consequences. Tyramine macrocycle **105** (employing a phenylethyl spacer) did not exhibit any binding to amides at all. Crystals of the *endo*-pyridyl macrocycle **102** suitable for investigation using a synchotron radiation source were obtained *via* slow evaporation of a solution of **102** in ethanol,[12] and crystals of the tyramine derived macrocycle **105** suitable for investigation *via* conventional crystallography were obtained from the slow evaporation of a solution of **105** in dichloromethane.[13] The *endo*-pyridyl macrocycle shows nicely how the rigid benzylic unit enforces a cavity on the macrocycle which, may be used to accommodate various guests (Figure 4.4). In this case no guest is bound and so the cavity attempts (unsuccessfully) to collapse

allowing aromatic stacking of the benzylic rings. The rigid benzylic spacer does not allow this to occur effectively, whereas tyramine macrocycle **105** which is much less rigid as a result of the extra $CH_2$ has the flexibility necessary for its cavity to collapse and the aromatic units to stack together effectively in the solid state (Figure 4.4). The same rationale is used to account for the low binding constant, as in solution if the cavity is collapsed it would prevent the binding of guests.

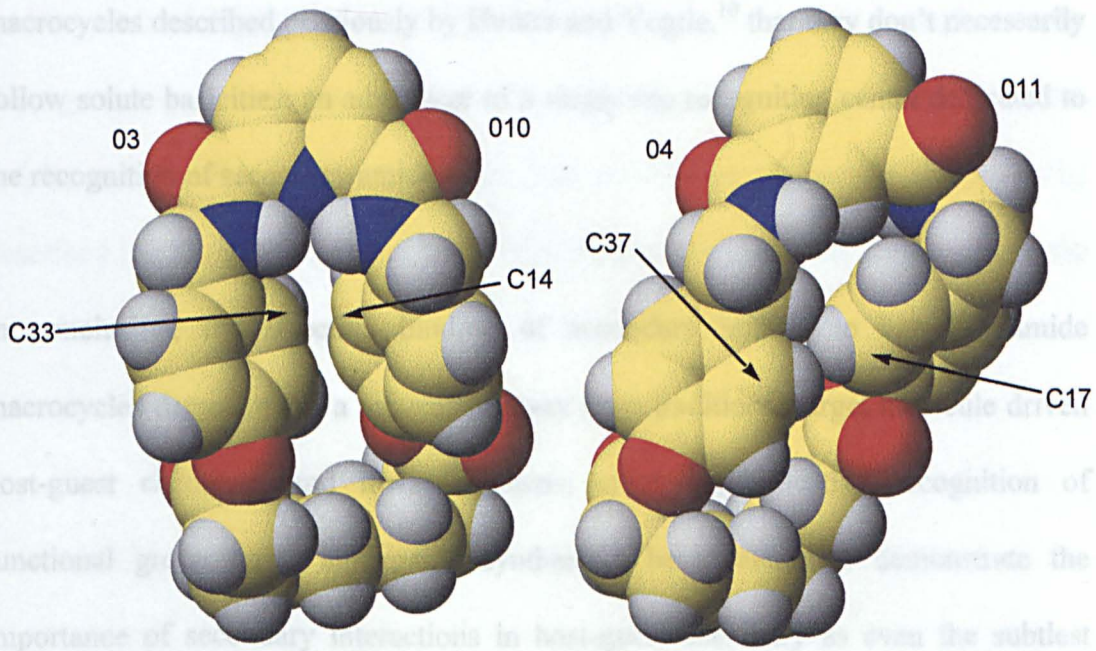


**Figure 4.4.** Solid state structure of the macrocycles **102** and **105** as determined by *X*-ray crystallography.[12] Carbon atoms are shown in yellow and carbon atoms; oxygen atoms are red, nitrogen dark blue and hydrogen white.

As the crystal structure of the methylated macrocycle **104** shows, these macrocycles demonstrate an ability to bind anions. It was therefore decided to assess the binding constants of the macrocycle **100** with halide anions (Table 4.1). The binding constants with chloride, bromide and iodide are all smaller than *N*-methylbenzamide, which is surprising considering that acyclic isophthalamide derivatives have been shown to bind anions with binding constants of up to $10^5$.[14] This is explained if several points are considered:

The large size of the anions might prevent them from entering and binding within macrocyclic cavity.

The aromatic rings of the benzylic unit direct electron density into the cavity, which will disfavour anion binding.

If the carbonyl functionality of the ester is pointing into the cavity it will disfavour anion binding.

Once again, the macrocycles described here offer the advantage over the tetralactam macrocycles described previously by Hunter and Vogtle,[10] that they don't necessarily follow solute basicities: an advantage of a single site recognition centre dedicated to the recognition of secondary amides.

In conclusion, the selective binding of secondary amides to benzylic amide macrocycles demonstrates a movement away from traditional target molecule driven host-guest chemistry and toward systems employing selective recognition of functional group types in organic synthesis. The results also demonstrate the importance of secondary interactions in host-guest chemistry as even the subtlest changes to structure can have dramatic effects! The potential use of these systems for peptide recognition, as catalysts and as reagents is now currently under investigation.

## 4.1. A first attempt at a thermodynamically controlled synthesis?

In this chapter (p. 95) the remarkable binding properties of mixed benzylic amide ester macrocycles have been described. In the following chapter the issue of a thermodynamically controlled synthesis of rotaxanes will be addressed for the first time. The Chapter describes a synthesis of a [2]rotaxane making use of the binding properties described in this chapter (p. 94) and the slippage concept outlined in chapter one (p. 18-20). Although essentially no successful outcome is obtained and no new methodology is described the chapter serves as a perfect example of why slippage is a poor route to rotaxanes and why thermodynamically controlled routes employing reversible covalent bond formations are necessary such as the one to be described in Chapter six (p 126). In addition the ideal size of a stopper to prevent the mixed benzylic amide-ester magic rings from falling off the dumbbell component of a rotaxane is discovered.

## 4.2. Experimental

### Preparation of 4-hydroxybenzylamine

The synthesis was carried out as is outlined in reference 5b

### *N,N'*-bis(4-hydroxybenzyl)isophthalamide

The synthesis was carried out as is outlined in reference 7

### *N,N'*-bis[(4-hydroxyphenyl)ethyl]isophthalamide

A mixture of isophthaloyl dichloride (1.52 g, 7.5 mmol) and triethylamine (1.14 g, 1.38 mL, 11.3 mmol) in anhydrous tetrahydrofuran (100 mL) was added dropwise over a period of one hour to a stirred suspension of tyramine (2.26 g, 16.5 mmol) in anhydrous tetrahydrofuran (150 mL) at room temperature, under argon. After stirring for a further 24 hours, the reaction mixture was filtered and the filtrate concentrated to give a yellow solid, which was purified by column chromatography to give a white solid. Yield: 1.82 g, 60 %; m.p. 231-235°C. $^{1}$H NMR (400 MHz, DMSO-$d_6$): $\delta$ = 2.74 (t, 4H, $J$ = 6.0 Hz, NHCH$_2$C$\underline{H}_2$), 3.43 (q, 4H, $J$ = 6.0 Hz, NHC$\underline{H}_2$CH$_2$), 6.64 (d, 4H, $J$ = 8.5 Hz, ArCH), 7.03 (d, 4H, $J$ = 8.5 Hz, ArC$\underline{H}$), 7.53 (t, 1H, $J$ = 7.5 Hz, ArC$\underline{H}$), 7.93 (dd, 2H, $J$ = 7.5 Hz, 1.5 Hz ArC$\underline{H}$), 8.28 (t, 1H, $J$ = 1.5 Hz ArC$\underline{H}$), 8.62 (t, 2H, $J$ = 6.0 Hz, N$\underline{H}$), 9.17 (s, 2H, O$\underline{H}$). $^{13}$C NMR (100 MHz, DMSO-$d_6$) $\delta$ = 34.67 (CH$_2$), 41.68 (CH$_2$), 115.50 (ArCH), 126.54 (ArCH), 128.63 (ArCH), 129.86 (from HMBC, q, ArC and ArCH), 133.70 (from HMQC, 2 x ArCH), 135.21 (q, ArC), 138.61 (q, Ar$\underline{C}$), 156.00 (q, Ar$\underline{C}$), 166.09 ($\underline{C}$O); FAB MS (*m*BNA matrix) *m/z* 405 [M+H]$^{+}$; anal. calcd. for $C_{24}H_{24}N_2O_4$(404): C, 71.3 %; H, 5.9 %; N, 6.9 %; found: C, 71.1 %; H, 6.1%; N, 6.8 %.

**_N,N'_-bis(4-hydroxybenzyl)3,5-pyridinedibenzamide**

To a stirred solution of hydroxybenzylamine (6.77 g, 55.0 mmol) and triethylamine (8.53 mL, 60.0 mmol) in anhydrous tetrahydrofuran (280 mL) was added dropwise pyridine-3,5-dicarbonyl dichloride (5.10 g, 25.0 mmol) in anhydrous tetrahydrofuran (280 mL). After sixteen hours, the resulting brown precipitate was filtered and the filtrate concentrated to 250 mL and hydrochloric acid added (0.5 M, 100 mL) followed by chloroform (100 mL). The organic layer was then washed with distilled water (2 x 100 mL), dried over magnesium sulphate, filtered and then concentrated to give an orange gum which was recrystallised from acetonitrile to give the product as a pale orange solid. Yield: 9.19 g, 97%; m.p. 209.9-211.0°C; $^{1}$H NMR (300 MHz, DMSO-$d_6$) $\delta$ = 4.39 (d, 4H, $J$ = 6.0 Hz, $C\underline{H}_2$), 6.71 (d, 4H, $J$ = 8.0 Hz, ArCH), 7.14 (d, 4H, $J$ = 8.0 Hz, ArCH), 8.64 (t, 1H $J$ = 2.0 Hz, PyCH), 9.12 (d, 2H, $J$ = 2.0 Hz, PyCH), 9.25 (t, 2H, $J$ = 6.0 Hz, NH), 9.32 (s, 2H, OH). $^{13}$C NMR (100 MHz, DMSO-$d_6$) $\delta$ = 46.2 ($CH_2$), 118.9 (ArCH), 133.0 (ArCH), 133.2 (ArCH), 133.5 (q, ArC), 137.9 (ArCH), 154.4 (q, ArC), 160.3 (q, ArC), 166.0 (CO) FAB MS (*m*BNA matrix): *m/z* 378 $[M+H]^+$; HRMS 377.1376 $[M+H]^+$ calculated for: $C_{21}H_{19}N_3O_4$ (+H), found: 377.1374

**_N,N'_-bis(4-hydroxybenzyl)-2,6-pyridinedibenzamide**

To a stirred solution containing 4-hydroxybenzylamine (2.65 g, 21.57 mmol) and triethylamine (3.0 mL, 21.57 mmol) in anhydrous tetrahydrofuran (150 mL) at –78°C was added dropwise over a period of one hour a solution containing 2,6-pyridine dicarbonyl chloride (2.00 g, 9.80 mmol) in anhydrous tetrahydrofuran (100 mL). The reaction mixture was then allowed to warm to room temperature and stir overnight after which it was filtered and washed with tetrahydrofuran (20 mL). The combined organic filtrate was then dried over magnesium sulphate, filtered and concentrated to

give the product as a yellow solid. Yield: 2.60 g, 73 %; m.p. 181.1-181.4°C; $^{1}$H NMR (400 MHz, DMSO-$d_6$) δ = 4.48 (d, 4H, *J* = 6.5 Hz, CONHC<u>H</u>$_2$), 6.71 (d, 4H, *J* = 8.5 Hz, ArCH), 7.12 (d, 4H, *J* = 8.5 Hz, ArCH), 8.21 (m, 3H, PyCH), 9.30 (s, 2H, OH), 9.80 (t, 2H, *J* = 6.5 Hz, NH); $^{13}$C NMR (100 MHz, DMSO-$d_6$) δ = 42.02 ($CH_2$), 115.44 (ArCH), 124.79 (ArCH), 128.61 (ArCH), 129.84 (q, ArC), 139.86 (ArCH), 149.13 (q, ArCH), 160.3 (q, ArC), 163.53 (CO); FAB MS (*m*BNA matrix): *m/z* 378 $[M+H]^+$; anal. calcd. for $C_{21}H_{19}N_3O_4$ (377): C, 66.83; H, 5.07; N, 11.13; found C, 66.46; H, 5.45; N, 10.94.

**Macrocycle 100**

The synthesis was carried out as is outlined in reference 7

**Macrocycle 101**

Under an atmosphere of argon, a stirred suspension of *N,N'*-bis(4-hydroxybenzyl)isophthalamide (0.50 g, 1.33 mmol), 1,10-dibromodecane (0.60 g, 1.99 mmol) and potassium carbonate (0.28 g, 1.99 mmol) in acetone (500 mL) was brought to reflux. The reaction mixture was then stirred over a period of forty-eight hours after which it was filtered and the solvent removed by rotary evaporation to leave a cream colored solid. This was then dried further in *vacuo* and then purified by column chromatography (4 % methanol/ dichloromethane) to give the product as a white solid. Yield: 0.24 g, 35 %; m.p. 247.1-248.9 °C; $^{1}$H NMR (400 MHz, $C_2D_2Cl_4$) δ = 1.18 (bm, 12H, alkyl $CH_2$), 1.33 (m, 4H, $CH_2$), 1.65 (p, 4H, *J* = 6.5 Hz, $COCH_2$), 3.84 (t, 4H, *J* = 6.5 Hz, $COCH_2$), 4.41 (d, 4H, *J* = 5.0 Hz, CONHC<u>H</u>$_2$), 6.28 (t, 2H, *J* = 5.0, CONH), 6.76 (d, 4H, *J* = 8.5 Hz, ArCH), 7.14 (d, 4H, *J* = 8.5 Hz, ArCH), 7.49 (t, 1H, *J* = 7.5 Hz, ArCH), 7.69 (s, 1H, ArCH), 7.95 (dd, 2H, *J* =

7.5 Hz, 1.5 Hz, ArCH); $^{13}$C NMR (100 MHz, $C_2D_2Cl_4$) δ = 26.80 (from HMQC, 2 x $CH_2$), 29.73 ($CH_2$), 30.45 ($CH_2$), 45.16 ($CH_2$), 68.59 ($CH_2$) 115.97 (ArCH), 124.75 (ArCH), 130.52 (q, ArC), 130.60 (ArCH), 130.87 (ArCH), 132.03 (ArCH), 135.63 (q, ArC), 159.81 (q, ArC), 167.30 (CO); FAB-MS: (*m*BNA matrix): *m/z* 515 $[M+H]^+$; anal. calcd. for $C_{32}H_{38}N_2O_4$ (514): C, 74.68 %; H, 7.44 %; N, 5.44 %; found: C, 74.97 %; H, 7.31 %; N, 5.25 %.

**Macrocycle 102**

Under an atmosphere of argon, suspensions of *N,N'*-bis(4-hydroxybenzyl)-2,6-pyridinedibenzamide (0.50 g, 1.38 mmol) in anhydrous tetrahydrofuran (100 mL) and sebacoyl dichloride (0.35 mL, 1.65 mmol) in anhydrous tetrahydrofuran (100 mL) were added simultaneously to a stirred solution of triethylamine (0.40 mL, 3.03 mmol) in anhydrous tetrahydrofuran (500 mL) over a period of one hour. The reaction mixture was stirred over a period of eighteen hours after which time a precipitate had formed. The reaction mixture was filtered and the solvent removed by rotary evaporation to leave a yellow oil. This was then dried further in *vacuo* giving a pale yellow foam. Column chromatography (1 % methanol/ dichloromethane) yielded the product as a white solid. Yield: 0.88 g, 52 %. m.p. 199.1-199.3°C; $^1$H NMR (400 MHz, $CDCl_3$) δ = 1.43 (m, 8H, $CH_2$), 1.59 (m, 4H, $CH_2$), 1.78 (m, 4H, $CH_2$), 2.59 (t, 4H, *J* = 6.5 Hz, $COCH_2$), 4.62 (d, 4H, *J* = 6.0 Hz, $CONHC\underline{H}_2$), 7.04 (d, 4H, *J* = 8.5 Hz, ArCH), 7.32 (d, 4H, *J* = 8.5 Hz, ArCH), 7.80 (t, 2H, *J* = 6.0 Hz, NH), 8.05 (t, 1H, *J* = 8.0 Hz, PyCH), 8.37 (d, 2H, *J* = 8.0 Hz, PyCH); $^{13}$C NMR (100 MHz, $CDCl_3$) δ = 25.14 ($CH_2$), 28.35 ($CH_2$), 28.83 ($CH_2$), 34.37 ($CH_2$), 43.54 ($CH_2$), 122.58 (ArCH), 125.57 (ArCH), 129.62 (ArCH), 135.59 (q, ArC), 139.61 (ArCH), 149.01 (q, ArC), 150.72 (q, ArC), 163.38 (CO), 172.68 (CO); FAB-MS (*m*BNA

matrix): *m/z* $[M+H]^+$; anal. calcd. for $C_{31}H_{33}N_3O_6$; C, 68.49 %; H, 6.12 %; N, 7.73 %; found C, 68.23 %; H, 5.87 %; N, 7.56 %.

**Macrocycle 103**

Under an atmosphere of argon, solutions of *N,N'*-bis(4-hydroxybenzyl)-3,5-pyridinedibenzamide (1.17 g, 3.1 mmol) in anhydrous tetrahydrofuran (100 mL) and sebacoyl dichloride (0.82 g, 3.4 mmol) in anhydrous tetrahydrofuran (100 mL) were added simultaneously to a stirred solution of triethylamine (0.91 mL, 6.5 mmol) in anhydrous tetrahydrofuran (900 mL) over a period of one hour. The reaction mixture was stirred over a period of eighteen hours after which time a precipitate had formed. The reaction mixture was filtered and the solvent removed by rotary evaporation to leave a yellow oil. This was then dried further in *vacuo* giving a pale yellow foam. Column chromatography (1 % methanol/ dichloromethane) yielded the product as a white solid. Yield: 0.88 g, 52 %. m.p. 215.2-215.7°C; $^1$H NMR (400 MHz, $CDCl_3$) δ = 1.37 (brm, 8H, $CH_2$), 1.72 (m, 4H, $CH_2$), 2.57 (t, 4H, $J$ = 6.5 Hz, $COCH_2$), 4.60 (d, 4H, $J$ = 5.5 Hz, $CONHC\underline{H}_2$), 6.49 (brm, 2H, NH), 7.06 (d, 4H, $J$ = 8.5 Hz, ArCH), 7.36 (d, 4H, $J$ = 8.5 Hz, ArCH), 8.04 (s, 1H, PyCH), 9.21 (s, 2H, PyCH); $^{13}$C NMR (100 MHz, $CDCl_3$), δ = 25.81 ($CH_2$), 29.14 ($CH_2$), 30.15 ($CH_2$), 34.44 ($CH_2$), 44.56 ($CH_2$), 122.59 (ArCH), 129.74 (ArCH), 130.29 (q, ArC), 131.49 (ArCH), 134.81 (q, ArC), 135.03 (q, ArC), 152.18 (ArCH), 165.58 (CO), 172.73 (CO); FAB-MS (*m*BNA matrix): *m/z* 544 $[M+H]^+$; anal. calcd. for $C_{31}H_{33}N_3O_6$ (543): C, 68.6 %; H, 6.1 %; N, 7.7 %; found C, 68.4 %; H, 6.2 %; N 7.7 %.

**Macrocycle 104**

To a stirred solution of Macrocycle **103** (0.04 g, 74 mmol) in THF (6 mL) was added dropwise a large excess of methyl iodide (2.00 mL). The reaction mixture was allowed to stir overnight and then dried *in vacuo* to leave a yellow solid which was

purified by column chromatography (methanol: chloroform, 1:99) then recrystallisation from acetonitrile to give the desired product. Yield: 0.04 g, 80 %; m.p. 159.9-162.2°C; $^{1}$H NMR (400 MHz, $CDCl_3$) δ 1.37 (bm, 8H, alkyl C$\underline{H_2}$), 1.68 (bm, 4H, alkyl C$\underline{H_2}$), 2.57 (t, 4H, $J$ = 6.5 Hz, COC$\underline{H_2}$), 4.12 (s, 3H, $NCH_3$), 4.57 (d, 4H, $J$ = 5.5 Hz, CONHC$\underline{H_2}$), 7.03 (d, 4H, $J$ = 8.5 Hz, ArCH), 7.47 (d, 4H, $J$ = 8.5 Hz, ArCH), 8.81 (bs, 2H, PyCH), 9.09 (brs, 1H, PyCH), 9.19 (bt, 2H, $J$ = 5.5 Hz, NH); $^{13}$C NMR (100 MHz, $CDCl_3$ from HMQC and HMBC), δ = 25.28 ($CH_2$), 30.06 ($CH_2$), 30.23 ($CH_2$), 34.32 ($CH_2$), 43.05 ($CH_2$), 49.85 ($CH_3$), 122.38 (ArCH), 130.57 (ArCH), 131.13 (q, ArC), 135.46 (q, ArC), 140.98 (ArCH), 146.61 (ArCH), 150.63 (q, ArC), 160.17 (CO), 173.17 (CO); FAB-MS (*m*BNA matrix): *m/z* 588 $[M\text{-}I]^+$; anal. calcd. for $C_{32}H_{36}N_3O_6I$ (715); C, 56.2 %; H, 5.4 %; N, 7.7 %; I, 17.5 %; found C, 56.4 %; H, 5.6 %; N, 7.6 %; I, 17.3 %.

**Macrocycle 105**

Under an atmosphere of argon, solutions of *N,N'*-bis(4-hydroxyphenylethyl)isophthalamide (0.28 g, 0.69 mmol) in anhydrous tetrahydrofuran (100 mL) and sebacoyl dichloride (0.17 g, 0.15 mL, 0.71 mmol) in anhydrous tetrahydrofuran (100 mL) were added simultaneously to a stirred solution of triethylamine (5.52 g, 7.60 mL, 54.6 mmol) in tetrahydrofuran (900 mL) over a period of one hour. The reaction mixture was stirred over a period of eighteen hours after which time a precipitate had formed. The reaction mixture was filtered and the solvent removed by rotary evaporation to leave a yellow oil. This was then dried further in *vacuo* giving a pale yellow foam. Column chromatography (1 % methanol/ dichloromethane) yielded the product as a white solid. Yield: 0.18 g, 46 %; m.p. 236-238°C; $^{1}$H NMR (400 MHz, $CDCl_3$) δ = 1.37 (bm, 8H, alkyl $CH_2$), 1.74 (m, 4H, $CH_2$), 2.51 (t, 4H, $J$ = 6.0 Hz, $COCH_2$), 2.94 (t, 4H, $J$ = 6.0 Hz, $CONHCH_2C\underline{H_2}$),

3.71 (q, 4H, $J$ = 6.0 Hz, CONHC$\underline{H}_2$CH$_2$), 6.26 (bt, 2H, $J$ = 6.0, NH), 6.98 (d, 4H, $J$ = 8 Hz, ArCH), 7.18 (d, 4H, $J$ = 8.0 Hz, ArCH), 7.42 (t, 1H, $J$ = 7.5 Hz, ArCH), 7.80 (dd, 2H, $J$ = 7.5 Hz, 1.5 Hz, ArCH) 7.87 (s, 1H, ArCH); $^{13}$C NMR (100 MHz, DMSO-$d_6$) δ = 25.24 ($CH_2$), 28.69 ($CH_2$), 28.94 ($CH_2$), 34.63 ($CH_2$), 34.75 ($CH_2$) 41.32 ($CH_2$), 122.12 (ArCH), 125.38 (ArCH), 129.38 (ArCH), 130.21 (ArCH), 130.46 (ArCH), 135.32 (q, Ar$\underline{C}$), 136.80 (q, ArC), 149.78 (q, ArC), 167.50 (CO), 172.84 (CO); FAB-MS: (*m*BNA matrix): *m/z* 571 $[M+H]^+$; anal. calcd. for $C_{34}H_{38}N_2O_6$ (570): C, 71.6 %; H, 6.6 %; N, 4.9 %; found: C, 71.5 %; H, 6.5 %; N, 4.8 %.

**Preparation of *N*-benzoyl glycine methyl ester**

The synthesis was carried out as is outlined in reference 15

**Preparation of *N*-benzoyl alanine methyl ester**

The synthesis was carried out as is outlined in reference 16

**$^1$H NMR titrations (general procedure)**

All host and guest compounds (except those described in the experimental) were purchased from commercial sources and dried thoroughly overnight in a vacuum oven before use. Deuterated solvents were dried over molecular sieves that had been pre-dried in an oven at 200°C for several days; a tiny amount of anhydrous $K_2CO_3$ was added to remove traces of HCl.

A sample of host was dissolved in deuterochloroform (generally concentrations of 0.5 mM-10 mM were used). A portion of this solution was used as the host NMR sample, and the remainder was used to dissolve a sample of guest, so that the concentration of host remained constant during the course of the titration. The $^1$H

NMR of the host solution was recorded and then successive aliquots of host guest solution were added to the host NMR sample recording the $^1H$ NMR after each addition. The changes of characteristic host signals were then analysed with purpose written software provided by Prof. C. A. Hunter on an Apple Macintosh™ computer. The program fits data to a binding model for a 1:1 binding isotherm to yield the association constant, the bound chemical shift, and if needed, the free chemical shift. This is achieved by solving equations (x-y) where $[H]_o$ is the total concentration of host, $[G]_o$ is the total concentration of guest, [H] is the concentration of unbound free host, [HG] is the concentration of host-guest complex, K is the association constant for the formation of the host-guest complex, $\Delta_f$ is the free chemical shift of the host and $\Delta_b$ is the limiting bound chemical shift of the host-guest complex.

$$[HG] = (1 + K[H]_o[G]_o - \sqrt{\{(1 + [H]_o[G]_o)^2 - 4K^2[H]_o[G]_o\}})/2K$$

$$[H] = [H]_o - [HG]$$

$$\Delta_{obs} = ([HG]/[H]_o)\Delta_b + ([H]/[H]_o)\Delta_f$$

## 4.2. References


1. (a) J. J. He, F. A. Quiocho, *Science* **1991**, *251*, 1497. (b) H. Lueke, F. A. Quiocho, *Nature* **1990**, *347*, 402 (c) F. A. Quiocho, J. W. Pflugrath, *Nature* **1985**, *314*, 402.
2. (a) H. E. Moser, P. B. Dervan, *Science* **1987**, *238*, 645-650. (b) J. D. Watson, F. H. C. Crick, *Nature* **1953**, *171*, 737-738.
3. (a) P. D. Henley, C. P. Waymark, I. Gillies, J. D. Kilburn, *J. Chem. Soc. Perkin Trans. 1* **2000**, 1021-1031. (b) T. Fessmann, J. D. Kilburn, *Angew. Chem. Int. Ed. Engl.* **1999**, *38*, 1993-1996. (c) M. Davies, M. Bonnat, F. Guillier, J. D. Kilburn, M. Bradley, *J. Org. Chem.* **1998**, *63*, 8696-8703. (d) J. Dowden, P. D. Edwards, S. S. Flack, J. D. Kilburn, *Chem. Eur. J.* 1999, 5, 79-89. (e) S. Goswami, R. J. Mukherjee, *Tetrahedron Lett.* **1997**, *38*, 1619-1622. (f) M. Bonnat, M. Bradley, J. D. Kilburn, *Tetrahedron Lett.* **1996**, *37*, 5409-5412 (g) C. P. Waymark, J. D. Kilburn, T. Gillies, *Tetrahedron Lett.* **1995**, *36*, 3051-3054. (h) F. P. Tecilla, R. P. Dixon, G. Slobadtkin, D. S. Alavi, A. D. Hamilton, *J. Am. Chem. Soc* **1990**, *112*, 9408-9410. (i) V. Hegde, P. Madhukar, J. D. Madura, R. P. Thummel, *J. Am. Chem. Soc.* **1990**, *112*, 4549-4550. (j) B. Asjew, P. Ballester, C. Buhr, K. S. Jeong, S. Jones, K. Parris, K. Williams, J. Rebek, Jr. *ibid*, **1989**, *111*, 1082-1090.
4. (a) L. Sebo, B. Schweizer, F. Diederich, *Helv. Chim. Acta.* **2000**, *83*, 80-92. (b) F. Werner, H-J. Schneider, *Helv. Chim. Acta*, **2000**, *83*, 465-478. (c) J. Scheerder, J. P. M. Van Duynhoven, J. F. J. Engebersen, D. N. Reinhoudt, *Angew. Chem. Int. Ed. Engl.* **1996**, *35*, 1090-1093.
5. (a) A. Metzeger, E. V. Anslyn, *Angew. Chem. Int. Ed. Engl.* **1998**, *37*, 649-651 (b) A. G. Johnston, D. A. Leigh, A. Murphy, J. P. Smart, *Bull. Chem. Soc. Belg.* **1996**, *105*, 721-727. (c) A. P. de Silva, H. Q. N. Gunaratne, C. P. McCoy, *Nature* 1993, *364*, 42-44.

6. V. Jubian, R. P. Dixon, A. D. Hamilton, *J. Am. Chem. Soc.* **1992**, *114*, 1120-1121.

7. D. A. Leigh, K. Moody, J. P. Smart, K. J. Watson, A. M. Z. Slawin, *Angew. Chem., Int. Ed. Engl.* **1996**, *35*, 306-310.

8. E. M. Arnett, E. J. Mitchell, T. S. S. R. Murty, *J. Am. Chem. Soc.* **1974**, *96*, 3875-3891.

9. A. P. Bisson, C. A. Hunter, J. C. Morales, K. Young, *Chem. Eur. J.* **1998**, *4*, 845-851.

10. (a) C. A. Hunter, *J. Am. Chem. Soc.* **1992**, *114*, 5303-5311. (b) H. Adams, F. J. Carver, C. A. Hunter, N. J. Osborne, *J. Chem. Soc., Chem. Commun.* **1996**, 2529-2530. (c) C. A. Hunter, *J. Chem. Soc., Chem. Commun.* **1991**, 749-750 (d) F. J. Carver, C. A. Hunter, R. J. Shannon, *J. Chem. Soc., Chem. Commun.* **1994**, 1277-1280. (e) F. Vögtle, S. Meier, R. Hoss, *Angew. Chem. Int. Ed. Engl.* **1992**, *31*, 1619. (f) C. Seel, A. H. Parham, O. Safarowsky, G. M. Hübner, F. Vögtle, *J. Org. Chem.* **1999**, *64*, 7236-7242.

11. $C_{32}H_{39}N_3O_{7.50}I$, M = 712.58, crystal size 0.10 x 0.02 x 0.20 mm, monoclinic $P2_1/a$ (no. 14), $a$ = 11.51(1), $b$ = 12.80(8), $c$ = 25.40(7) Å, $\beta$ = 93.72(4)°, V = 6145.6(5)Å$^3$, Z = 4, $\rho_{calcd}$ = 1.267 g cm$^{-3}$ Cu-Kα radiation (graphite monochromator, $\lambda$ = 1.54178 Å), $\mu$ = 71.1 cm$^{-1}$ , T = 293.0 K. 6171 data (5843 unique, $R_{int}$ = 0.132, 28.3<θ<52.5), were collected on a rigaku AFC7S diffractometer using narrow frames (16.0° in $\omega$) and were corrected linearly for absorption and linear beam decay (transmission 0.0718-1.0000). The structure was solved by direct methods and refined by full-matrix least-squares on $F^2$ values of all data to give $wR = \{\Sigma[w(F_o^2-F_c^2)^2]/\Sigma[w(F_o^2)^2]\}^{1/2}$ = 0.090, conventional $R$ =

0.102 for $F$ values of 1244 reflections with $F_o^2 > 2\sigma(F_o^2)$, $S$ = 4.27 for 236 parameters. Residual electron density extremes were 0.65 and –0.51 $Å^{-3}$.

12. $C_{31}H_{33}N_3O_6$, $M$ = 543.60, crystal size 0.15 x 0.08 x 0.04 mm, monoclinic $P2_1/c$, $a$ = 26.0296(17), $b$ = 10.9425(7), $c$ = 9.9122(6) Å, β = 98.635(2), $V$ = 2791.3(3)$Å^3$, $Z$ = 4, $\rho_{calcd}$ = 1.294 Mg $m^{-3}$; synchotron radiation (λ = 0.69290 Å), μ = 0.090 $mm^{-1}$, $T$ = 293(2)K. 14830 data (5255 unique, $R_{int}$ = 0.0385, 1.97<θ<25.00°), were collected on a Siemens SMART CCD diffractometer using narrow frames (0.3° in ω), and were corrected semi-empirically for absorption and incident beam decay. The structure was solved by direct methods and refined by full-matrix least-squares on $F^2$ values of all data (G.M.Sheldrick, SHELXTL manual, Siemens Analytical $X$-ray Instruments, Madison WI, USA, 1993, version 5.0) to give $wR = \{\Sigma[w(F_o^2-F_c^2)^2]/\Sigma[w(F_o^2)^2]\}^{1/2}$ = 0.1470, conventional $R$ = 0.0682 for $F$ values of 5255 reflections with $F_o^2 > 2\sigma(F_o^2)$, $S$ = 1.226 for 369 parameters. Residual electron density extremes were 0.254 and –0.255 $Å^{-3}$. Hydrogens were added in calculated positions and constrained to a Riding model.
13. Crystal data for **7** space group P1 (no. 2), $a$ = 9,1219(2), $b$ = 11.9357(3), $c$ = 16.5649(5) Å, $\alpha$ = 103.8720(10), $\beta$ = 97.3580(10), γ = 92.9630(10)°, $V$ = 1730.13(8) $Å^3$. Further information concerning this crystallographic investigation is currently unavailable as the structure is undergoing final refinement.
14. Kavallieratos, K.; de Gala, S. R.; Austin, D. J.; Crabtree, R. H. *J. Am. Chem. Soc.* 1997, *119*, 2325-2326.
15. M. Prein, P. J. Manly, A. Padwa, *Tetrahedron*, **1997**, *53*, 7777-7794.
16. K-D. Ginzel, P. Brungs, E. Stechan, *Tetrahedron*, **1989**, *45*, 1691-1701.a

**Acknowledgements:**

Thanks to Rizwana Nazreen who determined the binding constant of the macrocycles **103** and **104** with *N*-methylbenzamide.

Thanks to Gail Morris who determined the binding constants of the macrocycle **100** with all neutral guests and carried out the initial JOBS plots.

# Chapter Five

## 5. The Formation of Rotaxanes *via* Slow Slippage?

*Manuscript for submission to Chemical Communications*

Abstract: A peptide [2]rotaxane is assembled in a non-hydrogen-bonding solvent under thermodynamic control by simply mixing the individual components.

Due to a greater understanding of non-covalent interactions it has been possible to progress from the early catenane and rotaxane syntheses[1] to a level where it is possible to concentrate on the exploitation of the mechanical bond.[2] However, if interlocked architectures are ever to be constructed in useful quantities, then further improvements in synthetic methodology are necessary due to the limitations imposed by many of the *"capping"* (functionalisation of a linear thread circumscribed by a macrocycle) or *"clipping"* (synthesis of a macrocycle around a pre-formed thread) reactions which, are under kinetic control.[3] Of the many routes into rotaxanes that are now available to the researcher,[2] slippage[4,5] represents a real opportunity to synthesise rotaxanes under thermodynamic control[6] as it involves no chemical reaction making it compatible with many functionalities. Slippage relies on the small increase in cavity size that occurs to a macrocycle when it is heated allowing it to slip onto a dumbbell shaped thread whose stoppers have been judiciously chosen to allow such a process. The favourable interaction of the macrocycle with the thread prevents de-threading due to the thermodynamic stabilisation provided by the non-covalent interactions that are employed. Cooling results in the macrocycle becoming trapped upon the thread. Initial research into the formation of hydrogen bond-assembled rotaxanes using this approach has met with only moderate success.[5] The high temperatures required to give the macrocycle enough thermal energy to hurdle

the stopper reduce the non-covalent interactions that drive the threading. Here, for the first time, the serendipitous discovery of a slippage synthesis that works at ambient temperature is reported.

Leigh *et al.* recently reported the synthesis of hydrogen bond-assembled peptide rotaxanes whereby condensation of *para*-xylylenediamine and isophthaloyl dichloride in the presence of the thread **89** results in the synthesis of a rotaxane **90** in 62 % via *"clipping"* (Scheme 5.1).[7]

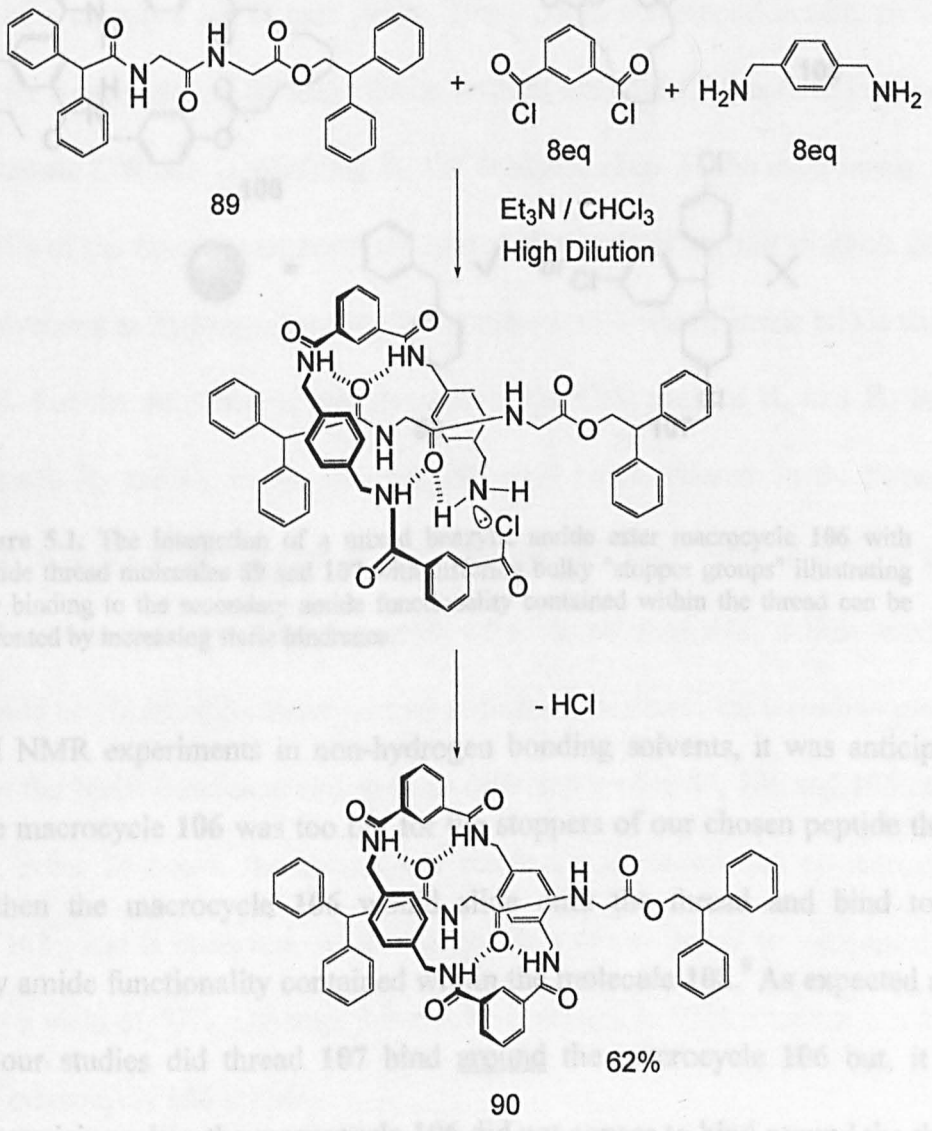


**Scheme 5.1.** The synthesis of a hydrogen bond-assembled peptide rotaxane **90** from thread **89** in 62 % using a "clipping" methodology.

Initially it was necessary to study which sizes of stopper would be suitable for the use of macrocycle **106** (Figure 5.1) in the synthesis of organic "magic" rod rotaxanes (rotaxanes constructed under thermodynamic control using reversible metathesis reactions).[8]

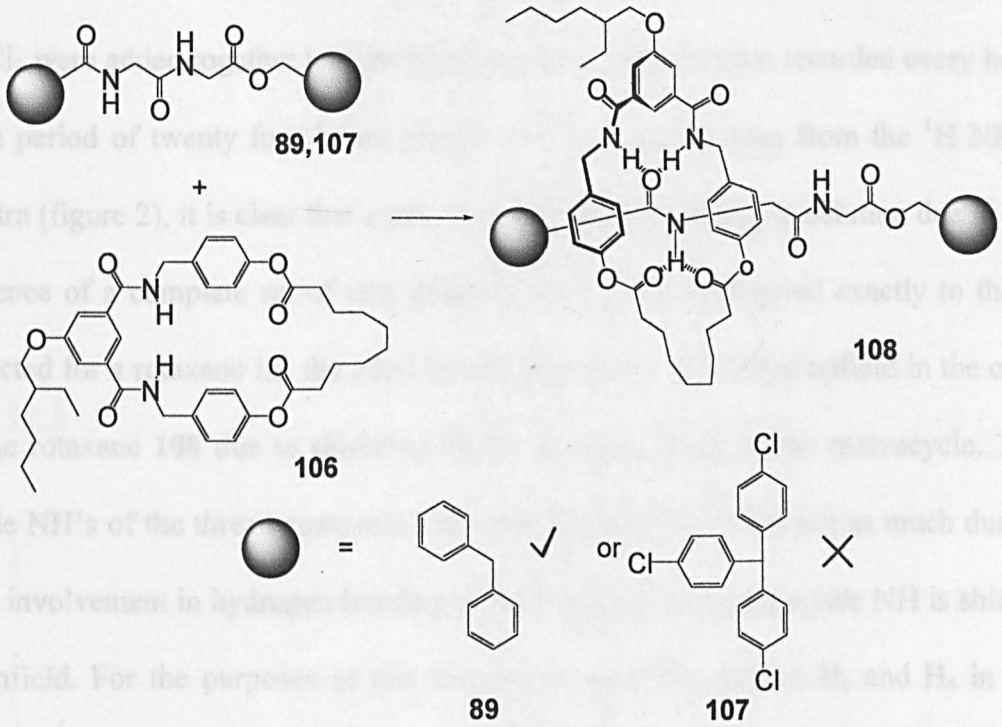


**Figure 5.1.** The interaction of a mixed benzylic amide ester macrocycle **106** with peptide thread molecules **89** and **107** with differing bulky "stopper groups" illustrating how binding to the secondary amide functionality contained within the thread can be prevented by increasing steric hindrance.

Using $^1$H NMR experiments in non-hydrogen bonding solvents, it was anticipated that if the macrocycle **106** was too big for the stoppers of our chosen peptide thread **89,107**, then the macrocycle **106** would slide onto the thread and bind to the secondary amide functionality contained within the molecule **108**.[9] As expected at no stage in our studies did thread **107** bind around the macrocycle **106** but, it was initially surprising when the macrocycle **106** did not appear to bind around the thread **89** (figure 5.1) as CPK modelling experiments had indicated the stoppers should be too small to hinder the threading of the macrocycle **106**. The $^1$H NMR spectrum of

the mixture was subsequently recorded again to confirm that this was true only to find that the presence of a second set of signals indicating not a time-averaged complex formation but the formation of a discreet molecule had occurred. It was decided to pursue this further to gain a greater understanding of the phenomenon and so solutions of the thread **89** and macrocycle **106** at identical concentrations of $CDCl_3$ were added together and the resulting $^1H$ NMR spectrum recorded every hour for a period of twenty four hours (figure 2).[†10] As can be seen from the $^1H$ NMR spectra (figure 2), it is clear that a new molecule **108** is forming in solution due to the presence of a complete set of new peaks. These peaks correspond exactly to those expected for a rotaxane i.e. the alkyl thread protons are all shifted upfield in the case of the rotaxane **108** due to shielding by the aromatic rings of the macrocycle. The amide NH's of the thread component are also shifted upfield but not as much due to their involvement in hydrogen bonding to the macrocycle whose amide NH is shifted downfield. For the purposes of this discussion, the $CH_2$ protons $H_c$ and $H_e$ in the thread **89** and $H_{c'}$ and $H_{e'}$ in the rotaxane **108** shall be considered. In the thread **89** they come at 4.7-4.8 ppm whilst in the rotaxane **108** they come at 2.9-3.0 ppm. Should the process involve the formation of a simple complex, a time-averaged signal would be observed for these protons indicating that here, the threading process is slow on the NMR timeframe and so three different species **89, 106** and **108** can be observed. After 24 hours, the system has reached equilibrium and no increase in rotaxane **108** yield is observed. At this stage, the ratio of thread to rotaxane is 3:2 indicating a yield of 40%, although this can be increased to 95% rotaxane if a 5 fold excess of macrocycle **106** is used.

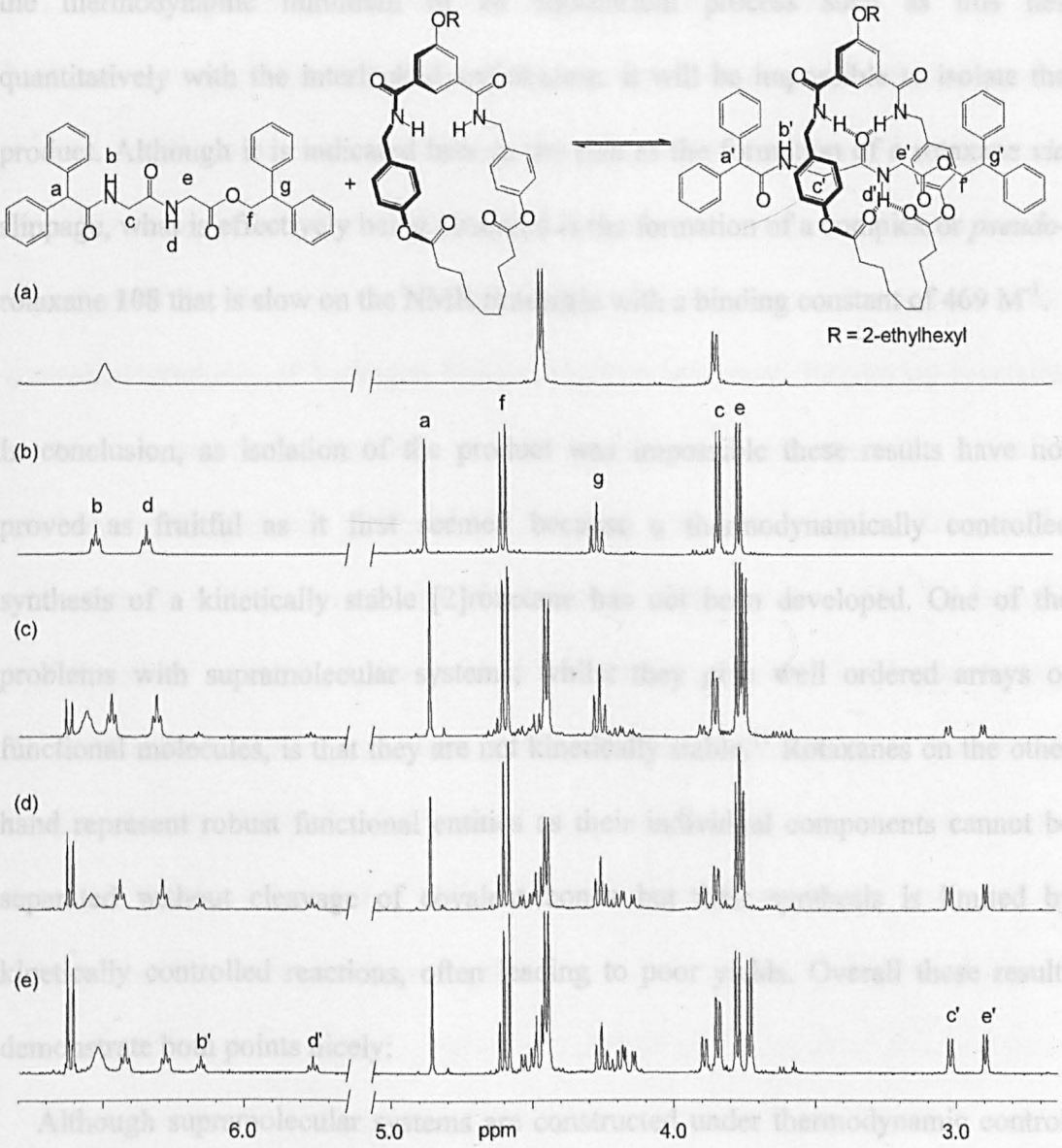


**Figure 5.2.** The formation of a rotaxane **108** *via* slow slippage illustrated by the change in the $^1$H NMR spectra (400 MHz, $CDCl_3$) a) macrocycle **106**, b) thread **89**, c) macrocycle **106** with thread **89** after 1 hour, d) macrocycle **106** with thread **89** after 6 hours, e) macrocycle **106** with thread **89** after 24 hours.

Having made this fortunate discovery, it was desirable to attempt purification of the rotaxane, which if successful would provide an efficient route into rotaxanes under thermodynamic control. Unfortunately, when chromatography of the reaction mixture is attempted, the rotaxane **108** decomposes. This is because although the system is under thermodynamic control, the product is not kinetically stable. In different environments, such as high temperatures, hydrogen-bonding solvents, high dilution etc. the thermodynamic minimum of equilibrium is changed and so unless

the thermodynamic minimum of an equilibrium process such as this lies quantitatively with the interlocked architecture, it will be impossible to isolate the product. Although it is indicated here in the title as the formation of a rotaxane *via* slippage, what is effectively being observed is the formation of a complex or *pseudo*-rotaxane **108** that is slow on the NMR timescale with a binding constant of 469 $M^{-1}$.

In conclusion, as isolation of the product was impossible these results have not proved as fruitful as it first seemed because a thermodynamically controlled synthesis of a kinetically stable [2]rotaxane has not been developed. One of the problems with supramolecular systems; whilst they give well ordered arrays of functional molecules, is that they are not kinetically stable.[11] Rotaxanes on the other hand represent robust functional entities as their individual components cannot be separated without cleavage of covalent bonds but their synthesis is limited by kinetically controlled reactions, often leading to poor yields. Overall these results demonstrate both points nicely:

Although supramolecular systems are constructed under thermodynamic control, the construction of functional arrays of molecules is limited by kinetic stability.

Constructing usable quantities of rotaxanes requires the development of thermodynamically controlled routes to rotaxanes that work using reversible chemical reactions and as a result give kinetically robust products.

## 5.1. A thermodynamically controlled rotaxane assembly process

In this chapter (p. 116), slippage (p. 18-21) has been shown to be a less than ideal method for the assembly of rotaxanes showing why the approach to rotaxane assembly to be described in the following chapter is necessary. In Chapter six, the objectives of the thesis are essentially realized to develop a true thermodynamically controlled synthesis of hydrogen bond-assembled rotaxanes. Employing reversible metathesis reactions (identified as suitable for thermodynamically controlled syntheses in Chapter one p. 22, 27-29), template sites containing one-three amides (shown to be suitable for rotaxane formation in Chapter two p. 48), 1,3-benzylic isophthalamide units (shown to be ideal for rotaxane assembly in Chapter three p. 72) macrocycles of the type whose binding of amide functionality is described in Chapter four (p. 95) and suitably sized stoppers found as a result of the studies described in this chapter (p. 116), Chapter six brings together many of the discoveries made in the previous chapters.

## 5.2. Supporting Information

### Diphenylacetylglycylglycine, 2,2-diphenylester 89

The compound was synthesized in the same way as is outlined in reference 7

### Macrocycle 106

The compound was synthesized in the same way as is outlined in reference 8

### †[2]rotaxane 108

Using a Brüker 400 MHz DPX NMR machine the $^1$H NMR sample of the thread **89** (0.012 g, 0.029 mmol, 5 mL) was recorded followed by the $^1$H NMR spectrum of the macrocycle **106** (0.020 g, 0.029 mmol, 5 mL). The two samples were then mixed together to give a sample of overall concentration 0.0365 M with respect to each component. Acquisition of the $^1$H NMR spectrum of this new sample (using the same machine) at regular intervals over a period of 24 hours indicated a new set of peaks for the glycylglycine $H_{c'}$ and $H_{e'}$ residues compatible with a rotaxane **108**. Mass spec. data was used to show that a complex had been formed. FAB-MS (*m*BNA matrix): *m/z* 1177 $[(MH)^+]$, 1214 $[(MK)^+]$. All attempts to isolate the rotaxane proved unsuccessful. Two-dimensional TLC showed that there was some decomposition of the product on silica.

## 5.3. References


1. (a) D. B. Amabilino, J. F. Stoddart, *Chem. Rev.* **1995**, *95*, 2725-2828; (b) G. Schill, *Catenanes, Rotaxanes and Knots*, Academic press, New York, **1971**.
2. (a) G. M. Hübner, J. Cläser, C. Seel, F. Vögtle, *Angew. Chem. Int. Ed. Engl.* **1999**, *38*, 383-386. (b) B. Mohr, M. Weck, J-P. Sauvage, R. H. Grubbs, *Angew. Chem. Int. Ed. Engl.* **1997**, *36*, 1308-1310.
3. Processes that utilise noncovalent forces to assemble an interlocked complex that is subsequently "captured" by irreversible bond formation ("self assembly with covalent modification") only operate under thermodynamic control before the final cyclization step [D. B. Amabilino, P. R. Ashton, L. Perez-Garcia, J. F. Stoddart, *Angew. Chem. Int. Ed. Engl.* **1995**, *34*, 2378-2380]. "Strict self assembly" pathways spontaneously convert components into products at thermodynamic equilibrium [D. Philp, J. F. Stoddart, *Angew. Chem. Int. Ed. Engl.* **1996**, *35*, 1154-1196.
4. (a) F. M. Raymo, K. N. Houk, J. F. Stoddart, *J. Am. Chem. Soc.***1998**, *120*, 9318-9322; (b) M. Asakawa, P. R. Asthton, R. Ballardini, V. Balzani, M. Bělohradský, M. T. Gandolfi, O. Kocian, L. Prodi, F. M. Raymo, J. F. Stoddart, M. Venturi, *J. Am. Chem. Soc.* **1997**, *119*, 302-310; (c) P. R. Ashton, M. Bělohradský, D. Philip, J. F. Stoddart, *J. Chem. Soc., Chem. Commun.* **1993**, *16*, 1274-1277; (d) P. R. Ashton, M. Bělohradský, D. Philp, J. F. Stoddart, *J. Chem. Soc., Chem. Commun.* **1993**, *16*, 1269-1274.
5. M. Handel, M. Pleovets, S. Gestermann, F. Vögtle, *Angew. Chem. Int. Ed. Engl.* **1997**, *36*, 1199-1201.
6. For selected examples of the synthesis of interlocked architectures constructed under thermodynamic control see: (a) K-Y. Jeong, J. S. Choi, S-Y. Chang, H-Y. Chang, *Angew. Chem. Int. Ed. Engl.* **2000**, *39*, 1692-1695; (b) S. J. Cantrill, S.

K. Rowan, J. F. Stoddart, *Org. Lett.* **1999**, *1*, 1363-1366; (c) A. C. Try, M. M. Harding, D. G. Hamilton, J. K. M. Sanders, *Chem. Commun.* **1998**, 723-724; (d) M. Fujita, F. Ibukuro, H. Hagihara, K. Ogura, *Nature*, **1994.**

7. D. A. Leigh, A. Murphy, J. P. Smart, A. M. Z. Slawin, *Angew. Chem. Int. Ed. Engl.* **1997**, *36*, 728-732.

8. For organic 'magic' rods see T. J. Kidd, D. A. Leigh, A. J. Wilson, *unpublished results*; For organic 'magic' rings see T. J. Kidd, D. A. Leigh, A. J. Wilson, *J. Am. Chem. Soc.* **1999**, *121*, 1599-1600.

9. It has previously been shown that secondary amides form 1:1 complexes with mixed benzylic amide ester macrocycles, C. Harris, D. A. Leigh, G. Morris, R. Nazreen, S. J. Teat, A. M. Z. Slawin, A. J. Wilson, J. K. Y Wong, *Unpublished results*.

10. Monitoring the $^{1}H$ NMR spectra after a period of 24 hours reveals no change as does heating the sample for a period of twelve hours at 40°C.

11. For selected examples see: (a) R. P. Sijbesma, F. H. Beijer, L. Brunsveld, B. J. B. Folmer, J. H. K. Ky Hirschberg, R. F. M. Lange, J. K. L. Lowe, E. W. Meijer, *Science*, **1997**, *278*, 1601-1605; (b) F. H. Beijer, H. Kooijman, A. L. Spek, R. P. Sijbesma, E. W. Meijer, *Angew. Chem. Int. Ed. Engl.* **1998**, *37*, 75-78; (c) J. P. Mathias, E. E. Simanek, J. A. Zerkowski, C. T. Seto, G. M. Whitesides, *J. Am. Chem. Soc.*, **1994**, *116*, 4316-4325.

# Chapter Six

## 6. Organic "Magic Rods": The Hydrogen Bond-Directed Assembly of Rotaxanes Under Thermodynamic Control

*As submitted to Chemical Communications*

Abstract: Peptide rotaxanes are assembled in high yield under thermodynamic control using hydrogen bonding interactions and cross olefin metathesis.

Whilst the use of non-covalent interactions in the templated assembly of interlocked architectures[1] leads to improved yields over statistical methods,[2] a common feature is that the final mechanically interlocking reaction is carried out under kinetic control with the exception of slippage[3] which is under thermodynamic control ("strict self assembly"[4]) at elevated temperatures. As a result, if *"clipping"* or *"capping"* does not occur *via* an already threaded precursor, "mistakes"- non-interlocked molecules- are produced that cannot be "corrected" (Figure 6.1).

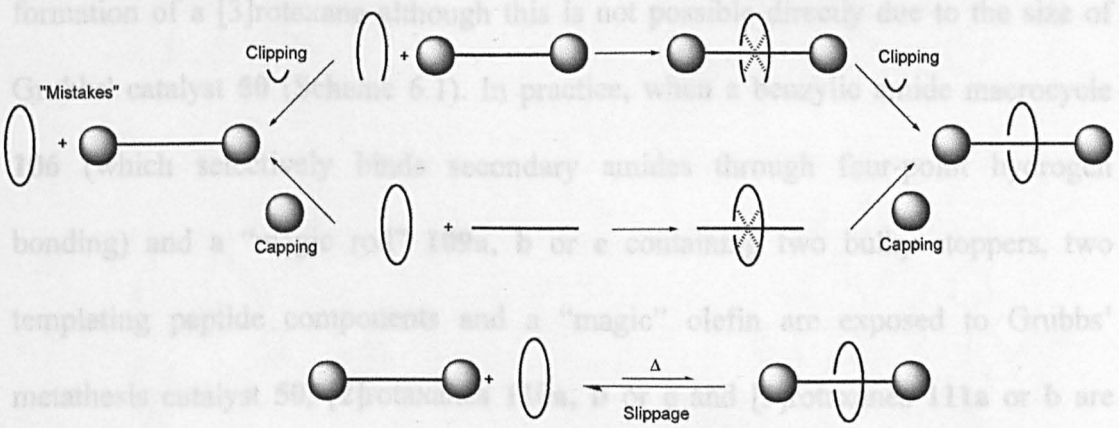


**Figure 6.1.** A cartoon representation of common interlocked architecture syntheses.

The synthesis of interlocked architectures under thermodynamic control has previously been achieved using weak, labile metal ligand bonds exploiting the

interactions that direct mechanical interlocking to construct catenanes in high yield[5] and more recently rotaxanes,[6] which can also be constructed under thermodynamic control using kinetically labile imine bonds.[7] Latterly, a "best of both worlds" approach incorporating organic rings, reversible ring opening metathesis reactions[8] and the hydrogen-bond directed self-assembly of benzylic amide macrocycles has shown the synthesis of kinetically robust catenanes under thermodynamic control in near quantitative yield is possible in a single step,[9] a processes which can be said to mimic the magicians trick of interlocking what appear to be "magic rings". Here the adaptation of this methodology to the synthesis of a new class of hydrogen bond assembled molecular shuttles under thermodynamic control is reported.

Schematically, the synthesis of rotaxanes in such a way relies on the use of a thread with bulky stoppers and a "magic" olefin in the centre. When the olefin is opened by Grubbs' catalyst **50**, it should be possible for a macrocycle to slip on and become trapped when the olefin is re-closed. This cycle can in theory continue on to the formation of a [3]rotaxane although this is not possible directly due to the size of Grubbs' catalyst **50** (Scheme 6.1). In practice, when a benzylic amide macrocycle **106** (which selectively binds secondary amides through four-point hydrogen bonding) and a "magic rod" **109a**, **b** or **c** containing two bulky stoppers, two templating peptide components and a "magic" olefin are exposed to Grubbs' metathesis catalyst **50**, [2]rotaxanes **110a, b** or **c** and [3]rotaxanes **111a** or **b** are formed in exactly this way (Scheme 6.1). As the metathesis reaction is reversible, the product distribution is determined only by the relative stabilities of the products; at high concentrations predominantly threaded species are obtained which can if so wished then be converted back to the non-interlocked components by diluting the reaction mixture. Since carbon-carbon double bonds are fundamentally robust,

rotaxanes produced in this way are kinetically stable when separated from the metathesis catalyst, moreover, this technique can be carried out at room temperature and so hydrogen bonding is maximised offering an advantage over slippage techniques which require heating.

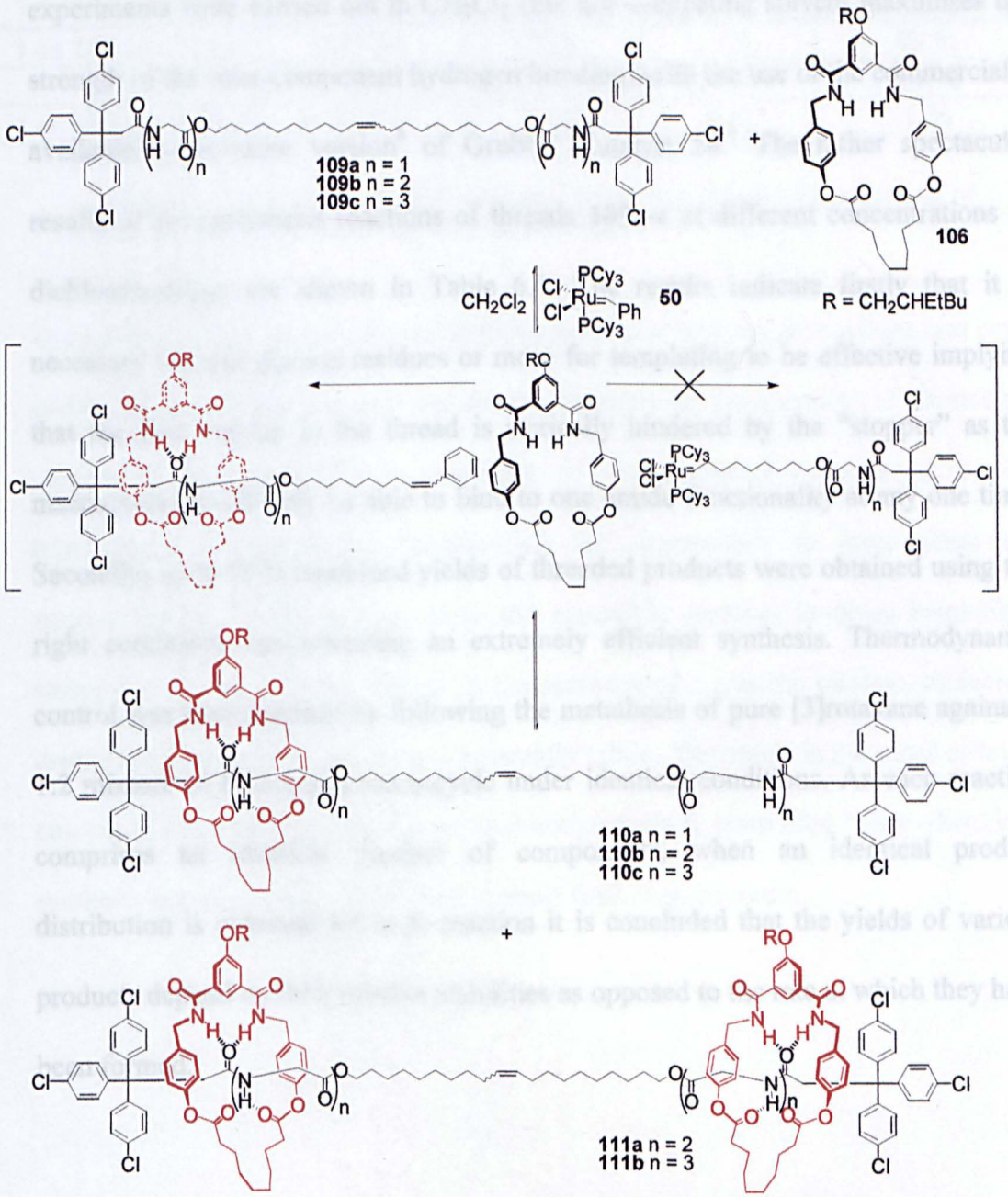


**Scheme 6.1.** The synthesis of [2]- and [3]rotaxanes **110a-c** and **111a-b** under thermodynamic control using a reversible threading strategy facilitated by olefin metathesis.

Obtaining a suitable macrocycle **106** was a relatively simple task as a result of previous work[9] whilst synthesis of the threads **109** were carried out in 4 steps from

simple amide and ester bond formations and a metathesis reaction in the final step. The extraordinarily long C20 alkyl chain threads described here were used because we found that shorter chains were not reactive enough either due to steric hindrance or the formation of metal chelates as proposed recently in the literature.[10] Metathesis experiments were carried out in $CH_2Cl_2$ (the non-competing solvent maximises the strength of the inter-component hydrogen bonding) with the use of the commercially available benzylidene version[8] of Grubbs' Catalyst **50**.† The rather spectacular results of the metathesis reactions of threads **109a-c** at different concentrations of dichloromethane are shown in Table 6.1. The results indicate firstly that it is necessary for two glycine residues or more for templating to be effective implying that the first residue in the thread is sterically hindered by the "stopper" as the macrocycle should only be able to bind to one amide functionality at any one time. Secondly, up to 95% combined yields of threaded products were obtained using the right conditions demonstrating an extremely efficient synthesis. Thermodynamic control was demonstrated by following the metathesis of pure [3]rotaxane against a 1:2 mixture of thread and macrocycle under identical conditions. As each reaction comprises an identical number of components, when an identical product distribution is obtained for each reaction it is concluded that the yields of various products depend on their relative stabilities as opposed to the rate at which they have been formed.

| Reactants | Concentration | [2]rotaxane | [3]rotaxane | Threaded products |
|---|---|---|---|---|
| 1 eq **106** and **109a** | 0.2 M | 15 % | 0 % | **15 %** |
| 1 eq **106** and **109b** | 0.2 M | 36 % | 20 % | **56 %** |
| 1 eq **106** and **109c** | 0.2 M | 34 % | 24 % | **58 %** |
| 5 eq **106** and **109b** | 0.2 M | 52% | 43 % | **95 %** |
| 1 eq **106** and **109b** | 0.05 M | 29 % | 11 % | **40 %** |
| **111a** | 0.05 M | 29 % | 11 % | **40 %** |
| 1 eq **106** and **109b** | 0.0002 M | 1 % | 0 % | **1 %** |

**Table 6.1.** Yields of "magic rod" rotaxanes **110a-c** and **111a-b** from metathesis of organic "magic rods" **109a-c** at various concentrations.

In conclusion, this combination of directed hydrogen bonding interactions and cross metathesis provides a powerful tool for the assembly (or disassembly) of interlocked compounds through built in recycling of non-preferred by-products, a key requirement in developing "engineering up" approaches to large functional supermolecules.[4] Significantly, since the reversible reaction involves breaking a strong C=C bond and only occurs in the presence of a specific catalyst, molecules assembled by this strategy are not inherently labile. The result is the most efficient one could hope for: an "intelligent" thermodynamically controlled "error-checking" synthesis combined with a kinetically robust final superstructure.

## 6.1. Designing and constructing interlocked architectures in high yield from scratch: A showcase for *"The Controlled Assembly of Interlocked Architectures"*

Although the previous four chapters and Appendix I culminating in this chapter have allowed the development of high-yielding routes to amide based interlocked architectures there is no way of fixing their conformational preference as is the case in template-directed routes to interlocked architectures employing metals. The following chapter makes use of all the information discovered in the previous five chapters and applies it to the design of an entirely new [2]catenate structure and subsequently synthesise for the first time, useful quantities of octahedral metal containing [2]catenates. This final chapter is a showcase for how careful well thought out design makes it possible to achieve *"The Controlled Assembly of Interlocked Architectures"* the title and goal of this thesis!

## 6.2. Supporting Information

### Discussion of $^1$H NMR data

The $^1$H NMR spectra of the glycylglycine "magic" rod rotaxanes and thread in $CDCl_3$ at 50°C are shown in Figure 6.4. The thread (Figure 6.2a) has glycylglycine protons $H_c$ that come in a non-shielded environment and so their signals appear around 3 ppm. The [2]rotaxane (Figure 6.2b) displays characteristic shifts for a threaded hydrogen bond assembled species[10] with the amide protons $H_C$ of the macrocycle shifting downfield due to deshielding and the glycylglycine protons $H_c$ all shifting upfield due to shielding. More significantly the glycylglycine protons $H_c$ are relatively broad indicating that the shuttling of the macrocycle along the axis of the thread is slow on the NMR timescale. Finally the [3] rotaxane (Figure 6.2c) is much the same as the [2] rotaxane in that a shielding pattern for the macrocyclic amide protons $H_C$ and the glycylglycine protons $H_c$ consistent with a threaded species is obtained. The main difference is that as each station of the thread is now occupied, the macrocycles are less free to move along the axis of the thread. The spectrum gives much sharper signals as both sides are occupied and the macrocycle spends more time shielding the $CH_2$'s of the glycine units so the shielding is more pronounced. Also of interest is the complex signal for the benzylic $CH_2$ of the macrocycle $H_D$ (a quartet of doublets, which at this temperature are beginning to coalesce) are observed which arise due to the two faces of the macrocycle being enantiotopic while in the [2]rotaxane, only a doublet is observed.

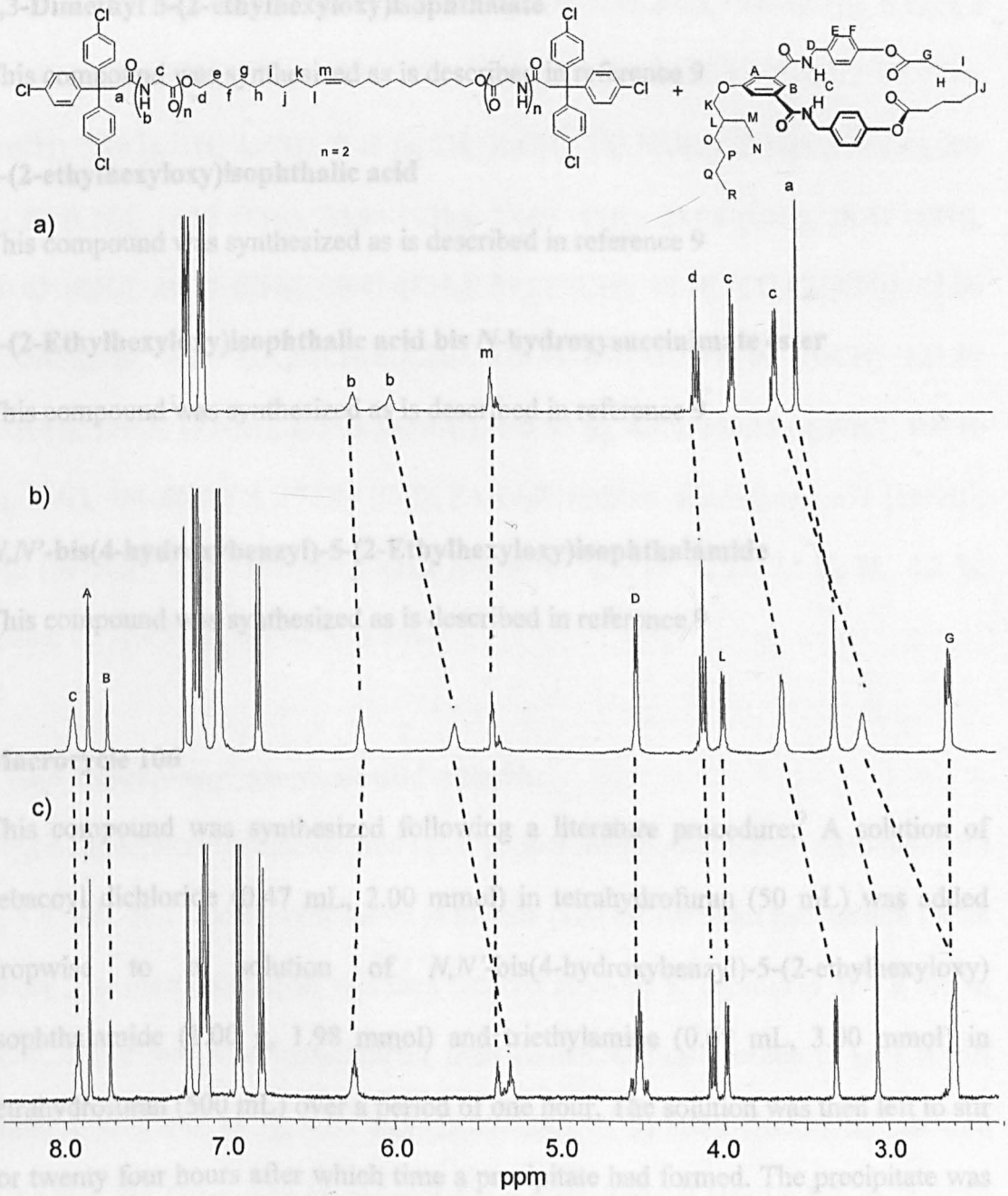


**Figure 6.2.** $^{1}H$ NMR spectra in $CDCl_3$ at 50°C of a) glycylglycine thread **109b**, (b) glycylglycine rotaxane **110b** and c) glycylglycine rotaxane **111a**.

## 4-hydroxybenzylamine

This compound was synthesized as is described in reference 11

## 5-hydroxyisophthalic acid dimethyl ester

This compound was synthesized as is described in reference 9

**1,3-Dimethyl 5-(2-ethylhexyloxy)isophthalate**

This compound was synthesized as is described in reference 9

**5-(2-ethylhexyloxy)isophthalic acid**

This compound was synthesized as is described in reference 9

**5-(2-Ethylhexyloxy)isophthalic acid bis *N*-hydroxysuccinimate ester**

This compound was synthesized as is described in reference 9

***N,N'*-bis(4-hydroxybenzyl)-5-(2-Ethylhexyloxy)isophthalamide**

This compound was synthesized as is described in reference 9

**Macrocycle 106**

This compound was synthesized following a literature procedure:[9] A solution of sebacoyl dichloride (0.47 mL, 2.00 mmol) in tetrahydrofuran (50 mL) was added dropwise to a solution of *N,N'*-bis(4-hydroxybenzyl)-5-(2-ethylhexyloxy) isophthalamide (1.00 g, 1.98 mmol) and triethylamine (0.69 mL, 3.00 mmol) in tetrahydrofuran (500 mL) over a period of one hour. The solution was then left to stir for twenty four hours after which time a precipitate had formed. The precipitate was filtered and the solvent removed in vacuo to leave a yellow solid that was then re-dissolved in 250 mL DCM. The organic solution was washed with HCl (0.2M, 50 mL) and $NaHCO_3$ solution (50 mL). The organic layer was dried over anhydrous magnesium sulphate and evaporated to dryness leaving a cream foam. Purification by column chromatography (dichloromethane: methanol, 99:1) afforded the macrocycle as a white solid: macrocycle **106**. Yield: 0.55 g, 41%; m.p. 117-119°C; $^1$H NMR (300 MHz, $CDCl_3$), $\delta$ = 0.86 (t, 6H, J = 6.8 Hz, 2x $CH_3$), 1.35 (m, 14H, 7 x alkyl $CH_2$), 1.65 (m, 7H, 3 x alkyl $CH_2$+ CH), 2.50 (t, J = 6.3 Hz, 4H, $CH_2C\underline{H}_2CO_2$), 3.83

(d, 2H, J = 5.8 Hz, $OC\underline{H}_2CH(Et)CH_2$), 4.42 (d, 4H, J = 5.4 Hz, $CONHC\underline{H}_2$), 6.62 (t, J = 5.4 Hz, 2H, $CON\underline{H}CH_2$), 6.97 (d, 4H, J = 8.3 Hz, ArCH), 7.22 (d, 4H, J = 8.3 Hz, ArCH) 7.24 (s, 1H, ArCH), 7.48 (s, 2H, ArCH); $^{13}C$ NMR (75 MHz, $CDCl_3$) δ = 11.10 ($CH_3$), 14.10 ($CH_3$), 23.04 ($CH_2$), 23.80 ($CH_2$), 24.88 ($CH_2$), 28.41 ($CH_2$), 29.03 ($CH_2$), 29.17 ($CH_2$), 30.45 ($CH_2$), 34.01 (CH), 39.28 ($CO_2\underline{C}H_2CH_2$), 43.60 ($CONH\underline{C}H_2$), 70.97 ($O\underline{C}H_2CH(Et)CH_2$), 115.71 (ArCH), 117.00 (ArCH), 121.87 (ArCH), 129.21 (ArCH), 135.38 (q, ArC), 135.92 (q, ArC), 150.15 (q, ArC), 160.10 (q, ArC), 166.68 (CO), 172.29 (CO); FAB-MS (*m*BNA matrix): *m/z* 671 $[M+H]^+$, 693 $[M+Na]^+$; anal. calcd. for $C_{40}H_{50}O_7N_2$ (670): C, 71.6 %; H, 7.5 %; N, 4.2 %; found: C, 71.9 %; H, 7.7 %; N, 4.5 %.

**Tris(4-chlorophenyl)propionic acid chloride**

Tris(4-chlorophenyl)propionic acid (15.0 g, 36.9 mmol) and oxaloyl dichloride (7.0 g, 4.9 mL, 55.5 mmol) were stirred in toluene (100 mL) at room temperature for 24 hours. The reaction mixture was then reduced in *vacuo* to dryness to give a brown solid, which was then recrystallised from dichloromethane/hexane to give an off white solid. Yield: 14.1g, 90%; m.p. 227.7-229.7°C; $^1H$ NMR (200 MHz, $CDCl_3$) δ = 4.63 (s, 2H, $CH_2$), 7.38 (d, 6H, *J* = 8.3, ArCH), 7.62 (d, 6H, *J* = 8.3 Hz, ArCH); $^{13}C$ NMR (75 MHz, $CDCl_3$) δ = 55.01 ($CH_2$), 58.32 (q, C), 128.79 (ArCH), 129.93 (ArCH), 133.10 (q, ArC), 142.76 (q, ArC), 169.80 (CO); anal. calcd. for $C_{21}H_{14}OCl_4$ (424): C, 59.4 %; H, 3.3 %; Cl, 33.5 %; found C, 59.6 %, H, 3.3 %, Cl, 33.5 %.

***N*-Tris(4-chlorophenyl)propionyl glycine methyl ester**

To a stirred solution of glycine methyl ester hydrochloride (2.00 g, 16.32 mmol) and triethylamine (3.46 g, 4.77 mL, 34.27 mmol) in dichloromethane (100 mL) was added dropwise a solution of tris(4-chlorophenyl)propionic acid chloride (7.27 g,

17.14 mmol) in dichloromethane (50 mL) over a period of 30 minutes. The resulting reaction mixture was then stirred for a further eighteen hours and then filtered. The solution was then washed with dilute HCl (0.2M) then saturated sodium bicarbonate solution and dried over magnesium sulphate. The reaction mixture was filtered, concentrated and then recrystallised from dichloromethane/hexane to give the product as a white solid. Yield: 6.12 g, 79 %; m.p. 147.5-149.3°C; $^{1}$H NMR (400 MHz, $CDCl_3$) δ = 3.53 (s, 2H, $C\underline{H}_2CONH$), 3.71 (s, 3H, $CH_3$), 3.76 (d, 2H, *J* = 5.0 Hz, $NHC\underline{H}_2CO_2$), 5.64 (bt, 1H, J = 5.0 Hz $CONHCH_2$), 7.18 (d, 6H, *J* = 8.5 Hz, ArCH), 7.27 (d, 6H, *J* = 8.5 Hz, ArCH); $^{13}$C NMR (100 MHz, $CDCl_3$) δ = 41.66 ($CH_2$), 48.02 ($CH_2$), 52.77 ($OCH_3$) 55.53 (q, C), 128.76 (ArCH), 130.75 (ArCH), 133.15 (q, ArC), 144.50 (q, ArC), 170.00 (CO), 170.26 (CO); FAB-MS (*m*BNA Matrix): *m/z* 476 $[M+H]^+$ ($^{35}$Cl); anal. calcd. for $C_{24}H_{20}O_3NCl_3$ (475): C, 60.63 %; H, 4.21 %; N, 2.95 %. found: C, 60.41 %; H, 4.23 %; N, 2.81.

**_N_-tris(4-chlorophenyl)propionyl glycylglycine ethyl ester**

To a stirred solution of glycylglycine ethyl ester hydrochloride (1.85 g, 9.43 mmol) and triethylamine (2.10 g, 2.88 mL, 20.80 mmol) in dichloromethane (100 mL) was added dropwise a solution of tris(4-chlorophenyl)propionic acid chloride (4.00 g, 9.43 mmol) in dichloromethane over a period 30 minutes. The resulting reaction mixture was then stirred for a further eighteen hours and then filtered. The solution was then washed with dilute HCl (0.2M, 50 mL) then saturated sodium bicarbonate solution (50 mL) and dried over magnesium sulphate. The reaction mixture was filtered, concentrated and then recrystallised from dichloromethane/hexane to give the product as a white solid. Yield: 1.51 g, 30 %; m.p. 183.6-185.4°C; $^{1}$H NMR (300 MHz, $CDCl_3$) δ = 1.28 (t, 3H, *J* = 7.3 Hz, $CH_2C\underline{H}_3$), 3.52 (s, 2H, $C\underline{H}_2CONH$), 3.66 (d, 2H, *J* = 5.2 Hz, $CONHC\underline{H}_2CO$), 3.90 (d, 2H, *J* = 5.2 Hz, $CONHC\underline{H}_2CO$) 4.19 (q,

2H, $J$ = 7.3 Hz, OC<u>H</u>$_2$CH$_3$), 6.06 (bt, 1H, $J$ = 5.2 Hz, CON<u>H</u>CH$_2$), 6.24 (bt, 1H, $J$ = 5.2 Hz, CON<u>H</u>CH$_2$), 7.14 (d, 6H, $J$ = 8.8 Hz, ArCH), 7.24 (d, 6H, $J$ = 8.8 Hz, ArCH); $^{13}$C NMR (75 MHz, $CDCl_3$) δ = 13.98 ($CH_3$), 40.98 ($CH_2$), 42.89 ($CH_2$), 47.21 ($CH_2$) 54.97 (q, C), 67.78 ($OCH_2$), 128.12 (ArCH), 130.25 (ArCH), 132.49 (q, ArC), 144.12 (q, ArC), 168.72 (CO), 169.36 (CO), 170.11 (CO); FAB-MS (*m*BNA matrix): *m/z* 547 $[M+H]^+$ ($^{35}$Cl); anal. calcd. for $C_{27}H_{25}O_4N_2Cl_3$ (547.5): C, 59.2 %; H, 4.6 %; N, 5.1 %; Cl, 19.4 %; found: C, 59.2 %; H, 4.6 %; N, 5.2 %; Cl, 19.2 %.

**_N_-Tris(4-chlorophenyl)propionyl glycylglycylglycine**

To a stirred solution of glycylglycylglycine (1.00 g, 4.61 mmol) and sodium hydroxide (0.37 g, 9.22 mmol) in water/ tetrahydrofuran (10 mL: 10mL) was added a solution of tris(4-chlorophenyl)propionic acid chloride (1.95 g, 4.61 mmol) in tetrahydrofuran (10 mL). The reaction mixture was allowed to stir for 1 hour after which time the reaction mixture was acidified with conc. HCl resulting in the formation of an oil. The tetrahydrofuran was removed in *vacuo* and the mixture extracted with ethyl acetate (4 x 50 mL). The reaction mixture was then evaporated to dryness and the resulting solid washed with dichloromethane (4 x 50 mL) to leave the product as a white solid. Yield: 1.76 g, 63 %; m.p. 147.1-149.0°C; $^1$H NMR (400 MHz, DMSO-$d_6$) δ = 3.48 (d, 2H, $J$ = 5.5, NHC<u>H</u>$_2$CO), 3.65 (s, 2H, C<u>H</u>$_2$CONH) 3.68 (d, 2H, $J$ = 5.5 Hz, NHC<u>H</u>$_2$CO), 3.74 (d, 2H, $J$ = 5.5 Hz, NHC<u>H</u>$_2$CO) 7.14 (d, 6H, $J$ = 9.0 Hz, ArCH), 7.32 (d, 6H, $J$ = 9.0 Hz, ArCH), 7.99 (t, 1H, $J$= 5.5 Hz, CON<u>H</u>CH$_2$), 8.06 (t, 1H, $J$= 5.5 Hz, CON<u>H</u>CH$_2$), 8.06 (t, 1H, $J$= 5.5 Hz, CON<u>H</u>CH$_2$); $^{13}$C NMR (75 MHz, DMSO-$d_6$) δ = 44.48 ($CH_2$), 45.15 ($CH_2$), 45.64 ($CH_2$), 49.66 ($CH_2$), 58.51 (q, C), 131.61 (ArCH), 134.79 (ArCH), 134.87 (q, ArC), 149.32 (q, ArC), 172.93 (CO), 173.04 (CO), 173.81 (CO), 175.00 (CO); FAB-MS (*m*BNA matrix): *m/z* 576 $[M+H]^+$ 597 $[M+Na]^+$ ($^{35}$Cl); anal. calcd. for

$C_{27}H_{24}O_5N_3Cl_3$ (576.5): C, 56.2 %; H, 4.1 %; N, 7.2 %; Cl, 18.4 %; found C, 56.3 %; H, 3.9 %; N, 7.0 %; Cl, 18.4 %.

**_N_-Tris(4-chlorophenyl)propionyl glycine undec-10-enyl ester**

A stirred solution containing *N*-tris(4-chlorophenyl)propionyl glycine ethyl ester (2.00 g, 4.070 mmol), undec-10-en-1-ol (0.82 mL, 4.070 mmol) and bis(dibutylchlorotin)oxide (10 mol %, 0.21 g, 0.407 mmol) was refluxed in anhydrous toluene (60 mL) for 1 hour. Toluene was then distilled off slowly over a period of 1 hour until only 10 mL remained. A further 50 mL toluene was added and once again removed by slow distillation. The solvent was then removed in *vacuo* and the reaction mixture purified by column chromatography (1% methanol/ dichloromethane) to give N-tris(4-chlorophenyl)propionyl glycine undec-10-enyl ester as a white foam. Yield: 2.34 g, 95 %; m.p. 69.3-70.3°C; $^1$H NMR (400 MHz, $CDCl_3$) $\delta$ = 1.29 (bm, 10H, 5 x $C\underline{H}_2$), 1.38 (bp, 2H, $J$ = 7.0, $C\underline{H}_2$), 1.61 (bp, 2H, $J$ = 7.0 Hz, $CH_2$), 2.05 (q, 2H, $J$ = 7.0 Hz, $CH_2$), 3.53 (s, 2H, $CH_2CONH$), 3.75 (d, 2H, $J$ = 5.0 Hz, $CONHC\underline{H}_2CO$), 4.09 (t, 2H, $J$ = 7.0 Hz, $CO_2C\underline{H}_2CH_2$), 4.98 (m, 2H, $CH_2CHC\underline{H}_2$), 5.60 (t, 1H, $J$ = 5.0 Hz, $CON\underline{H}CH_2CO$), 5.83 (m, 1H, $CH_2C\underline{H}CH_2$), 7.13 (d, 6H, $J$ = 8.0 Hz, ArCH), 7.27 (d, 6H, $J$ = 8.0 Hz, ArCH); $^{13}$C NMR (100 MHz, $CDCl_3$) $\delta$ = 26.16 ($CH_2$), 28.84 ($CH_2$), 29.30 ($CH_2$), 29.48 ($CH_2$), 29.57 ($CH_2$), 29.78 ($CH_2$), 29.82 ($CH_2$), 34.19 ($CH_2$), 41.76 ($CH_2$), 48.04 ($CH_2$), 55.55 (q, C) 66.14 ($CO_2\underline{C}H_2$), 114.57, ($CH_2CH\underline{C}H_2$), 128.75 (ArCH), 130.76 (ArCH), 133.14 (q, ArC), 139.58 ($CH_2\underline{C}HCH_2$), 144.53 (q, ArC), 169.94 (2 x CO from HMBC); FAB-MS (*m*BNA matrix): m/z 614 $[M+H]^+$ ($^{35}$Cl); anal. calcd. for $C_{34}H_{38}O_3NCl_3$ (614.5): C, 66.40 %; H, 6.23 %; N, 2.28 %; found C, 66.05 %; H, 6.25 %; N, 2.07 %.

**_N_-Tris(4-chlorophenyl)propionyl glycylglycine undec-10-enyl ester**

A stirred solution containing _N_-tris(4-chlorophenyl)propionyl glycylglycine ethyl ester (3.00 g, 5.490 mmol) undec-10-en-1-ol (1.10 mL, 5.490 mmol) and bis(dibutylchlorotin)oxide (5 mol %, 0.14 g, 0.274 mmol) was refluxed in anhydrous toluene (60 mL) for 1 hour. Toluene was then distilled off slowly over a period of 1 hour until only 10 mL remained. A further 50 mL toluene was added and once again removed by slow distillation. The solvent was then removed in *vacuo* and the reaction mixture purified by column chromatography (10 % ethyl acetate/ dichloromethane) to give the product as a white foam. Yield: 3.71 g, 97 %; m.p. 123.6-125.2°C; $^{1}$H NMR (400 MHz, $CDCl_3$) $\delta$ = 1.24-1.42 (bm, 12H, 6 x $C\underline{H}_2$), 1.63 (bm, 2H, $CH_2$), 2.04 (q, 2H, $J$ = 7.0 Hz, $CH_2$), 3.52 (s, 2H, $C\underline{H}_2CONH$), 3.66 (d, 2H, $J$ = 5.0 Hz, $CONHC\underline{H}_2CO$), 3.90 (d, 2H, $J$ = 5.0 Hz, $CONHC\underline{H}_2CO$), 4.12 (t, 2H, $J$ = 7.0 Hz, $OC\underline{H}_2CH_2$), 4.96 (m, 2H, $CH_2CHC\underline{H}_2$), 5.81 (m, 1H, $CH_2C\underline{H}CH_2$), 6.01 (t, 1H, $J$ = 5.0 Hz, $CON\underline{H}CH_2CO$), 6.20 (t, 1H, $J$ = 5.0 Hz, $CON\underline{H}CH_2CO$), 7.145 (d, 6H, $J$ = 8.5 Hz, ArCH), 7.238 (d, 6H, $J$ = 8.5 Hz, ArCH); $^{13}$C NMR (400 MHz, $CDCl_3$) $\delta$ = 26.22 ($CH_2$), 28.90 ($CH_2$), 29.31 ($CH_2$), 29.50 ($CH_2$), 29.61 (CH), 29.80 ($CH_2$), 29.85 ($CH_2$), 34.19 ($CH_2$), 41.45 ($CH_2$) 43.44 ($CH_2$), 47.68 ($CH_2$), 55.50 (q, C), 66.15 ($O\underline{C}H_2CH_2$), 114.58, ($CH_2CH\underline{C}H_2$), 128.66 (ArCH), 130.82 (ArCH), 133.02 (q, ArC), 139.57 ($CH_2\underline{C}HCH_2$), 144.71 (q, ArC), 169.36 (CO), 170.04 (CO), 170.71 (CO); FAB-MS (*m*BNA matrix): *m/z* 671 $[M+H]^+$ ($^{35}$Cl); anal. calcd. for $C_{36}H_{41}O_4N_2Cl_3$ (671.5): C, 64.33 %; H, 6.15 %; N, 4.17 %; found: C, 64.40 %; H, 6.09 %; N, 4.22 %.

**_N_-Tris(4-chlorophenyl)propionyl glycylglycylglycine undec-10-enyl ester**

_N_-Tris(4-chlorophenyl)propionyl glycylglycylglycine (4.00 g, 6.62 mmol), undec-10-en-1-ol (1.33 mL, 6.62 mmol) and dimethylaminopyridine (0.80 g, 6.62 mmol), were stirred in anhydrous dimethylformamide (100 mL) at O°C for 10 minutes. EDCI (1.26 g, 6.62 mmol) was then added and the reaction mixture allowed to warm to room temperature and stirred for a further 24 hours. The reaction mixture was diluted with water (200 mL) and extracted with ethyl acetate (5 x 100mL) and the organic extracts washed with 0.2M HCl (50 mL) and saturated sodium bicarbonate solution (50 mL). The organic layer was dried over magnesium sulphate, filtered and the solvent removed in *vacuo* to leave a white solid which was recrystallised from dichloromethane. Yield: 1.61 g, 33.3 %; m.p. 145.2-146.8°C; $^{1}$H NMR (400 MHz, $CDCl_3$) δ = 1.28 (bm, 10H, 5 x $CH_2$), 1.36 (bm, 2H, $CH_2$), 1.59 (bm, 2H, $CH_2$), 2.02 (m, 2H, $CH_2$), 3.57 (s, 2H, $C\underline{H}_2CONH$), 3.68 (d, 2H, $J$ = 5.5 Hz, $CONHC\underline{H}_2CO$), 3.75 (d, 2H, $J$ = 5.5 Hz, $CONHC\underline{H}_2CO$), 3.90 (d, 2H, $J$ = 5.5 Hz, $CONHC\underline{H}_2CO$), 4.01 (t, 2H, $J$ = 6.5 Hz, $OC\underline{H}_2CH_2$), 4.95 (m, 2H, $CH_2CHC\underline{H}_2$), 5.80 (m, 1H, $CH_2C\underline{H}CH_2$), 6.16 (bm, 1H, $CON\underline{H}CH_2CO$), 6.91 (bm, 1H, $CON\underline{H}CH_2CO$), 7.12 (d, 6H, $J$ = 9.5 Hz, $ArC\underline{H}$), 7.20 (d, 6H, $J$ = 9.5 Hz, ArCH) 7.31 (bm, 1H, $CON\underline{H}CH_2CO$); $^{13}$C NMR (100 MHz, $CDCl_3$) δ = 26.28 ($CH_2$), 28.90 ($CH_2$), 29.31 ($CH_2$), 29.67 ($CH_2$), 29.82 ($CH_2$), 29.87 ($CH_2$), 34.20 ($CH_2$), 41.48 ($CH_2$), 43.33 ($CH_2$), 43.51 ($CH_2$), 47.03 ($CH_2$), 55.58 ($CH_2$), 63.36 (q, C), 66.18 ($O\underline{C}H_2CH_2$), 114.60 ($CH_2CH\underline{C}H_2$), 128.55 (ArCH), 130.89 (ArCH), 132.87 (q, ArC), 139.57 ($CH_2\underline{C}HCH_2$), 144.87 (q, ArC), 169.40 (CO), 169.51 (CO), 170.21 (CO), 171.00 (CO); FAB-MS (*m*BNA matrix): *m/z* 728 $[M+H]^+$ ($^{35}$Cl); anal. calcd. for $C_{38}H_{44}O_5N_3Cl_3$ (728.5): C, 62.60 %; H, 6.08 %; N, 5.76 %; found: C, 62.46 %; H, 6.10 %; N, 5.60 %.

**General method for the preparation of amide based "magic rods".**

A closed schlenk tube with magnetic stirring bar was purged with argon. To this was added Grubbs' metathesis catalyst **50** (5 mol%). The schlenk tube was then sealed with parafilm and left under a constant stream of argon for ten minutes. Terminal alkene was dissolved in a sealed flask containing anhydrous dichloromethane, which was subsequently evacuated and purged with argon several times and then transferred to the schlenk tube using a syringe. The reaction was allowed to continue until no further change was observed by TLC and then the reaction mixture was evaporated to dryness and purified by chromatography.

**Thread 109a**

*N*-Tris(4-chlorophenyl)propionyl glycine undec-10-enyl ester (1.00 g, 1.628 mmol), Grubbs' Catalyst **50** (5 mol %, 0.07 g) and 40 mL dichloromethane. Chromatography: 1% methanol/ dichloromethane, product was isolated as a white foam. Yield: 0.88 g, 90%; m.p. 89.4-91.3°C; $^{1}$H NMR (400 MHz, $CDCl_3$) $\delta$ = 1.26-1.39 (bm, 24H, 12 x $CH_2$), 1.62 (bm, 4H, $CH_2$), 1.98 (bq, 4H, $J$ = 6.5 Hz, $CH_2$), 3.53 (s, 4H, $C\underline{H}_2CONH$), 3.76 (d, 4H, $J$ = 5.0 Hz, $CONHC\underline{H}_2CO_2$), 4.10 (t, 4H, $J$ = 6.5 Hz, $OC\underline{H}_2CH_2$), {*E*:*Z* ratio 5:1 2H, $CH_2C\underline{H}C\underline{H}CH_2$, 5.37 (*Z*, t, $J$ = 4.5 Hz), 5.400 (*E*, t, $J$ = 3.5 Hz)}, 5.58 (t, 2H, $J$ = 5.0 Hz, $CON\underline{H}CH_2$), 7.18 (d, 12H, $J$ = 8.5 Hz, ArCH), 7.28 (d, 12H, $J$ = 8.5 Hz, ArCH); $^{13}$C NMR (100 MHz $CDCl_3$) $\delta$ = 26.16 ($CH_2$), 27.60 ($CH_2$), 28.85 ($CH_2$), 29.53 ($CH_2$), 29.81 ($CH_2$), 30.03 ($CH_2$), 30.14 ($CH_2$) 33.00 $CH_2$), 41.76 ($CH_2$), 48.06 ($CH_2$), 55.54 (q, C), 66.16 ($O\underline{C}H_2CH_2$), 128.76 (ArCH), 130.28 ($CH_2\underline{C}H\underline{C}HCH_2$), 130.74 (ArCH), 133.14 (q, ArC), 144.49 (q, ArC), 169.91 (CO), 169.95 (CO); FAB-MS (*m*BNA matrix): *m/z* 1199 $[M+H]^+$ ($^{35}$Cl); anal. calcd. for $C_{66}H_{72}O_6N_2Cl_6$ (1198): C, 66.11 %; H, 6.01 %; N, 2.34 %; found: C, 65.76; H, 5.95 %; N, 2.14 %.

**Thread 109b**

*N*-Tris(4-chlorophenyl)propionyl glycylglycine undec-10-enyl ester (1.00 g, 1.49 mmol), Grubbs' Catalyst **50** (5 mol %, 0.06 g) and 40 mL dichloromethane. Chromatography: 5% methanol/ dichloromethane, product isolated as a white foam. Yield: 0.93 g, 95 %; m.p. 78.9-80.7°C; $^{1}$H NMR (400 MHz, $CDCl_3$) δ = 1.23-1.38 (bm, 24H, 12 x $CH_2$), 1.62 (bp, *J* = 7.0 Hz, 4H, $CH_2$), 1.96 (bq, 4H, *J* = 7.0 Hz, $CH_2$), 3.51 (s, 4H $C\underline{H}_2CONH$), 3.63 (d, 4H, *J* = 5.0 Hz, $CONHC\underline{H}_2CO$), 3.89 (d, 4H, *J* = 5.0 Hz, $CONHC\underline{H}_2CO$), 4.10 (t, 4H, *J* = 6.5 Hz, $OC\underline{H}_2CH_2$), {*E:Z* ratio 3:1 2H, $CH_2C\underline{H}C\underline{H}CH_2$, 5.35 (*Z*, m), 5.40 (*E*, m,)}, 6.31 (t, 2H, *J* = 5.0 Hz, $CH_2CON\underline{H}CH_2$), 6.39 (t, 2H, *J* = 5.0 Hz, $CH_2CON\underline{H}CH_2$), 7.13 (d, 12H, *J* = 9.0 Hz, ArCH), 7.22 (d, 12H, J = 9.0 Hz, ArCH); $^{13}$C NMR (100 MHz $CDCl_3$) δ = 26.21 ($CH_2$), 27.51 ($CH_2$), 28.89 ($CH_2$), 29.36 ($CH_2$), 29.50 ($CH_2$), 29.87 ($CH_2$), 30.01 ($CH_2$), 32.91 ($CH_2$), 41.49 ($CH_2$), 43.43 ($CH_2$), 47.79 ($CH_2$), 55.53 (q, C), 66.20 ($O\underline{C}H_2CH_2$), 128.69 (ArCH), 130.32 ($CH_2\underline{C}H\underline{C}HCH_2$), 130.79 (ArCH), 133.07 (q, ArC), 144.63 (q, ArC), 169.16 (CO), 170.06 (CO), 170.63 (CO); FAB-MS (*m*BNA matrix): *m/z* 1313 $[M+H]^+$ ($^{35}$Cl); $C_{70}H_{78}O_8N_4Cl_6$ (1312): C, 64.02 %; H, 5.95 %; N, 4.27 %; found C, 64.33 %; H, 6.25 %; N, 4.10 %.

**Thread 109c**

Due to the low solubility of the starting material in dichloromethane this reaction was carried out using tetrachloroethane (40 mL). *N*-tris(4-chlorophenyl)propionyl glycylglycylglycine undecenyl ester (1.00 g, 1.32 mmol), Grubbs' catalyst (5 mol %, 0.054 g). Chromatography (5% methanol/ dichloromethane, product isolated as a viscous oil. Yield: 0.69 g, 73.3 %; $^{1}$H NMR (400 MHz, $CDCl_3$) δ = 1.26 (bm, 24H, 12 x $CH_2$), 1.60 (bp, 4H, *J* = 7.0 Hz, $CH_2$), 1.96 (bq, 4H, *J* = 7.0 Hz, $CH_2$), 3.55 (s, 4H $C\underline{H}_2CONH$), 3.65 (d, 4H, *J* = 4.0 Hz, $CONHC\underline{H}_2CO$), 3.81 (d, 4H, *J* = 5.0 Hz,

CONHC$\underline{H}_2$CO), 3.89 (d, 4H, $J$ = 5.0 Hz, CONHC$\underline{H}_2$CO), 4.03 (t, 4H, $J$ = 7.0 Hz, OC$\underline{H}_2$CH$_2$), {*E*:*Z* ratio 4:1 2H, CH$_2$C$\underline{H}$C$\underline{H}$CH$_2$, 5.34 (*Z*, m), 5.36 (*E*, m)}, 6.73 (bm, 2H, CON$\underline{H}$CH$_2$), 6.04 (bm, 2H, $J$ = 5.0 Hz, CON$\underline{H}$CH$_2$), 7.12 (d, 12H, $J$ = 8.5 Hz, ArCH), 7.21 (d, 14H, $J$ = 8.5 Hz, 6ArCH and 2CON$\underline{H}$CH$_2$CO); $^{13}$C NMR (100 MHz CDCl$_3$) δ = 26.25 (CH$_2$), 27.50 (CH$_2$), 28.88 (CH$_2$), 29.28 (CH$_2$), 29.59 (CH$_2$), 29.84 (CH$_2$), 30.03 (CH$_2$), 32.87 (CH$_2$), 41.55 (CH$_2$), 43.23 (CH$_2$), 43.55 (CH$_2$), 47.34 (CH$_2$), 55.55 (q, C), 66.21 (O$\underline{C}$H$_2$CH$_2$), 128.61 (ArCH), 130.33 (CH$_2\underline{C}$H$\underline{C}$HCH$_2$), 130.84 (ArCH), 132.98 (q, ArC), 144.74 (q, ArC), 169.44 (CO), 169.55 (CO), 170.28 (CO) 171.01 (CO); FAB-MS (*m*BNA matrix): *m/z* 1427 [M+H]$^+$ ($^{35}$Cl); $C_{74}H_{84}O_{10}N_6Cl_6$ (1426): C, 62.27 %; H, 5.89 %; N, 5.89 %; found C, 62.09 %; H, 6.01 %; N, 5.72 %.

**General method for preparation of amide based "Magic rod" rotaxanes**

A closed flame-dried schlenk tube with magnetic stirring bar was purged with argon. To this was added Grubbs' metathesis catalyst **50**. The schlenk tube was then sealed with parafilm and left under a constant stream of argon for ten minutes. "magic rod" thread **109a,b** or **c** and macrocycle **106** were dissolved in a sealed flask containing anhydrous dichloromethane which was subsequently evacuated and purged with argon several times and then transferred to the schlenk tube using a syringe. The reaction was allowed to continue until no further change was observed by TLC at which point the reaction mixture was evaporated to dryness and purified by repeated chromatography.

**[2]rotaxane 110a**

Macrocycle **106** (0.0500 g, 0.0746 mmol), thread **109a** (0.0459 g, 0.0373 mmol), Grubbs' catalyst **50** (10 mol %, 0.0031 g, 0.0037 mmol). Chromatography: 1% methanol in dichloromethane followed by a second purification in 10% ethyl acetate in dichloromethane. Product isolated as a clear glass. Yield: 0.0105 g, 15 % relative to thread; $^{1}$H NMR (400 MHz, $CDCl_3$) $\delta$ = 0.96 (m, 6H, 2 x $CH_3$), 1.24-1.41 (bm, 32H, 16 x alkyl $CH_2$), 1.45 (bm, 8H, 4 x alkyl $CH_2$), 1.60 (p, 4H, $J$ = 6.5 Hz, $CH_2$), 1.69 (bm, 4H, $CH_2$), 1.83 (m, 1H, $OCH_2CH(Et)CH_2$), 1.98 (bm, 4H, $CH_2$), 2.63 (t, 4H, $J$ = 5.5 Hz, $COCH_2CH_2^{macrocycle}$), 3.10 (bm, 4H, $NHCH_2CO_2$), 3.19 (s, 4H, $CH_2CONH$), 3.98 (t, 4H, $J$ = 6.5 Hz, $OCH_2CH_2$), 4.03 (d, 2H, $J$ = 5.5 Hz, $OCH_2CH(Et)CH_2$), 4.49 (d, 4H, $J$ = 4.5 Hz, $CONHCH_2^{macrocycle}$), {*E*:*Z* ratio 3:1, 2H, $CH_2CHCHCH_2$, 5.37 (*Z*, m), 5.40 (*E*, m)}, 5.62 (t, 2H, $J$ = 5.5 Hz, $CONHCH_2CO$), 6.80 (d, 4H, J = 8.0 Hz, $ArCH^{macrocycle}$), 7.01 (d, 12H, $J$ = 8.0 Hz, ArCH), 7.12 (d, 4H, $J$ = 8.0 Hz, $ArCH^{macrocycle}$), 7.19 (d, 12H, $J$ = 8.0 Hz, ArCH), 7.40 (s, 1H, $ArCH^{macrocycle}$), 7.87 (s, 2H, $ArCH^{macrocycle}$), 7.98 (t, 2H, $J$ = 4.5 Hz, $CONHCH_2^{macrocycle}$); $^{13}$C NMR (100 MHz, $CDCl_3$) $\delta$ = 11.55 ($CH_3$), 14.52 ($CH_3$), 23.49 ($CH_2$), 24.28 ($CH_2$), 24.86 ($CH_2$), 26.16 ($CH_2$), 27.62 ($CH_2$), 28.42 ($CH_2$), 29.39 ($CH_2$), 29.48 ($CH_2$), 29.53 ($CH_2$), 29.57 ($CH_2$), 29.70 ($CH_2$), 29.91 ($CH_2$), 30.04 ($CH_2$), 30.16 ($CH_2$), 30.94 ($CH_2$), 34.01 ($CH_2$) 39.76 (CH), 41.25 ($CH_2$), 44.83 ($CH_2$), 47.73 ($CH_2$), 55.38 (q, C), 65.97 ($OCH_2CH_2$), 71.41 ($OCH_2CH(Et)CH_2$), 115.79 (ArCH), 118.58 (ArCH), 121.92 (ArCH), 128.75 (ArCH), 130.27 ($CH_2CHCHCH_2$), 130.84 (ArCH), 131.09 (ArCH), 132.87 (q, ArC) 135.90 (q, ArC), 144.51 q, ArC), 150.32 (q, ArC), 160.29 (q, ArC), 167.04 (q, ArC), 169.94 (CO), 170.05 (CO), 170.47 (CO), 173.40 (CO); FAB-MS (*m*BNA matrix): *m/z* 1869 $[M+H]^+$ ($^{35}$Cl).

**[2]rotaxane 110b**

Macrocycle **106** (0.0500 g, 0.0746 mmol), thread **109b** (0.0484 g, 0.0373 mmol), Grubbs' catalyst **50** (10 mol %, 0.0031 g, 0.0307 mmol). Chromatography: 5% methanol in dichloromethane. Product isolated as a clear glass. Yield: 0.0263 g, 35.5 % relative to thread; $^{1}$H NMR (400 MHz, $CDCl_3$) $\delta$ = 0.91 (m, 6H, 2 x $CH_3$), 1.22-1.37 (bm, 32H, 16 x alkyl $CH_2$), 1.38-1.56 (bm, 12H, 6 x alkyl $CH_2$), 1.58-1.63 (bm, 4H, 2 x $CH_2$), 1.78 (m, 1H, $OCH_2CH(Et)CH_2$), 1.95 (q, 4H, $J$ = 4.5 Hz, 2 x $CH_2$), 2.62 (t, 4H, $J$ = 5.0 Hz, $COCH_2CH_2^{macrocycle}$), 3.09 (vbs, 4H, $CH_2CONH$), 3.29 (bm, 4H, $CONHCH_2CO$), 3.62 (bm, 4H, $CONHCH_2CO$), 3.97 (d, 2H, $J$ = 6.0 Hz, $OCH_2CH(Et)CH_2$), 4.09 (t, 4H, $J$ = 7.5 Hz, $OCH_2CH_2$), 4.50 (d, 4H, $J$ = 5.0 Hz, $CONHCH_2^{macrocycle}$), {*E*:*Z* ratio 4:1, 2H, $CH_2CHCHCH_2$, 5.37 (*Z*, m), 5.40 (*E*, m)}, 5.89 (bm, 2H, $CONHCH_2$), 6.21 (bm, 2H, $CONHCH_2CO$), 6.80 (d, 4H, $J$ = 8.5 Hz, $ArCH^{macrocycle}$), 7.04 (d, 12H, $J$ = 8.0 Hz, ArCH), 7.16 (d, 12H, $J$ = 8.0 Hz, ArCH), 7.18 (d, 4H, $J$ = 8.5 Hz, $ArCH^{macrocycle}$), 7.70 (s, 1H, $ArCH^{macrocycle}$), 7.84 (s, 2H, $ArCH^{macrocycle}$), 8.09 (t, 2H, $J$ = 5.0 Hz, $CONHCH_2^{macrocycle}$); $^{13}$C NMR (100 MHz, $CDCl_3$) $\delta$ = 11.52 ($CH_3$), 14.52 ($CH_3$), 23.46 ($CH_2$), 24.26 ($CH_2$), 24.75 ($CH_2$), 26.21 ($CH_2$), 28.08 ($CH_2$), 28.73 ($CH_2$), 28.91 ($CH_2$), 29.20 ($CH_2$), 29.46 ($CH_2$), 29.52 ($CH_2$), 29.62 ($CH_2$), 29.88 ($CH_2$), 29.91 ($CH_2$), 30.10 ($CH_2$), 30.91 ($CH_2$), 32.93 ($CH_2$), 34.09 ($CH_2$) 39.73 (CH), 41.47 ($CH_2$), 44.61 ($CH_2$), 47.58 ($CH_2$), 55.34 (q, C), 66.04 ($OCH_2CH_2$), 71.38 ($OCH_2CH(Et)CH_2$), 116.03 (ArCH), 118.52 (ArCH), 122.03 (ArCH) 128.54 (ArCH), {*E*:*Z* ratio 4:1, 130.73 (*Z*, $CH_2CHCHCH_2$), 130.74 (*E*, $CH_2CHCHCH_2$)}, 130.88 (ArCH), 131.09 (ArCH), 132.91 (q, ArC) 135.64 (q, ArC), 136.41 (q, ArC), 144.75 (q, ArC), 150.12 (q, ArC), 160.32 (q, ArC), 166.79 (CO), 169.57 (CO), 169.76 (CO), 170.21 (CO), 174.26 (CO); FAB-MS (*m*BNA matrix): *m/z* 1984 $[M+H]^+$ ($^{35}$Cl 1 x $^{13}$C).

**[2]rotaxane 110c**

Macrocycle **106** (0.0500 g, 0.0746 mmol), thread **109c** (0.0554 g, 0.373 mmol), Grubbs' catalyst **50** (10 mol %, 0.0031 g, 0.0037 mmol). Chromatography: 10% methanol in dichloromethane. Product isolated as a clear glass. Yield: 0.0278 g, 35.5 % relative to thread. $^{1}$H NMR (400 MHz, $CDCl_3$) $\delta$ = 0.91 (m, 6H, 2 x $CH_3$), 1.20-1.36 (bm, 32H, 16 x alkyl $CH_2$), 1.39 (bm, 12H, 6 x alkyl $CH_2$), 1.55-1.71 (bm, 4H, 2 x $CH_2$), 1.738 (m, 1H, $OCH_2CH(Et)CH_2$), 1.95 (q, 4H, $J$ = 4.5 Hz, 2 x $CH_2$), 2.61 (t, 4H, $J$ = 6.0 Hz, $COCH_2CH_2^{macrocycle}$), 3.32 (bm, 8H, 4 x $CONHCH_2CO$), 3.54 (s, 4H, $CH_2CONH$), 3.78 (bm, 4H, $CONHCH_2CO$), 3.92 (d, 2H, $J$ = 5.0 Hz, $OCH_2CH(Et)CH_2$), 4.08 (t, 4H, $J$ = 7.0 Hz, $OCH_2CH_2$), 4.51 (bd, 4H, $CONHCH_2^{macrocycle}$), 5.36 (m, 2H, $CH_2CHCHCH_2$), 5.79 (vbm, 2H, $CONHCH_2CO$), 6.14 (bm, 2H, $CONHCH_2CO$), 6.66 (bm, 2H, $CONHCH_2CO$), 6.587 (d, 4H, $J$ = 8.5 Hz, $ArCH^{macrocycle}$), 7.06 (d, 12H, $J$ = 8.0 Hz, ArCH), 7.19 (m, 16H, 12 ArCH and 4 $ArCH^{macrocycle}$), 7.66 (s, 1H, $ArCH^{macrocycle}$), 7.80 (s, 2H, ArCH), 8.09 (t, 2H, $J$ = 5.0 Hz, $CONHCH_2^{macrocycle}$); $^{13}$C NMR (100 MHz, $CDCl_3$) $\delta$ = 11.47 ($CH_3$), 14.52 ($CH_3$), 23.48 ($CH_2$), 24.15 ($CH_2$), 24.74 ($CH_2$), 26.22 ($CH_2$), 28.14 ($CH_2$), 28.90 ($CH_2$), 29.17 ($CH_2$), 29.45 ($CH_2$), 29.62 ($CH_2$), 29.73 ($CH_2$), 29.81 ($CH_2$), 29.86 ($CH_2$), 29.97 ($CH_2$), 30.11 ($CH_2$), 30.81 ($CH_2$), 32.96 ($CH_2$), 34.09 ($CH_2$) 39.67 (CH), 41.58 ($CH_2$), 42.12 ($CH_2$), 44.63 ($CH_2$), 47.66 ($CH_2$), 55.45 (q, C), 66.13 ($OCH_2CH_2$), 71.56 ($OCH_2CH(Et)CH_2$), 116.11 (ArCH), 118.44 (ArCH), 122.20 (ArCH) 128.59 (ArCH), 128.73 (ArCH) {E:Z ratio 4:1 (Z, 130.29 $CH_2CHCHCH_2$), (E, 130.79 $CH_2CHCHCH_2$)}, 131.22 (ArCH), 132.95 (q, ArC) 135.76 (q, ArC), 136.40 (q, ArC), 144.67 (q, ArC), 150.22 (q, ArC), 160.29 (q, ArC), 166.78 (CO) 169.18 (CO), 169.36 (CO), 169.89 (CO), 170.01 (CO), 174.60 (CO); FAB-MS (*m*BNA matrix): *m/z* 2098 $[M+H]^+$ ($^{35}$Cl 1 x $^{13}$C).

**[3] rotaxane 111a**

Macrocycle **106** (0.0500 g, 0.0746 mmol), thread **109b** (0.0484 g, 0.0373 mmol), Grubbs' catalyst **50** (10 mol %, 0.0031 g, 0.0037 mmol). Chromatography: 1% methanol in dichloromethane followed by a second purification in 10% ethyl acetate in dichloromethane. Product isolated as a clear glass. Yield: 0.0223 g, 22.5 % relative to thread; $^{1}$H NMR (400 MHz, $CDCl_3$) $\delta$ = 0.91 (m, 12H, 4 x $CH_3$), 1.21-1.38 (bm, 48H, 24 x alkyl $CH_2$), 1.43 (bm, 16H, 8 x alkyl $CH_2$), 1.61 (bm, 4H, $CH_2$), 1.78 (m, 2H, $OCH_2CH(Et)CH_2$), 1.94 (bm, 4H, $CH_2$), 2.51 (d, 4H, $J$ = 6.0, $CONHCH_2CO$), 2.61 (m, 8H, $COCH_2CH_2^{macrocycle}$), 3.05 (s, 4H, $CH_2CONH$), 3.31 (d, 4H, $J$ = 5.0 Hz, $CONHCH_2CO$), 3.98 (d, 4H, $J$ = 6.0 Hz, $OCH_2CH(Et)CH_2$), 4.06 (t, 4H, $J$ = 6.5 Hz, $OCH_2CH_2$), 4.50 (dd, 4H, $J$ = 4.5 Hz, 14.5 Hz, $CONHCHH'^{macrocycle}$), 4.58 (dd, 4H, J= 4.5 Hz, 14.5 Hz, $CONHCHH'^{macrocycle}$), 5.37 (m, 4H, $CONHCH_2CO$ and $CH_2CHCHCH_2$), 6.32 (t, 2H, $J$ = 6.0 Hz, $CONHCH_2$), 6.80 (d, 8H, $J$ = 9.0 Hz, $ArCH^{macrocycle}$), 6.92 (d, 12H, $J$ = 8.5 Hz, ArCH), 7.127 (d, 12H, $J$ = 9.0 Hz, ArCH), 7.16 (d, 8H, $J$ = 8.5 Hz, $ArCH^{macrocycle}$), 7.71 (s, 2H, $ArCH^{macrocycle}$), 7.85 (s, 4H, $ArCH^{macrocycle}$), 8.09 (t, 4H, $J$ = 4.5 Hz, $CONHCH_2^{macrocycle}$); $^{13}$C NMR (100 MHz, $CDCl_3$) $\delta$ = 11.52 ($CH_3$), 14.52 ($CH_3$), 23.47 ($CH_2$), 24.26 ($CH_2$), 24.75 ($CH_2$), 26.23 ($CH_2$), 28.08 ($CH_2$), 28.78 ($CH_2$), 28.93 ($CH_2$), 29.20 ($CH_2$), 29.46 ($CH_2$), 29.60 ($CH_2$), 29.66 ($CH_2$), 29.88 ($CH_2$), 29.91 ($CH_2$), 30.08 ($CH_2$), 30.92 ($CH_2$), 33.03 ($CH_2$), 34.10 ($CH_2$) 39.73 ($OCH_2CH(Et)CH_2$), 41.40 ($CH_2$), 44.61 ($CH_2$), 47.57 ($CH_2$), 55.34 (q, C), 65.85 ($OCH_2CH_2$), 71.36 ($OCH_2CH(Et)CH_2$), 116.05 (ArCH), 118.52 (ArCH), 122.03 (ArCH), 128.33 (ArCH), {*E:Z* ratio 1:2, 128.50, (*E*, $CH_2CHCHCH_2$), 130.71 (*Z*, $CH_2CHCHCH_2$)}, 130.79 (ArCH), 131.09 (ArCH), 132.72 (q, ArC) 135.64 (q, ArC), 136.44 (q, ArC), 144.94 (q, ArC), 150.12 (q, ArC), 160.33 (q, ArC), 166.78 (CO),

169.57 (CO), 169.82 (CO), 170.22 (CO), 174.25 (CO); FAB-MS (*m*BNA matrix): *m/z* 2653 $[M+H]^+$ ($^{35}Cl + 4 \times {}^{13}C$).

**[3]rotaxane 111b**

Macrocycle **106** (0.0500 g, 0.0746 mmol), thread **109c** (0.0554 g, 0.0373 mmol), Grubbs' catalyst **50** (10 mol %, 0.0031 g, 0.0373 mmol). Chromatography: 1% methanol in dichloromethane. Product isolated as a clear glass. Yield: 0.0232 g, 22.5 % relative to thread; $^1$H NMR (400 MHz, $CDCl_3$) $\delta$ = 0.91 (m, 12H, 4 x $CH_3$), 1.20-1.36 (bm, 48H, 24 x alkyl $CH_2$), 1.36-1.54 (bm, 16H, 8 x alkyl $CH_2$), 1.64 (bm, 4H, 2 x $CH_2$), 1.74 (m, 2H, $OCH_2CH(Et)CH_2$), 1.95 (q, 4H, $J$ = 4.5 Hz, 2 x $CH_2$), 2.61 (t, 8H, $J$ = 5.5 Hz, $COCH_2CH_2^{macrocycle}$), 2.93 (d, 4H, $J$ = 5.5 Hz, $CONHCH_2CO$), 3.07 (d, 4H, $J$ = 5.5 Hz, $CONHCH_2CO$), 3.14 (s, 4H, $CH_2CONH$), 3.63 (d, 4H, $J$ = 5.5 Hz, $OCH_2CH(Et)CH_2$), 3.92 (d, 4H, $J$ = 5.5 Hz, $CONHCH_2CO$), 4.08 (t, 4H, $J$ = 6.5 Hz, $OCH_2CH_2$), 4.50 (dd, 4H, $J$ = 5.0 Hz, 14.0 Hz, $CONHCHH'^{macrocycle}$), 4.64 (dd, 4H, $J$ = 5.0 Hz, 14.0 Hz, $CONHCHH'^{macrocycle}$), 5.25 (t, 2H, $J$ = 5.5 Hz, $CONHCH_2CO$), {*E*:*Z* ratio 4:1, 2H, $CH_2CHCHCH_2$, 5.36 (*Z*, m), 5.40 (*E*, m)}, 5.8 (t, 2H, $J$ = 5.5 Hz, $CONHCH_2CO$), 6.43 (t, 2H, $J$ = 5.5 Hz, $CONHCH_2CO$), 6.87 (d, 8H, $J$ = 8.0 Hz, $ArCH^{macrocycle}$), 6.99 (d, 12H, $J$ = 9.0 Hz, ArCH), 7.17 (d, 12H, $J$ = 9.0 Hz, $ArCH^{macrocycle}$), 7.23 (d, 8H, $J$ = 8.0 Hz, $ArCH^{macrocycle}$), 7.66 (s, 2H, $ArCH^{macrocycle}$), 7.81 (s, 4H, $ArCH^{macrocycle}$), 8.03 (t, 4H, $J$ = 5.0 Hz, $CONHCH_2^{macrocycle}$); $^{13}$C NMR (100 MHz, $CDCl_3$) $\delta$ = 11.47 ($CH_3$), 14.52 ($CH_3$), 23.47 ($CH_2$), 24.17 ($CH_2$), 24.73 ($CH_2$), 26.22 ($CH_2$), 28.10 ($CH_2$), 28.92 ($CH_2$), 29.16 ($CH_2$), 29.42 ($CH_2$), 29.58 ($CH_2$), 29.64 ($CH_2$), 29.71 ($CH_2$), 29.85 ($CH_2$), 29.99 ($CH_2$), 30.07 ($CH_2$), 30.82 ($CH_2$), 33.02 ($CH_2$), 34.08 ($CH_2$) 39.67 (CH), 41.59 ($CH_2$), 42.08 ($CH_2$), 42.36 ($CH_2$), 47.61 ($CH_2$), 55.33 (q, C), 66.04 ($OCH_2CH_2$), 71.52 ($OCH_2CH(Et)CH_2$), 116.05 (ArCH), 118.46 (ArCH), 122.18 (ArCH) 128.50 (ArCH),

130.25 ($CH_2\underline{C}H\underline{C}HCH_2$), 130.73 (ArCH), 131.19 (ArCH), 132.84 (q, ArC) 135.75 (q, ArC), 136.52 (q, ArC), 144.77 (q, ArC), 150.20 (q, ArC), 160.30 (q, ArC), 166.70 (CO) 169.25 (CO), 169.44 (CO), 169.73 (CO), 169.88 (CO), 174.60 (CO); FAB-MS (*m*BNA matrix): m/z 2767 $[M+H]^+$ ($^{35}Cl$).

## 6.3. References

1. (a) G. M. Hübner, J. Cläser, C. Seel, F. Vögtle, *Angew. Chem. Int. Ed. Engl.* **1999**, *38*, 383-386; (b) B. Mohr, M. Weck, J-P. Sauvage, R. H. Grubbs, *Angew. Chem. Int. Ed. Engl.*, **1997**, *36*, 1308-1310; (c) D. A. Leigh, A. Murphy, J. P. Smart, A. M. Z. Slawin, *Angew. Chem. Int. Ed. Engl.* **1997**, *36*, 728-732; (d) S. Anderson, H. L. Anderson, *Angew. Chem. Int. Ed. Engl.* **1996**, *35*, 1956-1959; (e) D. B. Amabilino, J. F. Stoddart, *Chem. Rev.*, **1995**, *95*, 2725-2828; (f) A. Harada, J. Li, M. Kamachi, *Nature*, **1992**, *356*, 325-327.

2. G. Schill, *Catenanes, Rotaxanes and Knots*, Academic press, New York, **1971**.

3. (a) F. M. Raymo, K. N. Houk, J. F. Stoddart, *J. Am. Chem. Soc.*, **1998**, *120*, 9318-9322; (b) M. Asakawa, P. R. Asthton, R. Ballardini, V. Balzani, M. Bělohradský, M. T. Gandolfi, O. Kocian, L. Prodi, F. M. Raymo, J. F. Stoddart, M. Venturi, *J. Am. Chem. Soc.*, **1997**, *119*, 302-310; (c) M. Handel, M. Pleovets, S. Gestermann, F. Vögtle, *Angew. Chem. Int. Ed. Engl.* **1997**, *36*, 1199-1201; (d) P. R. Ashton, M. Bělohradský, D. Philip, J. F. Stoddart, *J. Chem. Soc., Chem. Comm.*, **1993**, 1274-1277; (e) P. R. Ashton, M. Bělohradský, D. Philp, J. F. Stoddart, *J. Chem. Soc., Chem. Comm.*, **1993**, *16*, 1269-1274.

4. Processes which utilise noncovalent forces to assemble an interlocked complex that is subsequently "captured" by irreversible bond formation ("self assembly with covalent modification") only operate under thermodynamic control before the final cyclization step [D. B. Amabilino, P. R. Ashton, L. Perez-Garcia, J. F. Stoddart, *Angew. Chem. Int. Ed. Engl.* **1995**, *34*, 2378-2380]. "Strict self assembly" pathways spontaneously convert components into products at thermodynamic equilibrium [D. Philp, J. F. Stoddart, *Angew. Chem. Int. Ed. Engl.* **1996**, *35*, 1154-1196.

5. (a) A. C. Try, M. M. Harding, D.G. Hamilton, J. K. M. Sanders, *Chem. Commun.* **1998**, 723-724; (b) M. Fujita, M. Aoyagi, F. Ibukuro, K. Ogura, K. Yamaguchi, *J. Am. Chem. Soc.*, **1998**, *120*, 611-612; (c) M. Fujita, F. Ibukuro, H. Seki, O. Kamo, M. Imanari, K. Ogura, *J. Am. Chem. Soc.*, **1996**, *118*, 899-900; (d) M. Fujita, F. Ibukuro, K. Yamaguchi, K. Ogura, *J. Am. Chem. Soc.*, **1995**, *117*, 4175-4176; (e) M. Fujita, F. Ibukuro, H. Hagihara, K. Ogura, *Nature*, **1994**, *367*, 720-723.

6. K-Y. Jeong, J. S. Choi, S-Y. Chang, H-Y. Chang, *Angew. Chem. Int. Ed. Engl.* **2000**, *39*, 1692-1695.

7. (a) S. J. Rowan, J. F. Stoddart, *Org. Lett.* **1999**, *1*, 1913-1916; (b) S. J. Cantrill, S. J. Rowan, J. F. Stoddart, *Org. Lett.* **1999**, *1*, 1363-1366.

8. (a) R. H. Grubbs, S. Chang, *Tetrahedron*, **1998**, *54*, 4413-4450; (b) S. K. Armstrong, *J. Chem. Soc., Perkin Trans. 1*, **1998**, 371-338; (c) M. Schuster, S. Blechert, *Angew. Chem. Int. Ed. Engl.* **1997**, *36*, 2036-2056; (d) P. Schwab, M. B. France, J. W. Ziller, R. H. Grubbs, *Angew. Chem. Int. Ed. Engl.* **1995**, *34*, 2039-2041.

9. For organic 'magic' rings see T. J. Kidd, D. A. Leigh, A. J. Wilson, *J. Am. Chem. Soc.*, **1999**, *121*, 1599-1600.

10. A. Furstner, K. Langemann, *J. Am. Chem. Soc.*, **1997**, *119*, 9130-9136.

11. A. G. Johnston, D. A. Leigh, A. Murphy, J. P. Smart, M. D. Deegan, *J. Am. Chem. Soc.* **1996**, *118*, 10662-10663.

# Chapter Seven

## 7. Benzylic imine catenates: Readily accessible octahedral analogues of the Sauvage catenanes

*As accepted by Angew. Chem. Int. Ed. Engl.*

Historically, one of the triumphs of coordination chemistry has been its application to the synthesis of mechanically interlocked molecular architectures, *i.e.* catenanes, rotaxanes and knots.[1-10] In 1984 Sauvage used the preferred tetrahedral geometry of Cu(I) to organize appropriately derivatized phenanthroline ligands into a fixed mutually-orthogonal orientation, whereupon a double macrocyclization reaction gave the [2]catenate **11** in 27% yield (Scheme 7.1a).[2] Subsequent studies on the system boosted yields to near quantitative levels (*via* ring closing metathesis, RCM)[3] and extended the interlocked architectures available to [*n*]catenates ($n$ = 2-8),[4] catenands (the demetallated, but still interlocked, ligands),[5] rotaxanes,[6] *pseudo*-rotaxanes[7] and knots[8]. Interlocked ligands can have remarkable properties; catenates are among the most stable complexes of Cu(I) that exist with a neutral species,[5] and catenands also stabilize[9] the ordinarily disfavored tetrahedral geometries of Ni(I) and Cu(0). However, although other metals have been introduced[9] and alternative trigonal bipyrimidal "stations" employed in redox-switchable systems,[10] the basic catenate assembly system based on a tetrahedral metal template and phenanthroline ligands has remained largely unchanged. Expanding this elegant strategy to include catenates based around octahedral centers is of obvious appeal (Scheme 7.1b),[11] and pioneering work in this regard has been carried out by Schröder,[12] Busch[13] and others,[1c,14] yet only two successful examples of octahedral catenates have been described to date.[1c,14] Here a simple, general and efficient synthesis of catenates with

an octahedral coordination geometry is reported using benzylic 2,6-diiminopyridine ligands. The catenates (M**112**$L_2$) are prepared either from preformed metal-ligand complexes (M**113**$_2L_2$) *via* RCM (Scheme 6.2a), or, in contrast to the Sauvage system, the binding sites can be assembled directly in the presence of the metal by reversible imine bond formation (Scheme 6.2b). The octahedral template is versatile, exemplified by the formation of catenates with every first row transition metal from manganese to zinc, cadmium from the second row, (at the time of writing, others have not been investigated) and a broad range of counter-ions. The *X*-ray crystal structure of a zinc(II) catenate, Zn*EE*-**112**$(ClO_4)_2$, confirms the interlocked architecture and shows that benzylic imine catenates are virtually isostructural with analogous hydrogen bond-assembled amphiphilic[15a] and "magic ring"[15b] benzylic amide catenanes.

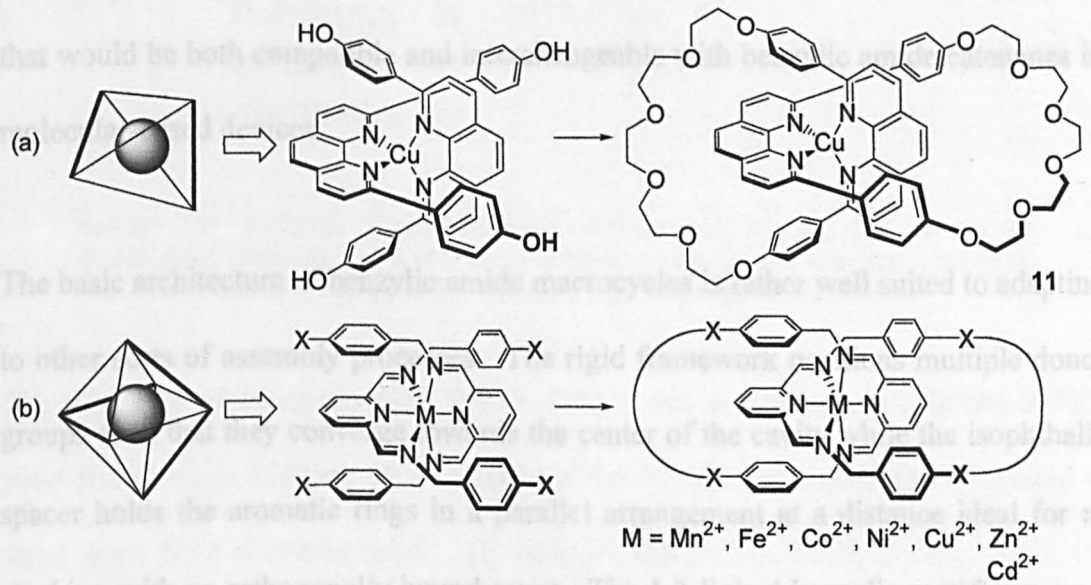


**Scheme 7.1.** The synthesis of catenates *via* the orthogonalization of coordinated ligands about (a) tetrahedral and (b) octahedral metal templates.

Preliminary results indicate that imine catenates can possess exceptional kinetic stability; the Zn*EE*-**112**$(ClO_4)_2$ catenate is not demetallated by 100 equivalents of the disodium salt of EDTA. However, treatment with $NaBH_4$ reduces the imine bonds

and permits demetallation of the ligand to give the corresponding benzylic amine catenand, *EE*-**115**. Re-metallation leads to a further class of more labile octahedral complexes, benzylic amine catenates (*e.g.* Zn*EE*-**115**$(ClO_4)_2$).

Hydrogen bond-assembled benzylic amide catenanes exhibit a broad range of dynamic properties. A cascade of intercomponent hydrogen bonds, π-stacking and van der Waals interactions ensure that circumrotation of the interlocked rings can occur over at least nine orders of magnitude depending on the structure, temperature and nature of the environment.[16] In contrast, the strong coordination bonds present in catenates lock the macrocyclic components in fixed positions or, in the absence of the metal, the rings rotate with virtually complete (but uncontrolled) freedom. This special kind of "on-off" dynamics, not readily available in the hydrogen bonded system, made it desirable to seek a route to metal-based catenates of a size and shape that would be both compatible and interchangeable with benzylic amide catenanes in molecular-based devices.

The basic architecture of benzylic amide macrocycles is rather well suited to adapting to other sorts of assembly processes. The rigid framework positions multiple donor groups such that they converge towards the center of the cavity while the isophthalic spacer holds the aromatic rings in a parallel arrangement at a distance ideal for π-stacking with an orthogonally bound guest. The 1,3-linked benzylic motif ensures a complete 180° turn for each fragment (in comparison to, say, the ~109° turn for a diphenylphenanthroline unit) holding the end groups in positions that promote intracomponent rather than intercomponent cyclizations. Thus the only changes necessary to change the hydrogen bonding system to one based around metal ion

chelation was to replace the amide groups with imines and, for stability reasons, the phenolic esters with ethers (Scheme 7.2).

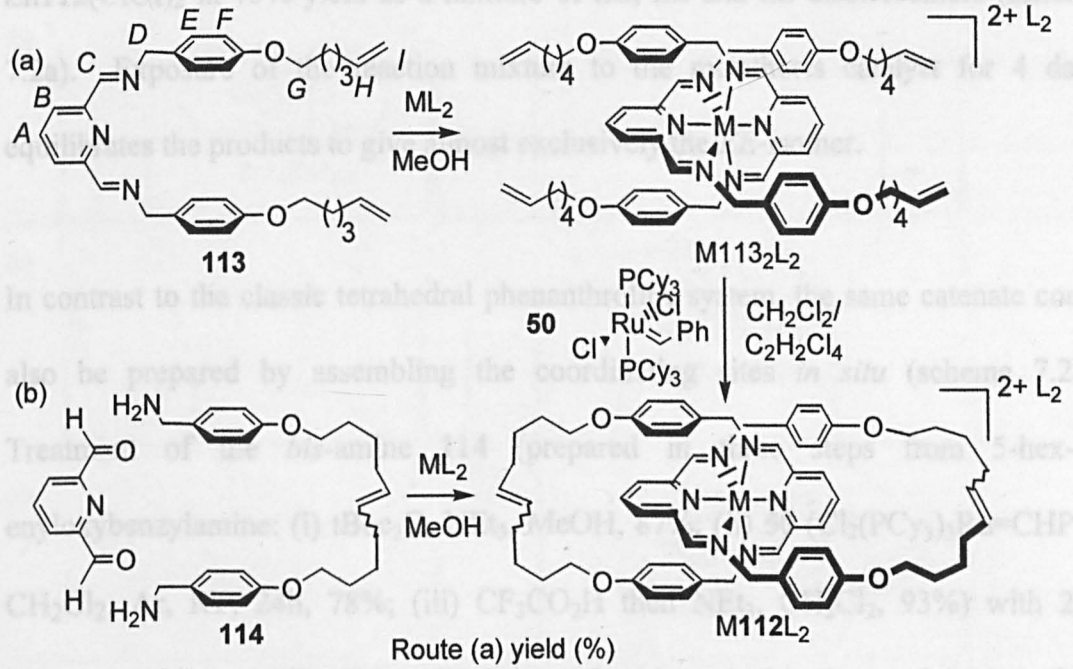


Route (a) yield (%)

| | | | |
|---|---|---|---|
| Mn**112**$(ClO_4)_2$ | 63 | Cu**112**$(ClO_4)_2$ | 61 |
| Fe**112**$Br_2$ | 75 | Zn**112**$(ClO_4)_2$ | 73 |
| Co**112**$(ClO_4)_2$ | 36 | Zn**112**$(BPh_4)_2$ | 81 |
| Co**112**$(BPh_4)_2$ | 41 | Cd**112**$(ClO_4)_2$ | 70 |
| Ni**112**$(ClO_4)_2$ | 32 | | |

**Scheme 7.2.** Synthesis of benzylic imine catenates, M**112**$L_2$, prepared *via* (a) the double macrocyclization of a preformed octahedral coordination complex (M**113**$_2L_2$), and (b) spontaneous metal-promoted assembly from non-chelated precursors.

The zinc(II) perchlorate complex Zn**113**$_2(ClO_4)_2$ was isolated as a precipitate in 83% yield from simple addition of a solution of the Schiff-base ligand **113** [prepared in three steps from 4-cyanophenol: (i) $HO(CH_2)_4CH{=}CH_2$, $Ph_3P$, DEAD, THF, 0°, 59%; (ii) $LiAlH_4$, THF, -78°C→reflux, 94%; (iii) 2,6-diformylpyridine, MeOH, 92%] in dichloromethane to a methanolic solution of $Zn(ClO_4)_2.6H_2O$. Imines are one of the few classes of substrates not normally compatible with olefin metathesis (indeed, the free Schiff-base ligand **113** cannot be converted into the macrocycle by RCM). However, pre-coordination ties up the imines and the tetra-olefin complex

Zn**113**$_2$($ClO_4$)$_2$ smoothly undergoes double macrocyclization *via* RCM with Grubbs' catalyst **50** ($Cl_2(PCy_3)_3Ru$=CHPh, $CH_2Cl_2$, Ar, RT, 4h) to give the zinc(II) catenate Zn**112**($ClO_4$)$_2$ in 73% yield as a mixture of *EE*, *EZ* and *ZZ* diastereomers (scheme 7.2a). Exposure of the reaction mixture to the metathesis catalyst for 4 days equilibrates the products to give almost exclusively the *EE*-isomer.

In contrast to the classic tetrahedral phenanthroline system, the same catenate could also be prepared by assembling the coordinating sites *in situ* (scheme 7.2b). Treatment of the *bis*-amine **114** (prepared in three steps from 5-hex-5'-enyloxybenzylamine: (i) $tBoc_2O$, $NEt_3$, MeOH, 87%; (ii) **50** ($Cl_2(PCy_3)_3Ru$=CHPh), $CH_2Cl_2$, Ar, RT, 24h, 78%; (iii) $CF_3CO_2H$ then $NEt_3$, $CH_2Cl_2$, 93%) with 2,6-diformylpyridine and $Zn(ClO_4)_2.6H_2O$ in methanol resulted in the precipitation of the catenate Zn*EE*-**112**($ClO_2$)$_2$ after one hour in 53% yield. In this case, the metal center orders the construction of the catenate about itself, *via* the reversible formation of four imine bonds from five components, as the lowest energy way it can satisfy its desired octahedral coordination geometry.

The $^1$H NMR spectra of the free ligand (**113**), zinc(II) precursor complex (Zn**113**$_2$($ClO_4$)$_2$) and zinc(II) catenate (Zn*EE*-**112**($ClO_4$)$_2$) are shown in Figure 7.1a-c. Shielding of the benzylic aromatic rings ($H_E$, $H_F$) in both the precursor complex (Figure 7.1b) and catenate (Figure 7.1c) with respect to the free ligand (Figure 7.1a) are indicative of the entwined (in the case of Zn**113**$_2$L$_2$) or interlocked (in the case of Zn*EE*-**112**L$_2$) architectures. It is interesting to note that there are subtle but significant differences in the shifts of all the non-alkyl chain resonances between Zn*EE*-**112**L$_2$ and Zn**113**$_2$L$_2$, indicating that a certain amount of reorganization of the ligands needs to occur during catenate formation.

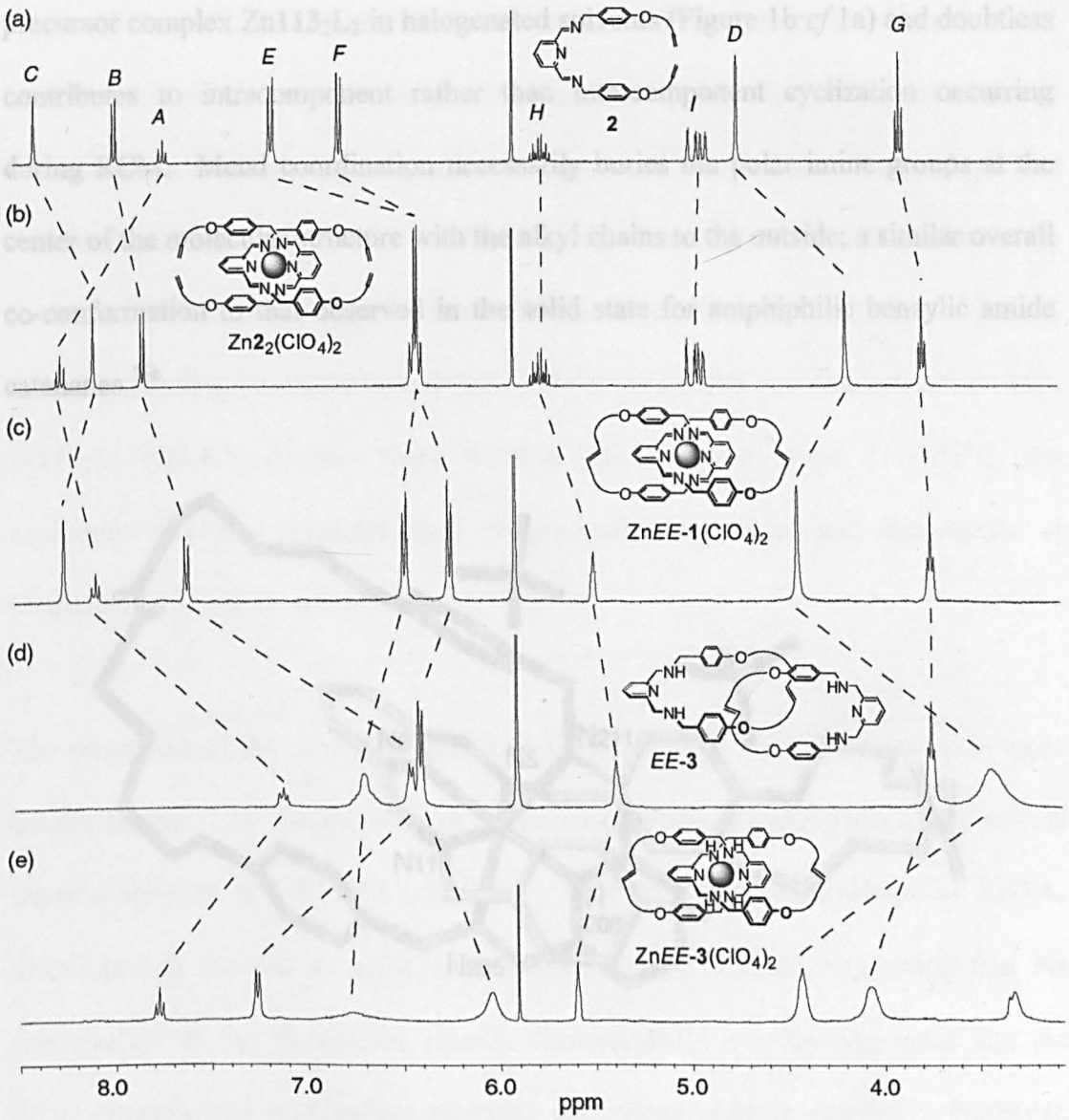


**Figure 7.1.** $^1$H NMR spectra (400 MHz, $C_2D_2Cl_4$, 298K) of (a) free Schiffs-base ligand **2**, (b) acyclic tetraolefin precursor complex Zn**113**$_2$(ClO$_4$), (c) benzylic imine catenate Zn*EE*-**112**(ClO$_4$)$_2$, (d) free benzylic amine catenand *EE*-**115**, and (e) benzylic amine catenate Zn*EE*-**115**(ClO$_4$)$_2$. The assignments correspond to the lettering shown in scheme 7.2.

Single crystals suitable for investigation by *X*-ray crystallography using a synchrotron source were obtained from slow vapor diffusion of diethyl ether into a solution of the *EE*-isomer of Zn**112**(ClO$_4$)$_2$ in acetonitrile.[17] The crystal structure (Figure 7.2) confirms the interlocked molecular architecture, the octahedral geometry of the coordinated zinc and the *E*-stereochemistry of the olefins in both rings. The benzylic groups of each macrocycle π-stack with the 2,6-diiminopyridine groups of the other interlocked ring, an interaction which is also clearly present in the non-cyclized

precursor complex Zn**113**$_2$L$_2$ in halogenated solvents (Figure 1b *cf* 1a) and doubtless contributes to intracomponent rather than intercomponent cyclization occurring during RCM. Metal coordination necessarily buries the polar imine groups at the center of the molecular structure with the alkyl chains to the outside; a similar overall co-conformation to that observed in the solid state for amphiphilic benzylic amide catenanes.[15a]

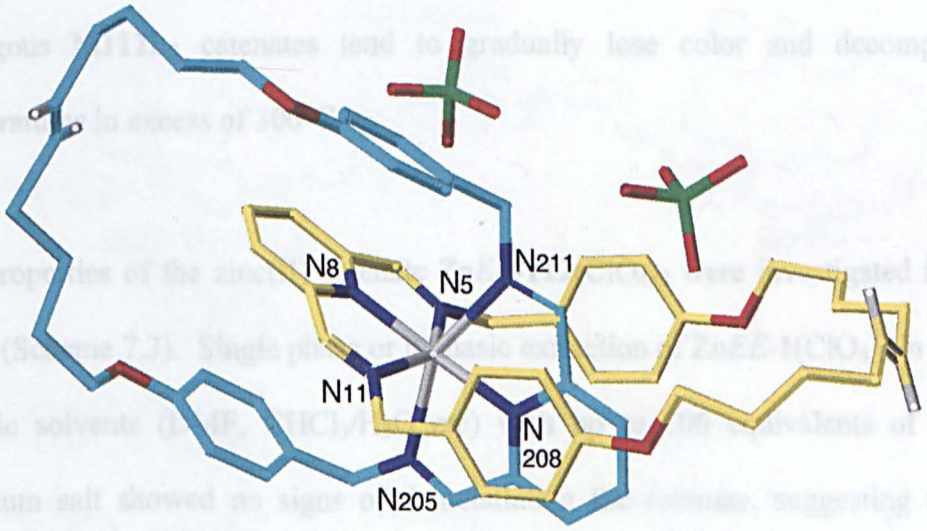


**Figure 7.2.** Solid state structure of the zinc(II) [2]catenate Zn*EE*-**112**$(ClO_4)_2$ as determined by *X*-ray crystallography.[17] Carbon atoms of one macrocycle are shown in light blue and those of the other in yellow; oxygen atoms are red, nitrogen dark blue, chlorine green, hydrogen white and zinc silver. Non-olefin hydrogen atoms and a molecule of acetonitrile are omitted for clarity. Selected bond lengths [Å]: Zn-N5 2.289, Zn-N8 2.048, Zn-N11 2.211, Zn-N205 2.264, Zn-N208 2.045, Zn-N211 2.276. Other selected interatomic distances [Å]: N5-N11 4.348, N8-N208 4.081, N205-N211 4.388. Ligand bite angles [°]: N5-Zn-N11 150.14, N205-Zn-N211 150.34.

The bite angle of the ligand in the *X*-ray structure of Zn*EE*-**112**$(ClO_4)_2$ is slightly smaller (150°) than other, non-cyclic, *bis*(2,6-diiminopyridine) complexes with Zn(II)[13] (151°) and Ni(II)[12,13] (151-156°) indicating that the ligand is able to adapt to the demands of its environment. Encouraged, the tolerance of the octahedral catenate assembly system was investigated by extending the RCM approach to metals both across and down the periodic table with respect to zinc (*i.e.* Mn←Zn and Cd). The

results (Scheme 7.2) were uniformly successful with the precursor complexes and catenates obtained in each case, often in good yields despite the mixture of diastereomers complicating the purification process.[18] Preliminary studies show that the same catenates can also be produced by the direct imine bond-formation route (Scheme 7.2b). Interestingly, all the catenates are much more thermally stable than the corresponding precursor complexes. Whilst the acyclic coordination compounds M**113**$_2$L$_2$ typically possess sharp melting points in the range 221-252°C, the analogous M**112**L$_2$ catenates tend to gradually lose color and decompose at temperatures in excess of 300°C.

The properties of the zinc(II) catenate Zn*EE*-**112**$(ClO_4)_2$ were investigated in more detail (Scheme 7.3). Single phase or biphasic extraction of Zn*EE*-**1**$(ClO_4)_2$ in various organic solvents (DMF, $CHCl_3/H_2O$ *etc*) with up to 100 equivalents of EDTA, disodium salt showed no signs of demetallating the catenate, suggesting that the combination of the directional, planar, diiminopyridyl coordinating motif and the tight, encapsulated architecture provides exceptional kinetic stability. However, reduction of the imines (Zn*EE*-**112**$(ClO_4)_2$, $NaBH_4$, EtOH, 1 h) followed by an aqueous EDTA, disodium salt wash, resulted in the free benzylic amine catenand *EE*-**115** (78%). Re-metallation ($Zn(ClO_4)_2$, MeOH) proceeds smoothly (~100%) to give the corresponding, clearly more labile, benzylic amine catenate, Zn*EE*-**115**$(ClO_4)_2$. The $^1$H NMR spectra of *EE*-**115** and Zn*EE*-**115**$(ClO_4)_2$ are shown in Figure 7.1d and e. The compact nature of the free ligand *EE*-**115** is convincingly demonstrated by the shielding of several resonances compared to the acyclic ligand **113**. Protons $H_E$ and $H_F$, for example, which intrinsically should be relatively unaffected by imine reduction, are shifted in *EE*-**115** by a similar magnitude to those in the Zn*EE*-**112**$(ClO_4)_2$ catenate and Zn**113**$_2(ClO_4)_2$ precursor complexes despite no directed

intercomponent interactions being present between the macrocycles in the catenand. The broad appearance of several resonances in the spectrum of the catenand are probably due to co-conformational exchange processes that are not fast on the NMR timescale at RT. The broadened peaks in the amine catenate Zn*EE*-**115**$L_2$, however, may be a result of multiple asymmetric centers being produced by coordination of the four now-prochiral nitrogen atoms.

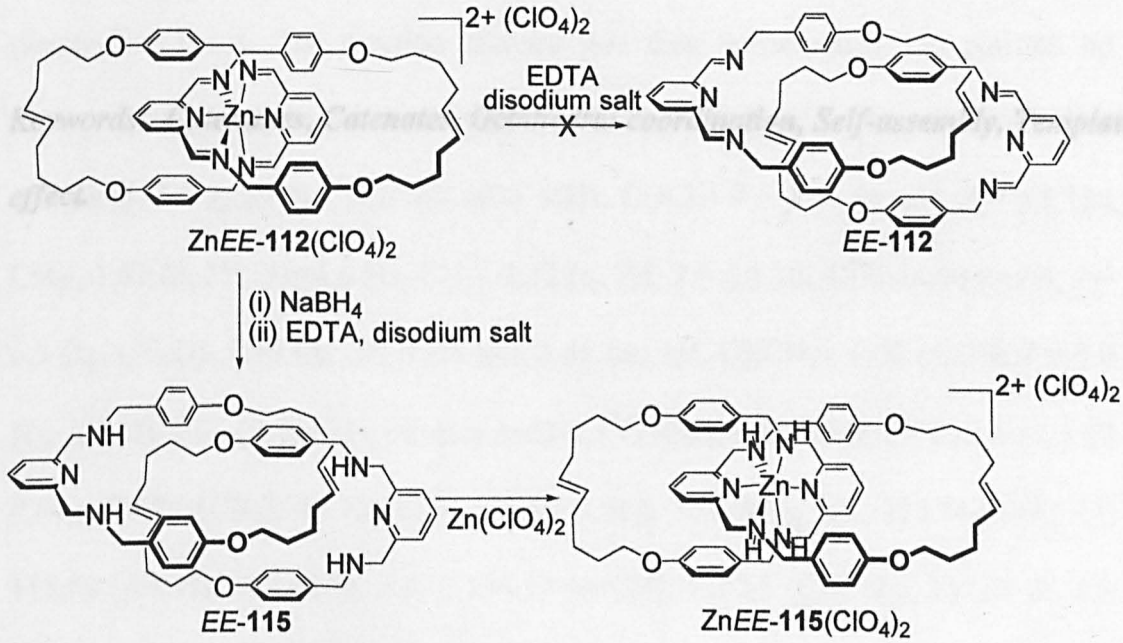


**Scheme 7.3.** The chemistry of an octahedral metal catenate. Direct demetallation with EDTA, disodium salt is unsuccessful, but reduction of the imines ($NaBH_4$) allows extraction of the zinc (EDTA, disodium salt) to give the free benzylic amine catenand, *EE*-**115**. Re-metallation ($Zn(ClO_4)_2$, MeOH) affords the benzylic amine catenate, Zn*EE*-**115**$(ClO_4)_2$.

In conclusion, a simple, versatile and effective route exists to octahedrally coordinated analogues of the Sauvage catenates, which should be both extendable to other metal-based interlocked architectures (such as rotaxanes, shuttles and knots) and interchangeable with hydrogen bond-assembled catenanes in possible molecular level devices. In addition to stabilizing unusual oxidation states and normally disfavored geometries, the wide range of metals that can adopt octahedral coordination patterns suggests that catenates could find uses in areas where

complexes with particularly high kinetic stabilities are required, such as radiotherapy[19] and magnetic resonance imaging[20]. Finally, it is noted that that metal complexes of 2,6-diminopyridine ligands also form an important new generation of non-metallocene olefin polymerization catalysts[21] and that intertwined versions of such structures exhibit novel forms of columnar liquid crystalline behavior.[22] The possible application of translationally switchable mechanically-interlocked architectures to these areas should be fascinating.

*Keywords:* ***Catenanes, Catenates, Octahedral coordination, Self-assembly, Template effect.***

## 7.2. Experimental

### 5-Hex-5'-enyloxybenzonitrile

To a stirred solution of 4-cyanophenol (5.0 g, 41.97 mmol), 5-hexenol (4.4 mL g, 62.96 mmol) and triphenylphosphine (11.0 g, 41.97 mmol) in anhydrous tetrahydrofuran (50 mL) at 0°C was added dropwise DEAD (6.6 mL, 41.97 mmol). The reaction was allowed to warm to room temperature and stirred for a further twenty-four hours. The reaction mixture was then concentrated and purified by passage through a short column of silica (hexane) yielding the product as a colourless oil. Yield: 5.2 g, 59 %; $^{1}$H NMR (400 MHz, $CDCl_3$) $\delta$ = 1.56 (p, 2H, $J$ = 6.5 Hz, $CH_2$), 1.81 (p, 2H, $J$ = 6.5 Hz, $CH_2$), 2.12 (q, 2H, $J$ = 6.5 Hz, $CH_2$), 4.00 (t, 2H, $J$ = 6.5 Hz, $CH_2O$), 5.00 (m, 2H, $CHC\underline{H}_2$), 5.81 (m, 1H, $C\underline{H}CH_2$), 6.92 (d, 2H, $J$ = 9.0 Hz, ArCH), 7.56 (d, 2H, $J$ = 9.0 Hz, ArCH); $^{13}$C NMR (100 MHz, $CDCl_3$) $\delta$ = 25.57 ($CH_2$), 28.79 ($CH_2$), 33.70 ($CH_2$), 68.58 ($CH_2$), 104.08 (q, C), 115.34 ($CH\underline{C}H_2$), 115.58 (ArCH), 119.68 (q, ArC), 134.33 (ArCH), 138.65 ($\underline{C}HCH_2$), 162.80 (q, C); MS-FAB (mNBA matrix): *m/z* 202 $[M+H]^+$.

### 5-Hex-5'-enyloxybenzylamine

To a 1M solution of lithium aluminium hydride in anhydrous tetrahydrofuran (45 mL) and rigorously inert (Ar) atmosphere at -78°C was added dropwise a solution of 5-hex-5'enyloxybenzonitrile (2.85 g, 15.24 mmol) in dry tetrahydrofuran (20 mL). The reaction mixture was then allowed to warm to room temperature then refluxed for three hours. The reaction mixture was then quenched by successive dropwise additions of water (1.27 mL), 15% aqueous sodium hydroxide solution (1.27 mL) and finally water (3.81 mL). Finally the reaction mixture was filtered through a plug of glass wool and the solvent removed in *vacuo* to give the product as a yellow oil.

Yield: 2.72 g, 93.5 %; $^1$H NMR (400 MHz, $CDCl_3$) δ = 1.57 (p, 2H, *J* = 7.0 Hz, $CH_2$), 1.79 (p, 2H, *J* = 7.0 Hz, $CH_2$), 2.12 (q, 2H, *J* = 7.0 Hz, $CH_2$), 3.79 (brs, 2H, $C\underline{H}_2NH_2$), 3.95 (t, 2H, *J* = 7.0, $CH_2O$), 5.00 (m, 2H, $CHC\underline{H}_2$), 5.82 (m, 1H, $C\underline{H}CH_2$), 6.86 (d, 2H, *J* = 8.5 Hz, ArCH), 7.21 (d, 2H, *J* = 8.5 Hz, ArCH); $^{13}$C NMR (100 MHz, $CDCl_3$) δ = 25.74 ($CH_2$), 29.14 ($CH_2$), 33.84 ($CH_2$), 46.31 ($CH_2$), 68.21 ($CH_2$), 114.77 (ArCH), 114.94 ($CHCH_2$), 129.52 (ArCH), 135.78 (q, ArC), 138.94 ($CHCH_2$), 158.44 (q, ArC); MS-FAB (mNBA matrix): m/z 206 $[M+H]^+$

**2,6-Diacetylpyridinebis(5-hex-5'-enyloxybenzylimine) 113**

A solution of 5-hex-5'-enyloxybenzylamine (1.50 g, 7.32 mmol), in methanol (50 mL) was added dropwise to a stirred solution of 2,6-diformylpyridine (0.49 g, 3.66 mmol) in methanol (10 mL). After stirring for one hour a white precipitate had formed which was filtered and washed with methanol (20 mL) then dried to give the title compound as a white crystalline solid. Yield: 1.72 g, 92 %; m.p. 100.6-102.6°C; $^1$H NMR (400 MHz, DMSO-$d_6$) δ = 1.49 (p, 4H, *J* = 7.53 Hz, $CH_2$), 1.70 (p, 4H, *J* = 7.5 Hz, $CH_2$), 2.08 (q, 4H, *J* = 7.5 Hz, $C\underline{H}_2CHCH_2$), 3.95 (t, 4H, *J* = 7.5 Hz, $OC\underline{H}_2CH_2$), 4.79 (brs, 4H, $CH_2^D$), 4.99 (m, 4H, $CHC\underline{H}_2^{\text{terminal alkene}}$), 5.82 (m, 2H, $C\underline{H}CH_2^{\text{terminal alkene}}$), 6.90 (d, 4H, *J* = 8.5 Hz, $ArCH^E$), 7.24 (d, 4H, *J* = 8.5 Hz, $ArCH^F$), 7.94 (m, 1H, $ArCH^A$), 8.02 (m, 2H, $ArCH^B$), 8.48 (s, 2H, $ArC\underline{H}N^C$), $^{13}$C NMR (100 MHz, DMSO-$d_6$) δ = 25.11 ($CH_2$), 28.51 ($CH_2$), 33.20 ($CH_2$), 63.50 ($CH_2$), 67.57 ($CH_2$), 114.76 (ArCH), 115.29 ($CHC\underline{H}_2^{\text{terminal alkene}}$), 122.13 ($C\underline{H}CH_2^{\text{terminal alkene}}$), 129.76 (ArCH), 131.04 (q, ArC), 138.13 (ArCH), 138.92 (ArCH), 145.39 (q, ArC), 158.10 (q, ArC), 162.05 (ArC{CH}N); FAB-MS (*m*BNA matrix): *m/z* = 510 $[M+H]^+$ anal. calcd. for $C_{33}H_{39}O_2N_3$ (509): C, 77.76 %; H, 7.71 %; N, 8.24 %, found: C, 77.56 %; H, 7.61 %; N, 8.23 %.

**Bis[2,6-diacetylpyridinebis(5-hex-5'-enyloxybenzylimine)]-zinc(II)perchlorate $Zn113_2(ClO_4)_2$**

To a stirred solution of zinc perchlorate hexahydrate (0.250 g, 0.67 mmol) in methanol (100 mL) was added dropwise a solution of 2,6-diacetylpyridinebis(5-hex-5'-enyloxybenzylimine) **113** (0.513 g, 1.00 mmol) in chloroform. The solution turned a cloudy white almost immediately and a precipitate began to form. After one and a half hours, the reaction mixture was filtered and the precipitate washed with methanol (30 mL) and dried to give the title compound as a white solid. Yield: 0.549 g, 64 %; mp 274.9-276.6°C; $^1$H NMR (400 MHz, DMSO-$d_6$) $\delta$ = 1.52 (p, 8H, $J$ = 7.5 Hz, $CH_2$), 1.72 (pentet, 8H, $J$ = 7.5 Hz, $CH_2$), 2.11 (q, 8H, $J$ = 7.5 Hz, $C\underline{H}_2CHCH_2$), 3.90 (t, 8H, $J$ = 7.5 Hz, $OC\underline{H}_2CH_2$), 4.26 (brs, 8H, $CH_2^D$), 5.01 (m, 8H, $CHC\underline{H}_2^{\text{terminal alkene}}$), 5.85 (m, 4H, $C\underline{H}CH_2^{\text{terminal alkene}}$), 6.50 (brs, 16H, $ArCH^E$ and $ArCH^F$), 8.02 (d, 4H, $J$ = 7.5 Hz, $ArCH^B$), 8.33 (s, 4H, $ArC\underline{H}N^C$), 8.53 (t, 2H, $J$ = 7.5 Hz, $ArCH^A$), $^{13}$C NMR (100 MHz, DMSO-$d_6$) $\delta$ = 25.11 ($CH_2$), 28.53 ($CH_2$), 33.26 ($CH_2$), 59.94 ($CH_2$), 67.63 ($CH_2$), 114.31 (ArCH), 115.36 ($CH\underline{C}H_2^{\text{terminal alkene}}$), 126.98 (q, ArC), 129.80 (ArCH), 130.22 (ArCH), 138.89 ($\underline{C}HCH_2^{\text{terminal alkene}}$), 144.56 (ArCH), 145.76 (q, ArC), 158.58 (q, ArC), 159.61 (ArC{$\underline{C}$H}N), FAB-MS (*m*BNA matrix): *m/z* = 1183 $[M\text{-}ClO_4^-]^+$ anal. calcd. for $C_{66}H_{78}O_{12}N_6Cl_2Zn$ (1281): C, 61.75 %; H, 6.12 %; N, 6.55 %, found: C, 61.58 %; H, 6.00 %; N, 6.40 %.

**[2]-bis[2,6-diacetylpyridine(1,10-dec-5-enyloxydibenzylimine)]-[zinc(II) perchlorate] catenate $Zn112(ClO_4)_2$**

A closed flame dried schlenk tube with magnetic stirring bar was purged with argon. To this was added Grubbs' metathesis catalyst **50** (0.02 g, 0.0243 mmol, 20 mol%). The schlenk tube was then sealed with parafilm and left under a constant stream of argon for ten minutes. $Zn113_2(ClO_4)_2$ (0.156 g, 0.122 mmol) was dissolved in a

sealed flask containing anhydrous dichloromethane (610 mL), which was subsequently evacuated and purged with argon several times and then transferred to the schlenk tube using a syringe. The reaction was allowed to continue until no further change was observed by TLC. The reaction mixture was then evaporated to dryness and purified by repeated chromatography (methanol 1-5%/ dichloromethane) to give the catenate **Zn112(ClO$_4$)$_2$** as a brownish solid. Yield: 0.112 g, 75 %; mp decomp ~350°C; $^1$H NMR (400 MHz, DMSO-d$_6$) δ = 1.58 (m, 8H, $CH_2$), 1.74 (m, 8H, $CH_2$), 2.12 (m, 8H, $C\underline{H}_2CHCHCH_2$), 3.85 (t, 8H, *J* = 6.5 Hz, $OC\underline{H}_2CH_2$), 4.49 (brs, 8H, $CH_2^D$), 5.61 (t, 4H, J = 3.0 Hz, $CH^{internal\ alkene}$), 6.36 (d, 8H, *J* = 8.0 Hz, $ArCH^E$), 6.53 (d, 8H, *J* = 8.0 Hz, $ArCH^F$), 7.70 (d, 4H, *J* = 8.0 Hz, $ArCH^B$), 8.42 (t, 2H, *J* = 8.0 Hz, $ArCH^A$), 8.50 (s, 4H, $ArCC\underline{H}N^C$), $^{13}$C NMR (100 MHz, DMSO-d$_6$) δ = 25.89 ($CH_2$), 28.05 ($CH_2$), 31.50 ($CH_2$), 60.76 ($CH_2$), 67.17 ($CH_2$), 113.91 (ArCH), 127.02 (q, ArC), 129.34 ($CH_2\underline{C}H\underline{C}HCH_2$), 129.97 (ArCH), 130.62 (ArCH), 144.37 (ArCH), 145.25 (q, ArC), 158.24 (q, ArC), 160.27 (ArC{$\underline{C}$H}N), FAB-MS (*m*BNA matrix): *m/z* = 1126 [M-$ClO_4^-$]$^+$ anal. calcd. for: $C_{62}H_{70}O_{12}N_6Cl_2Zn$ (1225) C, 60.66 %; H, 5.75 %; N, 5.75 %, found: C, 60.46 %; H, 5.97 %; N, 5.67 %.

**4-(*N-Tert*-butyloxycarbonylaminomethyl)-hex-5'-enyloxybenzene**

To a stirred solution of 5-Hex-5'-enyloxybenzylamine (2.00 g, 9.76 mmol) in methanol: triethylamine 9:1 (100 mL) at 0°C was added di-tert-butoxycarbonate (3.22 g 20.00 mmol). The reaction mixture was then allowed to warm to room temperature and stir for a further eighteen hours after which time the reaction mixture was concentrated under reduced pressure. The resulting brown oil was dissolved in chloroform and washed with 5% citric acid solution (100 mL) then water (2 x 100 mL) and dried over magnesium sulphate. Finally the reaction mixture was concentrated under reduced pressure to give the product as a pale yellow oil. Yield;

2.32 g, 87 %; $^{1}$H NMR (400 MHz, $CDCl_3$) δ = 1.45 (s, 9H, 3 x $CH_3$), 1.56 (p, 2H, *J* = 7.5 Hz, $CH_2$), 1.79 (p, 2H, *J* = 7.5 Hz, $CH_2$), 2.12 (q, 2H, *J* = 7.5 Hz, $CH_2$), 3.94 (t, 2H, *J* = 7.5 $OCH_2$), 4.23 (d, 2H, *J* = 5.5 Hz, $CH_2$), 4.77 (vbrs, 1H, NH), 5.00 (m, 2H, $CHC\underline{H}_2^{\text{terminal alkene}}$), 5.82 (m, 1H $C\underline{H}CH_2^{\text{terminal alkene}}$), 6.84 (d, 2H, *J* = 8.0 Hz, ArCH), 7.18 (d, 2H, *J* = 8.0 Hz, ArCH); $^{13}$C NMR (100 MHz, $CDCl_3$) δ = 23.05 ($CH_2$), 28.82 ($CH_3$), 29.10 ($CH_2$), 33.82 ($CH_2$), 44.59 ($CH_2$), 68.20 ($CH_2$), 79.73 (q, C), 114.98 (ArCH), 115.14 ($CH\underline{C}H_2^{\text{terminal alkene}}$), 129.21 (ArCH), 131.28 (q, ArC), 138.91 ($\underline{C}HCH_2^{\text{terminal alkene}}$), 156.24 (q, ArC), 158.83 (CO); FAB-MS (*m*BNA matrix): *m/z* 306 $[M+H]^+$.

**Bis-4-(*N-tert*-butyloxycarbonylaminomethyl)phenoxy-1,10-dec-5-ene**

A closed flame dried schlenk tube with magnetic stirring bar was purged with argon. To this was added Grubbs' metathesis catalyst **50** (0.13 g, 0.164 mmol, 5 mol%). The schlenk tube was then sealed with parafilm and left under a constant stream of argon for ten minutes. 4-(*N-tert*-butyloxycarbonylaminomethyl)-hex-5'-enyloxybenzene (1.00 g, 3.278 mmol) was dissolved in a sealed flask containing anhydrous dichloromethane (25 mL) which was subsequently evacuated and purged with argon several times and then transferred to the schlenk tube. The reaction was allowed to continue until no further change was observed by TLC. The reaction mixture was then evaporated to dryness and purified by column chromatography (dichloromethane) to give the compound as a greyish glassy solid. Yield; 0.75 g, 78 %; $^{1}$H NMR (400 MHz, $CDCl_3$) δ = 1.49 (s, 18H, 6 x $CH_3$), 1.55 (p, 4H, *J* = 7.0 Hz, $CH_2$), 1.80 (p, 4H, *J* = 7.0 Hz, $CH_2$), 2.09 (q, 4H, *J* = 7.0 Hz, $CH_2$), 3.97 (t, 4H, *J* = 7.0 Hz, $OCH_2$), 4.26 (d, 4H, *J* = 6.0 Hz, $CH_2$), 4.78 (brs, 2H, NH), 5.47 (p, 2H, *J* = 1.5 Hz, $CH^{\text{alkene}}$), 6.87 (d, 4H, *J* = 8.0 Hz, ArCH), 7.21 (d, 4H, *J* = 8.0 Hz, ArCH); $^{13}$C NMR (100 MHz, $CDCl_3$) δ = 26.35 ($CH_2$), 28.82 ($CH_3$), 29.12 ($CH_2$), 32.63

($CH_2$), 44.60 ($CH_2$), 68.29 ($CH_2$), 80.05 (q, C), 114.99 (ArC), 129.22 (ArCH), 130.73 ($CH_2CHCHCH_2$), 131.22 (q, ArCH), 156.23 (q, ArC), 158.85 (CO); FAB-MS (*m*BNA matrix): *m/z* 583 $[M+H]^+$.

**[2]-Bis[2,6-diacetylpyridine(1,10-dec-5-enyloxydibenzylimine)]-[zinc(II)perchlorate] catenate Zn112($ClO_4$)$_2$**

To a stirred solution containing bis-4-(*N-tert*-butyloxycarbonylaminomethyl) phenoxy-1,10-dec-5-ene (0.042 g, 0.072 mmol) in dichloromethane (20 mL) was added dropwise triflouroacetic acid (1 mL). The reaction mixture was allowed to stir for one hour after which time the reaction mixture was concentrated and dried thoroughly *in vacuo*. The resulting brown solid was then suspended in dichloromethane (20 mL) and triethylamine added (0.04 mL, 0.288 mmol). When all of the solid had dissolved, the reaction mixture was washed with water (5 x 20 mL), dried over magnesium sulphate and concentrated under reduced pressure to leave a cream colored foam. This and zinc perchlorate hexahydrate (0.131 g, 0.035 mmol) were dissolved in methanol (10 mL) to which was added dropwise a solution containing 2,6-pyridine dicarboxaldehyde (0.001 g, 0.007 mmol) in methanol. The reaction mixture was then allowed to stir at room temperature for three hours after which time the reaction mixture was concentrated then purified by column chromatography (5% methanol in dichloromethane) to yield the catenate **Zn113$_2$($ClO_4$)$_2$**. Experimental data as before.

**[2]-Bis[2,6-diacetylpyridine(1,10-dec-5-enyloxydibenzylamine)] catenane 115**

To a stirred solution of **Zn112($ClO_4$)$_2$** (0.050 g, 0.041 mmol) in ethanol (30 mL) was added sodium borohydride (0.009 g, 0.245 mmol). The reaction mixture turned pink in five minutes and was then allowed to stir for a further one hour. The reaction

mixture was then concentrated, dichloromethane added (50 mL), and then washed with saturated aqueous EDTA disodium salt solution (2 x 20 mL). The organic layer was then dried over magnesium sulphate, filtered and evaporated to dryness to give a pale pink solid. Yield: 0.031 g, 77.54 %; m.p. 182.6-183.7°C. $^{1}$H NMR (400 MHz, $CDCl_3$) δ = 5.53 (m, 8H, $CH_2$), 1.76 (m, 8H, $CH_2$), 2.06 (m, 8H, $CH_2$), 3.19 (brm, 4H, NH), 5.53 (d, 16 H, $J$ = 9.5 Hz, $C\underline{H}_2NHC\underline{H}_2$), 3.85 (t, 8H, $J$ = 6.0 Hz, $OC\underline{H}_2$), 5.45 (m, 4H, $CH^{\text{internal alkene}}$), 6.48 (d, 8H, $J$ = 8.5 Hz, ArCH), 6.61 (d, 4H, $J$ = 7.5 Hz, ArCH), 6.80 (d, 8H, $J$ = 8.5 Hz, ArCH), 7.29 (t, 2H, $J$ = 7.5 ArCH); $^{13}$C NMR (100 MHz, $CDCl_3$) δ = 26.64 ($CH_2$), 28.65 ($CH_2$), 31.18 ($CH_2$), 53.50 ($CH_2$), 53.89 ($CH_2$), 67.85 ($CH_2$), 114.61 (ArCH), 120.56 (ArCH), 128.74 (ArCH), 130.15 (ArCH), 130.87 ($CH_2\underline{C}H\underline{C}HCH_2$), 136.35 (ArCH), 155.79 (q, ArC), 158.88 (q, ArC); FAB-MS (*m*BNA matrix): *m/z* 972 $[M+H]^+$, 486 [macrocycle+H]$^+$; HRMS 971.6162 $[M+H]^+$ calculated for $C_{62}H_{79}N_6O_4$ (+H), Found: 971.6145

**Bis[2,6-diacetylpyridinebis(5-hex-5'-enyloxybenzylimine)]-copper(II) perchlorate Cu113$_2$(ClO$_4$)$_2$**

To a stirred solution of copper chloride (0.042 g, 0.314 mmol) in methanol 20 mL was added dropwise a solution of 2,6-diacetylpyridinebis(5-hex-5'-enyloxybenzylimine) **113** (0.400 g, 0.785 mmol) in dichloromethane and methanol (1:3 30 mL). To the stirring reaction mixture was added 15% perchloric acid (5 mL), which resulted in the formation of a green precipitate. This was filtered and washed with ether to give a green solid. Yield: 0.102 g, 78 %; m.p. 221°C decomp; FAB-MS (*m*BNA matrix): *m/z* = 1182 $[M\text{-}ClO_4^-]^+$ anal. calcd. for $C_{66}H_{78}O_{12}N_6Cl_2Cu$ (1280): C, 61.88 %; H, 6.09 %; N, 6.56 %, found: C, 60.80 %; H, 6.07 %; N, 6.31 %.

**Bis[2,6-diacetylpyridinebis(5-hex-5'-enyloxybenzylimine)]-nickel(II)perchlorate**

**$Ni113_2(ClO_4)_2$**

The procedure used was identical to that used for **$Zn113_2(ClO_4)_2$**, 2,6-diacetylpyridinebis(5-hex-5'-enyloxybenzylimine) **113** (0.100 g, 0.196 mmol), nickel(II)perchlorate hexahydrate (0.036 g, 0.098 mmol) Yield: 0.114 g, 91 %; m.p. 291.9-292.7°C ; FAB-MS (*m*BNA matrix): *m/z* = 1176 $[M\text{-}ClO_4^-]^+$ anal. calcd. for $C_{66}H_{78}O_{12}N_6Cl_2Ni$ (1275): C, 62.07 %; H, 6.11 %; N, 6.58 %, found: C, 61.93 %; H, 6.07 %; N, 6.50 %.

**Bis[2,6-diacetylpyridinebis(5-hex-5'-enyloxybenzylimine)]-cobalt(II)iodide**

**$Co113_2(I)_2$**

To a stirred solution of cobalt chloride hexahydrate (0.023 g, 0.098 mmol) in methanol 20 mL was added dropwise a solution of 2,6-diacetylpyridinebis(5-hex-5'-enyloxybenzylimine) **113** (0.100 g, 0.196 mmol) in dichloromethane and methanol (1:3 30 mL). To the stirring reaction mixture was added saturated potassium iodide solution (10 mL), which resulted in the formation of a dark red precipitate. This was filtered and washed with dichloromethane leaving a dark red solid. Yield: 0.125 g, 96%; m.p. 248.5-249.5°C; FAB-MS (mBNA matrix): *m/z* = 1204 $[M\text{-}I^-]^+$ anal. calcd. for $C_{66}H_{78}O_4N_6I_2Co$ (1331): C, 59.50 %; H, 5.86 %; N, 6.31 %, found: C, 59.12 %; H, 5.76 %; N, 6.11 %.

**Bis[2,6-diacetylpyridinebis(5-hex-5'-enyloxybenzylimine)]-iron(II)Bromide $Fe113_2(Br)_2$**

The procedure used was identical to that used for **$Co113_2(I)_2$** with the exception being that the following reagent were used: potassium bromide was used rather than potassium iodide, 2,6-diacetylpyridinebis(5-hex-5'-enyloxybenzylimine) **113** (0.100 g, 0.196 mmol), and iron(II)sulphate heptahydrate (0.027 g, 0.098 mmol) Yield: 0.110 g, 91 % m.p. 219.6-221.7°C; $^1$H NMR (400 MHz, DMSO-$d_6$) $\delta$ = 1.48 (p, 8H, *J* = 7.0 Hz, $CH_2$), 1.69 (p, 8H, *J* = 7.0 Hz, $CH_2$), 2.07 (q, 8H, *J* = 7.0 Hz, $C\underline{H}_2CHCH_2$), 3.63 (t, 8H, *J* = 7.0 Hz, $OC\underline{H}_2CH_2$), 3.91 (brs, 8H, $CH_2^D$), 4.99 (m, 8H, $CHC\underline{H}_2^{\text{terminal alkene}}$), 5.81 (m, 4H, $C\underline{H}CH_2^{\text{terminal alkene}}$), 6.40 (d, 8H, *J* = 8.5 Hz, ArCH) 6.64 (d, 8H, *J* = 8.5 Hz, ArCH), 7.93 (s, 4H, $ArCC\underline{H}N^C$), 8.20 (d, 4H, *J* = 7.5 Hz, $ArCH^B$), 8.40 (t, 2H, *J* = 7.5 Hz, $ArCH^A$); $^{13}$C NMR (100 MHz, DMSO-$d_6$) $\delta$ = 25.08 ($CH_2$), 28.45 ($CH_2$), 33.21 ($CH_2$), 60.44 ($CH_2$), 67.68 ($CH_2$), 114.54 (ArCH), 115.34 ($CH\underline{C}H_2^{\text{terminal alkene}}$), 125.20 (ArCH), 127.45 (q, ArC), 129.93 (ArCH), 136.36 (ArCH), 138.84 ($\underline{C}HCH_2^{\text{terminal alkene}}$), 158.83 (q, ArC), 159.66 (q, ArC), 169.32 (ArC{$\underline{C}$H}N), FAB-MS (*m*BNA matrix): *m/z* = 1155 $[M\text{-}Br^-]^+$ anal. calcd. for $C_{66}H_{78}O_4N_6Br_2Fe$ (1218): C, 63.94 %; H, 6.27 %; N, 6.88 %, found: C, 63.72 %; H, 6.31 %; N, 6.57 %.

**Bis[2,6-diacetylpyridinebis(5-hex-5'-enyloxybenzylimine)]-manganese(II) perchlorate $Mn113_2(ClO_4)_2$**

The procedure used was identical to that used for **$Zn113_2(ClO_4)_2$**, 2,6-diacetylpyridinebis(5-hex-5'-enyloxybenzylimine) **113** (0.100 g, 0.196 mmol), manganese(II)perchlorate hexahydrate (0.035 g, 0.098 mmol), Yield: 0.121 g, 96 %; m.p 278.9-280.4°C; FAB-MS (*m*BNA matrix): *m/z* = 1172 $[M\text{-}ClO_4^-]^+$ anal. calcd.

for $C_{66}H_{78}O_{12}N_6Cl_2Mn$ (1271): C, 62.26 %; H, 6.13 %; N, 6.60 %, found: C, 62.06 %; H, 6.08 %; N, 6.61 %.

**Bis[2,6-diacetylpyridinebis(5-Hex-5'-enyloxybenzylimine)]-cadmium(II) perchlorate Cd113$_2$(ClO$_4$)$_2$**

The procedure used was identical to that used for **Zn113$_2$(ClO$_4$)$_2$**, 2,6-diacetylpyridinebis(5-Hex-5'-enyloxybenzylimine) **113** (0.100 g, 0.1965 mmol), cadmium(II)perchlorate (0.031 g, 0.098 mmol) Yield: 0.102 g, 78 %; m.p. 244.5-245.9°C; $^1$H NMR (400 MHz, DMSO-d$_6$) $\delta$ = 1.52 (p, 8H, $J$ = 7.0 Hz, $CH_2$), 1.71 (p, 8H, $J$ = 7.0 Hz, $CH_2$), 2.12 (q, 8H, $J$ = 7.0 Hz, $C\underline{H}_2CHCH_2$), 3.81 (t, 8H, $J$ = 7.0 Hz, $OC\underline{H}_2CH_2$), 4.41 (brs, 8H, $CH_2^D$), 5.04 (m, 8H, $CHC\underline{H}_2^{\text{terminal alkene}}$), 5.86 (m, 4H, $C\underline{H}CH_2^{\text{terminal alkene}}$), 6.36 (d, 8H, $J$ = 8.5 Hz, ArCH), 6.61 (d, 8H, $J$ = 8.5 Hz, ArCH), 8.03 (d, 4H, $J$ = 8.0 Hz, $ArCH^B$), 8.47 (t, 2H, $J$ = 8.0 Hz, $ArCH^A$), 8.53 (s, 4H, $ArCC\underline{H}N^C$); $^{13}$C NMR (100 MHz, $C_2D_2Cl_4$) $\delta$ = 25.12 ($CH_2$), 28.53 ($CH_2$), 33.29 ($CH_2$), 60.68 ($CH_2$), 67.46 ($CH_2$), 114.04 (ArCH), 115.37 ($CH\underline{C}H_2^{\text{terminal alkene}}$), 127.88 (ArCH), 130.39 (q, ArC), 130.55 (ArCH from HMQC) 138.94 ($\underline{C}HCH_2^{\text{terminal alkene}}$), 143.58 (ArCH), 145. 47 (q, ArC), 158.53 (q, ArC), 159.77 (ArC{$\underline{C}$H}N); FAB-MS (*m*BNA matrix): *m/z* = 1229 [M-ClO$_4^-$]$^+$ anal. calcd. for $C_{68}H_{78}O_{12}N_4Cl_2Cd$ (1328): C, 59.59 %; H, 5.87 %; N, 6.32 %, found: C, 59.44 %; H, 5.83 %; N, 6.29 %.

**[2]-bis[2,6-diacetylpyridine(1,10-dec-5-enyloxydibenzylimine)]-[copper(II) perchlorate] catenate Cu112(ClO$_4$)$_2$**

The procedure used was identical to that used for catenate **Zn112(ClO$_4$)$_2$**. Grubbs' metathesis catalyst **50** (0.006 g, 0.008 mmol, 20 mol%), bis[2,6-diacetylpyridine(1,10-dec-5-enyloxydibenzylimine)]-copper(II)perchlorate

**Cu113$_2$(ClO$_4$)$_2$** (0.050 g, 0.039 mmol) Yield: 0.028 g, 59 %; m.p. decomposition ~300 °C; FAB-MS (*m*BNA matrix): *m/z* = 1126 [M-ClO$_4^-$]$^+$ anal. calcd. for: $C_{62}H_{70}O_{12}N_6Cl_2Cu$ (1224) C, 60.78 %; H, 5.72 %; N, 6.86 %, found: C, 60.64 %; H, 5.79 %; N, 6.73 %.

**[2]-bis[2,6-diacetylpyridine(1,10-dec-5-enyloxydibenzylimine)]-[nickel(II) perchlorate] catenate Ni112(ClO$_4$)$_2$**

The procedure used was identical to that used for catenate **Zn113(ClO$_4$)$_2$**. Grubbs' metathesis catalyst **50** (0.039 g, 0.047 mmol, 20 mol%), bis[2,6-diacetylpyridine(1,10-dec-5-enyloxydibenzylimine)]-nickel(II)perchlorate **Ni2$_2$(ClO$_4$)$_2$** (0.300 g, 0.235 mmol) Yield: 0.092 g, 32%; m.p. decomposition ~339 °C; FAB-MS (*m*BNA matrix): *m/z* = 1121 [M-ClO$_4^-$]$^+$ anal. calcd. for: $C_{62}H_{70}O_{12}N_6Cl_2Ni$ (1220) C, 61.00 %; H, 5.78 %; N, 6.88 %, found: C, 60.92 %; H, 5.89 %; N, 6.73 %.

**[2]-bis[2,6-diacetylpyridine(1,10-dec-5-enyloxydibenzylimine)]-[cobalt(II)iodide] catenate Co112(I)$_2$**

The procedure used was identical to that used for catenate **Zn113(ClO$_4$)$_2$**. Grubbs' metathesis catalyst **50** (0.037 g, 0.045 mmol, 20 mol%), bis[2,6-diacetylpyridine(1,10-dec-5-enyloxydibenzylimine)]-cobalt(II)iodide **Co113$_2$(I)$_2$** (0.300 g, 0.225 mmol) Yield: 0.103 g, 36%; m.p. decomposition ~321 °C; FAB-MS (*m*BNA matrix): *m/z* = 1021 [M-2I$^-$]$^+$ anal. calcd. for: $C_{62}H_{70}O_4N_6I_2Co$ (1275) C, 58.36 %; H, 5.53 %; N, 6.59 %, found: C, 58.12 %; H, 5.74 %; N, 6.50 %.

**[2]-bis[2,6-diacetylpyridine(1,10-dec-5-enyloxydibenzylimine)]-[iron(II) bromide] catenate Fe112(Br)$_2$**

The procedure used was identical to that used for catenate **Zn112(ClO$_4$)$_2$**. Grubbs' metathesis catalyst **50** (0.040 g, 0.049 mmol, 20 mol%), bis[2,6-diacetylpyridine(1,10-dec-5-enyloxydibenzylimine)]-iron(II)bromide **Fe113$_2$(Br)$_2$** (0.300 g, 0.243 mmol) Yield: 0.214 g, 75 %; m.p. decomposition ~350 °C; $^1$H NMR (400 MHz, DMSO-d$_6$) $\delta$ = 1.48 (bm, 8H, CH$_2$), 1.68 (bm, 8H, CH$_2$), 2.05 (brm, 8H, C$\underline{H}_2$CHCH$_2$), 3.72-4.02 (m, 16H, OC$\underline{H}_2$CH$_2$ + CH$_2^D$), 5.42 (t, 4H, $J$ = 4.0 Hz, CH$^{\text{internal alkene}}$), 6.57 (m, 8H, ArCH$^E$), 6.72 (d, 8H, $J$ = 9.0 Hz, ArCH$^F$), 7.92 (s, 4H, ArCC$\underline{H}$N$^C$), 8.43 (m, 4H, ArCH$^B$), 8.36 (m, 2H, ArCH$^A$); $^{13}$C NMR (100 MHz, DMSO-d$_6$) $\delta$ = 25.60 (CH$_2$), 28.16 (CH$_2$), 31.78 (CH$_2$), 59.24 (CH$_2$), 67.70 (CH$_2$), 114.80 (ArCH), 124.79 (q, ArC), 127.79 (ArCH), 130.16 (CH$_2$C$\underline{H}$C$\underline{H}$CH$_2$), 130.80 (ArCH), 136.40 (ArCH), 158.88 (q, ArC), 159.64 (q, ArC), 168.05 (ArC{C$\underline{H}$}NCH$_2$); FAB-MS (*m*BNA matrix): *m/z* = 1099 [M-Br$^-$]$^+$ anal. calcd. for: C$_{62}$H$_{70}$O$_4$N$_6$Br$_2$Fe (1172) C, 63.17 %; H, 5.98 %; N, 7.13 %, found: C, 62.88 %; H, 5.71 %; N, 7.25 %.

**[2]-bis[2,6-diacetylpyridine(1,10-dec-5-enyloxydibenzylimine)]-[manganese(II) perchlorate] catenate Mn112(ClO$_4$)$_2$**

The procedure used was identical to that used for catenate **Zn112(ClO$_4$)$_2$**. Grubbs' metathesis catalyst **50** (0.039 g, 0.047 mmol, 20 mol%), bis[2,6-diacetylpyridine(1,10-dec-5-enyloxydibenzylimine)]-manganese(II)perchlorate **Mn113$_2$(ClO$_4$)$_2$** (0.300 g, 0.236 mmol) Yield: 0.1724 g, 60 %; m.p. decomposition ~343 °C ; FAB-MS (*m*BNA matrix): *m/z* = 1116 [M-ClO$_4^-$]$^+$ anal. calcd. for: C$_{62}$H$_{70}$O$_{12}$N$_6$Cl$_2$Mn (1178) C, 61.15 %; H, 5.80 %; N, 6.90 %, found: C, 62.15 %; H, 6.19 %; N, 6.39 %.

**[2]-bis[2,6-diacetylpyridine(1,10-dec-5-enyloxydibenzylimine)]-[cadmium(II) perchlorate] catenate Cd112$(ClO_4)_2$**

The procedure used was identical to that used for catenate **Zn113$(ClO_4)_2$**. Grubbs' metathesis catalyst **50** (0.045 g, 0.037 mmol, 20 mol%), bis[2,6-diacetylpyridine(1,10-dec-5-enyloxydibenzylimine)]-cadmium(II)perchlorate **Cd113$_2(ClO_4)_2$** (0.300 g, 0.226 mmol). Yield: 0.202 g, 70 %; m.p. decomposition. ~344°C; $^1$H NMR (400 MHz, DMSO-$d_6$) $\delta$ = 1.61 (p, 8H, $J$ = 6.5 Hz, $CH_2$), 1.74 (p, 8H, $J$ = 6.5 Hz, $CH_2$), 2.14 (q, 8H, $J$ = 6.5 $C\underline{H}_2CHCH_2$), 3.75 (t, 8H, $J$ = 6.5 Hz, $OC\underline{H}_2CH_2$), 4.58 (brs, 8H, $CH_2^D$), 5.67 (t, 4H, $J$ = 3.5 Hz, $CH^{internal\ alkene}$), 6.24 (d, 8H, $J$ = 8.5 Hz, $ArCH^E$), 6.72 (d, 8H, $J$ = 8.5 Hz, $ArCH^F$), 7.80 (d, 4H, $J$ = 8.5 Hz, $ArCH^B$), 8.36 (t, 2H, $J$ = 8.5 Hz, $ArCH^A$), 8.59 (s, 4H, $ArCC\underline{H}N^C$); $^{13}$C NMR (100 MHz, DMSO-$d_6$) $\delta$ = 25.23 ($CH_2$), 28.02 ($CH_2$), 31.78 ($CH_2$), 59.24 ($CH_2$), 67.70 ($CH_2$), 114.75 (ArCH), 124.79 (q, ArC), 127.73 (ArCH), 130.17 ($CH_2C\underline{H}C\underline{H}CH_2$), 130.84 (ArCH), 136.40 (ArCH), 158.88 (q, ArC), 159.64 (q, ArC), 168.05 ($ArC\{C\underline{H}\}NCH_2$); (FAB-MS (*m*BNA matrix): *m/z* = 1175 $[M\text{-}ClO_4^-]^+$ anal. calcd. for: $C_{62}H_{70}O_{12}N_6Cl_2Cd$ (1225) C, 58.42 %; H, 5.54 %; N, 6.59 %, found: C, 58.03 %; H 5.70, %; N 6.79, %.

## 7.2. References


1. *Molecular Catenanes, Rotaxanes and Knots* (Eds.: J-P. Sauvage, C. Dietrich-Buchecker), Wiley-VCH, Weinheim, **1999**. For catenanes based on coordination bonds other than the Sauvage catenates see: (a) G-J. M. Gruter, F. J. J. de Kanter, P. R. Markies, T. Nomoto, O. S. Akkerman, F. Bicklehaupt, *J. Am. Chem. Soc.* **1993**, *115*, 12179-12180. (b) M. Fujita, F. Ibukuro, H. Hagihara, K. Ogura, *Nature* **1994**, *367*, 720-723. (c) C. Piguet, G. Bernardinelli, A. F. Williams, B. Bocquet, *Angew. Chem.* **1995**, *107*, 618-621; *Angew. Chem. Int. Ed. Engl.* **1995**, *34*, 582-584. (d) D. M. P. Mingos, J. Yau, S. Menzer, D. J. Williams, *Angew. Chem.* **1995**, *107*, 2045-2047; *Angew. Chem. Int. Ed. Engl.* **1995**, *34*, 1894-1895. (e) A. C. Try, M. M. Harding, D. G. Hamilton, J. K. M. Sanders, *Chem. Commun.* **1998**, 723-724. (f) D. Whang, K-M. Park, J. Heo, P. Ashton, K. Kim, *J. Am. Chem. Soc.* **1998**, *120*, 4899-4900. (g) C. P. McArdle, M. J. Irwin, M. C. Jennings, R .J. Puddephatt, *Angew. Chem.* **1999**, *111*, 3571-3573; *Angew. Chem. Int. Ed.* **1999**, *38*, 3376-3378. (h) M. Fujita, *Acc. Chem. Res.* **1999**, *32*, 53-61. For catenane-like coordination interpenetrating networks see: (i) S. R. Batten, R. Robson *Angew. Chem.* **1998**, *110*, 1558-1595; *Angew. Chem. Int. Ed.* **1998**, *37*, 1460-1494 and (j) A. J. Blake, N. R. Champness, H. Hubberstey, W-S. Li, M. A. Withersby, M. Schröder, *Coord. Chem. Rev.* **1999**, *183*, 117-138.
2. C. O. Dietrich-Buchecker, J-P. Sauvage, J-M. Kern, *J. Am. Chem. Soc.* **1984**, *106*, 3043-3045. For the earliest Cu(I) catenate synthesis, involving a threaded intermediate complex, see C. O. Dietrich-Buchecker, J-P. Sauvage, J-P. Kintzinger, *Tetrahedron Lett.*, **1983**, *24*, 5095-5098.
3. (a) B. Mohr, M. Weck, J-P. Sauvage, R. H. Grubbs, *Angew. Chem.* **1997**, *109*, 1365-1367; *Angew. Chem. Int. Ed. Engl.* **1997**, *36*, 1308-1310. (b) M. Weck, B. Mohr, J-P. Sauvage, R. H. Grubbs, *J. Org. Chem.* **1999**, *64*, 5463-5471.

4. F. Bitsch, C. O. Dietrich-Buchecker, A-K. Khémiss, J-P. Sauvage, A. V. Dosselaer, *J. Am. Chem. Soc.* **1991**, *113*, 4023-4025.

5. C. O. Dietrich-Buchecker, J-P. Sauvage, J-M. Kern, *J. Am. Chem. Soc.* **1989**, *111*, 7791-7800.

6. (a) C. Wu, P. R. Lecavalier, Y. X. Shen, H. W. Gibson, *Chem. Mater.* **1991**, *3*, 569-572. (b) J-C. Chambron, V. Heitz, J-P. Sauvage, *J. Chem. Soc., Chem. Commun.* **1992**, 1131-1133.

7. J-P. Collin, P. Gavinã, J-P, Sauvage, *J. Chem. Soc. Chem. Commun.*, **1996**, 2005-2006.

8. C. O. Dietrich-Buchecker, J-P. Sauvage, *Angew. Chem.* **1989**, *101*, 192; *Angew. Chem. Int. Ed. Engl.* **1989**, *28*, 189-192.

9. N. Armaroli, L. De Cola, V. Balzani, J-P. Sauvage, C. O. Dietrich-Buchecker, J-M. Kern, A. Bailal, *J. Chem. Soc., Dalton Trans.* **1993**, 3241-3247.

10. D. J. Cárdenas, A. Livoreil, J-P. Sauvage, *J. Am. Chem. Soc.* **1996**, *118*, 11980-11981.

11. The idea of using octahedral ligand geometries in catenane formation was actually proposed a decade *before* the Sauvage tetrahedral system was introduced [V. I. Sokolov, *Russ. Chem. Rev.* **1973** *42*, 452-463]. For more recent discussions of possible strategies to catenates based on octahedral metal templates see: (a) D. H. Busch, *J. Incl. Phenom.* **1992**, *12*, 389-395 and (b) N. V. Gerbeleu, V. B. Arion, J. Burgess, *Template Synthesis of Macrocyclic Compounds*, Wiley-VCH, Weinheim, **1999**.

12. A. J. Blake, A. J. Lavery, T. I. Hyde, M. J. Schröder, *Chem. Soc., Dalton Trans.* **1989**, 965-970.

13. A. L. Vance, N. W. Alcock, J. A. Heppert, D. H. Busch, *Inorg. Chem.* **1998**, *37*, 6912-6920.

14. J-P. Sauvage, M. Ward, *Inorg. Chem.* **1991**, *30*, 3869-3874.

15. (a) D. A. Leigh, K. Moody, J. P. Smart, K. J. Watson, A. M. Z. Slawin, *Angew. Chem.* **1996**, *108*, 321-326; *Angew. Chem. Int. Ed. Engl.* **1996**, *35*, 306-310. (b) T. J. Kidd, D. A. Leigh, A. J. Wilson, *J. Am. Chem. Soc.* **1999**, *121*, 1599-1600.

16. D. A. Leigh, A. Murphy, J.P. Smart, M. S. Deleuze, F. Zerbetto, *J. Am. Chem. Soc.* **1998**, *120*, 6458-6467.

17. $C_{62}H_{70}Cl_2N_6O_{12}Zn$ $(C_2H_3N)_{0.5}$, $M$ = 1248.04, crystal size 0.14 × 0.08 × 0.06mm, monoclinic $P2_1/c$, $a$ = 10.6258(5), $b$ = 17.4158(9), $c$ = 33.4757(18) Å, $\beta$ = 97.232(2)°, $V$ = 6145.6(5)Å$^3$, $Z$ = 4, $\rho_{calcd}$ = 1.349 Mg m$^{-3}$; synchrotron radiation (CCLRC Daresbury Laboratory Station 9.8, silicon monochromator, $\lambda$=0.69280 Å), $\mu$=0.553 mm$^{-1}$, $T$=150(2)K. 22797 data (7081 unique, $R_{int}$=0.0489, 1.65<$\theta$<21.00°), were collected on a Siemens SMART CCD diffractometer using narrow frames (0.2° in $\omega$), and were corrected semi-empirically for absorption and incident beam decay (transmission 0.83-1.00). The structure was solved by direct methods and refined by full-matrix least-squares on $F^2$ values of all data (G.M.Sheldrick, SHELXTL manual, Siemens Analytical *X*-ray Instruments, Madison WI, USA, 1994, version 5) to give $wR$ = $\{\Sigma[w(F_o^2-F_c^2)^2]/\Sigma[w(F_o^2)^2]\}^{1/2}$ = 0.2984, conventional $R$ = 0.1087 for $F$ values of 7081 reflections with $F_o^2>2\sigma(F_o^2)$, $S$ = 1.066 for 761 parameters. Residual electron density extremes were 0.974 and –0.563 Å$^{-3}$. The alkyl chain was modeled using both geometrical and displacement parameter restraints. Hydrogens were added in calculated positions and constrained to a Riding model. Crystallographic data for (excluding structure factors) have been deposited with the Cambridge Crystallographic Data Centre as supplementary publication number CCDC-147870. Copies of the data can be obtained free of

charge on application to The Director, CCDC, 12 Union Road, Cambridge CB2 1EZ, UK (fax: Int. code +1223-336-033; e-mail: teched@chemcrys.cam.ac.uk).

18. The yields listed in Scheme 7.2 are isolated yields after chromatography or recrystallization. Sometimes the mixture of olefin diastereomers complicates purification and, in particular, is a factor in the modest yields of Co**112**$L_2$ and Ni**112**$L_2$. All compounds gave satisfactory mass spectra, elemental analysis, and, with the exception of the paramagnetic catenates, $^{13}C$ and $^{1}H$ NMR data.
19. S. Jurisson, D. Berning, W. Jia, D. Ma, *Chem. Rev,* **1993**, *93*, 1137-1156.
20. D. Parker, *Chem. Bri*, **1994**, 818-822.
21. G. J. P. Britovsek, V. C. Gibson, D. F. Wass, *Angew. Chem. Int. Ed.* **1999**, *38*, 428-447; *Angew. Chem.* **1999**, *111*, 448-468.
22. L. Douce, A. El-ghayoury, A. Skoulios, R. Ziessel, *Chem. Commun.* **1999**, 2033-2034.

**Acknowledgments**

Thanks go to Dr. Paul J Lusby for the synthesis of **Zn112(BPh$_4$)$_2$ Co112(BPh$_4$)$_2$**

Thanks also to Drs. Steve Lacey, Tim Kidd, Gail Morris and Rizwana Nasreen for initial studies on this project and in particular the ligand design.

# Appendix I: Organic "Magic Rings": The Hydrogen Bond-Directed Assembly of Catenanes Under Thermodynamic Control

*J. Am. Chem. Soc.* **1999**, *121*, 1599−1600 

## Organic "Magic Rings": The Hydrogen Bond-Directed Assembly of Catenanes under Thermodynamic Control

Timothy J. Kidd,† David A. Leigh,*,† and Andrew J. Wilson†

*Department of Chemistry*
*University of Manchester Institute of Science and Technology*
*Sackville Street, Manchester M60 1QD, United Kingdom*

*Received August 31, 1998*
*Revised Manuscript Received December 14, 1998*

A common feature of most current strategies used to prepare mechanically interlocked rings (catenanes) is that the final macrocyclization reaction is generally carried out under *kinetic* control.[1,2] As a result, if ring closure does not proceed via an already threaded precursor, "mistakes"—noninterlocked macrocycles—are produced that cannot be "corrected". Catenane formation under *thermodynamic* control ("strict self-assembly"[2]) has previously been achieved with use of weak, reversibly formed, metal−ligand bonds[3] with the result that the strong intercomponent interactions normally employed to direct mechanical interlocking can be exploited to bring about very high yields of catenanes.[3b−g] In several celebrated examples,[3b−c] Fujita et al. have described systems where metallomacrocycles can be converted almost exclusively into [2]catenanes through hydrophobic binding—a feat noted as being reminiscent of the conjurors trick of interlocking seemingly "magic" rings. Here we report that a similar approach can be applied to wholly organic ring systems by exploiting the hydrogen bond-mediated assembly of self-complementary macrocycles and the current generation of highly versatile olefin metathesis catalysts[4] in reversible ring opening and closing (RORCM) reactions.[5−7] Under appropriate RORCM conditions (in which, possibly uniquely for a chemical transformation requiring external reagents, there is virtually[8] no net change in the number, type, stereochemistry, or sequence of covalent

**Scheme 1.** Thermodynamically Controlled Self-Assembly/Disassembly of Benzylic Amide Macrocycles and [2]Catenanes under RORCM[a]

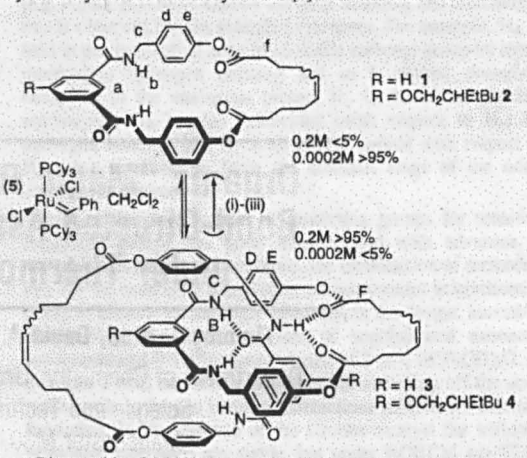


[a] Disassembly of the [2]catenanes into their component rings can also be achieved by switching off the intercomponent hydrogen bonding prior to RORCM: (i) $(CF_3CO)_2O$, Δ, 100%; (ii) **5**, $CH_2Cl_2$; (iii) MeOH, Δ, 100%.

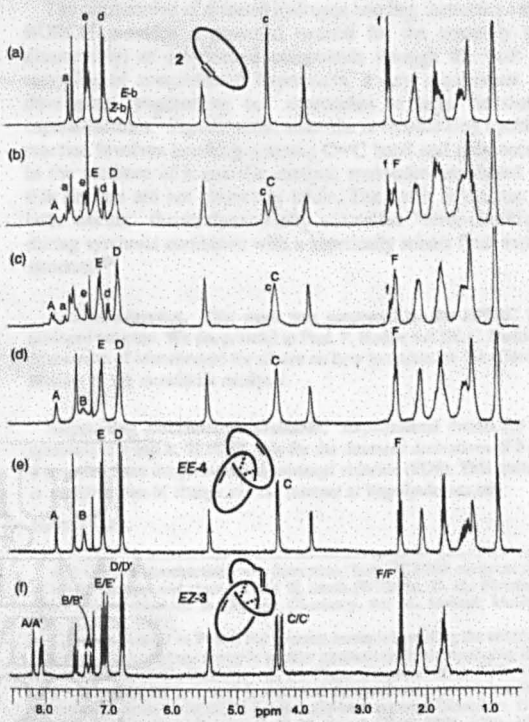


**Figure 1.** $^1$H NMR spectra (300 MHz, $CDCl_3$) of (a) the product mixture at equilibrium from RORCM from initial concentrations of **2**/**4** of 0.0002 M, (b) 0.002 M, (c) 0.02 M, and (d) 0.2 M; (e) homocircuit [2]catenane *EE*-**4**; and (f) heterocircuit [2]catenane *EZ*-**3**. Small case letters denote resonances from the noninterlocked macrocycle; upper case letters denote the equivalent resonances in the [2]catenanes.

† Current Address: Department of Chemistry, University of Warwick, Coventry CV4 7AL, United Kingdom.

(1) (a) Schill, G. *Catenanes, Rotaxanes and Knots*; Academic Press: New York, 1971. (b) Dietrich-Buchecker, C.; Sauvage, J.-P. *Bioorg. Chem. Frontiers* **1991**, *2*, 195−247. (c) Amabilino, D. B.; Stoddart, J. F. *Chem. Rev.* **1995**, *95*, 2725−2828. (d) Hunter, C. A. *J. Am. Chem. Soc.* **1992**, *114*, 5303−5311. (e) Vögtle, F.; Dünnwald, T.; Schmidt, T. *Acc. Chem. Res.* **1996**, *29*, 451−460. (f) Hamilton, D. G.; Sanders, J. K. M.; Davies, J. E.; Clegg, W.; Teat, S. J. *Chem. Commun.* **1997**, 897−898. DNA catenanes [Seeman, N. C. *Annu. Rev. Biophys. Biomol. Struct.* **1998**, *27*, 225−248] provide an exception to the kinetically controlled strategies.

(2) Processes which utilize noncovalent forces to assemble an interlocked complex that is subsequently "captured" by irreversible covalent bond formation ("self-assembly with covalent modification") only operate under thermodynamic control *before* the final cyclization step [Amabilino, D. B.; Ashton, P. R.; Pérez-García, L.; Stoddart, J. F. *Angew. Chem., Int. Ed. Engl.* **1995**, *34*, 2378−2380]. "Strict self-assembly" pathways spontaneously and reversibly convert components into products at thermodynamic equilibrium [Philp, D.; Stoddart, J. F. *Angew. Chem., Int. Ed. Engl.* **1996**, *35*, 1154−1196].

(3) (a) Gruter, G.-J. M.; de Kanter, F. J. J.; Markies, P. R.; Nomoto, T.; Akkerman, O. S.; Bickelhaupt, F. *J. Am. Chem. Soc.* **1993**, *115*, 12179−12180. (b) Fujita, M.; Ibukuro, F.; Hagihara, H.; Ogura, K. *Nature* **1994**, *367*, 720−723. (c) Fujita, M.; Ibukuro, F.; Yamaguchi, K.; Ogura, K. *J. Am. Chem. Soc.* **1995**, *117*, 4175−4176. (d) Fujita, M.; Ibukuro, F.; Seki, H.; Kamo, O.; Imanari, M.; Ogura, K. *J. Am. Chem. Soc.* **1996**, *118*, 899−900. (e) Fujita, M.; Aoyagi, M.; Ibukuro, F.; Ogura, K.; Yamaguchi, K. *J. Am. Chem. Soc.* **1998**, *120*, 611−612. (f) Whang, D.; Park, K.-M.; Heo, J.; Ashton, P.; Kim, K. *J. Am. Chem. Soc.* **1998**, *120*, 4899−4900. (g) Try, A. C.; Harding, M. M.; Hamilton, D. G.; Sanders, J. K. M. *Chem. Commun.* **1998**, 723−724.

(4) (a) Schwab, P.; France, M. B.; Ziller, J. W.; Grubbs, R. H. *Angew. Chem., Int. Ed. Engl.* **1995**, *34*, 2039−2041. (b) Schuster, M.; Blechert, S. *Angew. Chem., Int. Ed. Engl.* **1997**, *36*, 2036−2056. (c) Armstrong, S. K. *J. Chem. Soc., Perkin Trans. 1* **1998**, 371−388. (d) Grubbs, R. H.; Chang, S. *Tetrahedron* **1998**, *54*, 4413−4450.

(5) For tandem RORCM reactions which covert one ring system into a *different* ring system see: Zuercher, W. J.; Hashimoto, M.; Grubbs, R. H. *J. Am. Chem. Soc.* **1996**, *118*, 6634−6640.

(6) For a highly efficient catenane synthesis by ring closing metathesis (RCM) see: Mohr, B.; Weck, M.; Sauvage, J.-P.; Grubbs, R. H. *Angew. Chem., Int. Ed. Engl.* **1997**, *36*, 1308−1310.[13,14] For the synthesis of a molecular knot by RCM see: Dietrich-Buchecker, C.; Rapenne, G.; Sauvage, J.-P. *Chem. Commun.* **1997**, 2053−2054.

10.1021/ja983106r CCC: $18.00 
Published on Web 02/04/1999

bonds), isophthaloyl benzylic amide macrocycles possessing an internal olefin spontaneously self-assemble via interlocking to give [2]catenanes in >95% yield. Since carbon−carbon double bonds are fundamentally robust, catenanes produced in this way are kinetically stable when separated from the metathesis catalyst. Alternatively, they can be quantitatively converted back to their unlocked component macrocycles simply by diluting the RORCM reaction mixture or by "switching off" (by reversible trifluoroacetylation of the amides) the inter-macrocycle hydrogen bonding interactions prior to RORCM.

Benzylic amide macrocycles **1** and **2** were prepared according to methods given in the Supporting Information. The macrocycles were each isolated as mixtures of *E*- and *Z*-diastereomers and used as such in the metathesis experiments. RORCM was carried out in $CH_2Cl_2$ (the noncompeting solvent maximizes the strength of the inter-ring hydrogen bonding interactions) with use of the commercially available benzylidene version[4a] of Grubbs' catalyst, **5**.[9] At different concentrations the reactions yielded different product distributions, as evidenced by HPLC and $^1$H NMR spectroscopy (e.g. Figure 1a−d). At concentrations of 0.0002 M or less only simple macrocycle could be detected.[10] By using higher reaction concentrations, progressively more and more catenane (**3** or **4**) is produced until at equilibrium at 0.2 M >95% is a mixture of the three catenane diolefin isomers (*EE*, *EZ*, *ZZ*). Taking the product mixture from one metathesis reaction and reexposing it to catalyst at a different concentration converts the product distribution to that obtained if only the macrocycle (or catenane) is metathesized at that concentration, demonstrating that the reactions are truly under thermodynamic control. At concentrations higher than 0.2M mass spectrometry and analytical HPLC show that higher cyclic oligomers become increasingly abundant and the yield of catenane falls.

Saturated analogues of these amphiphilic benzylic amide catenanes have previously[11] been prepared in up to 18% yield by condensation of alkyl bis-acid chlorides and (masked) phenols and their interlocked nature confirmed by X-ray crystallography and a range of spectroscopic and spectrometric measurements. The saturated catenanes are easily distinguished from both their uninterlocked components and higher macrocycles by characteristic shifts in their $^1$H NMR spectra in $CDCl_3$ arising from the co-conformation adopted by the interlocked macrocycles to maximize intercomponent hydrogen bonding interactions.[11] The isomeric mixture of **3** and **4** produced in each olefin metathesis experiment was catalytically hydrogenated ($H_2$, Pd/C, 100%) and the resulting products shown to be identical to the saturated [2]-catenanes prepared unambiguously from the corresponding bisphenol and sebacoyl chloride.

In two cases (*EZ* isomer of **3**, *EE* isomer of **4**)[12] single catenane olefin isomers could actually be separated from the RORCM reaction mixture by preparative HPLC. The $^1$H NMR spectra of these individual diolefin isomers are shown in Figures 1e and 1f, respectively. Comparison of these spectra with those of **1** and **2** (e.g. Figure 1a) shows exactly the same shielding and deshielding trends observed for the saturated catenanes. For example, $H_A$ is held in the deshielding zone of an amide carbonyl group by inter-macrocycle hydrogen bonding and so is shifted *downfield* compared to the analogous proton, $H_a$, in the noninterlocked macrocycle; $H_B$ is also deshielded (with respect to $H_b$) by hydrogen bonding, but $H_{C-F}$ all appear *upfield* with respect to $H_{c-f}$ due to shielding from the aromatic rings of the other component macrocycle.

Just as the development of protecting groups for sensitive functional groups has gone hand-in-hand with advances in complex natural product synthesis, the introduction of methodology for the reversible modulation of noncovalent interactions is going to become increasingly important in the design, assembly, disassembly, and interconversion of sophisticated nanoscale superstructures.[13] Trifluoroacetylation of **3** or **4** ($(CF_3CO)_2O$, Δ) provides a mild and efficient method for switching off the inter-macrocycle hydrogen bonding interactions utilized for catenane formation. In the absence of the Grubbs catalyst the trifluoroacetylated catenanes are stable, but under RORCM conditions the rings smoothly dissociate to produce, after quantitative detrifluoroactylation (MeOH, Δ), the original component macrocycles **1** or **2**.

The combination of directed hydrogen bonding interactions and RORCM provides a powerful method for the assembly (or disassembly) of interlocked compounds through the built in recycling of nonpreferred byproducts, a key requirement in developing "engineering up" approaches to large functional supermolecules.[2] Significantly, since the reversible ring opening reaction involves breaking a strong C=C bond and only occurs in the presence of a specific catalyst, molecules assembled by this strategy are not inherently labile. The result is the best of both worlds: thermodynamically controlled "error-checking" during synthesis combined with a kinetically robust final superstructure.[14]

**Acknowledgment.** This work was supported by the EPSRC IPS managed program. We are grateful to Prof. P. Hodge and Dr. C. Ruddock (University of Manchester) for advice on how to maximize the effective lifetime of the metathesis catalysts.

**Supporting Information Available:** Experimental details for the synthesis of **1** and **2**; $^1$H NMR data for the saturated derivatives of **2** and **4** prepared from the phenols and sebacoyl chloride (PDF). This material is available free of charge via the Internet at http://pubs.acs.org.

JA983106R

(7) For evidence of some catenane formation during RORCM of macrocycles without recognition sites see: Wolovsky, R. *J. Am. Chem. Soc.* **1970**, *92*, 2132−2133; Wasserman, E.; Ben-Efraim, D. A.; Wolovsky, R. *J. Am. Chem. Soc.* **1970**, *92*, 2133−2135. For a recent discussion of the mechanism involved in those reactions see: Gruter, G.-J. M.; Akkerman, O. S.; Bickelhaupt, F. *Tetrahedron* **1996**, *52*, 2565−2572.

(8) The metathesis "catalyst" is actually a precatalyst or reaction initiator, so a small amount of macrocycle/catenane is lost through cross metathesis with the benzylidene ligand of **5**.

(9) General experimental procedure for RORCM: An anhydrous 0.0002−0.2 M solution of the olefin (0.35 mmol, **1** is not completely soluble in $CH_2Cl_2$ at 0.2 M and was used as a saturated suspension at that concentration) in freshly distilled dichloromethane was successively degassed and re-saturated with argon for at least 10 min before being injected directly into a flame-dried Schlenk tube containing the ruthenium carbene **5** (3−15 mg, 1−5 mol %) under a constant stream of argon with a gastight syringe. The reaction mixture was left stirring under a steady stream of argon for between 1 and 5 days until an unchanging product distribution was evidenced by analytical HPLC, then filtered through silica gel ($CHCl_3$/MeOH as eluent) to remove residual catalyst and leave catenane (using 0.2 M reaction concentration), macrocycle (0.0002 M), or mixtures thereof (0.02 and 0.002 M). Further purification with a Gilson 712 HPLC on a preparative column packed with Spherisorb S5W ($ClCH_2CH_2Cl$/*i*PrOH) allowed the separation of individual catenane diolefin isomers *EE*-**4** and *EZ*-**3**.

(10) The product distribution produced at equilibrium is independent of whether the starting material used is macrocycle, catenane, higher cyclooligomers, etc. or a mixture of these from another RORCM reaction. However, unstrained internal olefin metathesis is much slower than terminal olefin metathesis and the reactions normally require at least 24 h (and sometimes as long as 5 days with small catalyst loadings at dilute reaction concentrations) to undergo enough ring opening−ring closing cycles to allow the product distribution to reach a steady state. For such long reaction times decomposition of the catalyst by $O_2$ can be problematical and therefore the RORCM reactions require rigorous degassing before and during the experiment.

(11) Leigh, D. A.; Moody, K.; Smart, J. P.; Watson, K. J.; Slawin, A. M. Z. *Angew. Chem., Int. Ed. Engl.* **1996**, *35*, 306−310.

(12) Olefin stereochemistry was determined from $^{13}$C NMR chemical shifts of allylic carbons and characteristic IR bands [Williams, D. H.; Fleming, I. *Spectroscopic Methods in Organic Chemistry*, 4th ed., revised; McGraw-Hill: London, 1989].

(13) **Note Added in Proof.** For a recent example involving the temporary blocking of a cyclophane cavity in another catenane synthesis employing RCM see: Hamilton, D. G.; Sanders, J. K. M. *Chem. Commun.* **1998**, 1749−1750.

(14) **Note Added in Proof.** A π-electron rich/π-electron poor heterocircuit catenane synthesis by RORCM has recently been reported [Hamilton, D. G.; Feeder, N.; Teat, S. J.; Sanders, J. K. M. *New J. Chem.* **1998**, 1019−1021], although solubility-limited concentrations and slow reaction kinetics [see footnote 10] make the system only *quasi*-reversible thus far and consequently the product distribution is not under strict thermodynamic control.

# Appendix II: General Experimental Data

All melting points (m.p.) were determined using an Electrothermal 9100 melting point apparatus and are uncorrected.

$^{1}H$ and $^{13}C$ NMR spectra were recorded on a Brüker DPX 400 spectrometer at Warwick University and on a Brüker AC 300 or AC 200 at UMIST without any internal standard at 26 °C except where stated, and referenced to the residual solvent signal as internal standards ($CHCl_3$ at $\delta_H$: 7.27, s; $\delta_C$: 77.0, t; $C_2DHCl_4$ at $\delta_H$: 5.96, s; $\delta_C$: 78.0; [$D_5H$] DMSO at $\delta_H$: 2.54, m; $\delta_C$: 40.45, q). Chemical shifts are reported in parts per million (ppm) from high to low field. $^{1}H$-$^{1}H$ COSY, HMCQ, $^{13}C$ PENDANT, HMBC and GOESY were on occasion also recorded to enable more detailed assignment of $^{13}C$ and $^{1}H$ peaks.

Mass Spectrometry was carried out by the departmental services offered at Warwick University and UMIST.

C,H,N analyses were carried out by the departmental services offered at Warwick University and UMIST. At Warwick, the values are reported to 2 decimal places whilst at UMIST the values are reported to 1 decimal place. In addition no Cl analysis was routinely offered by the Warwick service.

Column chromatography was carried out using Kieselgel C60 (Merck, Germany) as the stationary phase.

TLC was performed on pre-coated silica gel plates (0.25 mm thick, $60F_{254}$, Merck, Germany). Plates were observed under UV light before being stained with either 8% sulphuric acid, potassium permangante solution or iodine vapour.

Reagents and anhydrous solvents used for reactions were purchased from Aldrich and were in general used without further purification. Isophthaloyl dichloride was

routinely recrystallised from hexane before use. Also, *p*-xylylene diamine was distilled under reduced pressure.